Vol. 96 No. 1, January 1, 1978 ISSN 0003-2670

ANALYTICA CHIMICA ACTA

International journal devoted to all branches of analytical chemistry

ELSEVIER SCIENTIFIC PUBLISHING COMPANY

ANALYTICA CHIMICA ACTA

International journal devoted to all branches of analytical chemistry
Revue internationale consacrée à tous les domaines de la chimie analytique
Internationale Zeitschrift für alle Gebiete der analytischen Chemie

PUBLICATION SCHEDULE FOR 1978 (incorporating the section on Computer Techniques and Optimization).

	J	F	M	A	M	J	J	A	S	O	N	D
Analytica Chimica Acta	96/1	96/2	97/1	97/2	98/1	98/2	99/1	99/2	100	101/1	101/2	102
Section on Computer Techniques and Optimization			103/1			103/2			103/3			103/4

Scope. *Analytica Chimica Acta* publishes original papers, short communications, and reviews dealing with every aspect of modern chemical analysis, both fundamental and applied. The section on *Computer Techniques and Optimization* is devoted to new developments in chemical analysis by the application of computer techniques and by interdisciplinary approaches, including statistics, systems theory and operation research.

Submission of Papers. Manuscripts (three copies) should be submitted to:
for *Analytica Chimica Acta*: Dr. A.M.G. Macdonald, Department of Chemistry, The University, P.O. Box 363, Birmingham B15 2TT, England;
for the section on *Computer Techniques and Optimization*: Dr. J.T. Clerc, Laboratorium für Organische Chemie, Swiss Federal Institute of Technology, Universitätstrasse 16, CH-8092 Zürich, Switzerland.

Information for Authors. Papers in English, French and German are published. There are no page charges. Manuscripts should conform in layout and style to the papers published in this Volume. Authors should consult Vol. 93, p. 379 for detailed information. Reprints of this information are available from the Editors or from: Elsevier Editorial Services Ltd., Mayfield House, 256 Banbury Road, Oxford OX2 7DE (Great Britain).

Reprints. Fifty reprints will be supplied free of charge. Additional reprints (minimum 100) can be ordered. An order form containing price quotations will be sent to the authors together with the proofs of their article.

Advertisements. Advertisement rates are available from the publisher.

Subscriptions. Subscriptions should be sent to: Elsevier Scientific Publishing Company, P.O. Box 211, Amsterdam, The Netherlands. The section on *Computer Techniques and Optimization* can be subscribed to separately.

Publication. *Analytica Chimica Acta* (including the section on *Computer Techniques and Optimization*) appears in 8 volumes in 1978. The subscription for 1978 (Vols. 96–103) is Dfl. 1000.00 plus Dfl. 120.00 (postage) (Total approx. US $463.71). The subscription for the *Computer Techniques and Optimization* section only (Vol. 103) is Dfl. 125 plus Dfl. 15.00 (postage) (Total approx. US $57.96). Journals are sent automatically by air mail to the U.S.A. and Canada at no extra cost and to Japan, Australia and New Zealand for a small additional postal charge. All earlier volumes (Vols. 1–87) are available at Dfl. 115.- (plus postage).

Claims for issues not received should be made within three months of publication of the issue, otherwise they cannot be honoured free of charge.

Printed in The Netherlands

Lasers in Chemistry

Proceedings of the Conference held at the Royal Institution, London, 31 May - 2 June 1977

edited by MICHAEL A. WEST, *The Royal Institution, London.*

As lasers and associated electro-optics have been developed in the past few years, chemists have rapidly adapted and used these new light sources in many diverse ways. This conference was held in order to review and discuss the present state-of-the-art in this fast-growing field and the proceedings contain 79 papers organized into seven sections. Each section, except one, contains a review paper by an invited speaker and a set of contributed papers which, taken together, indicate the overall scope of current research and point to likely future advances in a particular area. This volume will be of value to academic, government and industrial scientists as well as to technologists in chemistry, physics and electro-optics.

In the contents listed below, the main topics of the conference are given with the total number of papers in each section noted in parentheses. Limitation of space allows titles of only a few randomly selected papers to be mentioned.

CONTENTS: **1. Laser Raman and Other Scattering.** (10) Coherent anti-Stokes Raman spectroscopy *(J. P. E. Taran).* Raman rapid laser spectroscopy *(J. M. Beny, B. Sombret and F. Wallart).* **2. Pollution and Combustion.** (6) Long path IR absorption system for gaseous pollutants monitoring of the atmosphere *(F. Cappellani, G. Melandrone and G. Restelli).* Raman spectroscopic measurements of temperature in a natural gas/air flame *(L. Beardmore, H. G. M. Edwards, D. A. Long and T. K. Tan).* **3. Atomic and Molecular Spectroscopy** (18) Laser spectroscopy of gaseous free radicals and molecular ions *(A. Carrington).* Bimodal distribution of BaI vibrational states from the reaction BA + CF_3I *(G. P. Smith, J. C. Whitehead and R. N. Zare).* Molecular two-photon spectroscopy *(E. W. Schlag).* **4. Isotope Separation and Selective Excitation.** (8) Laser isotope separation *(C. P. Robinson, R. J. Jensen and C.D. Cantrell).* Near UV photophysics of gaseous UF_6 *(O.de Witte, R.Dumanchin, M. Michon and J. Chatelet).* **5. Infrared Photochemistry.** (8) High-power infrared laser chemistry *(W. Fuss, K. L. Kompa, D. Proch and W. E. Schmid).* **6. Fast Pulsed Techniques.** (14) Picosecond chemical kinetics *(G. Porter).* Laser flash photolysis studies on polymers using the light scattering detection method *(G. Beck, S. Beavan, G. Dobrowolski, D. Lindenau and W. Schnabel).* **7. Developments in Lasers and Laser Techniques.** (15) UV lasers: state of the art *(D. J. Bradley).* New analytic and spectroscopic tool - the opto-galvanic effect *(P. K. Schenck, D. S. King, K. C. Smyth, J. C. Travis and G. C. Turk).* **Author Index.**

Sept. 1977 xii + 438 pages US $69.50/Dfl. 170.00 ISBN 0-444-41630-7

ELSEVIER

P.O. Box 211, Amsterdam
The Netherlands
52 Vanderbilt Ave
New York, N.Y. 10017

The Dutch guilder price is definitive. US $ prices are subject to exchange rate fluctuations.

7057

Special Topics in Electrochemistry

edited by P. A. ROCK, *Department of Chemistry, University of California, U.S.A.*

In the last decade the field of electrochemistry has undergone rapid expansion. Several factors have contributed to this expansion but the major ones are undoubtedly the energy shortages, the desire for higher quality environments, and the greatly expanded efforts to understand bioelectric phenomena. Because of the rapid expansion of research efforts in electrochemistry, significant gaps have developed between the coverage of electrochemistry in existing chemistry textbooks and the research literature. The aim of this book is to bridge these gaps in several of the subfields of electrochemistry.

The material in this book is based mainly on papers presented at the Symposium entitled "Teaching of Electrochemistry" which was held on August 31, 1976 at the 172nd ACS Meeting in San Francisco, California. The symposium was sponsored by the Division of Chemical Education, Inc.

The level of presentation and the extent of the coverage of the various topics have been designed especially for senior and first-year graduate students who wish to survey the various research areas of contemporary electrochemistry. This work is also intended for chemistry teachers who wish to update and expand the coverage of electrochemistry in their courses.

CONTENTS: 1. Advanced Electrochemical Energy Systems *(L. R. McCoy).* 2. Photovoltaic Phenomena in Electrochemical Cells *(H. Gerischer).* 3. Electrochemical Synthesis *(Charles K. Mann and Margaret R. Asirvatham).* 4. Electrochemical Cells Without Liquid Junction *(Peter A. Rock).* 5. Species-Selective Electrochemical Sensors *(Peter A. Rock).* 6. Mechanisms of Electrochemical Oscillations *(Joel Keizer).* 7. Electrochemistry of Nerves *(Walter J. Moore).* 8. Theory and Applications of Electron Transfers at Electrodes and in Solution *(R. A. Marcus).* 9. On the Theory of Overvoltage for Electrode Processes Possessing Electron Transfer Mechanism *(R. A. Marcus).* 10. Electrostatic Free Energy and Other Properties of States Having Non-Equilibrium Polarization: Electrode Systems *(R. A. Marcus).*

Sept. 1977 viii + 224 pages US $39.50/Dfl. 97.00 ISBN 0-444-41627-7

ELSEVIER

P.O. Box 211, Amsterdam
The Netherlands
52 Vanderbilt Ave
New York, N.Y. 10017

The Dutch guilder price is definitive. US $ prices are subject to exchange rate fluctuations.

7058

Trace-Element Contamination of the Environment

DAVID PURVES, *Spectrochemistry Department, Edinburgh School of Agriculture, Edinburgh, Great Britain.*

FUNDAMENTAL ASPECTS OF POLLUTION CONTROL AND ENVIRONMENTAL SCIENCE, 1

The purpose of this book is to evaluate the global consequences of dispersal of trace elements, originally mined from localised limited deposits in the environment. Until now, this kind of environmental pollution has received less attention than the problem deserves for it could have profound ecological consequences in the long term.

This study provides a clear picture of the overall process of dispersion of trace elements in the biosphere and, within that perspective, highlights certain aspects of the subject. While consideration is given to problems arising from trace element contamination of the atmosphere and hydrosphere, the author focuses on the effects of contamination of the soil. The effects here will have serious and lasting consequences, as it is man's main source of food. Toxic trace elements in the soil can pass into plants and thence into food chains. Sources of trace-element contamination of the soil, the factors governing availability to plants and animals, and the nutritional consequences of soil contamination are therefore discussed at some length.

This book considers what previously appeared to be unrelated problems of environmental pollution and exhaustion of finite resources and reserves of metals such as cadmium, copper, lead, mercury, nickel and zinc, as aspects of a single global problem. It should therefore be of interest to environmentalists and conservationists, to those concerned with resource management and waste disposal, and to agricultural chemists and soil scientists.

July 1977 x + 260 pages US $34.75/Dfl. 85.00 ISBN 0-444-41570-X

ELSEVIER

P.O. Box 211, Amsterdam
The Netherlands
52 Vanderbilt Ave
New York, N.Y. 10017

The Dutch guilder price is definitive. US $ prices are subject to exchange rate fluctuations.

7053

ANALYTICA CHIMICA ACTA
VOL. 96 (1978)

ANALYTICA CHIMICA ACTA

International journal devoted to all branches of analytical chemistry

ELSEVIER SCIENTIFIC PUBLISHING COMPANY

Anal. Chim. Acta, Vol. 96 (1978)

Printed in The Netherlands

Analytica Chimica Acta, 96 (1978) 1—11

DETERMINATION OF TRACES OF MERCURY(II) BY INHIBITION OF AN ENZYME REACTOR ELECTRODE LOADED WITH IMMOBILIZED UREASE

LARS ÖGREN and GILLIS JOHANSSON*

Analytical Chemistry, University of Lund, P.O. Box 740, S-220 07 Lund (Sweden)

(Received 12th July 1977)

SUMMARY

Mercury (II) was determined in the range 0—0.7 nmol using urease immobilized in an enzyme reactor. Mercury inhibited the splitting of urea into bicarbonate and ammonia, the concentration of the latter being measured by an ammonia gas electrode. The sample volumes were 5 or 25 ml and the total mercury concentrations were 0—150 and 0—30 nmol l^{-1}, respectively. The reactor was regenerated by thioacetamide and EDTA between the samples. A derivation of the response equation showed that the inhibition should be a linear function of the amount of mercury and this was also found experimentally. The mercury was strongly bound to the urease, so the method should be useful for determination of free as well as complexed metal ions. Only silver and copper interfere.

It is well known that even trace amounts of metals and some other compounds may inhibit enzymatic reactions. A few cases have been reported in which the inhibition has been used analytically for the determination of inhibitor. A well known example is the determination of nerve gas and pesticides by the inhibition of choline esterases. Only a few reports have appeared concerning the determination of metals by enzyme inhibition. In most of these studies, urease has been used as a model enzyme.

The inhibition of urease by various metals has been studied systematically by Shaw [1] and Shaw and Raval [2]. A comparison between the inhibition of urease and the tendency of the metals to form slightly soluble sulphides has been made [3]. Torén and Burger [4] used a pH-stat kinetic method for metal determination; silver could be determined in the range $2—10 \times 10^{-8}$ M with a maximum error of 0.5 ng. A thermometric titration has been used for the determination of 1 ng Ag(I) ml^{-1} in solution [5]. Cadmium(II) in solutions containing 1—10 μg/10 ml has been determined by potentiometric titration [6].

Inhibition of enzymes has been used for the detection of metals in thin-layer chromatography. Urease provides detection limits in the range 3—0.02 μg of metal [7]. The lowest detection limits are obtained for mercury (0.02), copper (0.06), and silver (0.13). The method can also be used for organic mercury compounds [8] with detection limits of 0.03 μg for methoxy-

mercury chloride and phenylmercury acetate. A semi-quantitative visual agar-plate method with urease for mercury [9] provides a detection limit of 0.1—0.2 μg Hg(II).

Inhibition of the glucose—glucose oxidase system can also be used for metal determinations but with substantially higher detection limits [10]: $2—8 \times 10^{-5}$ M for mercury(II) and $2—10 \times 10^{-6}$ M for silver(I). Carbonic anhydrase inhibition gives a sensitivity [11] of about 2×10^{-4} M for silver nitrate. Mercury(II) (5×10^{-7} M) inhibits the glucosidase system, and this can be used for electrochemical detection [12]. Removal of the metal from a metalloenzyme can also be utilized analytically. The determination of zinc in the range 5—50 pg ml^{-1} with aminopeptidase can be cited as an example [13].

There should be some advantages in using the recently described enzyme-reactor electrode systems [14, 15] for metal determination and the present investigation was undertaken to evaluate the possibilities. Urease was selected because the technique of immobilization is well established, the immobilized enzyme is stable over long periods of time, the reaction products can be measured with very high selectivity, and the enzyme is very sensitive for traces of metals.

THEORY

An enzyme, E, is supposed to combine with a substrate, S, to a substrate—enzyme complex ES. This complex decomposes to a product P, the back-reaction of which is assumed to be negligible.

$$E + S \underset{k_{-1}}{\overset{k_1}{\rightleftarrows}} ES \xrightarrow{k_2} E + P \qquad (1)$$

The kinetics of this type of reaction has been derived by Michaelis and Menten [16]

$$\frac{dp}{dt} = k_2 e_0 (s_0 - p)/(K_m + s_0 - p) \qquad (2)$$

$$K_m = (e_0 - es)s/es = (k_{-1} + k_2)/k_1$$

(Lower case letters stand for concentrations, e_0 denotes the total concentration of enzyme, and s_0 the initial substrate concentration, t is the time and dp/dt the rate of product formation.) This theory has been applied to enzyme reactors, e.g. by Goldstein and Katchalski [17]. Their derivation can be extended to cover the present application. Suppose that a substrate with initial concentration s_0 is pumped through a reactor with an area A and length l, at a flow rate of q ml min^{-1}. Equation (2) will be valid for any position in the reactor if the time variable is replaced by the length co-ordinate l_x.

$$q \cdot t = l_x \cdot A \qquad (3)$$

Equation (3) is substituted into eqn. (2) which is integrated over the length of the reactor

$$e_0 k_2 \cdot A \cdot l/q = p + K_m \ln [s_0/(s_0 - p)] \quad (4)$$

The quantity $e_0 Al$ gives the amount of active enzyme in the reactor. If an inhibitor is introduced and bound irreversibly to some of the enzyme, only the quantity $(e_0 - e_i)Al$ of active enzyme remains. The amount of inhibited enzyme, $e_i Al$, should be proportional to the amount of inhibitor.

If the product concentrations before the inhibition, p_e, and after inhibition, p_i, are measured, the amount of inhibited enzyme can be found

$$[e_0 A \cdot l - (e_0 - e_i)A \cdot l] k_2/q = p_e - p_i + K_m \ln [(s_0 - p_i)/(s_0 - p_e)] \quad (5)$$

It is easier to study the behaviour of this equation if the conversion efficiency, $\eta = p/s_0$ is substituted into eqn. (5).

$$e_i \cdot A \cdot l = \frac{s_0 q}{k_2} \left[\eta_e - \eta_i + \frac{K_m}{s_0} \ln \left(\frac{1 - \eta_i}{1 - \eta_e} \right) \right] \quad (6)$$

The left-hand side of eqn. (6) represents the amount of metal for the present system. The square brackets on the right-hand side contain three terms; the first, η_e, is measured before a metal sample is introduced into the reactor and the second after the sample has passed through the reactor. The third term is logarithmic in these two measurable quantities. The influence of this term is determined by the Michaelis constant for the enzyme and the initial urea concentration. The amount of metal can thus be evaluated from a measurement of η_e and η_i if the constants are known. They can be collectively determined by calibration with metal solutions of known strengths.

In order to study the type of response curves to be expected, some simplification is desirable. For small values of η, eqn. (6) can be expanded

$$e_i \cdot A \cdot l = \frac{s_0 q}{k_2} (\eta_e - \eta_i) \left[1 + \frac{K_m}{s_0} + \frac{K_m}{s_0} \frac{(\eta_e + \eta_i)}{2} + \ldots + \right] \quad (7)$$

The amount of inhibited enzyme is in linear relation to the quantity $(\eta_e - \eta_i)$ for large values of s_0, i.e. when $s_0 \gg p$ and $s_0 > K_m$.

A more detailed study of eqn. (6) was undertaken by means of computer simulation. The percentage inhibition of the enzyme is given by $(\eta_e - \eta_i)100/\eta_e$. This quantity was plotted versus $e_i A l k_2/q$, which should be proportional to the amount of metal. The results obtained in the computer plots are shown in Fig. 1. Curve *a* represents the maximum sensitivity which can be obtained in a theoretical enzyme system; curves *b*—*e* are based on the K_m value of urease as determined earlier in an enzyme reactor [18], and on the use of reasonable concentrations of urea. The sensitivity, which can be defined as the slope of the plot in Fig. 1, decreases when the ratio K_m/s_0 increases. For a given K_m, a high substrate concentration is advantageous. There is an increased curvature in the response curves obtained at high values of η_e. A number of computer plots (not shown) indicated that the linearity was

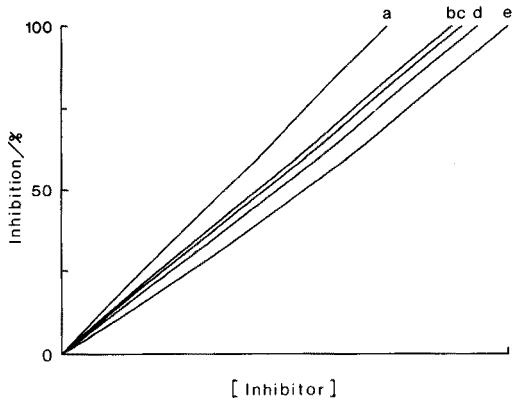

Fig. 1. Computer plot of eqn. (6) showing the percentage inhibition as a function of the inhibitor concentration in a sample of fixed size. Curves (a)—(e) are based on the constants; (a) $K_m/s_0 = 0.007$ $\eta_e = 0.01$, (b)—(e) $K_m/s_0 = 0.2$, $\eta_e = 0.01, 0.25, 0.50, 0.75$.

fairly good up to $\eta_e = 0.25$ even when $s_0 = K_m$. For $s_0 = 20K_m$, the linearity was good up to $\eta_e = 0.75$.

EXPERIMENTAL

Flow system

A schematic diagram is shown in Fig. 2. A two-channel pump (Pharmacia Fine Chemicals, Model P3) was fitted with 2.1-mm tubing and the motor speed was set so that the flow in each channel was 18.7 ml h^{-1}. A buffered urea solution was first pumped through an ion-exchange column (Chelex-100, 100-200 mesh, Na-form, i.d. 10 mm, length 95 mm) to remove traces of metal ions from the solution. The solution was then passed through the sample loop (Altex 4-way Rotary Valve, series 202) and next either through the enzyme reactor to a mixing T-joint or through a bypass directly to the T-joint. At the T-junction, the solution was made alkaline with a solution of 0.1 M NaOH containing 1 mM EDTA. The neutralization heat was removed in a heat-exchanger coil (Teflon tubing, 650 mm long, i.d. 0.5 mm, volume 140 μl). The ammonia concentration was determined with a flow-through ammonia electrode (EIL, Model 8002). The potential was measured with a pH meter (Radiometer, Model PH 640) and a potentiometric recorder in parallel.

Enzyme reactor

The enzyme reactor had an i.d. of 2.5 mm and a length of 2.2 mm between the two silver frits (1/8-in. diam., 0.015-mm holes; Reeve Angel, Cat. No. LA 200). The volume of the reactor was thus 14 μl. It was fitted with urease immobilized on CPG-10 controlled pore glass (Corning Glass Works, 120-200 mesh) by means of glutaraldehyde coupling as described earlier [14]. Two batches of enzyme were used, either U-1500 (4100 Sigma units/g) or

U-0251 (70 000 Sigma units/g) both made by Sigma Chemicals. Since the latter is much more active, only 3.1 mg of enzyme was taken per gram of glass, in contrast to 100 mg g^{-1} of glass for U-1500. The procedure has been described in detail [14].

Chemicals

The sodium hydroxide solution was made from a stock solution which had been boiled to expel ammonia and decrease the blank value. EDTA was added to prevent the formation of metal—ammine complexes at the electrode.

The substrate—buffer solution was made daily by dilution of stock solutions. It was 15 mM in urea, 25 mM in maleic acid buffer, and of pH 6.15. The stock solution of maleic acid was 0.1 M, adjusted to pH 6.00 with NaOH.

The metal stock solution was 10 mM in metal nitrate and 0.1 M in nitric acid. A secondary stock solution was made daily by dilution 1000 times. Sample solutions were made by diluting the secondary stock solution with 1 mM malic acid. The malic acid solution had previously been purified from metals by passage through a column of Chelex-100. The water used was purified with a Millipore-Q system, and all glass-ware was acid-washed and then soaked in purified water. Extensive purification is necessary only in preparation of the sample solutions, as other solutions are passed through the Chelex column in the flow system when necessary. The malic acid solution was of pH 5.3; at this pH it forms weak complexes with the metal ions, so that most of the metals are present in complexed form. The complexation and the buffering action together prevent precipitation as hydroxides and reduce ion-exchange adsorption on the walls of the containers and in the flow system.

The regeneration solution used was 10 mM in thioacetamide, 10 mM in EDTA and 0.1 M in Tris, adjusted to pH 7.0 with HCl.

Procedure

A buffered substrate solution is pumped through the enzyme reactor with the rotary valve in position A (Fig. 2). The substrate concentration is selected so that only about 3% of the urea is broken down to ammonia. The ammonia concentration, which under these conditions is proportional to the enzyme activity in the reactor, is sensed by the electrode and displayed on the pH-meter and recorder. For a constant flow rate and a constant temperature, a steady-state is obtained.

Next, the valve is changed to position B and 2.5 ml of water is passed through the reactor to displace the buffer—substrate solution. Then a sample or a standard solution containing metal ions can be passed through the reactor. The metal ions may bind the enzyme and deactivate part of it. A new portion of water is passed through the reactor before the valve position is changed.

If the sample contains metal ions which deactivate some of the enzyme the conversion of urea will be lower and a lower ammonia concentration will be displayed. The difference is a measure of the metal content of the sample.

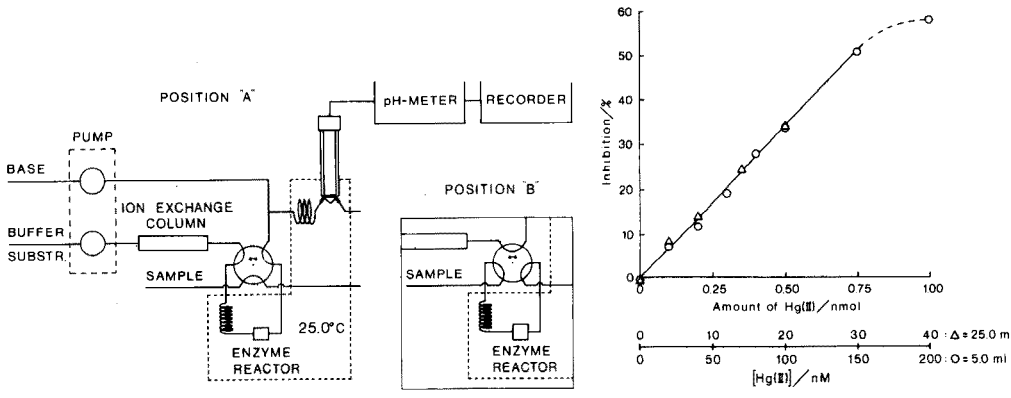

Fig. 2. Experimental arrangement for metal determinations with the enzyme reactor electrode.

Fig. 3. Percentage inhibition of the enzyme reactor as a function of the mercury concentration for two sample sizes. A scale giving the amount of mercury in the samples is shown for convenience.

The enzyme reactor can be regenerated by turning the valve to position B and passing 3 ml of regenerating solution through the reactor followed by 5 ml of water. The system is then ready for another sample.

RESULTS AND DISCUSSION

Mercury determination

A urea substrate solution was pumped through an enzyme reactor containing 3.1 mg of urease (U-0251) per gram of glutaraldehyde glass. The valves were in position A (see Fig. 2). The output voltage from the ammonia sensor reached a steady value within 3—4 minutes. The valve was switched to position B and 25 ml of 4×10^{-9} M mercury(II) solution was passed through the reactor at an approximate flow rate of 8 ml min^{-1}. The mercury(II) in the sample is bound to enzyme molecules which then become inactive. The valve was switched back to position A and the amount of ammonia produced from the urea substrate solution was again measured with the ammonia probe. Because of the mercury(II), the ammonia concentration was then lower. The relative decrease was calculated and plotted versus the mercury concentrations when a series of 25-ml samples were run as described. The results are shown in Fig. 3.

Another series of experiments was made with sample volumes of 5 ml but with 5 times higher mercury(II) concentrations. Figure 3 is provided with a scale for the total amount of mercury in each sample, and two concentration scales for 25- and 5-ml samples, respectively. It can be seen that the relative inhibition is a linear function of the mercury(II) concentration for a given sample size, and that, if the sample size is varied, it is a linear function of the

amount of mercury. This shows that the mercury(II) in the sample is quantitatively removed from the sample and bound to the enzyme in the reactor. For more than 50% relative inhibition, the linear relationship breaks down, probably because the flow is unevenly distributed in the minute reactor bed. Enzyme beds along the main flow paths become saturated with a resultant breakthrough of mercury.

The Michaelis constant for soluble urease has been reported [19] to be 19 mM. For urease immobilized in a reactor similar to that used here, a value of 3.1 mM has been reported [18] at a flow rate of 0.44 ml min^{-1}. The substrate concentration was 15 mM; K_m/s_0 then becomes 0.2, and η_e is 0.033. Equation (6) or (7) then predicts a linear response, in agreement with the results shown in Fig. 3 for relative inhibitions below 50%. Equation (6) also predicts that the values of K_m/s_0 and η_e give about 85% of the maximum sensitivity which can be obtained with the amount of enzyme used (Fig. 1). The sensitivity is the slope of the line in Fig. 3. The only practical way of increasing the sensitivity further is, therefore, either to decrease the reactor volume or to decrease the density of enzyme on the glass spheres.

A few initial experiments were made with a different procedure. The flow of sample solution was mixed with a flow of buffer—substrate solution and pumped through the reactor. Valves were then not needed, and the inhibition could be recorded continuously. The disadvantage of this method was that the metal ions formed complexes with the ammonia produced or with impurities in the substrate—buffer solution. The method was also slower and less reproducible than that described above. This procedure was therefore not examined further.

Mercury(II)—enzyme complex formation

Once mercury(II) had been bound to the enzyme, large amounts of substrate—buffer solution could be passed through the reactor without changes in the relative inhibition. It can therefore be concluded that the mercury(II)—enzyme complex is much stronger than the complexes between mercury(II) and maleic acid or ammonia.

Strong complex formers are required for regeneration of the enzyme. Various solutions (2 ml) were passed quickly through a partly (85%) inhibited reactor. The results, shown in Table 1, were normalized to that of the thioacetamide—EDTA solution, and the values reflect both kinetic and equilibrium effects. The conditional stability constants at pH 7 for the predominant mercury(II) complex were also calculated from literature data [20—23]. The enzyme concentration in the reactor is not a well defined quantity; the concentration including the volume of the glass is less than 10^{-4} M. The stability of the mercury(II)—enzyme complex must be much larger than, for example, that of the mercury(II)—EDTA complex, as a large volume of the latter can be passed through the reactor with only a small decrease in the inhibition.

At first sight, cysteine is a very efficient regeneration agent, reactivating

TABLE 1

Regeneration of the reactor by passing 2 ml of complex former in 0.10 M Tris—HCl, pH 7.0, quickly through an 85% inhibited reactor

Complex former	Conc. (mM)	Relative regeneration (%)	log K[a]
Thioacetamide EDTA	10 10	100	—
EDTA	5	5	15.5 (HgL) [20, 21, 23]
Thioacetamide	5	12	18.7 (HgL_3) [22, 23]
Thiourea	5	3	20.9 (HgL_3) [20, 21, 23]
Cysteine	5	620	6.4 (HgL) [21, 23]
Histidine	5	0	13.0 (HgL_2) [21, 23]
Methionine	5	0	4.0 (HgL_2) [21, 23]

[a] K = conditional complex constant corrected for pH effects on both the ligand and the metal. The constant relates to the dominant complex shown in parentheses. The figures in brackets are reference numbers.

more enzyme than the thioacetamide—EDTA solution. The level of activity obtained with cysteine increased with the number of regenerations but the sensitivity towards mercury(II) as an inhibitor decreased rapidly. The reagent was therefore unsuitable for use with the present analytical method, as the increase in activity seemed to result from a chemical reaction rather than from complex formation with mercury(II). In contrast to the effects observed with cysteine, a regeneration solution consisting of thioacetamide—EDTA always gave a definite and reproducible level of enzyme activity. The sensitivity for mercury(II) was constant even after a large number of inhibition—regeneration cycles. EDTA is not necessary for removal of mercury(II), but it is necessary if inhibition has been caused by metals such as Ag(I) and Cu(II).

Metals other than mercury

When samples containing 0.25 and 0.5 nmol of silver(I) were run through the reactor, the initial inhibition was high, but decreased with time because the silver(I)—ammine complexes were strong enough to remove the metal from the enzyme. When the recorded value was extrapolated back to the time of sample injection, the sensitivity obtained was almost the same as for mercury(II).

All the results reported above relate to urease from batch number U-0251. The following study for other metals was made with batch U-1500. No inhibition was observed with 5-ml samples which were 0.1 or 1 μM in Ni(II), Zn(II), Cd(II) or Pd(II), when they were introduced at a flow rate of about 1 ml min^{-1}. For copper(II) the amount of inhibition depended on the flow rate: 5 ml of 1 μM copper(II) solution produced 5% inhibition at 15 ml min^{-1} and 25% inhibition at 0.3 ml min^{-1}. At 0.3 ml min^{-1}, a 4 μM solution of

zinc(II) also produced some inhibition (6%). Mercury(II), however, showed no flow dependence between 1 ml min^{-1} and 20 ml min^{-1}. At 0.3 ml min^{-1}, there was a slight decrease, probably caused by adsorption on the container walls.

Under the conditions described in the Experimental, the method is selective for mercury, with a selectivity factor of 1000 and probably much more over the metals Ni(II), Cd(II), Pb(II) and Zn(II). The selectivity over copper depends on the rate of sample injection, and the factor may vary between 50 and 1000. There is initially practically no selectivity for mercury over silver, but the presence of silver can easily be seen on the recorder. The inhibition for silver(I) (and copper(II)) decreases rapidly with time.

Number of metal ions per enzyme molecule

The urea batch U-1500 was found to contain 10.0% N (Kjeldahl method). When the immobilization procedure was used with 100 mg of enzyme taken for each gram of glass, 2.6 mg N was bound to each gram of glass when a correction (0.6 mg N/g glass) had been applied for the nitrogen from the propylamine silanization. If all nitrogen-containing compounds in the enzyme batch immobilize with the same probability, 26 mg of protein should be bound to each gram of dry glass.

A reactor contains 4.7 mg of dry enzyme-glass, and if all the protein is assumed to be urease (m.w. 480 000 [24]), there should be 0.25 nmol of enzyme present. The calibration curves were similar to those of Fig. 3 when enzyme batches were prepared from U-1500. The curves were extrapolated to 100% inhibition and the amount of mercury(II) was read. Three reactors, each made from separate immobilizations, required 0.8, 0.9 and 1.8 nmol of mercury(II), respectively, for complete inhibition. Nitrogen was determined on the last reactor. The number of mercury(II) ions per enzyme molecule was then calculated to be 3.2, 3.6, and 7.2, respectively.

It has been reported that urease contains six sub-units [25]; there seem to be 3—4 sulfhydryl active sites per molecule [26]. The total number of —SH groups which can be titrated with silver nitrate was found [27] to be 109 ± 7. It is also possible to differentiate the —SH groups according to reactivity [28]; there are 26—28 highly reactive groups, 7—9 less reactive groups and, on unfolding of the chain, another 45—50 groups. Inhibitor studies with hydroxamic acid have shown that two inhibitor molecules are bound to each urease molecule [29].

The precision of the present determination of the number of mercury ions required to inhibit one urease molecule, is low. The amount of protein was determined only for the material in the last reactor, it may be different in the others. The volume, 14 μl, in the reactor cannot be precisely determined with the silver frits used. Some of the urease may be destroyed during the immobilization procedure and there may also be other nitrogen-containing material bound to the glass.

The conclusion which can be drawn is that the number of mercury ions is too low to correspond to binding even only of the more reactive —SH groups. It is more likely that a small number, perhaps one or two, per sub-unit or active site is sufficient to cause inhibition of the enzyme activity.

Differences in the enzyme batches

When the activity of a reactor containing enzyme from batch U-0251 was measured before any inhibition was attempted, the value obtained was low. After inhibition with 5 ml of 10 μM Hg(II) solution and regeneration, the activity was much higher. The initial activity was only 2% of the activity obtained after the inhibition—regeneration cycle. Regeneration solution alone did not increase the activity. No corresponding phenomena were observed with enzyme from batch U-1500. The activities of the soluble enzymes were checked and found to be in agreement with the specifications given by Sigma Chemicals. A possible explanation is that an inhibitor bound to the enzyme was displaced by mercury and washed away. The differences between the batches may also have been caused by differences in the immobilization procedure; much less of the batch U-0251 enzyme was used and there may have been differences in the binding. Addition of mercury may have caused conformational changes which restored some of the activity.

Reactors made from enzyme batch U-1500 showed a slightly sigmoidal calibration curve for mercury. A small amount of metal ions seemed to be bound before inhibition could start. This batch was less pure and may have contained some impurity which formed a complex with mercury(II) stronger than the mercury(II)—urease complex. The reproducibility of the reactors made from U-1500 was less satisfactory and a longer time was required to obtain stable potential values. The inhibition was different if the same amount of mercury(II) was introduced in different sample volumes. The impurities in this batch seem to give the reactors less desirable properties.

Increasing the sensitivity

As mentioned above, the values of η_e and K_m/s_0 were selected so that the sensitivity was close to the optimum (85%). It can be seen from eqn. (6) or (7) that the sensitivity can be changed by varying the quantity $e_i Al$. In this study, reactors with $A \times l = 14$ μl were used, and it is not practical to reduce the volume further. The remaining parameter is e_i, the amount of active enzyme. As shown above, impure enzyme preparations which were less active produced various side effects so that it seems better to use less of a pure enzyme. If a small amount of enzyme is present per gram of glass, there will be more bonds between each enzyme molecule and the alkylamino groups on the glass. The activity of immobilized U-0251 urease was less than that expected from the specification of the soluble enzyme. The low concentration of enzyme used with this batch caused denaturation, some of which could be restored by a mercury inhibition—regeneration cycle. In retrospect, it might have been better to use more than 3.1 mg of

urease U-0251 per gram of glass in the immobilization procedure and to reduce e_i by other means.

One way to reduce the amount of enzyme immobilized in a given volume is to use glass with a large pore diameter. A glass with 2000-Å pore size gave 1.4 times less activity and 1.8 times higher sensitivity than the glass with 700-Å pore size used earlier; the surface area is lower per gram of glass, the larger the pore diameter. Other possibilities might be to decrease the pore size so that less enzyme can penetrate into the glass, or to dilute the enzyme-glass with a glass with an inactive surface, but these possibilities were not examined. A batch of immobilized enzyme was treated with 0.1% ethanolamine for 75 min at pH 6 and 4°C; the activity was decreased 2.3 times and the sensitivity for mercury was increased 2.8 times.

This work was supported by grants from the Swedish Board for Technical Development, STU. Dr. H.-G. Karlsson, STU, initiated the project and gave valuable suggestions.

REFERENCES

1 W. H. R. Shaw, J. Am. Chem. Soc., 76 (1954) 2160.
2 W. H. R. Shaw and D. N. Raval, J. Am. Chem. Soc., 83 (1961) 3184.
3 R. B. Hughes, S. A. Katz and S. E. Stubbins, Enzymologia, 36 (1969) 332.
4 E. C. Torén Jr. and F. J. Burger, Mikrochim. Acta, (1968) 1049.
5 J. N. Baldridge and N. D. Jespersen, Anal. Lett., 8 (1975) 683.
6 H. Weisz and K. Rothmaier, Anal. Chim. Acta, 80 (1975) 351.
7 F. Geike, Z. Anal. Chem., 258 (1972) 284.
8 F. Geike and I. Schupman, J. Chromatogr., 72 (1972) 153.
9 E. Sandi, K. Soos, R. Liebman and A. Hellwig, Chem. Tech., 22 (1970) 557.
10 E. C. Torén Jr. and F. J. Burger, Mikrochim. Acta, (1968) 538.
11 J. Maguire and N. Watkin, Bull. Environ. Contam. Toxicol., 13 (1975) 625.
12 G. G. Guilbault and D. N. Kramer, Anal. Biochem., 18 (1967) 313.
13 P. Lehky and E. A. Stein, Anal. Chim. Acta, 70 (1974) 85.
14 G. Johansson and L. Ögren, Anal. Chim. Acta, 84 (1976) 23.
15 G. Johansson, K. Edström and L. Ögren, Anal. Chim. Acta, 85 (1976) 55.
16 L. Michaelis and M. L. Menten, Biochem. Z., 49 (1913) 333.
17 L. Goldstein and E. Katchalski, Z. Anal. Chem., 243 (1968) 375.
18 G. Johansson and L. Ögren, in E. Pungor (Ed.), Ion-selective Electrodes, Akadémiai Kiadó, Budapest, 1977, p. 93.
19 F. J. Reithel in P. D. Boyer (Ed.), The Enzymes, Vol. 4, Academic Press, New York, 1971, p. 4.
20 J. J. Christensen and R. M. Izatt, Handbook of Metal Ligand Heats, M. Dekker, New York, 1970.
21 R. M. Smith and A. E. Martell, Critical Stability Constants, Vol. 1: Amino Acids, Plenum, New York, 1974.
22 D. M. King, N. I. Kolby and J. W. Price, J. Electroanal. Chem., 40 (1972) 295.
23 L.-G. Sillén, Chemical Society, London 1964, Suppl. No. 1, London 1971.
24 W. N. Fishbein, K. Nagarajan and W. Scurzi, J. Biol. Chem., 248 (1973) 7870.
25 F. J. Reithel, J. E. Robbins and G. Gorin, Arch. Biochem. Biophys., 108 (1964) 409.
26 J. F. Ambrose, G. B. Kistiakowsky and A. G. Kridl, J. Am. Chem. Soc., 73 (1951) 1232
27 P. Mildner, B. Mihanovic and D. Winterstreiger-Cvoriscec, Croat. Chem. Acta, 44 (1972) 407.
28 A. Andrews and F. J. Reithel, Arch. Biochem. Biophys., 141 (1970) 538.
29 K. Kobashi, J. Hase and T. Komai, Biochem. Biophys. Res. Commun., 23 (1966) 34.

Analytica Chimica Acta, 96 (1978) 13—22

THE FORMATION OF MIXED COPPER SULFIDE—SILVER SULFIDE MEMBRANES FOR COPPER(II)-SELECTIVE ELECTRODES
Part III. The Electrode Response in the Presence of Complexing Agents

G. J. M. HEIJNE and W. E. van der LINDEN*

Laboratory for Analytical Chemistry, University of Amsterdam, Nieuwe Achtergracht 166, Amsterdam (The Netherlands)

(Received 30th June 1977)

SUMMARY

The behaviour of a copper(II)-selective electrode made of ternary copper/silver sulfide, in the presence of complexing agents is discussed. Potential vs. pH curves indicate that in the case of Trien and Tetren, the electrode response reflects the situation in the bulk solution when both the free ligand and its copper(II) complex are present; when only the ligand is present, a small amount of the complex is probably formed near the surface, by dissolution of the membrane material. Similar results were found with citrate and glycine. In the case of EDTA and NTA, however, the response of the electrode is quite different; the concentrations of free copper(II) measured are higher than those expected from chemical equilibrium calculations for the bulk solution. The curves for solutions with and without the complex coincide and show an anomalous dependence on the side-reaction coefficient, $\alpha_{L(H)}$. No explanation has been found for this behaviour. There is good agreement between stability constants for copper complexes or precipitates of Trien, Tetren, hydroxide and sulfide, obtained with this electrode and those given in the literature. The results indicate that Tetren or Trien should be preferred to EDTA and NTA for the preparation of metal buffer solutions.

It has already been shown [1] that the value of the potential of copper(II)-selective electrodes at low concentrations of free copper(II) is more positive than the value calculated on the assumption of chemical equilibrium in the solution. Evidence has been given [2] that electrodes made of precipitates which contain the mineral jalpaite ($Ag_{1.5}\,Cu_{0.5}\,S$) have the best response characteristics. Hence the presence of copper(I) must be considered. In solubility measurements, it was found that extraordinarily large amounts of copper ions were dissolved (about 10^6 times larger than could be expected from the solubility products given in the literature [3]). The results of several experiments suggested that these high copper concentrations might be caused by oxidation of copper(I) by the general reaction $Cu_2S \rightleftarrows 2Cu^+ + S^{2-} \rightleftarrows CuS + Cu^{2+} + 2e^-$; or in the case of jalpaite $4Ag_{1.5}\,Cu_{0.5}\,S \rightleftarrows 3Ag_2S + CuS + Cu^{2+} + 2e^-$.

Several authors [4—6] have discussed theoretically the response of electrodes based on mixed sulfide precipitates, and especially the standard

potentials, but these papers do not elucidate the problem of the high value of the lower limit of detection. Koebel [5], as well as Buck and Shepard [6], have discussed the complications arising in the case of copper sulfide, since at least five different stoichiometric compositions are known [7]. In both papers deviations were reported between the calculated and the experimental standard potentials for the system copper sulfide—silver sulfide. Ternary compounds have not been considered. Morf et al. [8] tried to explain the high detection limits found for silver sulfide electrodes by postulating for the membrane material a silver defect activity, which would cause the observed levelling of the electrode response below a certain concentration. This explanation was questioned by Buck [9] and the results of Morf et al. could not be verified experimentally by Crombie et al. [10].

Recently, two studies have been published on the response of copper sulfide-based electrodes which contained copper(I). Hepel et al. [11] considered electrodes made of the non-stoichiometric materials, $Cu_{1.98}S$ and $Cu_{1.86}S$, and presented a model in which the response of the electrode to copper(II) is based on a reduction reaction at the surface of the membrane: $CuS\ (n\text{-}s) + Cu^{2+} + 2e^- \rightleftarrows Cu_2S\ (n\text{-}s)$, where (n-s) indicates that non-stoichiometric solid phases are involved. In order to verify the potential equation derived, measurements were made in copper(II) and copper(I) solutions; the close agreement between theory and experiment found seems to be caused partly by the inconsequent use of standard potential data.

Hulanicki and Lewenstam [12], working with a single-crystal electrode of chalcocite (Cu_2S), explained the response on the basis of an ion-exchange reaction: $Cu_2S + Cu^{2+} \rightleftarrows CuS + 2Cu^+$. They reported good agreement between theory and experiment, but results of calibrations below 10^{-5} M copper(II) were not presented, which makes it difficult to verify their hypothesis. However, on the basis of this model, levelling of the electrode response to copper(II) is predicted when very small amounts of copper(I) are present, because this type of electrode is essentially sensitive to copper(I). These authors found a difference in the behaviour of the electrode during titrations of copper(II) with EDTA or Tetren. With Tetren, the experimental and calculated values of the potential agreed, whereas with EDTA the experimental values were high, which suggests higher concentrations of free copper(II) in excess of ligand than could be expected on the basis of chemical equilibrium. The explanation of this phenomenon [12] is based on the assumption that copper(I) forms weaker complexes with EDTA than with Tetren. Thus, with EDTA there is a relatively larger concentration of free copper(I), which determines the potential after the equivalence point, while with Tetren copper(I) is also complexed. No explanation was given for the amount of copper(I) present (2.5×10^{-11} M), but it is larger than can be expected from solubility alone.

The response of copper(II)-selective electrodes in solutions containing complexing agents has often been discussed [13—18]. El-Taras et al. [18] reported linear responses towards citrate, glycine and other ligands in the

case of electrodes made of copper sulfide with silicone rubber as the matrix. In the other studies, generally the response of the electrode has been measured as a function of pH at constant concentrations of the ligand, both in the presence and in the absence of copper(II), in order to establish optimum conditions for titrations. In an extensive study of the effects of complexing agents, Nakagawa et al. [15] determined the stability constants of the copper(II) complexes; difficulties occurred when EDTA or NTA was used, and no stability constants could be calculated.

In the present paper, more information is given about the electrode response observed in solutions containing complexing agents. It is important to find an answer to the problems mentioned above, not only from a theoretical point of view, but also because EDTA and NTA have been proposed for metal buffers for the calibration of electrodes [14, 19]. The experimental data show that copper(II)-selective electrodes can have a linear Nernstian response down to about 10^{-20} M of free copper(II) when Tetren or Trien is used.

THEORY OF COMPLEXATION

An extensive treatment of the theory of complexation in relation to i.s.e., by the approach of Ringbom [20] with side-reaction coefficients, α, has been given by Hansen et al. [14]. For convenience, some of the important equations will be given here; charges are omitted, where no ambiguity results. The concentration of free copper(II) in a solution containing ligand L which forms only 1:1 complexes with copper(II) can be written as:

$$p[Cu] = \log \beta_{CuL} + \log (\alpha_{ML}/\alpha L) + \log ([L']/[ML']) \quad (1)$$

where β_{CuL} is the stability constant of the complex CuL. The primed concentrations include those species formed by side-reactions, e.g. $[A'] = \alpha_A [A]$, where α are side-reaction coefficients: $\alpha_A = \alpha_{A(B,C)} = 1 + \beta_{AB}[B] + \beta_{AB_2}[B]^2 + ... + \beta_{AC}[C] + ...$ The copper(II) concentration arising from dissolution of copper(II) sulfide can be calculated from

$$[Cu^{2+}] = (K_{so}^{CuS} \cdot \alpha_{S(H)}/\alpha_{Cu^{2+}})^{\frac{1}{2}} \quad (2)$$

When no ligand is present, only copper hydroxides can be formed:

$$\alpha_{Cu^{2+}} = \alpha_{Cu(OH)} = 1 + \beta_{CuOH}[OH^-] + \beta_{Cu(OH)_2}[OH^-]^2 + ... \quad (3)$$

but when a ligand is present, complexation must be considered. In this case of dissolution equilibrium, this complexation is a side-reaction, hence

$$\alpha_{Cu} = \alpha_{Cu(L,OH)} = 1 + \beta_{CuL}[L] + \beta_{CuOH}[OH] + \beta_{Cu(OH)_2}[OH]^2 + ... \quad (4)$$

Analogously, for copper(I) in equilibrium with Cu_2S

$$[Cu^+] = (2K_{so}^{Cu_2S} \alpha_{S(H)}/(\alpha_{Cu^+}))^{\frac{1}{3}} \quad (5)$$

EXPERIMENTAL

The preparation of the electrodes and the equipment used have been described before [1]. The concentration of acetate buffer was 0.05 M. pH measurements were made with an Electrofact 7G 11 glass electrode vs. SCE, and read with a Radiometer pHM 22 meter, calibrated at pH 6.50.

All chemicals used were of analytical-reagent grade.

The response of the copper-i.s.e. in the presence of ligands was recorded as a function of pH for pH 2—12 by addition of 1 M potassium hydroxide solutions to the medium which contained 0.1 M potassium nitrate and 0.01 M nitric acid. In the case of sulfide ion, the direction of the pH change was reversed, 1 M nitric acid being added to the 0.1 M potassium nitrate—0.01 M potassium hydroxide medium.

RESULTS AND DISCUSSION

Response of the electrode to copper(II) and sulfide ions

The electrode was calibrated frequently to check that no change in the response characteristics occurred. The calibration curves did not change during one month, obeying the equation

$$E = E' + S \log a_{Cu^{2+}} = 89 + 29.7 \log a_{Cu^{2+}} \quad (6)$$

The value of S varied between 29.6 and 29.8 mV/decade; this variation was considered negligible in further calculations.

The response of the electrode to sulfide ion was recorded by varying the pH of a solution containing 10^{-3} M sodium sulfide. The free S^{2-} concentration was calculated from the stability constants $\beta_{HS}^{H} = 10^{12.6}$ and $\beta_{H_2S}^{2H} = 10^{19.5}$ [20]. Concentrations were converted to activities by using a value of 0.38 for the activity coefficient of the sulfide ion [21].

Figure 1 shows the variation of the potential as a function of both pH and pS. The pS plot is linear over at least fifteen decades, the equation being

$$E = -829 - 25.9 \log a_{S^{2-}} \quad (7)$$

After these measurements the surface of the electrode was tarnished, and the response to copper(II) diminished slightly. Intersection of the E vs. log $a_{Cu^{2+}}$ curve with the E vs. log $a_{S^{2-}}$ curve led to a value for the solubility product $a_{Cu^{2+}} \cdot a_{S^{2-}} = 10^{-33}$. Therefore it can be concluded that in sulfide medium, as well as in more concentrated copper(II) solutions, the response is based on solubility equilibria, as is generally assumed.

Response of the electrode as a function of pH

Figure 2 shows the response of the electrode as a function of pH for solutions containing 0.1 M KNO_3 alone, and 0.1 M KNO_3 in the presence of 10^{-3} M copper(II). In the presence of copper(II) the curve shows a decrease above pH 6.5, indicating hydrolysis of copper(II). From the slope of about

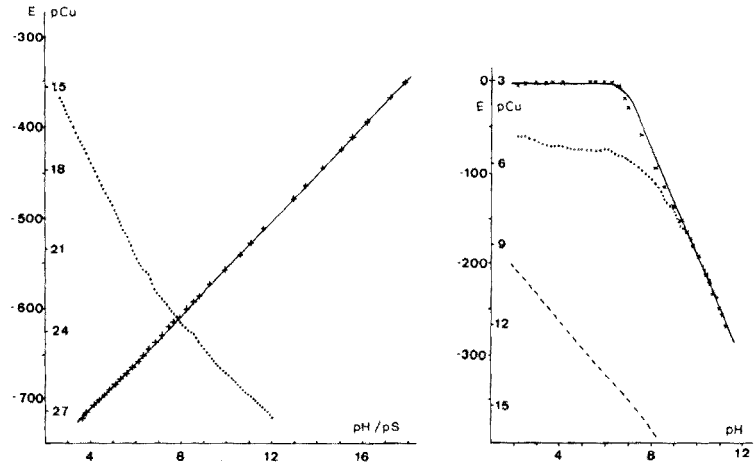

Fig. 1. Response of the copper-i.s.e. in 10^{-3} M sodium sulfide vs. pH (.....) and vs. sulfide activity (x—x—x).

Fig. 2. Response of the copper-i.s.e. vs. pH in 10^{-3} M copper nitrate (x) and in 0.1 M potassium nitrate (•). The curves drawn were calculated from $\log K_{so}(Cu(OH)_2) = -17.3$ (——) and from eqn. (2) (------).

60 mV/decade, it can be concluded that two hydroxyl ions are involved; i.e. $Cu(OH)_2$ is formed either as a complex or as a precipitate. The corresponding stability constant or solubility product was calculated: $\log \beta(Cu(OH)_2) = 14.3$, $\log K_{so}(Cu(OH)_2) = -17.3$. The E—pH curve calculated on the basis of these constants is also shown in Fig. 2. The small deviation in the pH range 6.5—9 might be due to the formation of $CuOH^+$. The literature values are: $\log \beta(CuOH) = 6.0—7.5$, $\log \beta(Cu(OH)_2) = 13.2$ and 14.3 [3], and $\log K_{so}(Cu(OH)_2) = -18.8$ [22], or -19.0 to -20.0 [3]. Although in the present experiments complete equilibrium was probably not attained at the electrode surface, the correspondence of the present results with the literature values is fairly good.

In the absence of copper(II) in the solution, one might expect an E—pH curve corresponding to eqn. (2). However, experiments showed a much larger concentration of copper(II), while at higher pH values the coincidence with the curve for 10^{-3} M copper(II) also indicated that, at least at the surface of the electrode, relatively large amounts of copper(II) were present, which agrees with the enhanced solubility reported previously [2].

Response of the electrode in the presence of complexing agents

Measurements were made in solutions containing either 10^{-3} M ligand or 2×10^{-3} M ligand and 1×10^{-3} M copper(II). The results are presented in Fig. 3 for EDTA, NTA, Trien, Tetren, glycine and citrate; Fig. 3 also shows the calculated E—pH curves based on the assumption of a dissolution

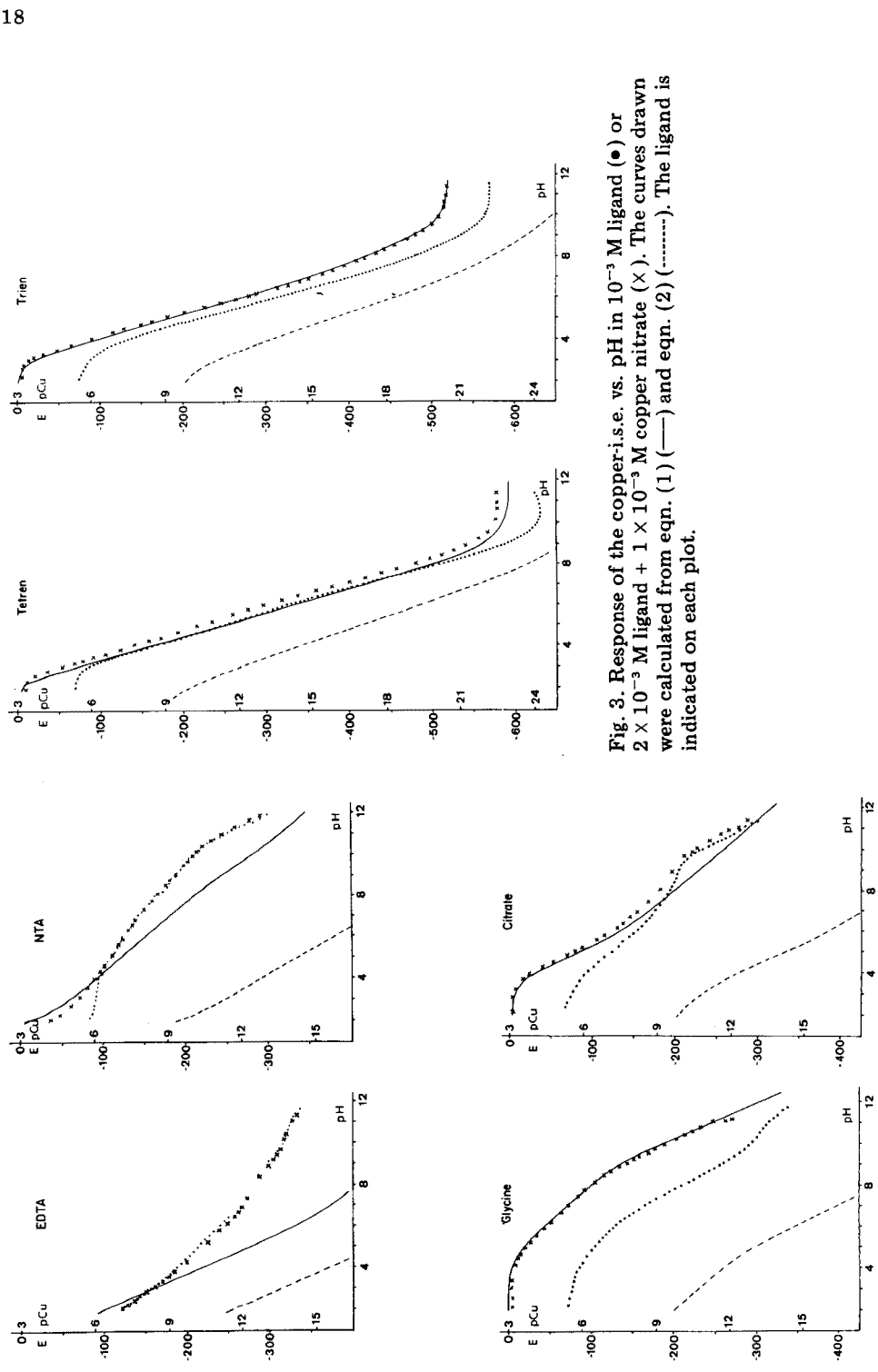

Fig. 3. Response of the copper-i.s.e. vs. pH in 10^{-3} M ligand (•) or 2×10^{-3} M ligand + 1×10^{-3} M copper nitrate (×). The curves drawn were calculated from eqn. (1) (——) and eqn. (2) (-------). The ligand is indicated on each plot.

equilibrium at the electrode surface (eqns. 2, and 4) and the curve based on the assumption that the concentration of copper(II) at the electrode surface equals the free copper(II) concentration in the bulk of the solution, calculated from eqn. (1). The values of the constants used for these calculations are summarized in Table 1; the value of $\beta_{Cu(OH)_2}$ was taken from Fig. 2.

There is fairly good agreement between the E—pH curves calculated from eqn. (1) and the experimental curves for solutions containing copper(II) in the presence of an excess of Trien, Tetren, glycine and citrate. This is strong proof that in these cases the conditions at the electrode surface are similar to those in the bulk solution. The fact that the experimental curves in the presence of ligand alone are approximately parallel to the curves obtained with copper(II) (at least above pH 4), indicates that essentially the same solution exists, although the concentration of the copper complex at the surface is somewhat lower when only the ligand is present. This again can be explained only by enhanced solubility of the membrane material, accompanied by a certain amount of complex formation near the surface.

The behaviour of EDTA and NTA was quite different. The copper(II) concentrations indicated by the electrode were much larger than could be calculated on the basis of complexation equilibrium in the bulk solution. Another striking feature was the coincidence of the E—pH curves obtained in the presence of copper complex with an excess of ligand, and in the presence of ligand alone, suggesting that the response of the electrode depends only on the free ligand concentration in the solution.

Similar behaviour has been observed by Nakagawa et al. [15], who found that the stability constants for several ligands agreed very well with those given in the literature, except for EDTA and NTA. In these latter two cases, apparent coordination numbers of about 1/2 and 2/3 occurred for EDTA and NTA respectively, values which are highly improbable.

In the present study, it was found that the E—pH curves for solutions containing 10^{-3} M ligand could be fitted very well to the equation

TABLE 1

Logarithmic values of the stability constants [3, 20] used for the calculation of free copper concentrations

Complexing agent	β^{H}_{HL}	$\beta^{2H}_{H_2L}$	$\beta^{3H}_{H_3L}$	$\beta^{4H}_{H_4L}$	$\beta^{5H}_{H_5L}$	β^{L}_{CuL}	$\beta^{2L}_{CuL_2}$	β^{H}_{CuLH}	β^{OH}_{CuLOH}
Hydroxide	14.00						14.3		
EDTA	10.34	16.58	19.33	21.40		18.8		3.0	2.5
NTA	9.81	12.38	14.35			12.7	16.3		4.7
Trien	10.00	19.28	26.03	29.43		20.4		3.6	
Tetren	9.68	18.78	26.86	31.58	34.56	22.8			5.18
Glycine	9.70	12.20				8.1	15.1		
Citrate	5.68	10.03	12.90			5.9		3.20 (β_2 = 6.4)	9.66

$$E = E'' - S \log (1/\alpha^{n}_{L(H)})$$

where S = 29.7 mV/decade. For EDTA, E'' = −316 mV and n = 1/2; for NTA, E'' = −225 mV and n = 2/3. The small deviation of the potential to more negative values at high pH can be attributed to the influence of hydrolysis of copper(II) (see Fig. 2).

These conclusions were confirmed by the results of titrations of copper(II) with EDTA and Tetren (Fig. 4) as well as of these ligands with copper(II) (Fig. 5). From eqn. (1) it can be seen that after the equivalence point the concentration of free copper depends only on the ratio [L']/[CuL'] at a fixed pH. This ratio is a function of the titration parameter, f, only, and is independent of the initial concentration. Figure 4 shows that this behaviour was found for Tetren, but not for EDTA. A closer examination showed that the response again depended on the free EDTA concentration. In Figure 5 all curves should coincide at f = 0.5, where [L'] = [CuL']. This again happened for Tetren, but not for EDTA.

Finally, the influence of complexing agents was studied by means of calibration curves, E vs. log [L], in acetate buffer, pH 4.7. The results obtained for EDTA, Trien and Tetren are presented in Fig. 6. Solutions with the ligand alone and solutions containing the complex as well were compared. Again EDTA showed a different behaviour, not only because

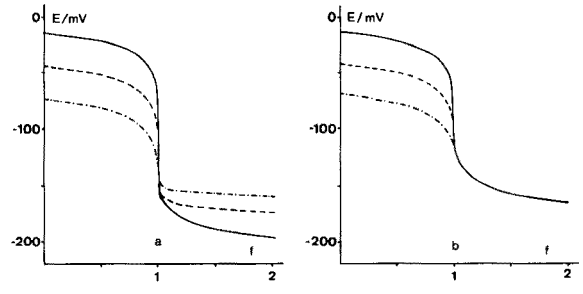

Fig. 4. Titration of copper(II) with EDTA (a) and Tetren (b) at copper concentrations of 10^{-3} M (——), 10^{-4} M (------) and 10^{-5} M (— · —) at pH 4.7.

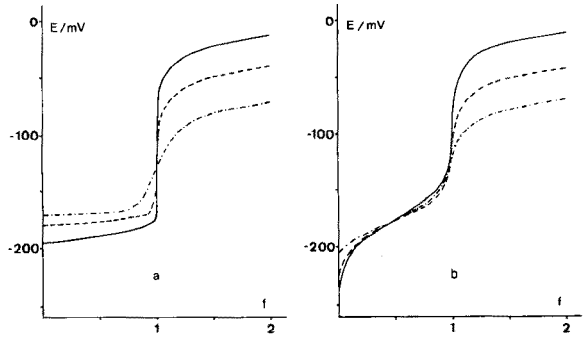

Fig. 5. Titration of EDTA (a) and Tetren (b) with copper(II) at ligand concentrations of 10^{-3} M (——), 10^{-4} M (-------) and 10^{-5} M (— · —) at pH 4.7.

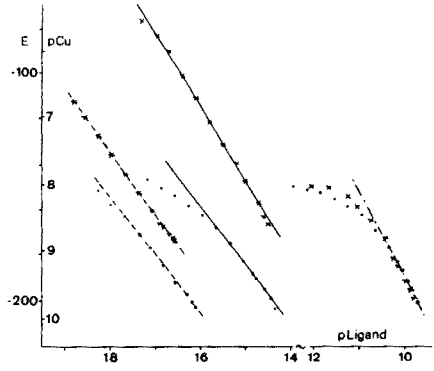

Fig. 6. Calibration curves of the response of the copper-i.s.e. vs. Trien (——), Tetren (-------) and EDTA (—·—) in the presence of 1×10^{-3} M copper—ligand complex (×) or without complex (•) at pH 4.7.

both curves coincided, which indicates that the response is governed only by the free ligand concentration and is unaffected by the concentration of the complex in the bulk solution, but also because of the very steep slope at high ligand concentrations (—40 mV/decade).

In the presence of 10^{-3} M complex, the responses were: $E = -640 - 32.9$ log [Trien] for Trien, and $E = -634 - 27.8$ log [Tetren] for Tetren. Combination of these equations with eqn. (6), taking [CuL] = 10^{-3} M, results in values of the logarithmic stability constants of about 20.3 and 22.2 respectively, which are in good agreement with the literature values (Table 1).

For Trien and Tetren the results of all experiments indicate that in the presence of the corresponding copper(II) complex and an excess of the ligand, the situation at the surface reflects exactly the situation in the bulk solution. In the case of EDTA and NTA, an increased concentration of copper(II) is observed; this can be attributed only to enhanced dissolution of the membrane material. If the concentration measured reflected the bulk concentration, the membrane would be completely dissolved in a short time. As this is not the case, evidently the observed concentration applies only to a small volume near the surface of the electrode, and some kind of steady state has to be adopted.

To account for the different behaviour of the polyamines on the one hand and the polyaminopolycarboxylic acids on the other, it is necessary to look for differences in their properties. Apart from the assumptions introduced by Hulanicki and Lewenstam [12] with respect to a possible difference in the stability of copper(I) complexes of EDTA and Tetren, no difference can be found other than the electrical charge of the species in the solution. In the case of polyamines like Trien and Tetren, the ligands themselves as well as their metal complexes are positively charged, while for polyaminopolycarboxylic acids like EDTA and NTA, both ligands and complexes are negatively charged in the pH-region under study.

Recently, Wu and Yang [23] tested the adsorption of metals ions on copper(II) sulfide precipitates and found strong adsorption of copper(II) ions on copper sulfide. If such an adsorption occurred at the membrane surface, the negatively charged polyaminopolycarboxylic acids or their metal complexes could reach the surface, whereas positively charged polyamines or their complexes would be repelled. A stronger attack and dissolution of the membrane surface would therefore be expected in the former case, in agreement with the results reported above.

Although it is believed that it is not merely by chance that the factor $\alpha_{L(H)}^{1/2}$ was found for EDTA and $\alpha_{L(H)}^{2/3}$ for NTA, these factors cannot be explained satisfactorily at the moment. Nevertheless, these results indicate that EDTA and NTA should not be used for the preparation of metal buffers [14, 19], but should be replaced by Trien or Tetren.

The authors express their gratitude to B. ter Laan for experimental help and to Prof. Dr. G. den Boef for his advice during the preparation of the manuscript.

REFERENCES

1 G. J. M. Heijne, W. E. van der Linden and G. den Boef, Anal. Chim. Acta, 89 (1977) 287.
2 G. J. M. Heijne and W. E. van der Linden, Anal. Chim. Acta, in press.
3 L. G. Sillén and A. E. Martell, Stability Constants, Spec. Publ. no. 17, The Chemical Society, London, 1964; Supplement no. 1, Special Publ. no. 25, 1971.
4 M. Sato, Electrochim. Acta, 11 (1966) 361.
5 M. Koebel, Anal. Chem., 46 (1974) 1559.
6 R. P. Buck and V. R. Shepard, Anal. Chem., 46 (1974) 2097.
7 H. J. Mathieu and H. Rickert, Z. Phys. Chem., N.F., 79 (1972) 315.
8 W. E. Morf, G. Kahr and W. Simon, Anal. Chem., 46 (1974) 1538.
9 R. P. Buck, Anal. Chem., 48 (1976) 23R.
10 D. J. Crombie, G. J. Moody and J. D. R. Thomas, Anal. Chim. Acta, 80 (1975) 1.
11 T. Hepel, M. Hepel and M. Leszko, Analyst, 102 (1977) 132.
12 A. Hulanicki and A. Lewenstam, Talanta, 23 (1976) 661.
13 J. W. Ross and M. S. Frant, Anal. Chem., 41 (1969) 1900.
14 E. H. Hansen, C. G. Lamm and J. Růžička, Anal. Chim. Acta, 59 (1972) 403.
15 G. Nakagawa, H. Wada and T. Hayakawa, Bull. Chem. Soc. Jpn., 48 (1975) 424.
16 A. Hulanicki, M. Trojanowicz and M. Cichy, Talanta, 23 (1976) 47.
17 V. K. Olson, J. D. Carr, R. D. Hargens and R. K. Forcé, Anal. Chem., 48 (1976) 1228.
18 M. F. El-Taras, E. Pungor and G. Nagy, Anal. Chim. Acta, 82 (1976) 285.
19 R. Blum and H. M. Fog, J. Electroanal. Chem., 34 (1972) 485.
20 A. Ringbom, Complexation in Analytical Chemistry, Interscience, New York, 1963.
21 J. Kielland, J. Am. Chem. Soc., 59 (1937) 1675.
22 M. Pourbaix, Atlas of Electrochemical Equilibria in Aqueous Solutions, Pergamon Press, Oxford, 1966, p. 384.
23 C. C. Wu and M. H. Yang, Anal. Chim. Acta, 84 (1976) 335.

Analytica Chimica Acta, 96 (1978) 23—29

CONTINUOUS MONITORING OF A HEAVY WATER PLANT EFFLUENT WITH A SULPHIDE-SELECTIVE ELECTRODE§

J. GULENS*

General Chemistry Branch, Atomic Energy of Canada Ltd., Chalk River Nuclear Laboratories, Chalk River, Ontario K0J 1J0 (Canada)

K. JESSOME and C. K. MACNEIL**

Port Hawkesbury Heavy Water Plant, Atomic Energy of Canada Ltd., Port Hawkesbury, Nova Scotia B0E 2V0 (Canada)

(Received 24th June 1977)

SUMMARY

A monitor, based on a sulphide ion-selective electrode, has been developed and applied to measure the total dissolved sulphide concentration (0.01—100 mg kg^{-1}) in heavy water plant effluents. The monitor is reliable and accurate, and has minimal maintenance and calibration requirements under continuous operation. The Orion 94-16A sulphide electrode gives Nernstian response to sulphide concentrations as low as ca. 0.01 mg kg^{-1} in strongly alkaline solutions in the presence of anti-oxidants, but its sensitivity decreases with use. One electrode failed to give Nernstian response to sulphide concentrations below 1 mg kg^{-1}.

Heavy water is used as a moderator and coolant in the Canadian nuclear power reactor CANDU (CANadian, Deuterium, Uranium). This heavy water is produced by the Girdler-Sulphide process, a bithermal isotopic exchange process between counter-current flows of water and hydrogen sulphide gas. Hydrogen sulphide is extremely toxic to man and the environment; because the process liquid effluent from the first enrichment stage is saturated with H_2S, it is passed through a steam stripper to remove the gas before the water is returned to the environment. A continuous monitor based on a sulphide-selective electrode was developed and tested at the Chalk River Nuclear Laboratories (CRNL) to measure the total dissolved sulphide content of the liquid effluent from the stripper [1]. The sample was adjusted to pH 14 with sodium hydroxide; under the conditions used, the sulphide concentration measured is directly related to the concentration of total dissolved sulphide [1, 2]. The monitor was installed at the Port Hawkesbury Heavy Water Plant, in the plant laboratory, where a sample of the stripper effluent

§ This paper was presented at the 1977 Pittsburgh Conference.

**Present address: New Brunswick Electric Power Commission, 527 King Street, Fredericton, New Brunswick E3B 4X1, Canada.

was piped to it, The monitor performed reliably and accurately at the plant over a four-month evaluation period, and this paper reports operating experience with it.

EXPERIMENTAL

Monitor

A schematic diagram of the monitor is shown in Fig. 1. The effluent was sampled at a constant rate by a peristaltic pump (Sage Model 371A), mixed with a constant amount of sodium hydroxide, and passed through a thermostatted mixing chamber into the Plexiglas cell containing the electrodes. The potential of the sulphide-selective electrode (Orion 94-16A) was measured by a digital voltmeter (Orion 801) relative to a saturated calomel reference electrode. The latter was thermostatted and separated from the sample solution by a 0.1 M KCl liquid bridge. The analog output voltage from the voltmeter was stored on a strip-chart recorder. To attain maximum precision on the recorder, the analog output was biased against a known and constant reference voltage (Fig. 2).

Except for the tubing used in the pump and for the Plexiglas cell, all components in the monitor were of stainless steel. The volume of the lines (1.6-mm diameter) from the sampling point to the exit of the cell was ca. 15 ml. The ratio of flow (sample: sodium hydroxide) was governed by the interior diameters of the pump tubing used and was normally 10:1 or 5:1. This ratio was checked frequently. The concentration of sodium hydroxide used in the monitor was changed with any change in the ratio of

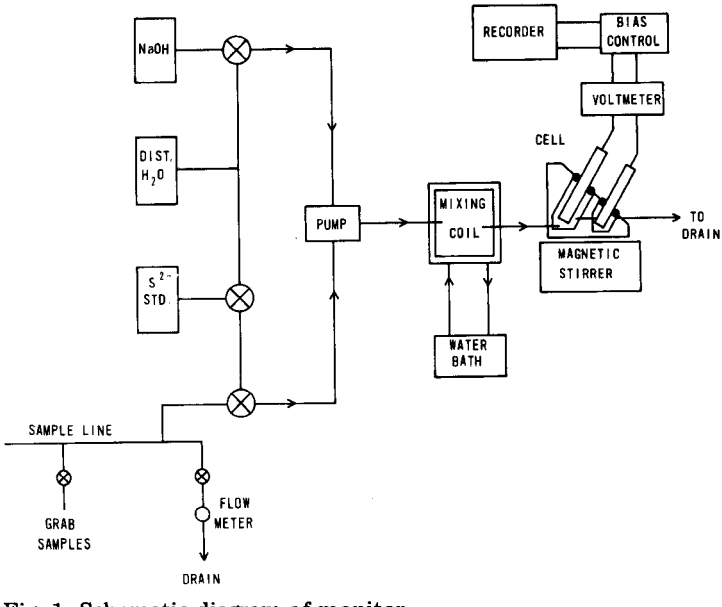

Fig. 1. Schematic diagram of monitor.

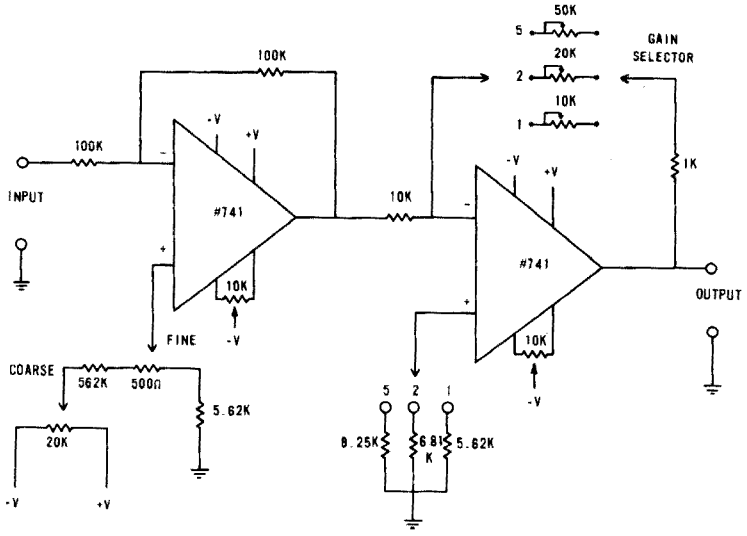

Fig. 2. Circuit diagram for bias control unit.

flow rates, so that the final concentration was ⩾1 M. Total flow through the monitor was ca. 25 ml min^{-1}, and with a 10:1 flow ratio, a 25-l container of 10 M sodium hydroxide—0.01 M ascorbic acid was consumed in 6 days.

Solutions

All solutions were prepared from reagent-grade chemicals and double-distilled water. A stock (1000 mg kg^{-1}) sulphide solution was prepared in 1 M sodium hydroxide—10% (v/v) hydrazine from $Na_2S \cdot 9H_2O$ crystals, and was standardized by potentiometric titration with a 0.1 M lead nitrate solution [3]. Dilute standard solutions in 1 M sodium hydroxide—0.1 M ascorbic acid were prepared daily from the concentrated stock solution and used in calibrating the monitor.

The calibration curve for the sulphide electrode was prepared by the standard addition procedure. To verify the accuracy of the monitor, the sulphide concentrations of certain samples were determined by wet analysis, either spectrophotometrically with methylene blue [4] or iodimetrically [5].

RESULTS

Calibration

Earlier work [1, 2] had shown that the electrode could be calibrated with Nernstian response to total dissolved sulphide levels as low as about 1×10^{-7} M (0.003 mg kg^{-1}), provided that the sodium hydroxide solution contained excess of reducing agent (ascorbic acid or hydrazine) to remove dissolved oxygen. The monitor was calibrated manually at the 1-mg kg^{-1} level, initially every other day, but later only once a week. The repeatability of the calibration, or electrode drift, was usually ±0.5 mV with only rare excursions

to ±2 mV, and this was determined from the digital display of the voltmeter. The drift of the bias control unit was less than 5% and was determined independently of the electrode drift by the position of the recorder pen after the voltmeter had been calibrated.

Response

The response time of the monitor, for 90% of the expected signal, was 75—90 s for a change in concentration of the sample at the inlet from 10^{-5} M to 10^{-6} M.

A full-scale recorder deflection could be set to correspond to any change in concentration desired, ranging from one to over four orders of magnitude, by selection of the appropriate bias control gain and recorder span values. The monitor was used most frequently to cover the range of 0.01—100 mg kg^{-1} for total dissolved sulphide. Performance of the monitor during a period of plant instability is presented in Fig. 3, which illustrates the rapid response of the monitor to both large and small changes in concentration, and the need for the monitor to be sensitive as well as having a wide range of response. These recorded variations in sulphide concentration correlate with known periods of plant instability.

Accuracy

Samples of steam condensate were collected in plastic bottles containing zinc acetate crystals for spectrophotometric determination, or containing sodium hydroxide pellets and ascorbic acid powder for the ion-selective electrode analysis, and then brought immediately to the laboratory for analysis. Table 1 compares the results obtained from the monitor with those obtained by wet analysis.

Interferences

Oxygen dissolved in the sodium hydroxide interfered, but this interference was removed by the addition of a reducing agent such as ascorbic acid.

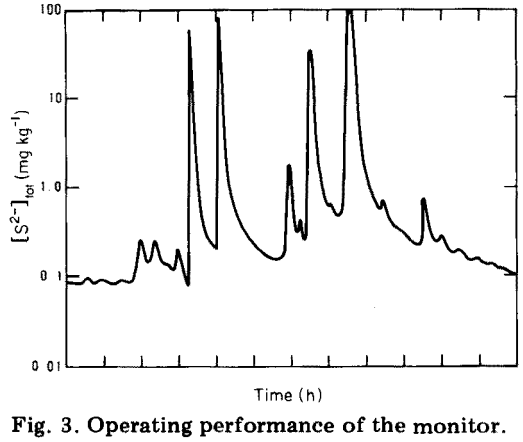

Fig. 3. Operating performance of the monitor.

TABLE 1

Analyzer results compared to wet analysis
(Results are given as S_7^{2-} mg kg^{-1})

Sample		Analyzer	Spectrophotometric	Titrimetric
Steam condensate	3/12/76	0.24	0.26	—
	4/13/76	0.004	<0.005	—
	5/12/76	0.004	<0.005	—
Stripper effluent		0.16	0.19	—
Diluted process samples	5/25/76	45	—	54
	5/26/76	1200	—	1330

Changing from a sodium hydroxide solution containing 0.01 M ascorbic acid to one without it caused the apparent sulphide concentration to decrease by ca. 30% at the 1-mg kg^{-1} level, while at sulphide levels below 0.1 mg kg^{-1}, the concentration would decrease by many orders of magnitude. Oil present in the effluent interfered with the quantitative, but not the qualitative, performance of the monitor. Gradual accumulation of oil on the electrode surface increased the response time and decreased the accuracy of the measurements by 20—30% at the 1-mg kg^{-1} sulphide level. Oil fouling was particularly noticeable after periods of plant instabilities, but the electrodes could be cleaned simply with tissue paper.

Maintenance

The monitor required only 2—3 man-hours per week for maintenance and calibration. Once a week, fresh sodium hydroxide—ascorbic acid solution was prepared, the monitor was flushed with detergent solution and rinsed with distilled water, and then calibrated. At the same time, the liquid levels were checked in the reference electrode, liquid-junction bridge and circulating water bath. The flow rates of sample and sodium hydroxide were measured every two weeks. Silicone-rubber tubing was used to pump the sample and was replaced once a month when the sample temperature was 303—313 K. During the winter months when the sample line to the laboratory was steam-heated, the temperature of the sample entering the monitor was ca. 343 K and the silicone tubing would last only a week before rupturing. Tygon tubing was used instead, and was replaced once a month. Tygon was the only tubing that could stand up to the concentrated sodium hydroxide solution.

Problems

Rupture of the pump tubing caused the largest problems. Rupture of the sample line constituted a potentially serious hazard for laboratory personnel as the sample could contain large amounts of dissolved hydrogen

sulphide (10^2—10^3 mg kg^{-1}) during plant upsets. Spilled concentrated sodium hydroxide from ruptured tubing corroded components of the monitor and also constituted a safety hazard. Metering pumps with Teflon bellows are being substituted for the peristaltic pumps in an attempt to alleviate these problems.

A sulphide electrode failed to respond in a Nernstian manner to concentrations below 1 mg kg^{-1}, even after polishing, after three weeks of continuous duty in the monitor and was replaced with a new sulphide electrode which performed satisfactorily for the remaining twelve weeks of the evaluation period. The failed electrode had been used previously in testing the monitor at CRNL for several months.

DISCUSSION

The performance of the monitor under continuous operation, in an admittedly ideal environment of the plant laboratory, was excellent. The monitor performed reliably and accurately, and required relatively little maintenance. The plant operators acquired sufficient confidence in the monitor that they considered interfacing it with the plant computer.

The ability to follow changes in the electrode potential both directly via the digital voltmeter and via the recorder tracings proved to be very valuable. Off-scale excursions of the recorder pen, corresponding to either high or low concentrations, could be readily verified by interpolating on the calibration curve the sulphide concentration that corresponded to the measured potential. In addition, the electrode drift could be determined independently of the drift of the bias control during calibration.

As presently constituted, the monitor is not suitable for field installation. The prime impediment to its use in the field is the need to adjust the sample to pH 14. This requires the use of pumps to add the sodium hydroxide and to control the flow ratio of sample to sodium hydroxide. The variable and unpredictable life-time of pump tubing under conditions of continuous operation, elevated sample temperatures (323—353 K) and corrosive chemicals (5—10 M sodium hydroxide) counsel against its use in a field instrument. High sample flow rates are used to give the required rapid response and result in a high consumption rate of sodium hydroxide. Storage of large volumes of sodium hydroxide in the field is not practical because of the need to remove dissolved oxygen, and to keep it from freezing during the winter. The need to thermostat both the electrodes (because of their large temperature coefficients) and the sample adds to the complexity of the monitor and further mitigates against its use in the field. Other approaches to sample conditioning are being investigated to overcome these problems and to find a reliable, maintenance-free system suitable for field use. A promising approach uses "passive addition" of reagent [6], wherein the accuracy of the monitor is not affected by changes in the flow rate, and the reagent diffuses through a barrier into the sample stream (pumps are then not required).

The limit of Nernstian response of the sulphide electrode is ca. 10^{-7} M total dissolved sulphide, provided that the solution contains excess of reducing agent to keep it free of dissolved oxygen. With increasing use, the electrodes have an increasingly negative deviation from the Nernstian slope at low concentrations, and their surfaces acquire a dull film or tarnish [1]. These surface films could be removed by polishing the electrodes on polishing strips (Orion Research 94-82-01), thereby restoring the sensitivity of the electrode to at least the 0.1-mg kg^{-1} level. The use of a one-point calibration at the 1-mg kg^{-1} level in the monitor therefore appeared reasonable.

The electrode in the monitor that did not give Nernstian response at the 1-mg kg^{-1} level was subsequently tested in the laboratory at CRNL. After extensive polishing with moist alumina on felt cloth, Nernstian response was again attained at the 1-mg kg^{-1} level, but at concentrations below 0.1 mg kg^{-1}, large deviations from Nernstian response were still observed. Other workers [7] have also noted such decreases in the sensitivity of the sulphide electrode and the beneficial effects of polishing the surface. Experiments investigating the nature and cause of this decreased sensitivity are underway. This loss of sensitivity of the electrode has serious implications for applications of this monitor to samples (steam condensate, cooling water and environmental samples) which contain low levels (0.005—0.1 mg kg^{-1}) of total dissolved sulphide.

REFERENCES

1 J. Gulens and B. Labbate, Atomic Energy of Canada Ltd., Report AECL-5542 (1976).
2 D. J. Crombie, G. J. Moody and J. D. R. Thomas, Anal. Chim. Acta, 80 (1975) 1.
3 Orion Research Incorporated Instruction Manual, Sulphide Electrode 94-16, (1974).
4 G. D. Patterson, in D. F. Boltz (Ed.), Colorimetric Determination of Nonmetals, Interscience-Wiley, New York, 1958, p. 261.
5 A. I. Vogel, Quantitative Inorganic Analysis, 3rd edn., Longmans, London, 1961, p. 370.
6 J. W. Ross Jr., Orion Research Incorporated, personal communication (1977). This approach is being used in the Orion Model 1500 Sodium Monitor, SLeD (Sodium Leak Detector).
7 F. C. Hill, Glace Bay Heavy Water Plant, Glace Bay, Nova Scotia, personal communication, 1976.

Analytica Chimica Acta, 96 (1978) 31—36

KINETIC DETERMINATION OF IODIDE AND OSMIUM(VIII) WITH A CHLORAMINE-T-SELECTIVE ELECTRODE

M. A. KOUPPARIS and T. P. HADJIIOANNOU*

Laboratory of Analytical Chemistry, University of Athens, Athens (Greece)

(Received 20th May 1977)

SUMMARY

A kinetic potentiometric method for the microdetermination of iodide and osmium based on their catalytic effect on the chloramine-T—arsenic(III) reaction is described. The reaction is monitored with a chloramine-T-selective electrode. The time required for the potential to change by a preselected amount is measured automatically and related directly to the iodide or osmium concentration. Trace amounts of iodide in the range 1.5—30 μg and of osmium in the range 10—150 μg can be determined with relative errors and standard deviations of about 1—2%.

Kinetic methods have received increased attention in recent years, particularly with regard to trace analysis. Ion-selective electrodes have been used as sensitive sensors in kinetic studies and analysis [1—9]. Recently, a new chloramine-T-selective membrane electrode has been described [10]; this electrode was applied to the determination of chloramine-T (CAT), ascorbic acid, and arsenic(III) by direct potentiometry or by potentiometric titration. The rapid response of the CAT-selective electrode to changes in chloramine-T concentration makes it a valuable sensor for following the rate of chloramine-T reactions. In this paper a kinetic potentiometric method is described for the microdetermination of iodide and osmium(VIII), based on their catalytic effect on the chloramine-T—arsenic(III) reaction, which is monitored with the chloramine-T-selective electrode. The time required for the consumption of a fixed amount of chloramine-T, and therefore for the potential to increase by a preselected amount (25.0 and 20.0 mV for iodide and osmium, respectively), is measured automatically with a solid-state "double switching" network and related directly to the iodide or osmium concentration. Commercial equipment and an auxiliary relay system are easily combined and provide automatic results shortly after the start of the reaction. Trace amounts of iodide in the range 1.5—30 μg and of osmium in the range 10—150 μg can be determined with relative errors and relative standard deviations of about 1—2%.

EXPERIMENTAL

Instrumentation

The electrodes, the reaction cell and the recording system were the same as previously reported [10]. The distance between the electrodes and their positions in the reaction cell were rigidly maintained during all measurements. The reaction cell was emptied by suction. All measurements were made under constant stirring with a magnetic stirring bar, at such a rate that no bubbles or vortex were formed, and in the absence of direct sunlight to avoid hydrolysis of chloramine-T. The measurement and control systems were the same as previously reported [5]. Times were measured with a digital Heath-Schlumberger Timer (SM-102 A). A block diagram of the system is shown in Fig. 1.

Reagents

All solutions were prepared with twice-distilled deionized water from reagent-grade materials.

Chloramine-T solutions. For a 0.100 M stock solution, dissolve 28.17 g of chloramine-T trihydrate (Merck) in water, dilute to 1 l and store in an amber bottle. This solution is stable for at least one month. Prepare more dilute solutions fresh daily by appropriate dilution.

Sodium arsenite solution, 0.100 M. Dissolve 13.00 g of $NaAsO_2$ in about 800 ml of water, adjust the pH to 7 with 5 M H_2SO_4 and dilute with water to 1 l.

Standard iodide solutions. For the stock solution (100 ppm of iodide) dissolve 0.1308 g of dried (P_2O_5) potassium iodide in water and dilute to exactly 1 l in a volumetric flask; store in an amber bottle in the refrigerator. Prepare working standards (0.2, 0.5, 1 and 2 ppm) from the stock solution by suitable dilution.

Standard osmium(VIII) solutions. For the stock solution (100.0 ppm) dissolve 0.1336 g of OsO_4 in 1 l of 0.05 M NaOH solution. Prepare working standards (0.5, 2.5, 5 and 10 ppm) from the stock solution by dilution with 0.01 M NaOH solution.

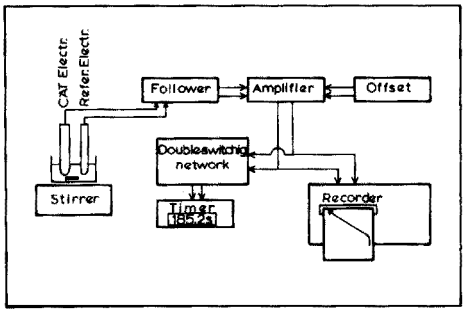

Fig. 1. Block diagram of the automatic measurement and control system.

Phosphate buffer, pH 6.0 and 7.0. Mix 10.0 ml of 3.0 M NaH_2PO_4 solution and about 80 ml of water, adjust with 2 M NaOH to pH 6.0 and 7.0, respectively, and dilute to 100 ml.

Procedure

Determination of iodide. Into the thermostated reaction cell kept at 25.0°C, pipet 5.00 ml of 0.0100 M chloramine-T solution, 2.00 ml of phosphate buffer pH 6.0 and 15.00 ml of iodide standard or sample solution. Start the stirrer, and after the potential has stabilized at a value E_0 (after about 20 s) adjust the recorder pen to one side (lower potential) of the chart. Adjust the potentiometers on the control system so that the time measurement starts at E_1 and stops at E_2 ($\Delta E = E_2 - E_1 = (E_0 + 30.0) - (E_0 + 5.0) = 25.0$ mV). Reset the Start button on the timer and inject 1.00 ml of 0.100 M sodium arsenite solution into the reaction cell with a 1.00-ml syringe. The analysis is completed automatically and the number on the timer (time in hundredths of a second) is recorded. Empty the cell with suction. Repeat the procedure for each analysis without changing the potential levels on the control system.

Determination of osmium. Proceed as for the determination of iodide, but use the buffer pH 7.0 and adjust the potentiometer on the control system so that the time measurement stops at $E_2' = E_0 + 25.0$ ($\Delta E = 20.0$ mV).

Calculations

Working curves are prepared to read ppm of iodide or osmium by plotting $1000/\Delta t$ values vs. iodide or osmium concentration of the standards.

RESULTS AND DISCUSSION

In any kinetic method, the choice of initial reactant concentrations is governed by the reaction rate, the experimental techniques and the sensitivity of the measurement system. The chloramine-T concentration chosen, 2.2×10^{-3} M, is a compromise to ensure small blanks and a linear potential change of at least 50 mV before approaching the lower limit of the linear response of the chloramine-T selective electrode.

Figure 2 shows the effect of arsenite concentration on the rate of the uncatalyzed reaction. The reaction rate and the blank increase with increasing arsenite concentration. The arsenite concentration chosen, 4.3×10^{-3} M, is a compromise to ensure small blanks and measurement times in the range 20—200 s. Recorded curves for the uncatalyzed and the iodide-catalyzed chloramine-T—arsenic(III) reaction at various pH levels are shown in Fig. 3. Similar curves for the osmium(VIII)-catalyzed chloramine-T—arsenic(III) reaction are shown in Fig. 4. It can be seen that the rate of both the uncatalyzed and the catalyzed reactions increases with decreasing pH. The potential of the chloramine-T-selective electrode is practically independent of pH in the range 5—8 [10]. ApH of 6.0 was chosen as optimum

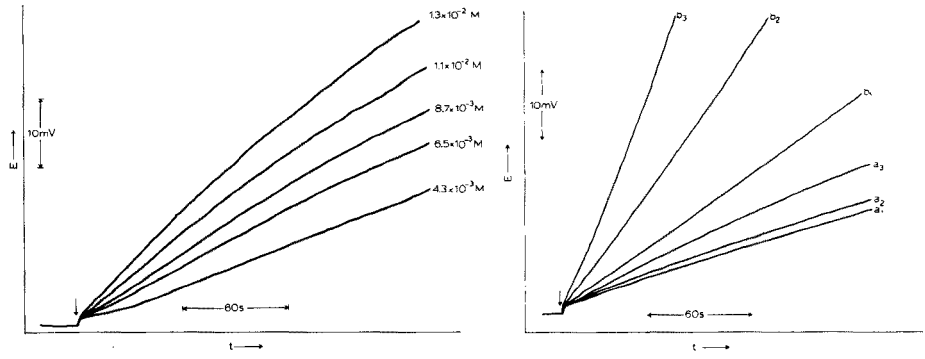

Fig. 2. Recorded curves of cell voltage vs. time for the uncatalyzed chloramine-T—arsenic(III) reaction at various arsenite concentrations. Other conditions as under Procedure.

Fig. 3. Recorded curves of cell voltage vs. time for the uncatalyzed (a) and the iodide-catalyzed (b) chloramine-T—As(III) reaction at various acidities. Iodide concentration, 1.00 ppm, pH: (1) 7.2; (2) 6.8; (3) 6.2. Other conditions as under Procedure.

for the iodide determination. For the osmium determination a pH of 7.0 was chosen because at pH 6.0 the measurement times are very short.

The voltage interval must be large enough that the measurement error is small in comparison. Voltage intervals of 25.0 and 20.0 mV were chosen for the iodide and osmium determination, respectively. Figure 5 shows typical recorded curves and the corresponding working curve for the iodide-catalyzed chloramine-T—arsenic(III) reaction. Similar curves are shown in Fig. 6 for osmium. After initiation of the reaction, a premeasurement time of a few

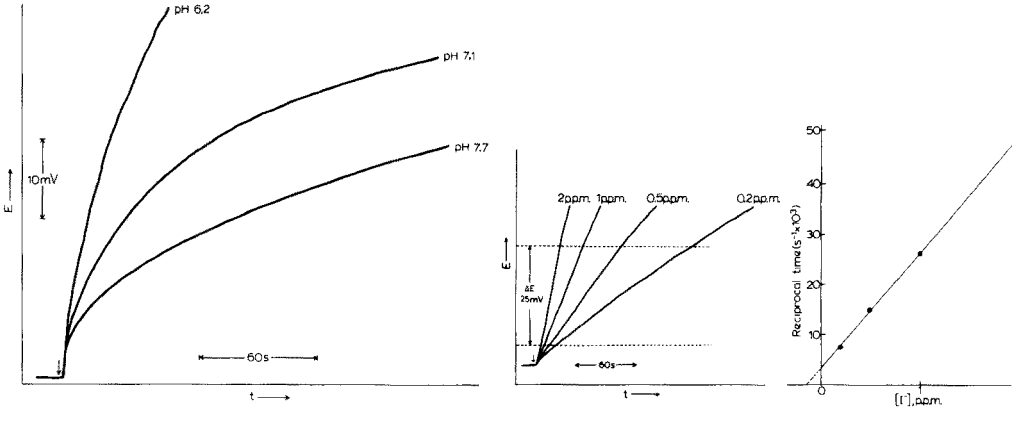

Fig. 4. Recorded curves of cell voltage vs. time for the osmium-catalyzed chloramine-T—As(III) reaction at various acidities. Osmium(VIII) concentration, 5.00 ppm. Other conditions as under Procedure.

Fig. 5. Recorded curves of cell voltage vs. time for the chloramine-T—arsenic(III) reaction in the presence of iodide, and the corresponding working curve. Other conditions as under Procedure.

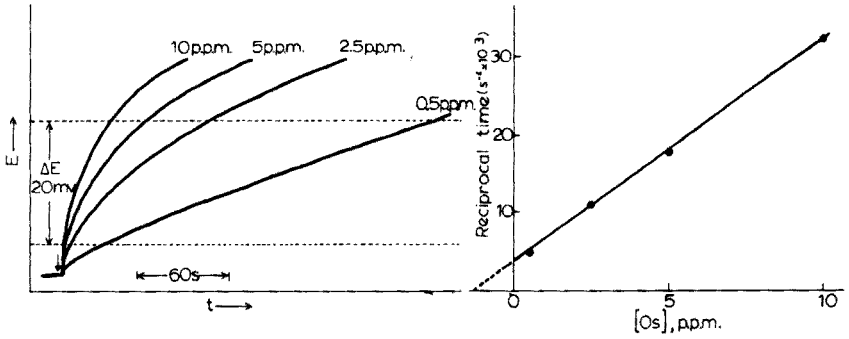

Fig. 6. Recorded curves of cell voltage vs. time for the chloramine-T—arsenic(III) reaction in the presence of osmium, and the corresponding working curve. Other conditions as under Procedure.

seconds is desirable to ensure thorough mixing of the reagents. The pre-measurement time is controlled by appropriate setting of the potentiometers on the control system. A premeasurement time corresponding to a 5.0 mV change was chosen.

Analysis of aqueous iodide and osmium solutions of known concentrations gave the results shown in Table 1. Amounts of iodide in the range 1.5—30 μg and of osmium in the range 10—150 μg can be determined with relative errors of about 1—2%. The relative standard deviation was 1.5% for a 0.5 ppm of iodide sample (n = 6) and 0.7% for a 5 ppm of osmium sample (n = 6).

TABLE 1

Results for aqueous iodide and osmium(VIII) solutions

Reciprocal time ($s^{-1} \times 10^3$)	Ion in 15-ml sample (μg)		Error (%)
	Taken	Found[a]	
Iodide			
5.32	1.50	1.56	+4.0
10.00	4.50	4.55	+1.1
19.3	10.5	10.5	—
30.7	18.0	17.8	−1.1
44.7	27.0	26.7	−1.1
		Av.	1.5
Osmium(VIII)			
5.82	11.2	11.7	+4.5
11.0	37.5	38.5	+2.7
17.7	75.0	73.3	−2.3
32.4	150	150	—
		Av.	2.4

[a]From the straight-line working curve; average of two values.

Any substance which reacts with chloramine-T or arsenic(III) at pH 6—7 would interfere and should be eliminated prior to the measurement. Several ions were tested for their effect on the chloramine-T—arsenic(III) reaction. The following ions had no effect at a concentration of 100 ppm: Co(II), Cr(III), Ru(III), Ir(III), Rh(III), Fe(III), Pt(IV), Au(III), Mn(II), and Ni(II). Bromide has no catalytic effect but the bromine formed interferes with the chloramine-T electrode response because of its action on the electrode membrane.

These kinetic methods developed for the microdetermination of iodide and osmium have no particular advantage in sensitivity in comparison with other methods, but they are superior in terms of low cost, indifference to optical problems and simplicity because of the ion-selective electrode. Furthermore, they demonstrate the possibilities of the CAT-selective electrode in kinetic analysis and studies.

The authors are grateful to C. E. Efstathiou for valuable assistance.

REFERENCES

1 G. A. Rechnitz, Analytical Studies on Ion-Selective Membrane Electrodes, in R. A. Durst, Ion-Selective Electrodes, Nat. Bur. Stand. (U.S.) Spec. Publ. No. 314, 1969, p. 330.
2 H. I. Thomson and G. A. Rechnitz, Anal. Chem., 44 (1972) 300.
3 K. Toth and E. Pungor, Anal. Chim. Acta, 64 (1973) 417.
4 T. P. Hadjiioannou, D. S. Papastathopoulos, M. I. Karayannis and A. K. Vassiloglou, Chim. Chron., New Series, 3 (1974) 13.
5 C. E. Efstathiou and T. P. Hadjiioannou, Anal. Chem., 47 (1975) 864.
6 C. E. Efstathiou and T. P. Hadjiioannou, Anal. Chim. Acta, 89 (1977) 55.
7 C. E. Efstathiou and T. P. Hadjiioannou, Anal. Chim. Acta, 89 (1977) 391.
8 C. E. Efstathiou and T. P. Hadjiioannou, Talanta, 24 (1977) 270.
9 D. S. Papastathopoulos and G. A. Rechnitz, Anal. Chem., 47 (1975) 1792.
10 M. A. Koupparis and T. P. Hadjiioannou, Anal. Chim. Acta, 94 (1977) 367.

Analytica Chimica Acta, 96 (1978) 37—43

A CARBON-ROD ATOMIZER FOR THE DETERMINATION OF CADMIUM AND LEAD IN PLANT MATERIALS AND SOIL EXTRACTS Part III. Simultaneous Determination of Cadmium by Atomic Fluorescence and Lead by Atomic Absorption Spectrometry

A. M. URE*, M. P. HERNANDEZ-ARTIGA** and M. C. MITCHELL

Department of Spectrochemistry, The Macaulay Institute for Soil Research, Craigiebuckler, Aberdeen AB9 2QJ (Gt. Britain)

(Received 1st August 1977)

SUMMARY

An apparatus and technique for the simultaneous determination of cadmium by atomic fluorescence and lead by atomic absorption spectrometry are described. A common dithizone—chloroform extraction procedure is used for the analysis of plant material and soil extracts with the carbon-rod atomizer. Detection limits in solution of 0.002 ppm for cadmium and 0.035 ppm for lead are obtained with a precision of ±2—6% and minimal interference effects.

The determination of cadmium by atomic absorption spectrometry with a carbon-rod atomizer and a solvent extraction procedure has been discussed in Part I of this series [1]. The apparatus has now been modified so that lead is determined by atomic absorption and cadmium, simultaneously, by non-dispersive atomic fluorescence. The method uses a single-pass solvent extraction procedure for the two elements and a carbon-rod atomizer whose rod-geometry has been modified for atomic fluorescence as described in Part II [2].

Various types of carbon and graphite electrothermal atomizers [3—10] have been employed for atomic fluorescence spectrometry and their use has been reviewed by several authors [11—17]. Those most commonly used have been variants of the carbon filament or carbon rod design [4, 6], similar to that used in Part I [1] for atomic absorption spectrometry. This consisted of a carbon-rod with a central sample-well, sited between two small regions of reduced rod-diameter. However, this type of atomizer, in common use for atomic absorption spectrometry, has been described as unsuitable for atomic fluorescence spectrometry [18] and an alternative design has been offered [8]. The rod-atomizer used in the present work provides superior precision for atomic fluorescence without impairing its performance for atomic absorption

**On leave from: Departamento de Quimica Analitica, Facultad de Ciencias, Universidad de Murcia, Murcia, Spain.

spectrometry. The determination of cadmium makes use of non-dispersive atomic fluorescence spectrometry with a solar-blind photomultiplier as first described by Larkins et al. [19, 20]. Although atomic fluorescence spectrometry with carbon or graphite electrothermal atomizers has been widely discussed and its potential assessed, applications to practical analysis have been few. These include the analysis of engine and other oils [21—23], water particulates [24], and biological materials [10, 25].

EXPERIMENTAL

Sample preparation

Solutions of plant material were prepared as described in Part I [1] by dissolving a weight of ash (450°C) equivalent to 1 g of oven-dried (80°C) plant material, in 10 ml of 0.06 M HCl.

Concentrated solutions were prepared from acetic acid extracts of soils and sewage sludges (20 g in 800 ml of 0.5 M acetic acid) in a final volume of 10—50 ml of 0.06 M HCl as described in Part I [1].

Simultaneous solvent extraction procedure for cadmium and lead

A 5-ml aliquot of these dilute hydrochloric acid solutions, buffered with 4 ml of purified ammonium citrate solution (400 g l^{-1}) is extracted twice with 2 ml of 0.2% (w/v) dithizone in chloroform at pH 9 and the organic phases are bulked for analysis. This extraction procedure, detailed in Part I [1], is quantitative up to about 0.5 ppm for cadmium and 3 ppm for lead. To reduce the lead blank to an acceptable level, it was found necessary to purify the ammonium citrate solution by solvent extraction with dithizone in chloroform [26].

Standard solutions

A series of mixed cadmium and lead standard solutions, with concentrations appropriate to the analysis and within the concentration range 0.002—0.5 ppm for cadmium and 0.05—10 ppm lead, are made in 0.06 M HCl from 1000-ppm stock solutions prepared from ignited cadmium oxide or AnalaR cadmium sulphate and AnalaR lead nitrate.

Calibration curves of fluorescence intensity versus concentration for cadmium are linear up to 0.3 ppm with slight curvature from 0.3 to 0.5 ppm. For lead, the calibration of absorbance versus concentration becomes non-linear above about 2 ppm when the 217.0-nm resonance line is used. A linear calibration curve is obtained up to about 3 ppm when the less sensitive 283.3-nm line is used. Curvature above this concentration is mainly due to the decreasing effectiveness of the extraction procedure, but useful analysis can be made for lead up to about 10 ppm at the 283.3-nm line.

Apparatus

The apparatus shown in Fig. 1 was designed and constructed in the laboratory.

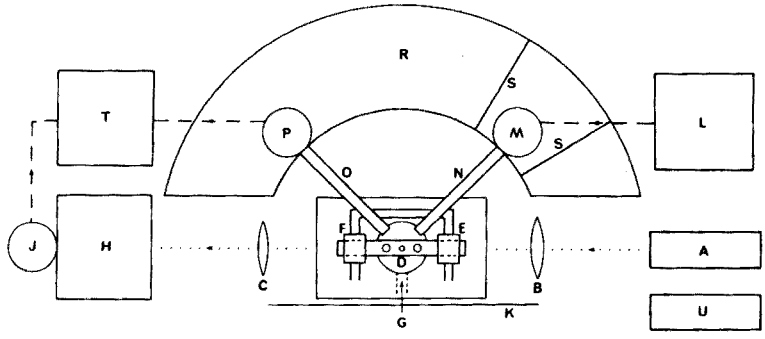

Fig. 1. Schematic diagram of the apparatus showing cadmium hollow-cathode lamp (A), lenses (B, C), carbon rod (D), in water-cooled terminal blocks (E, F) argon sheath supply (G), monochromator (H), photomultiplier (J), hinged door (K), power supply (L), for cadmium discharge lamp (M), solar blind photomultiplier (P), light guides (N, O), chamber (R), light baffles (S), twin-pen recorder (T), and alternative hydrogen lamp (U).

The atomic absorption portion [1] is converted for lead analysis by replacing the cadmium hollow-cathode lamp at A, Fig. 1. This portion consists of the hollow-cathode lamp A, lenses B and C, carbon rod D (Morganite, Grade SG-905-J carbon) mounted in water-cooled stainless steel terminal blocks E and F, laminar argon gas sheath supply G, monochromator H (Rank-Hilger D292), and hinged door K, to prevent ambient light reaching the photomultiplier J (1P28). The irradiating source, M, for the atomic fluorescence section is a Philips Spectrum Discharge Lamp for cadmium (type 93162E.E27) supplied from a variable-transformer-controlled 240-V, 50-Hz mains-operated power unit L, and mounted, together with the solar blind photomultiplier P (Hammamatsu R166), in an aluminium chamber R, containing light baffles S, to prevent light from the source M, leaking into the photomultiplier housing. The graph of lamp voltage versus fluorescence intensity has an approximately gaussian form [27] with a region between about 110 and 140 V where the intensity changes little with voltage. Use is made of this to stabilize the fluorescence intensity against supply voltage changes by operating the lamp at about 120 V from a variable transformer itself supplied from a constant voltage transformer. Light from the source M illuminates a small region of about 2 mm in diameter at a height of about 3 mm above the sample-well through a 5-cm long u.v.-transmitting light guide N (Schott, Mainz, W. Germany). This is mounted in an aluminium tube that can be moved to position the incident light beam. A similar light guide, O, is used to collect and direct the emitted fluorescence onto the solar blind photomultiplier cathode. The outputs of the two photomultipliers, J and P, develop voltages in their appropriate load resistors (30 K) which in turn supply a two-pen recorder T. A hydrogen lamp, U, is mounted as an alternative source to the hollow-cathode lamp to monitor background effects but is not required in practice.

Accurate initial positioning of the carbon-rod is essential to ensure that

the irradiating light beam and the collector of the emitted fluorescence are aligned on the atomic vapour column above the sample well. Further, since the rod may move slightly during a long series of analyses as a result of differential friction at the two terminal blocks and the expansion and contraction of the rod, its position should be checked periodically. To achieve this, a circular spot of light of the same diameter as the sample-well is projected from an optical system (not shown in Fig. 1) mounted above the rod and sharply focussed at the bottom of the well. Misalignment of the rod can thus easily be detected and corrected.

Operation

After the rod has been cleaned by preheating until no absorption or fluorescence signal is observed, a 5-μl aliquot of the dithizone-in-chloroform extract is pipetted into the sample-well of the rod as described in Part I [1]. After drying by heating for 1 min at 6 A, and ashing for 2 min at 16 A, the cadmium and lead are atomized at a current of 90 A. The procedure differs from that used for cadmium [1] by the change from ashing for 1 min at 10 A to 2 min at 16 A. After cooling, a replicate atomization of each sample is made to ensure that occasional pipetting errors are detected.

Interference effects

As was found by atomic absorption [1], no interference effects were obtained for cadmium by atomic fluorescence nor for lead by atomic absorption, from 5000 ppm calcium, 1500 ppm potassium, 1600 ppm magnesium, 1000 ppm phosphorus, 500 ppm aluminium, chromium, manganese or sodium, or 100 ppm zinc in the aqueous solution before extraction. Depressive interference was found from 100 ppm copper on cadmium (25%) and lead (40%) and from 500 ppm iron on lead (50%) but not on cadmium. At a concentration of 100 ppm, iron did not affect the lead atomic absorption signal.

RESULTS AND DISCUSSION

The precisions of the determination of cadmium by atomic fluorescence and of cadmium and lead by atomic absorption are shown in Table 1.

The theoretical detection limit (DL) for lead by atomic absorption spectrometry (a.a.s.), defined by DL = blank + 3τ, where τ is the standard deviation of a small signal near the blank level, is limited principally by the typical reagent blank (0.03 ppm) to about 0.035 ppm.

The smallest concentration of cadmium determinable by atomic fluorescence spectrometry (a.f.s.) is not restricted by the reagent blank level but by the inability of the simple detection system to reject the light emitted from the hot rod. The detection limit of 0.0002 ppm is not, therefore, achieved and in practice the lowest measurable concentration is about 0.002 ppm.

TABLE 1

Precision of atomic fluorescence (a.f.s.) determination of cadmium and atomic absorption (a.a.s.) determination of cadmium and lead

Cd solution concentration (ppm)	R.s.d. (%)		Pb solution concentration (ppm)	R.s.d. (%)
	A.a.s.	A.f.s.		A.a.s.
0.01	—	5.6	0.1	3.6
0.05	3.3	4.2	1.0	1.6
0.1	3.2	2.4	—	—

TABLE 2

Simultaneous comparative analyses of solutions of ashed plant material for cadmium by a.a.s. and by a.f.s.

Sample	Solution content (ppm) A.a.s.	Solution content (ppm) A.f.s.	Deviation (ppm) (A.f.s.—A.a.s.)	Mean deviation (ppm)
1	0.018	0.020	+0.002	+0.003
2	0.023	0.026	+0.003	
3	0.026	0.029	+0.003	
4	0.068	0.070	+0.002	
5	0.080	0.086	+0.006	

By replacing the lead hollow-cathode lamp with a cadmium lamp, a comparison (Table 2) of the cadmium contents of solutions of different plant ashes by the present a.f.s. method can be made simultaneously with those obtained by the a.a.s. method already validated [1]. This shows that, apart from a small positive bias of about 0.003 on average, the accuracy of the a.f.s. method is good.

The accuracy of the method for the determination of lead is indicated (Table 3) by the agreement with results obtained by a quantitative (±10%) d.c. arc optical emission spectrometric method after a concentration procedure [28] and with the U.S. National Bureau of Standards certificated value for the Orchard Leaf Standard Reference Material 1571. The values for cadmium content, determined by a.f.s. at the same time, are also shown in Table 3. The cadmium content of 0.17 ppm for N.B.S. Orchard Leaf SRM 1571 is significantly higher than the certificate value 0.11 ± 0.016 but is in close agreement with the value of 0.16 obtained by the a.a.s. method described in Part I [1].

The method is further validated by the results presented in Tables 4 and 5, for the acetic acid-extractable contents of cadmium and lead in some soils obtained by this method together with contents of cadmium by atomic absorption flame spectrometry.

TABLE 3

Comparison of plant contents (ppm oven-dry) of lead by the present a.a.s. method with those by a d.c.-arc optical emission spectrometric method (Emiss.) [28] and with certificated content of N.B.S. Orchard Leaf SRM 1571. The cadmium content was determined simultaneously by a.f.s.

Sample	Lead content		Cadmium content A.f.s.
	A.a.s.	Emiss.	
Mixed herbage	1.1	1.0	0.12
Barley straw	2.3	1.8	0.12
Potato shaws	4.7	4.4	0.81
Pine needles	6.0	6.5	0.24
SRM 1571	42	45 ± 3[a]	0.17

[a]Certificated content.

TABLE 4

Acetic acid-extractable cadmium and lead contents of soils expressed as ppm in dry soil, obtained by the present method and by a flame a.a.s. method

Soil No.	Cadmium (Present method)	Cadmium (A.a.s.)	Lead (Present method)
1	0.09	0.08	0.59
2	0.06	0.05	0.40
3	0.11	0.09	0.24
4	0.21	0.20	0.86
5	0.14	0.15	0.50

TABLE 5

Acetic acid-extractable cadmium and lead contents of soils treated with sewage sludges expressed as ppm dry soil, obtained by the present method and by a flame a.a.s. method

Sewage sludge	Cadmium (Present method)	Cadmium (A.a.s.)	Lead (Present method)
1	0.58	0.53	3.1
2	1.2	1.30	4.3
3	1.3	1.46	3.9
4	0.39	0.29	1.4
5	0.30	0.29	1.8
6	0.19	0.19	1.3
7	0.37	0.33	2.3
8	0.49	0.54	2.5
9	1.0	1.13	3.1
10	0.60	0.69	3.8

The method has been in routine use for several months and is proving of considerable value for the analysis of agricultural materials for these two elements, particularly in view of the current interest in toxic environmental pollutants.

We gratefully acknowledge the award of a grant from the Spanish Ministry of Education and Science to one of us (M.P.H.A.) during the course of this work.

REFERENCES

1 A. M. Ure and M. C. Mitchell, Anal. Chim. Acta, 87 (1976) 283. (Part I).
2 A. M. Ure and M. P. Hernandez-Artiga, Anal. Chim. Acta, 94 (1977) 195. (Part II).
3 H. Massmann, Spectrochim. Acta, Part B, 23 (1968) 215.
4 T. S. West and X. K. Williams, Anal. Chim. Acta, 45 (1969) 27.
5 T. S. West, J. Pure Appl. Chem., 25 (1971) 47.
6 J. F. Alder and T. S. West, Anal. Chim. Acta, 51 (1970) 365.
7 J. D. Winefordner, in R. M. Dagnall and G. F. Kirkbright (Eds.) Atomic Absorption Spectroscopy, Plenary Lectures Int. At. Abs. Spectroscopy Conf., Sheffield, 1969, Butterworths, 1970, p. 35.
8 M. D. Amos, P. A. Bennet, K. G. Brodie, P. W. Y. Lung and J. P. Matoušek, Anal. Chem., 43 (1971) 211.
9 A. Montaser, S. R. Goode and S. R. Crouche, Anal. Chem., 46 (1974) 597.
10 B. R. Bartschmid, Flameless non-dispersive atomic fluorescence spectrometry, University of Houston, Ph.D. Thesis, 1974.
11 G. F. Kirkbright and T. S. West, Chem. Br., 8 (1972) 428.
12 G. F. Kirkbright, Analyst (London), 96 (1971) 609.
13 T. S. West and M. S. Cresser, Appl. Spectrosc. Rev., 7 (1973) 79.
14 R. F. Browner, Analyst (London), 99 (1974) 617.
15 T. S. West, Proc. Anal. Div. Chem. Soc., 13 (1976) 266.
16 A. Montaser and S. R. Crouch, Anal. Chem., 46 (1974) 1817.
17 H. Massmann, Proc. Anal. Div. Chem. Soc., 13 (1976) 258.
18 M. D. Amos, Am. Lab., August (1970) 33.
19 P. L. Larkins, R. M. Lowe, J. V. Sullivan and A. Walsh, Spectrochim. Acta, Part B, 24 (1969) 187.
20 P. L. Larkins, Spectrochim. Acta, Part B, 26 (1971) 477.
21 B. M. Patel and J. D. Winefordner, Anal. Chim. Acta, 64 (1973) 135.
22 B. M. Patel, R. D. Reeves, R. F. Browner, C. J. Molnar and J. D. Winefordner, Appl. Spectrosc., 27 (1973) 171.
23 I. D. Guzeev, E. S. Blinova, I. A. Mairow and V. V. Nedler, Ind. Lab., 39 (1973) 165.
24 Yu. I. Belyaev and V. N. Oreshkin, Okeanologiya, 14 (1974) 917.
25 S. A. Clyburn, G. R. Serio, B. R. Bartschmid, J. E. Evans and C. Veillon, Anal. Biochem., 63 (1975) 231.
26 F. W. Church, J. Ind. Hyg. Toxicol., 29 (1971) 34.
27 P. A. Bennett, Resonance Lines, 1 (1969) 1.
28 R. L. Mitchell and R. O. Scott, J. Soc. Chem. Ind., 66 (1947) 330.

Analytica Chimica Acta, 96 (1978) 45—54

ATOMIC ABSORPTION INHIBITION RELEASE TITRATION AS A METHOD OF STUDYING RELEASING AND INHIBITING EFFECTS
Studies of the Mechanism of Formation of Calcium Phosphate Compounds

D. STOJANOVIĆ[§], J. BRADSHAW and J. D. WINEFORDNER*
Department of Chemistry, University of Florida, Gainesville, FL 32611 (U.S.A.)
(Received 6th July 1977)

SUMMARY

The results of releasing and inhibiting studies by means of a new, semi-automatic technique termed atomic absorption inhibiting release titration (a.a.i.r.t.) are reported. This method is based on the releasing or inhibition effect (enhancement or depression, respectively) of an atomic absorption signal by a given chemical component; namely, the releasing element is titrated by a solution of magnesium chloride and phosphoric acid while the magnesium signal is monitored by atomic absorption flame spectrometry. This method was employed for the continuous observation and explanation of processes occurring during evaporation/vaporization. On the basis of the mole ratios obtained at characteristic points on the titration curves, a possible mechanism of tricalcium phosphate formation is presented. It was established that this compound was formed through a chain of intermediate compounds of the $xCaO \cdot yP_2O_5$ type.

Studies on interferences and ways of eliminating or minimizing them successfully are important in both atomic emission and atomic absorption flame spectrometry. However, efforts have been directed mainly towards obtaining analytically reliable results, especially when one element is determined in the presence of an interfering one. Some authors have studied the mechanisms of interferences resulting from the inhibition caused by several anions [1—3] (chemical inhibition interference). Very few data are available on the mechanism of eliminating or minimizing this type of interference by the application of releasing agents [4, 5], because of the lack of sensitive and simple methods for such investigations. Obviously, releasing and inhibiting effects are similar in that they both involve the processes of thermostable compounds.

A mechanism explaining the releasing effect is based on shifts in the chemical processes involved during droplet evaporation/vaporization. There is no conclusive evidence about the stage of the life of the droplet during which compound formation actually occurs. Thus, the releasing element forms less stable compounds with the interfering element, and

§ Present address: Institute for the Application of Nuclear Energy in Agriculture, Veterinary Medicine and Forestry ZEMUN, Baranjska 15, P.O. Box 46, Yugoslavia.

during evaporation/vaporization of the spray droplets, these compounds form preferentially leaving the required element unbound [6].

Although this mechanism has been generally accepted, there are still no methods by which the dynamic processes in vaporizing particles can be followed. The introduction of such methods would help to decide whether the dynamic processes occur only within evaporating droplets, or occur within and between the particles formed after solvent evaporation. The work described below was designed to elucidate partially the problems of both releasing and inhibiting effects; calcium phosphate compounds and the mechanism of their formation were examined. A new titration method, based on releasing and inhibition effects, was utilized. For continuous monitoring of changes in the titrated solution, and of the processes occurring in the flame after aspiration of this solution, the atomic absorption of magnesium was measured.

The principle of this method, termed atomic absorption inhibition release titration [7] (a.a.i.r.t.), is as follows: solutions of a releasing element (in this case, $CaCl_2$ solution) are titrated with a stock solution of magnesium chloride and phosphoric acid, with simultaneous aspiration of the titrand into the flame. The changes in the magnesium atomic absorption signal are recorded. This method has been employed for the determination of rare earths [8] and some other elements [9]. The technique is similar to that applied by Huber et al. [10—12] in their work on atomic absorption inhibition titrations (a.a.i.t.). A.a.i.t. utilizes the inhibition of magnesium atomic absorption by various anions whereas in a.a.i.r.t., inhibition is preceded by the releasing effect; thus the name of this technique accords with the order of events during the titration.

The a.a.i.t. method was developed as a result of studies of inhibition by anions forming refractory compounds: a definite volume of solution of anion inhibitor (X) is titrated by the metal cation stock solution (M) while the atomic absorption signal for the metal is monitored. During evaporation vaporization of the titrand droplets, thermostable compound(s) of metal and cation (MX) are formed. Initially, the absorption signal is very small and remains small until the total amount of anion has reacted with the metal: $X + M \rightarrow MX$. Further addition of titrant causes a rapid increase in the metal absorption, allowing the end-point to be determined.

In 1957, Gaydon [13] pointed out that interference effects in flame photometry were sometimes caused by alteration in chemical reaction rates and equilibria. Dinin [5] later supplied evidence that chemical equilibria in aqueous solutions play a large part in inhibiting and releasing effects.

The series of events in the a.a.i.r.t. method is as follows. If the solution of the releasing element, E, is titrated with a standard solution containing metal, M, and anion inhibitor, X, and the titrand is aspirated into a flame, then the releasing element will form a stable compound with the anion during the vaporization of the particle, leaving the metal unbound. This reaction can be generally represented by

$$E + (M + X) \leftrightarrows EX + M \qquad (1)$$

If the atomic absorption of the metal, M, is measured during the titration, the absorption will increase until the total amount of releasing element has reacted stoichiometrically with the anion. On further addition of the titrant, the atomic absorption of metal M decreases, which is considered the titration end-point. Obviously, at the end-point of titration, the inhibition effect ($X + M \rightarrow MX$) is again present. However, reaction (1) cannot be applied directly to the reaction products because it may proceed by a series of steps.

It is impossible to predict all the ways in which reaction (1) can be established and shifted. However, it is certain that several characteristics, e.g., shape of the titration curve, sharpness of the change at the end-point, number of characteristic points on the titration curve, etc., depend on the metal-to-anion concentration ratio in the titrant, on the concentration of releasing element, and on the flame conditions (temperature, composition, etc.).

EXPERIMENTAL

Instrumentation and solutions

A Unicam SP90 atomic absorption spectrometer and a Sargent-Welsh Model SRG recorder were used. A hydrogen—air flame was used with a single-slot premix laminar burner (0.45 × 100 mm); the normal SP90 acetylene-gas burner top (0.3 × 100 mm) was replaced by the new top because of the increased hydrogen flow rate (over 5 l min^{-1}) and the concomitant loss of hydrogen through the drainage opening.

Compressed air was used as the oxidant; the flow rate was controlled by the UNICAM regulator built into the apparatus. The hydrogen flow rate was controlled by a Beckman regulator. For all measurements, the monochromator slit width was fixed at 80 μm and the burner height at 1 cm above the burner top. Solutions were introduced into the nebulizer-burner by means of a tygon capillary tube connected to the nebulizer and passing through a peristaltic pump (from a Technicon AutoAnalyzer).

Unicam magnesium (285.2 nm) and calcium (422.7 nm) hollow-cathode lamps were operated at 4 mA and 10 mA, respectively.

A standard calcium(II) solution was prepared by dissolving $CaCO_3$ (reagent grade) in a minimal volume of HCl and diluting to volume with water. A magnesium(II) solution was prepared from $MgCl_2 \cdot 6H_2O$ (reagent grade) and standardized complexiметrically. Phosphate solutions were obtained by dilution of a stock 0.1 M H_3PO_4 solution (reagent grade). Standard solutions of $MgCl_2$ and H_3PO_4 were prepared by mixing exact volumes of solutions of known concentration. Distilled water was used for dilutions.

Procedure

An aliquot of standard calcium(II) solution was pipetted into a 100-ml beaker and diluted to 50 ml with water. The recorder was set to zero absorption while water was aspirated. The tygon capillary was then placed in

the solution; simultaneously, the titrant was added by activating the peristaltic pump, and the absorption of magnesium was followed. The titration was usually continued after the end-point, until the absorption reached a constant value. The rate of titrant delivery could be varied (1—3 ml min^{-1}). However, care was taken to ensure that the titrant delivery rate was approximately equal to the normal pneumatic nebulization rate.

RESULTS AND DISCUSSION

To determine the shapes of the titration curves, calcium chloride solutions were titrated with a standard magnesium chloride solution containing various phosphate concentrations. Titration curves have the same shape (Fig. 1) whether the phosphate concentration in the titrant is 350 or 450 ppm. However, when the phosphate concentration in the titrant is 200 ppm, the shape of the titration curve is altered (Fig. 2).

Phosphate-to-calcium mole ratios (Table 1) at the characteristic points (a, b, ...) on the titration curves (Fig. 1) indicate that up to point *d* calcium reacts with phosphate in an approximately constant ratio, regardless of the varying phosphate concentration in the titrant. However, phosphate-to-calcium mole ratios at point *e* on the curves differ when the phosphate concentration is changed. It can therefore be concluded that the reaction between calcium and phosphate is complete at point *d*, and that up to point *e*,

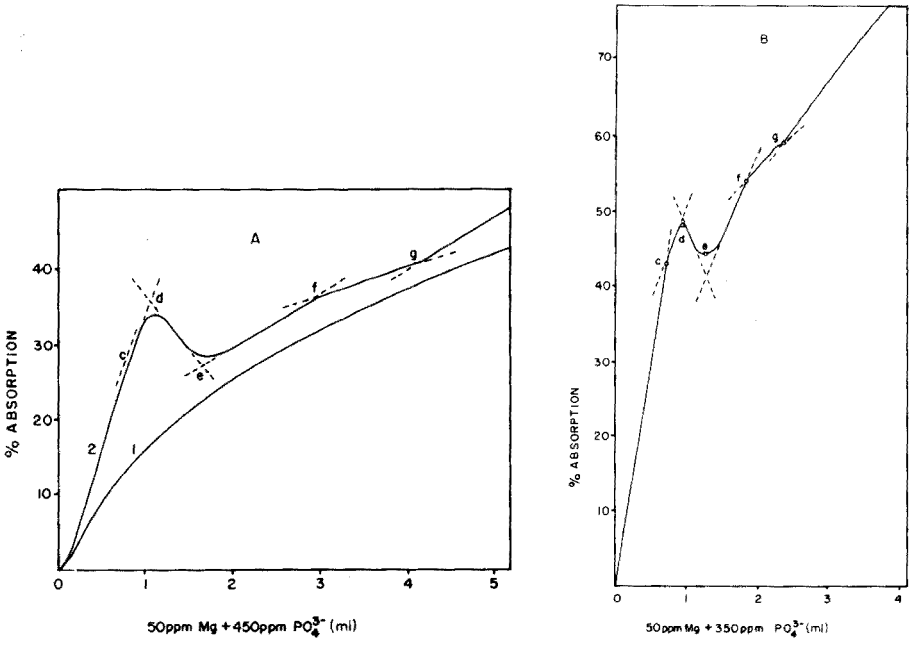

Fig. 1. A. Titration of 50 ml of water (1) and 6-ppm calcium solution (2). B. Titration of 4-ppm calcium solution. Air flow rate, 3.5 l min^{-1}. Hydrogen flow rate, 9.3 l min^{-1}.

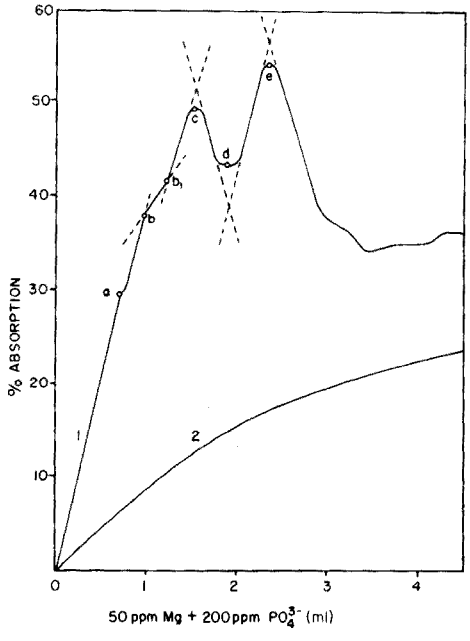

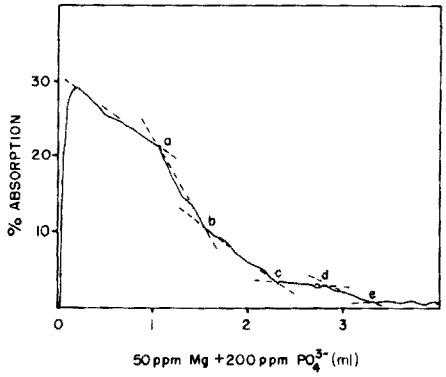

Fig. 2. Titration of 50 ml of water (2) and 4-ppm calcium solution. Flow rates as in Fig. 1.

Fig. 3. Titration of 8-ppm calcium with monitoring of the calcium signal. Flow rates as in Fig. 1.

TABLE 1

Phosphate-to-calcium mole ratios at the successive characteristic points on the titration curves with titrants containing 50 ppm Mg and 450 or 350 ppm phosphate

Ca (ppm)	450 ppm PO_4^{3-}			350 ppm PO_4^{3-}		
	Ratios at points			Ratios at points		
	c	*d*	*e*	*c*	*d*	*e*
4	0.50	0.67	1.04	0.53	0.68	0.93
6	0.48	0.67	1.03	0.53	0.67	0.89
8	0.49	0.67	1.02	0.50	0.66	0.91
Mean values	0.49	0.67	1.03	0.52	0.67	0.91

a compound is formed between magnesium and phosphate. The decrease in absorption after point *d* can be explained in the same way. Further details about the compounds between magnesium and phosphate at point *e*, as well as at some other characteristic points on the curves will be reported elsewhere.

The phosphate-to-calcium mole ratio at point *d* suggests the formation of thermally stable tricalcium phosphate. This finding is in accordance with the

results of Fukushima [2] and Popham and Schrenk [14], but not with those of Yofé and Finkelstein [4]. On the basis of the mean values of PO_4^{3-}/Ca^{2+} ratios at points *c* and *d*, the reactions occurring in the vaporizing droplets are probably: at point *c* ($PO_4^{3-}/Ca^{2+} \approx 0.51$)

$$4CaCl_2 + 2H_3PO_4 + H_2O \rightarrow 4CaO \cdot P_2O_5 + 8HCl \quad (2)$$

and at point *d* ($PO_4^{3-}/Ca^{2+} \approx 0.67$)

$$3CaCl_2 + 2H_3PO_4 \rightarrow 3CaO \cdot P_2O_5 + 6HCl \quad (3)$$

Tricalcium phosphate is probably formed via a tetracalcium phosphate intermediate.

The shapes of the titration curves (Fig. 1) indicate that magnesium absorption increases in the region from 0 to point *c*. Table 2 shows that in the region from 0 to point *c*, the Mg^{2+}/Ca^{2+} atomic ratios are essentially constant if the Mg^{2+}/PO_4^{3-} ratio in the titrant is constant. Because the magnesium absorption increases up to point *d* in Fig. 1, vaporization of the solute particles most likely results in MgO. Therefore, during the a.a.i.r. titration of $CaCl_2$ with $MgCl_2$—H_3PO_4 solution, the reaction products are mixed oxides with variable magnesium content. Consideration of reactions (2) and (3), as well as the Mg^{2+}/Ca^{2+} ratios, suggests that the formula of the mixed oxide is $4CaO \cdot P_2O_5 \cdot MgO$ at point *c* on the titration curves and $3CaO \cdot P_2O_5 \cdot MgO$ at point *d* (see Table2).

However, if the titrant contains 50 ppm of magnesium chloride and 200 ppm of phosphoric acid, then a double peaked curve results (Fig. 2). From the phosphate/calcium mole ratios (Table 3) and the results in Fig. 2, it is evident that the magnesium absorption increases up to point *c* where $PO_4^{3-}/Ca^{2+} \approx 0.51$. As in the previous case, it can be assumed that the magnesium absorption increases up to point *c* because of the reaction of Ca^{2+} with PO_4^{3-}, while Mg^{2+} remains largely unbound as MgO.

TABLE 2

Magnesium-to-calcium atomic ratios (Mg/Ca) at the successive characteristic points on the titration curves with titrants containing 50 ppm Mg and 450 or 350 ppm phosphate

Ca (ppm)	450 ppm PO_4^{3-}			350 ppm PO_4^{3-}		
	Ratios at points			Ratios at points		
	c	*d*	*e*	*c*	*d*	*e*
4	0.22	0.30	0.45	0.27	0.33	0.52
6	0.21	0.29	0.44	0.26	0.37	0.48
8	0.21	0.29	0.44	0.27	0.35	0.50
Mean values	0.21[a]	0.29[b]	0.44	0.27[a]	0.35[b]	0.50

[a]Possible formula of the mixed oxide is $4CaO \cdot P_2O_5 \cdot MgO$.
[b]Possible formula of the mixed oxide is $3CaO \cdot P_2O_5 \cdot MgO$.

TABLE 3

Phosphate-to-calcium mole ratios at the successive characteristic points on the titration curves for a titrant containing 50 ppm Mg and 200 ppm PO_4^{3-}

Ca (ppm)	*a*	*b*	b_1	*c*	*d*	*e*	*d* (corrected) = $e - (d - c)$[b]
2	0.25	0.35[a]	0.39	0.55[a]	0.71[a]	0.85	0.69
3	0.25	0.34	0.39	0.52	0.67	0.84	0.69
4	0.26	0.30	0.35[a]	0.50	0.63	0.77	0.64
5	0.25	0.31	0.40	0.51	0.63	0.77	0.65
Mean values	0.25	0.32	0.39	0.51	0.64	0.81	0.67

[a]These values are not taken into account.
[b]See text.

It is possible that after an equilibrium is established leading to the formation of tetracalcium phosphate (point *c* on the curve), magnesium absorption decreases owing to the formation of a thermostable compound between magnesium and phosphate (point *d*). If this assumption is correct, the increase in magnesium absorption between points *d* and *e* could be explained by the repeated effect of calcium as a releasing agent. However, because the ratio of Ca^{2+}/PO_4^{3-}at point *d* is very close to the stochiometric ratio corresponding to the formation of tricalcium phosphate, an alternative explanation is needed: during the formation of tricalcium phosphate, the formation of a thermostable compound between tricalcium phosphate and magnesium oxide may take place. To verify this, calcium chloride solutions were titrated with the magnesium chloride—phosphoric acid solution (50 ppm Mg + 200 ppm PO_4^{3-}) by measuring changes in the calcium atomic

TABLE 4

Phosphate-to-calcium mole ratios at successive characteristic points on the titration curve for a titrant containing 50 ppm Mg and 200 ppm PO_4^{3-} when the calcium signal is monitored

Ca (ppm)	*a*	*b*	*c*	*d*	*e*	*e* (corrected) = $e - (d - c)$[a]
8	0.25	0.33	0.51	0.63	0.76	0.64
10	0.24	0.35	0.51	0.64	0.74	0.61
12	0.23	0.34	0.50	0.64	0.73	0.59
Mean values	0.24	0.34	0.51	0.64	0.74	0.61[b]

[a]See text.
[b]Corrected mole ratio mean values at point *e* in this Table are lower than the corresponding values in Table 3. This can be explained by the higher consumption of titrant for achieving the titration end-point. In this titration, the phosphate concentration is somewhat lower and that of calcium higher than in the titration represented by Table 4. Undoubtedly, this is why a portion of $CaCl_2$ is lost during aspiration before the end-point is reached.

absorption (see Fig. 3). The phosphate-to-calcium mole ratios at characteristic points are given in Table 4. The calcium absorption decreases until a PO_4^{3-}/Ca^{2+} ratio of about 0.50 is obtained; it then remains constant at PO_4^{3-}/Ca^{2+} ratios of 0.50 to 0.64, and finally decreases further until a PO_4^{3-}/Ca^{2+} ratio of about 0.74 is obtained. The constant absorption of calcium for ratios of 0.50—0.64 suggests that the decrease in absorption after point *c* on the curve (Fig. 2) is caused by magnesium reactions with phosphate.

It can be concluded that the reaction between calcium and phosphate is complete at point *e*. If it is assumed that the amount of phosphate between points *c* and *d* is consumed in the reaction with magnesium, then subtraction of this amount of phosphate (*d* − *c*) from the total moles of phosphate at point *e* gives the moles of phosphate which reacted with calcium. This value is presented in Tables 3 and 4 as *e* corrected.

Means and standard deviations of the PO_4^{3-}/Ca^{2+} mole ratios are given in Table 5. On the basis of the mean mole ratios at the characteristic points,

TABLE 5

Reproducibility of measurements from the results of 5 titrations with a 50 ppm Mg 200 ppm PO_4^{3-} solution

Point on curve	Titration of 4 ppm Ca			Titration of 8 ppm Ca[a]		
	Mean mole ratios PO_4/Ca	*s*	s_r (%)	Mean mole ratios PO_4/Ca	*s*	s_r (%)
a	0.256	0.005	1.95	0.242	0.008	3.30
b	0.326	0.013	3.98	0.340	0.016	4.70
b_1	0.380	0.020	5.26	-	—	—
c	0.514	0.016	3.11	0.512	0.017	3.32
d	0.650	0.019	2.92	—	—	—
e	—	—	—	0.744	0.024	3.23

[a]With monitoring of the calcium signal.

TABLE 6

Possible mechanism of formation of calcium phosphate compounds

Point at the curve	Mole ratio[a] PO_4/Ca	Reaction in evaporation of droplets		Product
a	0.25	$8CaCl_2 + 2H_3PO_4 + 5H_2O$	→	$8CaO \cdot P_2O_5 + 16\ HCl$
b	0.33	$6CaCl_2 + 2H_3PO_4 + 3H_2O$	→	$6CaO \cdot P_2O_5 + 12HCl$
b_1[b]	0.39	$5CaCl_2 + 2H_3PO_4 + 2H_2O$	→	$5CaO \cdot P_2O_5 + 10HCl$
c	0.51	$4CaCl_2 + 2H_3PO_4 + H_2O$	→	$4CaO \cdot P_2O_5 + 8HCl$
$e_{corrected}$	0.64	$3CaCl_2 + 2H_3PO_4$	→	$3CaO \cdot P_2O_5 + 6HCl$

[a]Mean values of the ratios given in Tables 3 and 4 are given here.
[b]Differentiation of particles with such a ratio in the case of a.a.i.r. titration of calcium chloride on the curve, shown in Fig. 3, is a result of the high sensitivity of the a.a.s. method for magnesium. This ratio cannot be differentiated in Fig. 3.

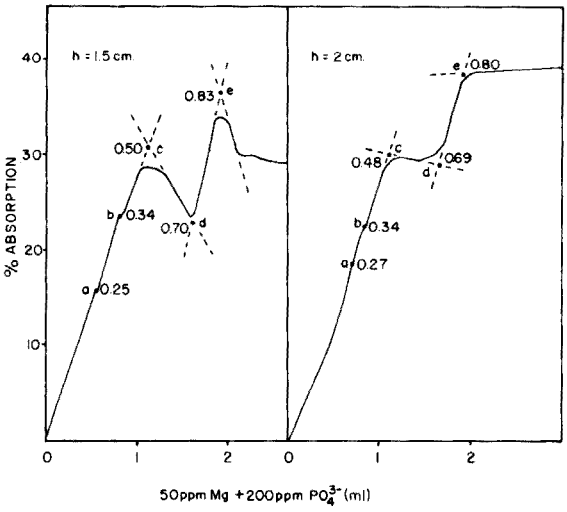

Fig. 4. Titration of 4-ppm calcium with measurements at different heights above the burner top. Flow rates as in Fig. 1.

chemical equations can be formulated which represent the reactions taking place during the vaporization of the solute particles. These equations (Table 6) represent the most probable mechanism leading ultimately to the formation of tricalcium phosphate.

The compounds listed in Table 6 may be taken as the products formed from tricalcium phosphate and various molar quantities of calcium oxide. The existence of particles with such mole ratios at various heights in an air/hydrogen flame above the burner top was shown by performing the a.a.i.r. titration at two heights (Fig. 4). The PO_4^{3-}/Ca^{2+} mole ratios thus obtained (values on curves) agree reasonably with the mean values given in Table 3.

One of the authors (D. S.) thanks the International Atomic Energy Agency for the opportunity of working at the University of Florida. This work was supported by AF-AFOSR-F44620-76-C-0005.

REFERENCES

1 C. Th. J. Alkemade and M. H. Voorhuis, Z. Anal. Chem., 163 (1958) 91.
2 S. Fukushima, Microchim. Acta, 4 (1959) 596.
3 W. T. Elwell and J. A. F. Gidley, Atomic Absorption Spectrophotometry, 2nd edn., Pergamon Press, London, 1966.
4 Y. Yofé and R. Finkelstein, Anal. Chim. Acta, 19 (1958) 166.
5 J. I. Dinin, Anal. Chem., 32 (1960) 11, 1475.
6 Y. Yofé, R. Avni and M. Stiller, Anal. Chim. Acta, 28 (1963) 331.
7 D. Stojanović, V. Vajgand and M. Djurdjević, Abstracts 6th Yugoslav Conference on General and Applied Spectroscopy, Bled, October 1976, No. AA2.
8 V. Vajgand and D. Stojanović, Chem. Anal. (Warsaw), 20 (1975) 973.

9 V. Vajgand, D. Stojanović and M. Djurdjević, Bull. Soc. Chim. (Beograd), 39 (1974) 61
10 R. V. Looyenga and C. O. Huber, Anal. Chem., 43 (1971) 498; Anal. Chim. Acta, 55 (1971) 179.
11 W. E. Crawford, C. Y. Lin and C. O. Huber, Anal. Chim. Acta, 64 (1973) 387.
12 C. I. Lin and C. O. Huber, Anal. Chem., 44 (1972) 13, 2200.
13 A. G. Gaydon, The Spectroscopy of Flames, Wiley, New York, 1957, p. 323.
14 E. R. Popham and W. C. Schrenk, Developments in Applied Spectroscopy, Vol. 7A P. 189, E. L. Grove and Alfred J. Perkins (Eds.), Plenum Press, New York, 1969.

Analytica Chimica Acta, 96 (1978) 55—62

INTERFERENCE EFFECTS IN A CAPILLARY ARC EXCITATION SOURCE FOR EMISSION SPECTROMETRY

M. KUBOTA

National Chemical Laboratory for Industry, 1-chome, Honmachi, Shibuya-ku, Tokyo (Japan)

(Received 14th June 1977)

SUMMARY

The effects of major constituents (K, Zn, and phosphate) on the emission intensities of eighteen selected analytes in a d.c. capillary arc plasma provided with a nebulizer—desolvation apparatus, are reported. Potassium and zinc enhance the emission from most of the analytes, especially that from the elements of medium ionization potential. Cesium added in excess as a buffer reduces the cation interferences to negligible proportions. The presence of phosphate results in a marked decrease in the excitation temperature of the plasma. Depression effects of phosphate, observed for all the analytes tested but Mg, Se, and La, are probably due to the reduced temperature.

Many workers have used d.c. arc plasmas as excitation sources for emission spectrometric analysis. The plasmas are of either the current-carrying type or the current-free type. The capillary arc plasma, which was developed for exciting a fine aerosol produced from solid metal samples [1], is a small, wall-stabilized arc of the former type. Gray [2] used the plasma as an ion source for mass-spectrometric analysis of solutions. The capability of the plasma as an emission spectrometric excitation source for solution analysis has been demonstrated by Denton et al. [3], who introduced solutions into the plasma with a tantalum-filament atomizer. A modified capillary arc excitation source has been combined with a nebulizer—desolvation system to permit continuous sample introduction [4]. The excitation source operated with argon flow rates of less than 2 l min^{-1} and could be used with the same ease as chemical combustion flames. The capillary arc analytical technique is competitive in sensitivity with spectrometric methods based on chemical flames or current-free arcs such as plasma jets.

This paper reports interference effects of major constituents (matrices) on the emission intensities of analytes observed in the capillary arc spectrometric analysis of solutions.

EXPERIMENTAL

Apparatus and procedure

The sample desolvation device, capillary arc source unit, and non-integrating photoelectric read-out system have been described previously [4]. The apparatus and operating conditions are listed in Table 1. Argon was used as a nebulizing and plasma-forming gas. A separate stream of argon was introduced around the cathode to reduce electrode consumption. No additive gas was used in the present study.

Analytes and spectral lines

The analytes were chosen so as to include elements of low, medium, and high ionization potential, and refractory elements that tend to form stable oxides in the plasma. The spectral lines selected are the most sensitive for each element, being free from spectral interferences. The analytes and analytical lines are listed in Table 2.

Both the atom and ion lines for calcium, iron, cadmium, and tungsten were used for investigating interferences whose extent depends on the type of spectral line.

Reagents

Pure aqueous solutions containing the analytes separately were prepared from 1 or 2 mg ml^{-1} stock solutions. The analyte concentrations used (Table 3) are approximately 20—200 times the concentrations of the detection limits estimated by preliminary experiments.

TABLE 1

Experimental apparatus and operating conditions

Capillary arc excitation source	
Spray gas	Argon at 1.15 l min^{-1}
Cathode gas	Argon at 0.10 l min^{-1}
Excitation	6.0 A at 35 V d.c.
Spectrometer system	
Spectrometer	JEOL 1.25-m Czerny-Turner mount, model 125B
Grating	Concave, 1200 lines mm^{-1}, blazed for 300 nm
Dispersion	0.62 nm mm^{-1} in the first order
Slit widths	7-μm entrance; 50-μm exit
Detector system	
Photomultiplier	Hamamatsu TV R453
High volt. power supply	Power Designs Inc., model 2K20
Dynode supply volt.	750 V d.c.
Amplifier	Takeda Riken d.c. picoammeter
Recorder	Hitachi strip chart recorder, model 056

TABLE 2

Analytes, spectral lines, excitation potentials (V_{ex}), ionization potentials (V_i), and dissociation energies of monoxides (E_d)

Group	Analyte	Line (nm)	V_{ex} (eV)[a]	V_i (eV)[a]	E_d (eV)[b]
Low ionization potential element	Cs	I 455.53	2.72	3.893	—
	Rb	I 421.55	2.94	4.176	—
Medium ionization potential element	Ba	II 455.40	2.72	5.210	5.75
	Al	I 396.15	3.14	5.984	4.6
	Ga	I 417.20	3.07	6.00	3.0
	Ca	I 422.67	2.93	6.111	4.3
		II 393.36	3.15		
	Sn	I 270.65	4.78	7.342	5.40
	Ni	I 341.47	3.65	7.633	$\leqslant$4.2
	Mg	II 279.55	4.43	7.644	4.1
	Fe	I 371.99	3.33	7.87	4.3
		II 259.94	4.77		
High ionization potential element	Sb	I 259.80	5.82	8.639	4
	Cd	I 228.80	5.41	8.991	$<$3.8
		II 226.50	5.47		
	Te	I 214.27	5.78	9.01	3.9
	Se	I 203.98	6.32	9.75	4.3
Stable monoxide forming element	La	II 408.67	3.03	5.61	8.2
	V	I 437.92	3.13	6.74	6.4
	Zr	II 339.19	3.82	6.84	7.8
	W	I 400.87	3.45	7.98	6.8
		II 239.70	5.56		

[a]Taken from ref. 5. [b]Taken from ref. 6.

TABLE 3

Analyte concentrations in solutions

Analyte	Concentration ($\mu g\ ml^{-1}$)
Ca, Mg	1
Ba, Al, Ga, Sn, Ni, Fe, Cd, V, Zr	10
Sb, Te, La, W	100
Cs, Rb, Se	500

Potassium chloride, zinc chloride, and ammonium dihydrogen-phosphate were selected as representatives of major constituents with a cation of low and high ionization potential, and an anion (phosphate), respectively. It is common practice to add an easily ionized element in excess to diminish ionization interferences [7—9]. Cesium (as CsCl), which has a lower

ionization potential (3.893 eV) than potassium (4.339 eV), was used as a spectroscopic buffer. Reagent-grade chemicals were dissolved in dilute hydrochloric acid to obtain potassium, zinc, phosphate, and cesium concomitant solutions. An appropriate series of test solutions was prepared from the stock and the concomitant solutions. All solutions, acidified to 0.1 M with hydrochloric acid, were stored in polyethylene containers.

Measurements

The relative emission intensity of a spectral line, I, is represented by $I = s_{l+b} - s_b$ where s_{l+b} is the gross line signal defined as the signal obtained at the line wavelength and s_b is the background signal. These signals were obtained as means of ten repeated recordings for each solution.

The term "interference effect" refers to a change in the relative intensity produced by a cation or anion present as a "matrix" ion in a test solution. The size of the interference effect, X is expressed as $X = (I_m - I_0)/I_0$, where I_m and I_0 are the relative intensities observed when the test solution with an analyte and matrix and the pure aqueous solution with the analyte are nebulized, respectively.

Excitation temperatures were measured to ascertain effects of major constituents on the physical characteristics of the plasma. The excitation temperature was calculated from the observed relative intensities of two iron lines Fe (I)273.55 nm and Fe (I)273.73 nm. Transition probabilities and statistical weights were taken from the American Institute of Physics Handbook [10].

RESULTS AND DISCUSSION

Interference effects of major constituents

Potassium chloride solutions have often been used to obtain lower detection limits in stabilized arc and plasma jet emission spectrometry [7, 8, 11, 12]. The lower detection limits reported seem to result from an increase in line emission as well as a decrease in background emission caused by the addition of potassium. The effects of potassium on the emission intensities of the selected analytical lines are presented in Fig. 1. Obviously, potassium enhanced the emission intensities of all the analytes tested except zirconium and tungsten. The enhancement effect was most significant for the elements of medium ionization potential. The values X for the ion lines of calcium, iron, cadmium, and tungsten were smaller than those for the atom lines of the respective elements. Presumably this is due to potassium suppressing the ionization of these species in the plasma.

Figure 1 also shows the interference caused by zinc, which has a high ionization potential (9.391 eV). Enhancement, which was smaller than that caused by potassium, was observed for the analytes of medium and high ionization potential (excluding antimony), while depression was found for the analytes of low ionization potential and oxide-forming elements except for lanthanum.

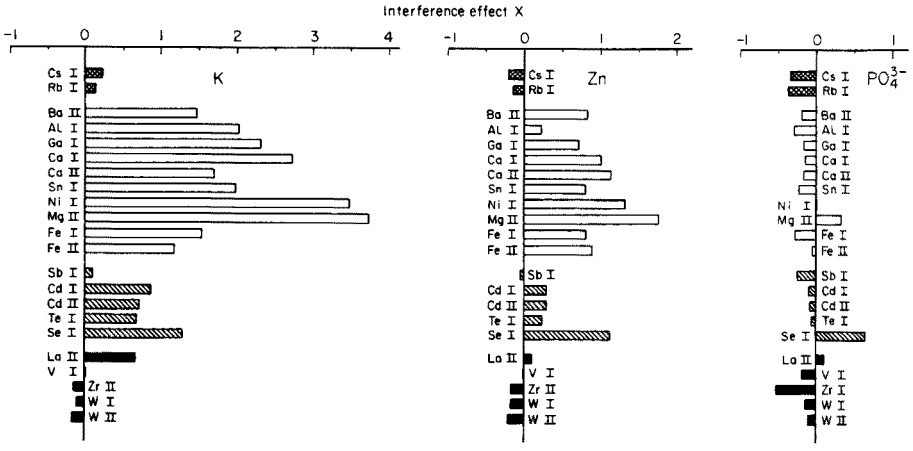

Fig. 1. Effects of potassium (2 mg ml^{-1}; 0.0512 mol KCl), zinc (2 mg ml^{-1}; 0.0301 mol $ZnCl_2$) and phosphate (2 mg ml^{-1}; 0.0211 mol PO_4) on the emission intensities of the analytical lines.

The depressing effect of phosphate on the emission of calcium has been reported by various workers [8, 11—13]. The interference from phosphate on the emission intensities of the 18 elements is shown in Fig. 1. It can be seen that phosphate depressed the emission intensities of most of the analytes examined as well as the intensity of calcium. Depression was most significant for the zirconium line. No obvious correlation was observed between the extent of the interference effect and the classified elements.

Excitation temperatures

Measurements of the excitation temperature were made for an aqueous iron solution (1 mg ml^{-1}), and for test solutions containing 1 mg Fe ml^{-1} and potassium, zinc, or phosphate (2 mg ml^{-1}) The results are listed in Table 4. Potassium or zinc decreased the excitation temperature slightly. Therefore, the enhancements shown in Fig. 1 appear to be associated with a change in the efficiency of introducing the sample aerosol into the plasma. Marinković and Vickers [14] stated that the large thermal gradient at the edge of a stabilized d.c. arc without potassium chloride tends to prevent the aerosol from entering the higher temperature regions of the arc. The enhancement of the emission intensities of the iron lines by potassium or zinc may be due to

TABLE 4

Excitation temperatures of the plasma (1 mg Fe ml^{-1} was present in all cases)

Concomitant	—	K	Zn	PO_4^{3-}
Temperature (K)	4830	4720	4740	4330

improved atomization of the sample aerosol introduced efficiently into the hot regions of the capillary arc.

The presence of phosphate resulted in a drastic decrease (ca. 500 K) in the excitation temperature. It seems likely that the depressing effect of phosphate on the emission intensities of many elements as well as iron, can be ascribed to the lower temperature causing reduced efficiencies of both atomization and excitation of the analytes.

Buffering effects of cesium

The emission intensity of the Fe (II)259.94 nm line and the background intensity measured as a function of cesium concentration are shown in Fig. 2. The measurements were made with test solutions containing iron (10 μg ml^{-1}) and cesium at varying concentrations. In the range exceeding 0.05 mol of cesium chloride (6.645 mg Cs ml^{-1}), the line intensity remained nearly constant, whereas the background intensity decreased with increasing cesium concentration.

The effects of cesium chloride (0.05 mol) on the interferences from potassium, zinc, and phosphate were investigated. Aluminium, cadmium, and zirconium were taken as analytes representing medium- and high-ionization potential metals and refractory metals, respectively. The buffering effect of cesium on the interference caused by potassium on the emission intensities

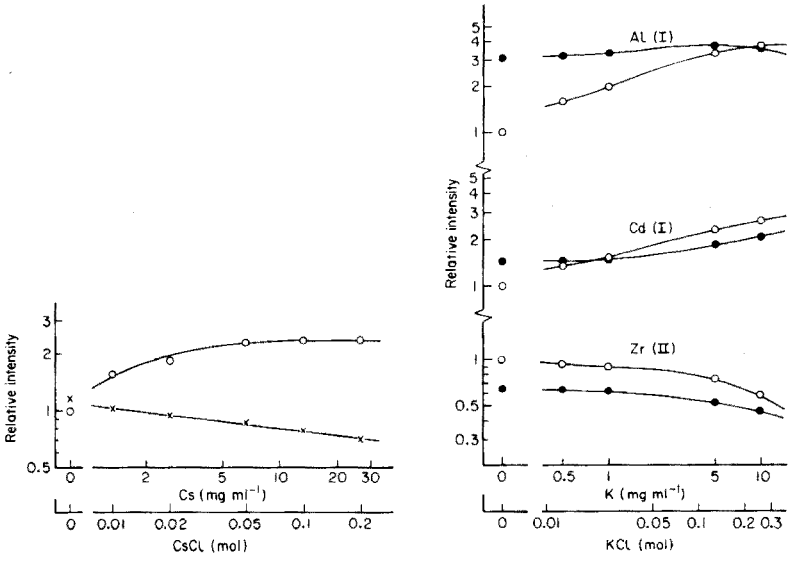

Fig. 2. Changes in the iron line and background intensities with cesium concentration. (○) FeII 259.94 nm line. (×) Background at 259.94 nm.

Fig. 3. Buffer effect of cesium on the intensity changes of Al, Cd, and Zr lines with potassium concentration. (○) Without CsCl. (●) With 0.05 mol CsCl.

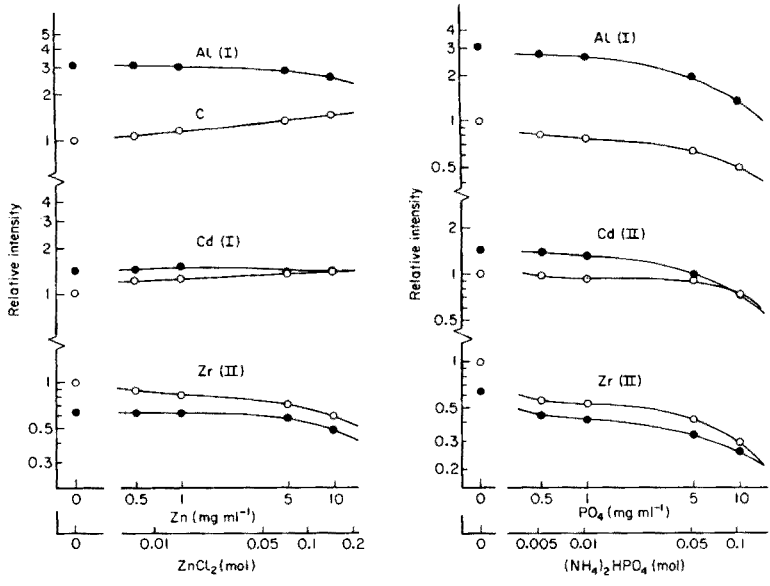

Fig. 4. Buffer effect of cesium on the intensity changes of Al, Cd, and Zr lines with zinc concentration. (○) Without CsCl. (●) With 0.05 mol CsCl.

Fig. 5. Buffer effect of cesium on the intensity changes of Al, Cd, and Zr lines with phosphate concentration. (○) Without CsCl. (●) With 0.05 mol CsCl.

of these analytes is shown in Fig. 3. Clearly, cesium decreased changes in the emission intensities with potassium concentration.

Similar results for the buffering effect of cesium on the interference from zinc are given in Fig. 4. With cesium, the interference was negligible up to 5 mg Zn ml^{-1}.

The interference from phosphate could not be reduced by addition of cesium chloride (Fig. 5). A slight reduction in this interference was observed when the arc current was raised to 10 A. Figure 1 shows that the phosphate interference is generally less important than the cation interferences. However, care must be taken in analyses of elements such as aluminium, zirconium, and selenium in the presence of phosphate at concentrations above 0.5 mg ml^{-1}.

REFERENCES

1 J. L. Jones, R. L. Dahlquist and R. E. Hoyt, Appl. Spectrosc., 25 (1971) 628.
2 A. L. Gray, Analyst, 100 (1975) 289.
3 H. Denton, B. L. Sharp and T. S. West, Talanta, 22 (1975) 379.
4 M. Kubota, Anal. Chim. Acta, 88 (1977) 79.

5 A. N. Zaidel', V. K. Pokof'ev, S. M. Raiskii, V. A. Slavnyi and E. Ya. Shreider, Tables of Spectral Lines, IFI/PLENUM, 1970, p. 351.
6 A. G. Gaydon, Dissociation Energies and Spectra of Diatomic Molecules, Chapman and Hall, 1968, p. 260.
7 P. M. McElfresh and M. L. Parsons, Anal. Chem., 46 (1974) 1021.
8 W. E. Rippetoe and T. J. Vickers, Anal. Chem., 47 (1975) 2082.
9 R. K. Skogerboe, I. T. Urasa and G. N. Coleman, Appl. Spectrosc., 30 (1976) 500.
10 D. E. Gray (Ed.), American Institute of Physics Handbook, 2nd edn., McGraw-Hill, 1963, p. 7—93.
11 M. Marinković and B. Dimitrijević, Spectrochim. Acta, Part B, 23 (1968) 257.
12 W. E. Rippetoe, E. R. Johnson and T. J. Vickers, Anal. Chem., 47 (1975) 436.
13 D. A. Murdick, Jr. and E. H. Piepmeier, Anal. Chem., 46 (1974) 678.
14 M. Marinković and T. J. Vickers, Appl. Spectrosc., 25 (1971) 319.

Analytica Chimica Acta, 96 (1978) 63—67

DETERMINATION OF BARIUM IN POTABLE WATERS AND SEDIMENTS BY CARBON-FURNACE ATOMIC EMISSION SPECTROMETRY

L. EBDON*

Department of Chemistry, Sheffield City Polytechnic, Pond Street, Sheffield S1 1WB (Gt. Britain)

R. C. HUTTON and J. M. OTTAWAY

Department of Pure and Applied Chemistry, University of Strathclyde, Cathedral Street, Glasgow G1 1XL (Gt. Britain)

(Received 13th June 1977)

SUMMARY

A method is described for the determination of barium in potable waters and sediments by carbon-furnace atomic emission spectrometry. The method has been evaluated for river, reservoir and borehole water and a river sediment. Calcium does not interfere. The working range, 0.01—0.2 μg Ba ml^{-1}, is adequate to meet even the most stringent water quality regulations. The limit of detection (2σ) for barium in deionized water is 0.0008 μg ml^{-1} and in potable water 0.002 μg ml^{-1}. The relative standard deviation is typically 4.7%. Results are compared with those obtained by atomic absorption spectrometry with a nitrous oxide—acetylene flame.

Although the toxicity of barium compounds in moderately large doses is well known, little attention has been given to its presence in drinking water in trace amounts. The level of barium in solution is normally limited by the concentration of sulphate and thus large concentrations are not expected in natural waters. The acknowledgement that new sources of potable water must be found to prevent serious future water shortages has led to increased interest in trace metal levels, as the quality of potential new sources is investigated. The World Health Organisation international standard (1963) [1] for barium is 1.0 μg ml^{-1}, which is given as the limit at which actual danger may arise. The U.S. Public Health Service in 1962 gave this same level as grounds for rejection of water for potable supply [2], and the 1.0 μg ml^{-1} level has been confirmed as the maximum permissible level in drinking and general agricultural waters in the U.S.A. [3]. It has been estimated that the range in U.S. water supplies is between 0.7 ng ml^{-1} and 0.9 μg ml^{-1} [4]. A recent E.E.C. Council Directive concerning the quality required of surface water intended for the abstraction of drinking water set two limits for barium [5]. The upper limit (1 μg ml^{-1}) is intended to apply to waters subject to normal or intensive physical and chemical treatment and disinfection, and the lower limit (0.1 μg ml^{-1}) to waters subject

to simple physical treatment, e.g. rapid filtration and disinfection. This directive poses some problems for the water industry in developing methods for the determination of barium with sufficient accuracy and precision.

This paper describes a method for the determination of barium in potable waters from a region where barium-containing minerals are found, by means of carbon-furnace atomic emission spectrometry. Barium was determined in potable waters in the range 0.10—0.18 $\mu g\ ml^{-1}$ by direct calibration. Barium may also be found in natural waters as suspended solids at times of spate, and therefore the method was also successfully applied to a typical sediment sample.

Frequently, trace metals are determined in potable waters by atomic spectrometry with flame atom cells. The use of the nitrous oxide—acetylene flame for the determination of barium provides better sensitivity than the air—acetylene flame. In the hotter flame, the atomic absorption detection limit in pure water is reported as 0.02 $\mu g\ ml^{-1}$ at 553.5 nm [6]. The use of atomic emission allows lower levels to be detected in the same flame; the detection limit is 0.002 $\mu g\ ml^{-1}$ at 553.5 nm [7]. The presence of excess of calcium, however, causes severe problems as the CaOH band at 553—555 nm overlaps the 553.5-nm barium line [8, 9]. This results in considerable deterioration of the detection limit in most practical samples and indeed barium can be measured in the presence of excess of calcium only in the nitrous oxide—acetylene flame [10]. Without some form of background correction, preferably based on wavelength modulation [11], the accurate determination of barium in the presence of excess of calcium is impossible by flame atomic emission spectrometry even when nitrous oxide—acetylene is used. While some workers report that the atomic absorption determination is possible in this flame, others disagree and either propose further improvements to the instrumentation, such as flame separation, or employ a chemical separation of barium from the calcium prior to atomization. This controversy has recently been discussed [12]. Recent work [13] has shown that barium can be determined in potable waters by atomic absorption in the nitrous oxide—acetylene flame only if flame conditions are rigorously controlled; with care a detection limit of 0.1 $\mu g\ ml^{-1}$ for a typical water can be achieved.

It has been shown that interferences from calcium in barium determinations are much reduced when an electrothermal atomizer is used [12, 14]. Moreover, the detection limits for barium determinations by carbon-furnace atomic emission spectrometry are significantly better than those obtained by carbon-furnace atomic absorption measurements [15, 16]. Recently, barium has been determined down to 0.036 $\mu g\ g^{-1}$ in calcium carbonate rocks by carbon-furnace atomic emission spectrometry [12]. Simultaneous background correction, by wavelength modulation, was successfully employed to overcome possible interferences from molecular calcium interferences [17]. In the determination of barium with a nitrous oxide—acetylene flame, it is necessary to add an ionization suppressor, but ionization of barium in a carbon furnace is much less [16, 18] and for the potable water analysis reported here such a precaution was unnecessary.

Thus it would appear that carbon-furnace atomic emission spectrometry offers an appropriately speedy, selective and sensitive method of determining barium in potable waters at levels which are well below those given in the E.E.C. Directive.

EXPERIMENTAL

Apparatus

A Perkin-Elmer Model 306 atomic absorption/emission spectrometer equipped with an HGA-72 heated graphite atomizer, was used. The spectrometer was connected to a Servoscribe RE 541.20 potentiometric strip-chart recorder. The operation of this instrument for carbon-furnace atomic-emission measurements has been described elsewhere [15, 19]. The instrumental parameters were:

Wavelength	553.5 nm	Atomization	6 s at 2700°C
Slit width	0.4 nm	Mode	Stopped flow
Purge gas	Argon at 1.5 l min^{-1} (20 lb in^{-2})	Sample volume	50 μl
Drying	50 s at 100°C	Chart speed	2 cm s^{-1}
Charring	10 s at 1000°C	Recorder f.s.d.	5 mV

Reagents

AnalaR-grade reagents were used throughout and all solutions were prepared and diluted with de-ionized water. A stock barium solution (100 μg Ba ml^{-1}) was prepared in 1% (v/v) nitric acid and diluted as required.

Preparation of samples

The water samples were acidified with nitric acid, 0.3 ml of concentrated acid to 50 ml of sample, immediately after collection and refrigerated until analyzed. The sediment sample was dried at 105°C and a sub-250 μm sample (1 g) was digested with concentrated nitric acid (5 ml). The digest was filtered (Whatman No. 1) to remove excess of silica and made up to 100 ml.

RESULTS AND DISCUSSION

Table 1 lists the levels of barium found in various water samples by the present method; for comparison, the levels found by atomic absorption in a nitrous oxide—acetylene flame, and the calcium levels found similarly [13], are also given. In Table 2, the determination of barium in the sediment sample is compared with the results found with a nitrous oxide—acetylene flame. It can be seen that within the limitations imposed by the poor precision of the flame method, for which the relative standard deviation is about 15% at this level, good agreement is obtained between the two methods. In two cases the levels determined in the flame appear to be higher than those obtained using the furnace. Comparison of results obtained by direct

TABLE 1

Determination of barium in potable waters

Sample	Ba (c.f.a.e.s.)[a] (μg ml^{-1})			Ba (a.a.s.)[b] (μg ml^{-1})	Ca (a.a.s.)[b] (μg ml^{-1})
	1[c]	2[c]	3[d]		
Ogston Reservoir	0.10	0.11	0.10	0.1	69
Ogston Final	0.10	0.10	0.10	0.1	78
River Derwent	0.17	0.18	0.18	0.3	82
River Amber	0.11	0.12	0.13	0.15	83
Peakshole	0.12	0.11	0.11	0.2	69

[a]Carbon-furnace atomic emission spectrometry.
[b]Atomic absorption spectrometry with a nitrous oxide—acetylene flame [13].
[c]Direct calibration.
[d]Standard additions.

TABLE 2

Barium in sediment from River Noe, Edale

	Ba (c.f.a.e.s.)[a]			Ba (a.a.s.)[b]	Ca (a.a.s.)[b]
	1[c]	2[c]	3[d]		
Sediment (mg kg^{-1} dry solid)	175	180	188	200	5000

[a—d]See footnotes to Table 1.

calibration with aqueous barium solutions and by standard additions on samples diluted 1 + 1, shows no significant difference, which indicates that for determinations of barium in potable water by carbon-furnace atomic emission spectrometry, direct calibration is quite adequate. The standard addition graphs were parallel to calibration graphs obtained with aqueous solutions, indicating that there was no suppression of ionization by the constituents of these water samples. If samples of higher sodium or potassium content were to be analyzed, the addition of caesium as an ionization buffer to all samples and standard solutions would be necessary [12].

The calcium in the waters analyzed gave no significant signals above the variation of the tube background in the spectral region used (555 and 552 nm). Although calcium molecular emission background has been measured in a furnace at levels as low as 100 μg ml^{-1} [17], levels as high as 4000 μg Ca ml^{-1} have been found to give negligible chemical interferences in the determination of 0.5 μg Ba ml^{-1} [12], and any calcium molecular emission interference, if observed, could be corrected by wavelength modulation.

The calibration graphs were linear up to 0.2 μg Ba ml^{-1} and the optimum working range was found to be 0.01—0.2 μg Ba ml^{-1}. The limit of detection

(2σ) for barium in deionized water was found to be 0.0008 $\mu g\ ml^{-1}$ and for potable water 0.002 $\mu g\ ml^{-1}$. A relative standard deviation of 4.7% was obtained when the barium content of the River Amber sample was determined eleven times.

Conclusion

Carbon-furnace atomic emission spectrometry offers a simple and sufficiently sensitive technique for these determinations. Any atomic absorption instrument fitted with a carbon furnace could be easily converted to emission operation, and it has been demonstrated [20] that detection limits within an order of the best can be achieved on many other commercial instruments. In some cases, simple minor modifications to limit the entrance slit may be necessary.

We are indebted to the Severn-Trent Water Authority, Derwent Division, for the supply of samples and for the flame analysis results. The award of a grant from the Royal Society to J. M. O. for the purchase of the HGA-72 atomizer is gratefully acknowledged.

REFERENCES

1 International Standards for Drinking Water, World Health Organisation, 1963.
2 United States Public Health Service standards, 1962.
3 Report of Committee on Water Quality Criteria, F.W.P.C.A., U.S. Dept. of Interior, 1968.
4 P. L. Brezonik in A. J. Rubin (Ed.), Aqueous-Environmental Chemistry of Metals, Ann Arbor Science, Michigan, 1974, p. 174.
5 Council Directive 75/440/EEC, Official Journal of the European Communities (Legislation, English Edition), 18 L 194 (1975) 26.
6 G. D. Christian and F. J. Feldman, Appl. Spectrosc., 25 (1971) 660.
7 E. E. Pickett and S. R. Koirtyohann, Spectrochim. Acta, Part B, 23 (1968) 235.
8 S. R. Koirtyohann and E. E. Pickett, Anal. Chem., 38 (1966) 585.
9 J. Van der Hurk, Tj. Hollander and C. Th. J. Alkemade, J. Quant. Spectrosc. Radiat. Transfer, 13 (1973) 273.
10 S. R. Koirtyohann and E. E. Pickett, Spectrochim. Acta, Part B, 23 (1968) 673.
11 W. Snelleman, T. C. Rains, K. W. Yee, H. D. Cook and O. Menis, Anal. Chem., 42 (1970) 394.
12 R. C. Hutton, J. M. Ottaway, T. C. Rains and M. S. Epstein, Analyst, 102 (1977) 429.
13 L. Ebdon and D. R. Lees, to be published.
14 K. C. Thompson and R. G. Godden, Analyst, 100 (1975) 198.
15 J. M. Ottaway and F. Shaw, Appl. Spectrosc., 31 (1977) 12.
16 M. S. Epstein, T. C. Rains and T. C. O'Haver, Appl. Spectrosc., 30 (1976) 324.
17 R. C. Hutton, J. M. Ottaway, M. S. Epstein and T. C. Rains, Analyst, 102 (1977) 658
18 J. M. Ottaway and F. Shaw, Analyst, 101 (1976) 582.
19 J. M. Ottaway and F. Shaw, Analyst, 100 (1975) 438.
20 D. Littlejohn and J. M. Ottaway, Analyst, 102 (1977) 553.

Analytica Chimica Acta, 96 (1978) 69—75

DETERMINATION OF GERMANIUM BY ATOMIC ABSORPTION SPECTROMETRY AFTER SOLVENT EXTRACTION -- ENHANCEMENT OF SENSITIVITY BY A NEBULIZER EFFECT

SHIGERU SHIMOMURA*, HIROMU SAKURAI, HIDEYOSHI MORITA and YOSHIKI MINO

Faculty of Pharmaceutical Sciences, University of Tokushima, Tokushima, 770 (Japan)

(Received 17th June 1977)

SUMMARY

Germanium can be determined by atomic absorption spectrometry after extraction into n-butyl ether. Germanium is first extracted with n-butyl ether from 8 M hydrochloric acid, and the extract is shaken again with 12 M hydrochloric acid. A ca. 5-fold enhancement of sensitivity is obtained compared with an earlier procedure based on methyl isobutyl ketone. This enhancement is ascribed to a "nebulizer effect", and is probably due to the different chemical forms of germanium produced when germanium is extracted from various concentrations of hydrochloric acid.

In the determination of germanium by atomic absorption spectrometry (a.a.s.), it is difficult to obtain high sensitivity owing to the formation of highly stable oxide species in the flame, similarly to vanadium, molybdenum and titanium. Amos and Willis [1] obtained a sensitivity of only 120 μg Ge ml^{-1} for 1% absorption, using the 265.12—265.16-nm doublet of germanium, in both fuel-rich air—acetylene and air—hydrogen flames. However, with a nitrous oxide—acetylene flame, Amos and Willis [1] and Manning [2] reported sensitivities of 1.5 μg and 2.5 μg Ge ml^{-1}, respectively. Popham and Schrenk [3] found a limit of detection of 0.5 μg Ge ml^{-1} with the same flame system, using a (1 + 1) acetone—water solvent system. Kirkbright et al. [4] reported that the low background of the argon-separated nitrous oxide—acetylene flame enabled the limit of detection to be lowered to 0.2 μg Ge ml^{-1}.

Several workers have investigated the a.a.s. of germanium after solvent extraction. Yanagisawa et al. [5] reported that the extraction method with methyl isobutyl ketone (MIBK) provided a ca. 10-fold absorption enhancement over that obtained in spraying the aqueous solution with the same flame system as Manning used. Pollock [6] determined germanium in limonite by a.a.s. after extraction with MIBK.

It is well-known that the solubility of MIBK in the aqueous layer increases at high hydrochloric acid concentrations. Yanagisawa et al. [5] observed an absorption, which was probably due to hydrochloric acid in MIBK, even when the MIBK layer contained no germanium. For these reasons, MIBK

cannot be recommended for determinations of germanium by solvent extractions in which a high concentration of hydrochloric acid is required.

This paper deals with the determination of germanium by a.a.s. after solvent extraction with n-butyl ether.

A new extraction procedure for germanium is proposed; a ca. 5-fold enhancement of sensitivity was achieved compared with the sensitivity obtained by the method previously reported [5, 6]. This enhancing phenomenon is considered as a "nebulizer effect". It was also examined by means of Raman spectrometry, to establish the chemical forms of germanium present.

EXPERIMENTAL

Apparatus

A Shimadzu MAF atomic absorption spectrophotometer equipped with a Nippon Jarrell—Ash high-temperature slot burner was used with a two-pass optical system. A Hamamatsu TV hollow-cathode lamp L-233 was used as radiation source at a lamp current of 14 mA. The light beam was 10 mm above the burner head. The flow rates of nitrous oxide and acetylene were kept constant at 3.2 l min^{-1} and 4.5 l min^{-1}, respectively.

A Nippon Bunko R-800 laser Raman spectrophotometer equipped with an argon laser (Spectra Physics, model 164 ion laser with model 265 exciter), and a Hitachi 124 spectrophotometer were also used. An electric shaker was used for extractions.

Materials

Stock solutions of germanium (500 ppm) were prepared as reported previously [7]. All solvents were of special-reagent grade. Germanium tetrachloride (99.99999%) was obtained from Wako Pure Chemical Industries. Other chemicals used were of reagent grade or the highest quality available.

Procedures

Atomic absorption measurements. Solutions (30 ml) containing 200 μg of germanium in various concentrations of hydrochloric acid were transferred to separatory funnels and 10 ml of organic solvent was added. After shaking for 3 min, the aqueous layer was discarded. The organic layer obtained here is called organic layer (I). This layer was shaken again with 2 ml of 12 M hydrochloric acid by shaking for 3 min and the aqueous layer was discarded. This organic layer is called organic layer (II). The atomic absorption of germanium was measured at the 265.12—265.16 nm doublet.

There was no difference in absorbance between n-butyl ether alone and n-butyl ether which had been treated as above, hence n-butyl ether was used as reference.

In the final recommended procedure, 10 ml of the neutralized sample solution was transferred to a separatory funnel together with 20 ml of 12 M

hydrochloric acid. After extraction with 10 ml of n-butyl ether for 3 min, the aqueous layer was discarded. The organic layer was shaken well with 2 ml of 12 M hydrochloric acid for 3 min. The aqueous layer was discarded and the organic layer transferred to a new glass-stoppered test tube for atomic absorption analysis.

Spectrophotometric measurements. Solutions (20 ml) containing 50 μg of germanium in various concentrations of hydrochloric acid were extracted with 10 ml of n-butyl ether by shaking for 3 min. The aqueous layer was poured into a new separatory funnel, and adjusted to a constant volume of 60 ml which was 9 M in hydrochloric acid. The solution was extracted with 10 ml of carbon tetrachloride for 3 min. An aliquot (2 ml) of the organic layer was transferred to a 10-ml volumetric flask, 5 ml of ethanol and 1 ml of phenylfluorone solution (1.9×10^{-3} M) were added, and the resultant solution was measured after dilution to 10 ml with ethanol [8].

Water and hydrochloric acid contents of n-butyl ether. Water was determined by the Karl Fisher method [9]. To measure the acid uptake, 5 ml of n-butyl ether was shaken with various concentrations of hydrochloric acid. The hydrochloric acid in the n-butyl ether layer was extracted into water (20 ml), and then the separated aqueous layer was back-titrated with 0.1 M hydrochloric acid after the addition of an excess (known) amount of sodium carbonate.

RESULTS AND DISCUSSION

Choice of solvent

The effect of the concentration of hydrochloric acid on the extraction of germanium into various solvents such as MIBK, n-butyl ether, n-butyl acetate and isoamyl acetate was studied. Extraction was done at a 3:1 volume ratio (aqueous to organic). The volume changes of the organic layers after extraction are shown in Fig. 1. The solubility of MIBK in aqueous solution increased remarkably above 7 M hydrochloric acid, while that of n-butyl ether was not influenced by the concentration of hydrochloric acid.

The maximum absorption for germanium was obtained when germanium was extracted with n-butyl ether from 10 M hydrochloric acid or above (Fig. 2). A ca. 5-fold absorbance enhancement was obtained compared to the earlier method [5, 6] in which germanium was extracted with MIBK from 8 M hydrochloric acid.

These results indicate that n-butyl ether is a more suitable solvent than MIBK and the others which have been used conventionally for extraction of germanium.

Extraction curves

The extraction curves I and II in Fig. 3 represent the absorbances obtained when organic layers (I) and (II) were aspirated, respectively. From curve I, it may be concluded that complete extraction of germanium is achieved from 11 M and above hydrochloric acid. However, germanium is

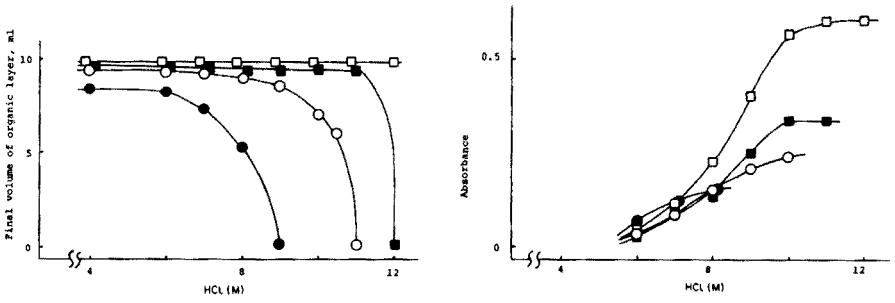

Fig. 1. Final volume of organic layer (I) after extraction. Initial volumes, 10 ml of solven and 30 ml of hydrochloric acid. —□— n-butyl ether, —■— isoamyl acetate, —○— n-butyl acetate, —●— methyl isobutyl ketone.

Fig. 2. Effect of hydrochloric acid concentration on atomic absorption of germanium in the organic layer (I). —□— n-butyl ether, —■— isoamyl acetate, —○— n-butyl acetate, —●— methyl isobutyl ketone.

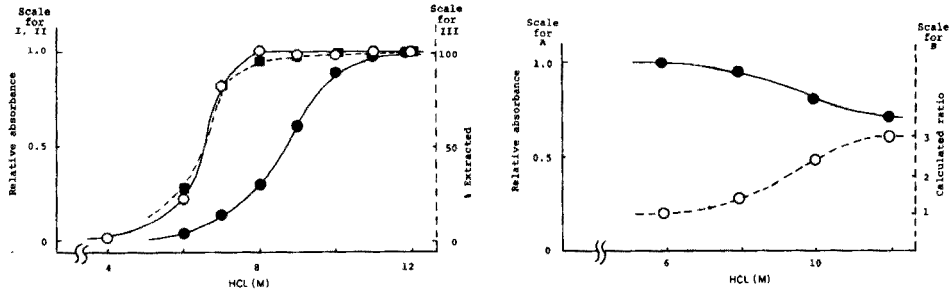

Fig. 3. Extraction curves of germanium with n-butyl ether. I, absorbance in n-butyl ether layer (I) (—●—); II, absorbance in n-butyl ether layer (II) (—○—); III, colorimetric method (—■—).

Fig. 4. Effect of hydrochloric acid concentration on amount of germanium. A, amount of germanium in drain (—●—); B, calculated ratio of amount of germanium introduced to flame to that in aspirated n-butyl ether (—○—).

completely extracted into n-butyl ether even from 8 M hydrochloric acid, as shown in curve II, which was obtained by shaking organic layer (I) again with 12 M hydrochloric acid. This curve II agrees closely with the extraction curve III obtained by the colorimetric method [8]. These results indicate that a higher sensitivity is provided when the n-butyl ether layer containing a certain amount of germanium is shaken with 12 M hydrochloric acid. The absorbance was trebled by shaking the n-butyl ether layer with 12 M hydrochloric acid compared with the results from 8 M hydrochloric acid.

This phenomenon might be attributed to the following three causes [10]: (1) aspiration efficiency depending on changes of viscosity, density or surface tension of the solvent; (2) nebulizer efficiency arising from changes in the distribution of droplet size in the aerosol and from the vaporization of

solvent; and (3) changes in flame conditions or atomization efficiency. Because neither the aspiration rate nor the amount of the solvent introduced into the flame changed when the n-butyl ether layers containing germanium extracted from various concentrations of hydrochloric acid were sprayed, it was considered that the first and second possibilities did not contribute to the enhancement of sensitivity. However, it was thought probable that some other effect in the nebulizer was active, although the third point has not been resolved as yet.

Nebulizer effect

In order to investigate this effect in the nebulizer, the amount of germanium in the drain when n-butyl ether layer (I) was aspirated was measured (Fig. 4). The amount of germanium in the drain decreased as the concentration of hydrochloric acid increased, i.e. the amount of germanium introduced into the flame increased with the concentration of hydrochloric acid. About 14% of the aspirated n-butyl ether was introduced into the flame, and the ratio of the amount of germanium introduced into the flame to that in the aspirated n-butyl ether was calculated as follows.

The equation relating to the amount of germanium is

$$C_o = R \cdot C_d + (1 - R)C_f \quad (1)$$

where C_o, C_d and C_f are, respectively, the amounts of Ge in the aspirated n-butyl ether, in the drain, and introduced into the flame; and R is the ratio of the volume of the drain to that of aspirated n-butyl ether (R = 0.86 in this case). Thus, by rearrangement,

$$C_f/C_o = (C_o - R \cdot C_d)/C_o(1 - R) \quad (2)$$

Curve B in Fig. 4 shows this ratio calculated for various concentrations of hydrochloric acid; this curve corresponds to curve I, which is the apparent extraction curve, in Fig. 3.

Consequently, the change in sensitivity is mainly due to the difference in the ratio of amount of germanium in the flame to that in the organic layer when germanium is extracted from different concentrations of hydrochloric acid. It is apparently a kind of "nebulizer effect".

The chemical forms of germanium in n-butyl ether

It was considered that this nebulizer effect was due to differences between the chemical forms of germanium present in 8 M hydrochloric acid and in higher concentrations of hydrochloric acid. The chemical forms of germanium in n-butyl ether layers extracted from 8, 9, 10 and 12 M hydrochloric acid were studied by Raman spectroscopy (Fig. 5).

The germanium extracted from 12 M hydrochloric acid showed a sharp peak at 397 cm^{-1} similar to the spectrum of germanium tetrachloride, but that from 8 M hydrochloric acid exhibited a broad peak at 405 cm^{-1} without the peak at 397 cm^{-1}. The chemical form of germanium obviously depended

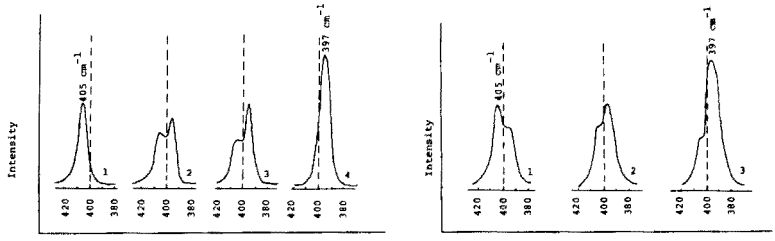

Fig. 5. Raman spectra of germanium in n-butyl ether (I). n-Butyl ether shaken with the corresponding concentrations of hydrochloric acid without germanium was used as reference. Curves 1—4: 8, 9, 10 and 12 M hydrochloric acid, respectively. Spectra were measured with a laser source (514.5 nm); the curves were recorded 16 times and smoothed twice.

Fig. 6. Raman spectra of germanium tetrachloride in the presence of water. n-Butyl ether was used as reference. Curves 1—3: 0.11%, 0.06% and 0.01% of water, respectively. Measuring conditions as in Fig. 5.

on the concentration of hydrochloric acid, and the form of germanium extracted from 12 M hydrochloric acid was the same as germanium tetrachloride, which is volatile even at ordinary temperatures (b.p., 83°C).

To examine further the chemical forms of germanium in n-butyl ether extracted from 8 M hydrochloric acid, the Raman spectra of germanium tetrachloride were measured in n-butyl ether containing various amounts of water (Fig. 6). The peak at 397 cm^{-1} was shifted to 405 cm^{-1} with increase in water content. Figure 7 shows the amounts of both water and hydrochloric acid in n-butyl ether layers shaken with various concentrations of hydrochloric acid. The amount of water in the n-butyl layer was almost independent of the concentration of hydrochloric acid, while the amount of acid in the organic layer increased at concentrations of 8 M and above. In the organic layer shaken with 12 M hydrochloric acid, the acid concentration was very much higher than that of water.

It was presumed that the peak at 405 cm^{-1} is related to both the water and hydrochloric acid contents in the organic layer; hence, the germanium

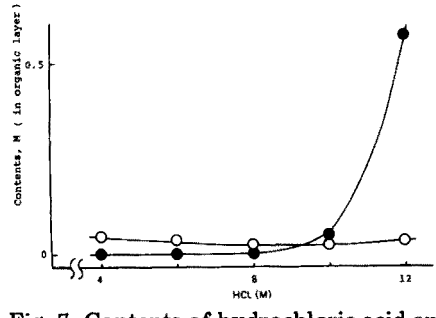

Fig. 7. Contents of hydrochloric acid and water in n-butyl ether layer (I). —○— water, —●—, hydrochloric acid.

TABLE 1

Comparison of this n-butyl ether method with an earlier MIBK method [5, 6]

	HCl (M)	Sensitivity (ppm for 1% absorption)
This method	8, 12 (2 steps)	0.13
Earlier method	8	0.68

extracted from 8 M hydrochloric acid exists in a different chemical form, which is less volatile than germanium tetrachloride, from that extracted from 12 M hydrochloric acid. Consequently, the phenomenon shown in Fig. 3 can be attributed to the different volatilities of the germanium chlorides formed when germanium is extracted from various concentrations of hydrochloric acid.

In this connection, in atomic absorption spectrometry with a premix burner, some workers have observed different peak profiles caused by differences in the volatilities of forms of the metal. Trent [11] and Odashima and Kumagai [12] reported such profiles in the determination of tetramethyllead and tetraethyllead in gasoline, and in the determination of both mercury(II) chloride and mercury(II) nitrate, respectively. These phenomena were based on the difference in original chemical forms, but in the present work the different forms of germanium were produced when the element was extracted from different concentrations of hydrochloric acid.

Extraction procedure of germanium

The above results led to a recommended procedure (mentioned under Experimental) for the determination of germanium. This procedure, which does not require a large amount of 12 M hydrochloric acid, is better than a single extraction method from 10 M hydrochloric acid or above. The procedure resulted in a significant increase in sensitivity compared to the MIBK method (Table 1). The standard deviation for a 10-ppm sample was 2.1% for 8 consecutive measurements.

REFERENCES

1 M. D. Amos and J. B. Willis, Spectrochim. Acta, 22 (1966) 1325.
2 D. C. Manning, At. Absorpt. Newsl., 6 (1967) 35.
3 E. R. Popham and W. G. Schrenk, Spectrochim. Acta, Part B, 23 (1968) 543.
4 G. F. Kirkbright, M. Sargent and T. S. West, Talanta, 16 (1969) 1467.
5 M. Yanagisawa, M. Suzuki and T. Takeuchi. Anal. Chim. Acta, 46 (1969) 152.
6 E. N. Pollock, At. Absorpt. Newsl., 10 (1971) 77.
7 S. Shimomura, H. Sakurai, H. Morita, Y. Mino and M. Inoue, Anal. Chim. Acta, 91 (1977) 421.
8 R. Yamaguchi and A. Murata, Jpn. Anal., 9 (1960) 959.
9 J. Mitchell, Jr., Anal. Chem., 23 (1951) 1069.
10 J. E. Allan, Spectrochim. Acta, 17 (1960) 467.
11 D. J. Trent, At. Absorpt. Newsl., 4 (1963) 348.
12 T. Odashima and Y. Kumpagai, At. Absorpt. Newsl., 12 (1973) 39.

Analytica Chimica Acta, 96 (1978) 77—82

ATOMIC ABSORPTION SPECTROMETRY OF BISMUTH WITH ELECTROTHERMAL ATOMIZATION FROM METAL ATOMIZERS

KIYOHISA OHTA and MASAMI SUZUKI*

Department of Chemistry, Faculty of Engineering, Mie University, Kamihama-cho, Tsu, Mie-ken 514 (Japan)

(Received 1st June 1977)

SUMMARY

Synchroscope traces of atomic absorption signals generated during heating of bismuth salts in a metal micro-tube atomizer show features which are characteristic for bismuth when a fast-response amplifier is used. Atomization profiles of bismuth with a molybdenum micro-tube are complicated for inorganic compounds and some complexes, but addition of thiourea improves the absorption profiles and increases sensitivity. Tantalum and tungsten micro-tubes were used for comparison. The interferences of other metals on bismuth absorption and the determination of bismuth in aluminum samples are also described.

Several papers have described the atomic absorption spectrometry of bismuth with electrothermal atomization. Headridge and Smith [1] determined bismuth in lead and iron with an induction-heated graphite furnace, and found a sensitivity of 1.4×10^{-9} g. Langmyhr et al. [2] atomized bismuth at 1400°C in a graphite furnace heated by a high-frequency induction generator. Barnett and McLaughlin [3] atomized bismuth at 2500°C in a Perkin-Elmer HGA-2100 graphite furnace. Frech [4] used a Massmann type graphite furnace for atomization of bismuth in combination with a temperature-controlled heating device. In these papers, measurements were made with a conventional amplifier system. In the present work, the flameless atomization of bismuth in a metal micro-tube atomizer was investigated with a fast-response amplifier system and the complex atomization characteristics of bismuth were established.

EXPERIMENTAL

Apparatus

The monochromator, photomultiplier, signal control unit, dual-beam synchroscope and recorder were the same as used previously [5]. The light source was a bismuth hollow-cathode lamp (Hamamatsu TV Co.). The analytical wavelength was 233.06 nm and the slit width was chosen so as to give a spectral band pass of ca. 0.02 nm. A deuterium lamp (Original Hanau D200F) was used for background correction.

The metal micro-tube atomizer (1.5-mm diameter and 25-mm long) and absorption chamber (300-ml volume) have been described [6]. The method

of measuring the tube temperature has also been described [5]. Argon was used as purge gas in the absorption chamber with hydrogen. All sample solutions were injected with a glass micro-pipet.

Reagents

Bismuth stock solutions were prepared by dissolving bismuth metal in nitric acid. Bismuth chloride solution was prepared by heating bismuth nitrate with hydrochloric acid. All reagents were of analytical-reagent grade, and deionized-distilled water was used in all dilutions.

RESULTS AND DISCUSSION

Atomization of bismuth from various compounds and complexes

Bismuth was atomized from various compounds and complexes to establish its atomization characteristics. Diethyldithiocarbamate, oxinate and iodide complexes were prepared as described in the literature [7—9]. Figures 1 and 2 show the synchroscope traces of the bismuth absorption for the various compounds and complexes. The sample solution (1 μl) was placed in the micro-tube and dehydrated at 100°C, followed by ashing at 200°C. Then, bismuth was atomized by heating so as to give a final temperature of 1700, 2200 or 2400°C. As can be seen from Figs. 1 and 2 two absorption peaks appeared in atomization from nitrate, chloride, carbamate and oxinate. The

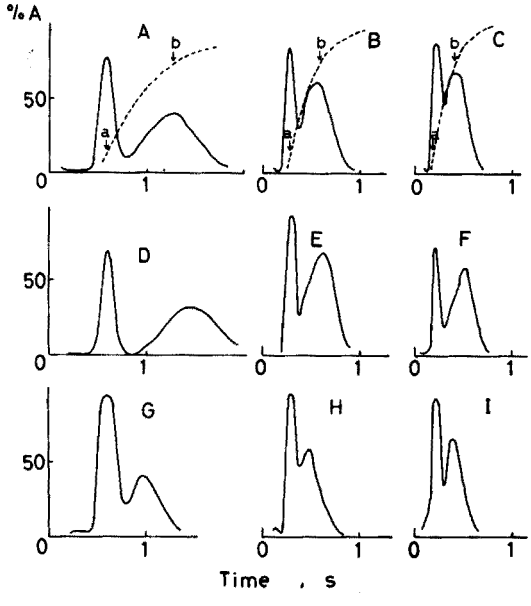

Fig. 1. Synchroscope traces of bismuth atomization in a molybdenum micro-tube atomizer. A, B and C, nitrate. D, E and F, chloride. G, H and I, DDTC complex. Maximum temperatures, 1700°C for A, D and G; 2200°C for B, E and H; 2400°C for C, F and I. Gas flow rates, 480 ml Ar min^{-1}; 20 ml H_2 min^{-1}. Dashed curves show the curves of temperature increase: (a) 1000°C and (b) 1500°C.

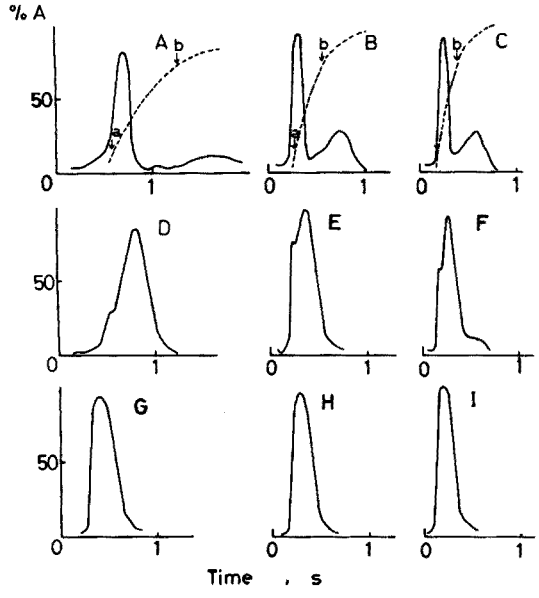

Fig. 2. Synchroscope traces of bismuth atomization in a molybdenum micro-tube atomizer. A, B and C, oxinate. D, E and F, iodide complex. G, H and I, thiourea added. Maximum temperatures for A—I, gas flow rates, and temperature increases (a) and (b) are exactly the same as in Fig. 1.

first peak appeared at about 1000°C for almost all samples, whereas the second peak was observed at different temperatures for each sample. The first absorption may result from atomization of bismuth metal, which is produced by the partial reduction of bismuth salts. The temperature at which the first absorption commenced corresponds to the atomization temperature of bismuth metal. Bismuth has a low melting point (271°C) and a relatively high vapor pressure (1 mm Hg at 934°C). The second absorption is assumed to originate from a bismuth complex. It might be considered that the second absorption results from atomization of some bismuth compound, such as trichloride, which sublimes in hydrogen, but this is insufficient to elucidate the second absorption. It seems reasonable to assume that bismuth undergoes an interaction with molybdenum.

Only a single peak was observed when a conventional amplifier system was used, presumably because of an insufficient speed of response.

Only one absorption peak appeared in atomization from the iodide complex (Fig. 2). The shoulder of the absorption profile was due to background absorption. The atomization temperature of bismuth from the iodide complex was higher than that of the other compounds and complexes. Bismuth iodide is known to be sublimed in hydrogen. The higher atomization temperature may have resulted from some difficulty in the dissociation of iodide.

A single absorption peak was also observed in atomization from bismuth nitrate containing thiourea. In this case, bismuth atomized at a relatively low

temperature. Urea did not show the same effect on bismuth absorption. Sulfide formation was observed in the ashing step. Although the role of thiourea is unknown, sulfide formation may be effective in the atomization of bismuth. Bismuth sulfide is reduced readily in hydrogen. Thiourea also served to increase the sensitivity for bismuth to 9×10^{-13} g (1% absorption).

The hydrogen flow in the absorption chamber had some effects on the absorption profile of bismuth. For atomization from bismuth chloride and nitrate, the first absorption peak first became lower and then increased with increasing hydrogen flow. A hydrogen flow of 20 ml min^{-1} is recommended.

In order to compare the results obtained with a molybdenum atomizer, atomization of bismuth was also examined with tantalum and tungsten micro-tubes. Their dimensions were the same as those of the molybdenum tube. In the tantalum atomizer, two absorption peaks were shown for atomization from inorganic compounds, but the second peak was close to the first peak. These profiles were not reproducible: sometimes absorption appeared as a single peak. The acidity of the sample solution appeared to affect the atomization profiles. The aqueous bismuth solution was 0.1 M in acid for the present work. The tantalum tube lost its metallic lustre and showed poor electric conduction after only ten measurements.

With the tungsten micro-tube, the absorption profiles showed pronounced tailing and the atomization temperatures giving maximum absorption shifted to higher regions.

The gas flow did not affect the absorption in tantalum and tungsten atomizers except that the absorption peak tended to decrease as the hydrogen flow increased.

Tantalum and tungsten are more resistant chemically than molybdenum. The reactivity of the evaporation surface may affect the atomization profiles of bismuth. McIntyre et al. [10] reported that little chemical interaction occurs between copper and a molybdenum surface, and that cobalt and nickel undergo little or no interaction with molybdenum. They concluded that molybdenum is an inert, reproducible, and durable evaporation surface for the determination of cobalt, nickel and copper. However, it seems reasonable to assume from the present work that molybdenum has some effect on bismuth atomization, probably owing to some surface interaction between the two metals.

The complex atomization profile was specific for bismuth, and was not shown by other metals such as copper, cobalt, lead and gallium.

Interferences

Figure 3 shows the synchroscope traces for the atomization of bismuth in the presence of lead, copper and silver. Iodide complexes were extracted into methyl isobutyl ketone. As can be seen from Fig. 3, lead, copper and silver seriously affected the bismuth absorption even in small amounts. The same interference phenomena were shown for the carbamate complex and inorganic compounds. Thiourea served to depress the interferences in the atomization of bismuth (Fig. 3).

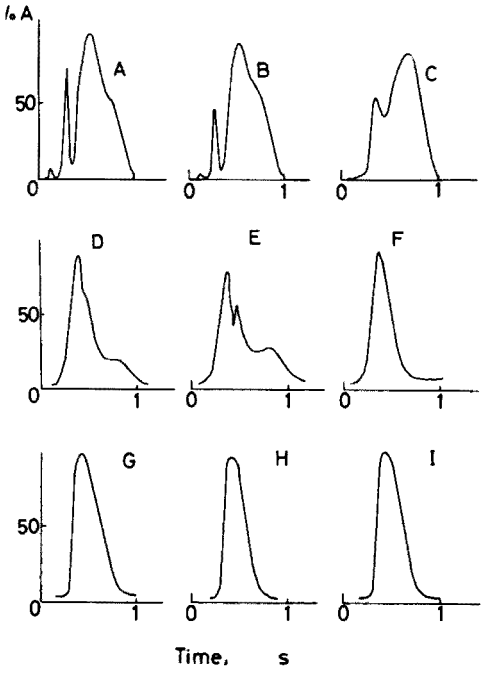

Fig. 3. Synchroscope traces of interferences on bismuth absorption in a molybdenum micro-tube atomizer. A, DDTC complexes of Bi (0.5 ng) and Pb (1 ng). B, DDTC complexes of Bi (0.5 ng) and Cu (1 ng). C, DDTC complexes of Bi (0.5 ng) and Ag (1 ng). D, iodide complexes of Bi (0.5 ng) and Pb (1 ng). E, iodide complexes of Bi (0.5 ng) and Cu (1 ng). F, iodide complexes of Bi (0.5 ng) and Ag (1 ng). G, Bi (0.5 ng) and Pb (1 ng) in the presence of thiourea. H, Bi (0.5 ng) and Cu (1 ng) in the presence of thiourea. I, Bi (0.5 ng) and Ag (1 ng) in the presence of thiourea. Gas flow rates, 480 ml Ar min^{-1} and 20 ml H_2 min^{-1}. Maximum temperature, 2200°C.

With the tantalum atomizer, only small effects were shown with 10-fold amounts of lead, copper and silver, whereas the interferences were complex with the tungsten atomizer.

Determination of bismuth in aluminum with the molybdenum micro-tube atomizer

Flameless atomic absorption spectrometry with the molybdenum micro-tube atomizer was applied to the determination of bismuth in aluminum. Solvent extraction was used for eliminating the major interference.

Procedure. Dissolve 0.1 g of sample in 6 M hydrochloric acid, and evaporate the solution to dryness on a water bath. Heat the residue with 6 M hydrochloric acid, and, after cooling, dilute to 100 ml with water in a volumetric flask. To 1—5 ml of this solution, add 1 ml of EDTA solution (3%) and 2.5 ml of citric acid solution (50%). Adjust the pH to 11—12. Add 1 ml of sodium diethyldithiocarbamate solution (2.5%) and extract with 5 ml of carbon tetrachloride. Evaporate the organic phase to dryness and heat with

TABLE 1

Determination of bismuth in aluminum

Sample	Bismuth found (%)[a]	
	Proposed method	Polarography
Aluminum No. 1	0.029 ± 0.004	0.028
Aluminum No. 2	0.026 ± 0.002	0.03

[a]Three or four determinations.

10 ml of 12 M hydrochloric acid to dryness. After adding 5 ml of 0.2 M hydrochloric acid to the residue, add 1 ml of thiourea solution (50%) and dilute to 10 ml. Place an aliquot of the solution into the micro-tube atomizer and atomize bismuth. Prepare a calibration curve by treating bismuth standard solution as above.

Table 1 shows the results obtained for aluminum samples. Lower results were obtained when the sample solutions were analyzed with the addition of thiourea without extraction. As is apparent, the procedure based on extraction is adequate for accurate determinations of bismuth in aluminum.

Conclusions

Bismuth has complex atomization characteristics with the molybdenum micro-tube atomizer, especially for atomization from inorganic compounds. The addition of thiourea to the sample solution improved the absorption profile and sensitivity toward bismuth. Thiourea was also useful for suppression of interferences.

The bismuth absorption signals were reproducible for the molybdenum tube, but not for the tantalum tube. The surface conditions of tantalum appeared to be responsible for the poorer reproducibility of the signals. Although the tungsten tube gave a reproducibility comparable to that obtained with the molybdenum tube, the sensitivity of the bismuth determination was poor.

REFERENCES

1 J. B. Headridge and D. R. Smith, Talanta, 19 (1972) 833.
2 F. J. Langmyhr, R. Solberg and L. T. Wold, Anal. Chim. Acta, 69 (1974) 267.
3 W. B. Barnett and E. A. McLaughlin, Jr., Anal. Chim. Acta, 80 (1975) 285.
4 W. Frech, Z. Anal. Chem., 275 (1975) 353.
5 K. Ohta and M. Suzuki, Anal. Chim. Acta, 83 (1976) 381.
6 K. Ohta and M. Suzuki, Talanta, 22 (1975) 465.
7 R. A. Chalmers and D. M. Dick, Anal. Chim. Acta, 31 (1964) 520.
8 T. Moeller, Ind. Eng. Chem. Anal. Ed., 15 (1943) 346.
9 H. Goto and Y. Kakita, J. Chem. Soc. Jpn., 82 (1961) 1212.
10 N. S. McIntyre, M. G. Cook and D. G. Boase, Anal. Chem., 46 (1974) 1983.

Analytica Chimica Acta, 96 (1978) 83—88

TRACE MERCURY ANALYSIS IN BIOLOGICAL MATERIAL: USE OF ^{203}Hg-LABELLED METHYLMERCURY CHLORIDE FOR IN VIVO LABELLING OF FISH TO STUDY THE EFFICACY OF VARIOUS WET ASHING PROCEDURES

D. C. STUART

Slowpoke Nuclear Reactor, Life Sciences Building, Dalhousie University, Halifax, Nova Scotia B3H 4J1 (Canada)

(Received 20th May 1977)

SUMMARY

Several wet ashing techniques for trace mercury analysis by cold vapour atomic absorption have been evaluated with radiotracer mercury, and in particular fish labelled in vivo with ^{203}Hg-tagged methylmercury chloride. Partial digestion methods suffer from strong matrix effects; these include incomplete extraction from the sample, hold-back of mercury in the extraction solution during the reduction/aeration step, and alteration of the aeration release pattern so as to cause low results if measurement is based on peak height. A complete digestion method is outlined; this gives good results and is tentatively recommended pending further tests with other types of biological samples.

Because of the importance of trace analysis for mercury in the environment [1—7], a careful evaluation of the analytical techniques utilized to gather information on the problem was instituted.

Of the methods for the trace analysis of mercury available, the most widely used is the cold vapour a.a.s. method [7, 8], critical investigations of which are being published [9, 10]. For this technique, as well as for most others, mercury must be separated from the biological matrix before determination. There is ample evidence in the literature [7] to indicate that this step is extremely difficult.

This report outlines an evaluation of various wet ashing techniques. The samples were labelled in vivo with radiotracer mercury to simulate as closely as possible the conditions met in a typical environmental analysis. Fish were chosen as suitable specimens, as they concentrate mercury from their environment [11], mainly in a methylated form [12—15]. Furthermore, the analysis of fish is currently of concern.

Partial digestion techniques have become popular although they have been applied mainly to biological fluids. Since the matrix is not completely destroyed, this method relies on complete extraction of the mercury from the matrix and the breaking of any carbon—mercury bonds to give mercury(II) in solution. The advantage of this type of digestion is that high temperatures

are unnecessary, and so volatilization of mercury should be less likely than in complete ashing techniques. A complete wet ashing procedure may, however, be necessary to remove various strong matrix effects which occur [16—19], even when analyzing urine samples [20], although losses of mercury occur through volatilization during wet ashing at elevated temperatures [17, 21—26]. Campbell and Head [27] have reviewed early techniques, and research carried out by the S.A.C. Analytical Methods Committee [28] is pertinent. None of these methods appears to be wholly satisfactory when all of the literature quoted is taken into account, especially as the current concentration level of analytical interest is orders of magnitude lower than that considered in most of these publications.

During this study a method of wet ashing which appears to give excellent results was found, and is presented as a tentatively recommended procedure.

EXPERIMENTAL

The in vivo labelling of fish with $CH_3—^{203}HgCl$

A five-gallon tank containing several species of small fish was set up. Methylmercury chloride, labelled with ^{203}Hg (purchased from ICN) was added to the water. The fish, left in this environment for several months to allow natural incorporation of the tracer, took up some of the radiotracer and contained ca. 60 ppb based on activity measurements. The fish were used in the experiments described in the following section.

Evaluation of wet ashing techniques

Partial digestion methods. The methods studied are outlined briefly in Table 1; the procedures were applied to samples of the labelled fish. Initially, the possibility of loss from volatilization of extracted mercury from open containers was investigated. Each method mentioned in this section was checked first by the use of inorganic Hg(II) radiotracer and then portions of the labelled fish.

After following the prescribed treatment, the samples were filtered; the amounts of tracer mercury remaining in the residue and extracted into the filtrate were measured. In methods (4) and (5) (see Table 1), the analysis was completed by reduction/aeration and a.a.s. The amounts of tracer aerated and remaining in the sample were also measured.

All measurements of tracer radioactivity were made with a 7.56 cm × 7.56 cm NaI(Tl) well-type detector connected to a Canberra model 8100 multi-channel pulse-height analyzer.

Complete digestion method. A weighed portion of sample was placed in a 250-ml round-bottomed flask, connected to an efficient reflux condenser (Graham-type). Ground-glass joints were treated with a small amount of concentrated sulphuric acid. All reagents were added through the top of the condenser. Concentrated sulphuric acid (10 ml) was added and the sample allowed to soak. Heat was then applied with a burner to begin charring the

TABLE 1

Partial digestion methods applied to radiotracer-labelled fish

Brief outline of methods	Tracer remaining in residue, %	References
(1) Digest solution: 150 ml 6% $KMnO_4$ + 20 ml 18 M H_2SO_4; to 1-g sample, add 1.5 ml of digest solution, and allow to stand overnight add 0.3 ml 20% NH_6OHHCl.	98.4	[21, 29—32]
(2) As (1), but heat at 60°C overnight.	90.3	[33]
(3) To 0.1-g sample, add 2.0 ml 11 M HCl + 100 mg $NaNO_3$, and allow to stand overnight; add 10 ml H_2O and filter.	13[a]	[34]
(4) To 0.1-g sample, add 0.4 ml H_2SO_4; heat to 50°C, cool, and add cautiously 3 ml of 6% $KMnO_4$; heat again and allow to cool; repeat this step twice; cool and add 20% NH_2OHHCl.	42	[35, 36]
(5) Digest solution: $HClO_4$—HNO_3 = 5:1; to 0.2-g sample, add 1.5 ml of digest solution and place in a 70—75°C water bath overnight; cool, add 1 ml H_2O, add 5 drops NH_2OHHCl.	15 (in alkaline residue)	[37]

[a]Apparent 35% loss by volatilization.

sample, and 3 ml of fuming nitric acid (90%) were added. Vigorous heating was used to ash the sample completely. Additional nitric acid was added as required. Considerable amounts of nitrogen oxides escaped through the top of the condenser. After complete ashing (clear solution), the digested sample was left to cool.

This method was tested by using aliquots of CH_3—$^{203}HgCl$. The samples taken contained about 4×10^{-9} g of tracer. After the ashing procedure, carrier mercury was added and precipitated as mercury(II) sulphide, filtered, dried and weighed, and the activity was measured. These samples were compared with the activity of standard aliquots taken at the same time. These were counted immediately; then carrier mercury was added with $KMnO_4$ to promote exchange, and precipitated as mercury(II) sulphide, which was filtered, dried, weighed, and counted in order to reproduce geometry and attenuation effects in the samples [7].

Another test was carried out with portions of the labelled fish. The tracer activities of the samples were determined before and after ashing; the tracer was recovered by precipitation, as described in the previous paragraph.

More portions of labelled fish were ashed by the procedure outlined, and the analysis was completed by reduction/aeration and atomic absorption [9].

Finally, portions of a standard reference material (Bowen's kale) were analyzed.

RESULTS AND DISCUSSION

Partial digestion methods

In the study of possible volatilization loss with inorganic radiotracers, significant loss was noted in only one case: that of pretreatment of the tracer in alkaline solution. This treatment is normally only recommended for homogenization of fish, and in the case of the fish, loss was not observed.

The extraction performance of the methods tested with the labelled fish is shown in Table 1. With Skare's procedure [37], the residue from the pretreatment in alkaline solution contained 15% of the radiotracer. The procedure of Toribara and Shields [34] resulted in a 35% loss of the tracer by volatilization.

Completion of the analysis by reduction/aeration and a.a.s. showed that for the procedure of Jacobs et al. [35, 36], only 43% and 37% of the tracer were aerated from two aliquots of the filtrate; with the procedure of Skare [37], 58% and 75% were aerated. The rest of the tracer remained in solution. This effect was the same as that observed for the addition of too much hydroxylammonium chloride [10], but that was not the cause of the hold-back effect in this experiment as great care was taken to add minimal amounts The effect must, therefore, be attributed to a matrix interference from some component of the partially ashed biological sample.

In addition, sample absorption peaks were considerably drawn out in time relative to standards, even though the standards were prepared with the reagents added to the samples. This effect must also be attributed to interference caused by the partially ashed matrix; the interference may be corrected satisfactorily by measuring peak area, rather than peak height [10].

Complete digestion method

The volumes given may be adjusted for the amount of sample taken. The important factor appears to be that an excess of sulphuric acid over other components be maintained until after complete ashing and just before analysis; water must not be added to the mixture before ashing.

Table 2 gives results for a tracer experiment to investigate the performance of the outlined method with $CH_3{}^{203}HgCl$ samples of ca. 4×10^{-9} g. Table 3

TABLE 2

Tracer mercury loss on wet ashing (mercury added as CH_3HgCl)

Order aliquot taken	Specific activity[a]	Mean
(2) Standard	581	593
(5) Standard	605	
(1) Sample	579	
(3) Sample	600	600
(4) Sample	620	

[a]Counts per 200 s per mg yield of carrier. Amount of tracer used was ca. 4×10^{-9} g.

TABLE 3

Tracer mercury loss on wet ashing from in vivo labelled fish

Sample	Weight (mg)	Activity recovered (as % of initial)[a]
Dried fish head	32	92
Fresh body	132	92
Fresh body	128	93

[a]7% reduction in measured activity from attenuation by the precipitate and different counting geometry.

shows results for in vivo labelled fish (in this case, a 3% decrease results from a different counting geometry, and a 4% decrease from greater attenuation of the γ-rays by mercury(II) sulphide [7], so that complete recovery of the tracer results in an activity recovery of 93% of the initial activity). Both experiments indicate complete recovery of the tracer mercury.

In the reduction/aeration step, it is necessary to use tin(II) in dilute sulphuric acid rather than hydrochloric acid to achieve complete aeration.

Analyses of samples (ca. 780 mg) of Bowen's kale [38] by this method gave 165 and 168 ppb, in good agreement with Bowen's mean value of 166 ppb [39].

The results obtained suggest that nothing short of a complete wet ashing suffices to eliminate matrix effects sufficiently to obtain accurate results. Partial digestion techniques appear to be inadequate.

The financial support of the National Research Council of Canada is gratefully acknowledged. This research was carried out in partial fulfilment of Ph.D. requirements in the laboratories of Professor K. Fritze, McMaster University, whose advice and encouragement have been deeply appreciated.

REFERENCES

1 K. Ljunggren, B. Sjostrand, A. G. Johnels, M. Olsson, G. Otterlind, and T. Westermark, IAEA Proc. Symp. Nucl. Techniques Environ. Pollut., Oct. 26—30, 1970, pp. 373—405.
2 H. Ackefors, Proc. Roy. Soc., Ser. B, 177 (1971) 365.
3 N. Grant, Environment 13 (May, 1971) 2.
4 H. R. Jones, Mercury Pollution Control, Noyes Data Corp., Park Ridge, N.J., 1971.
5 F. M. D'Itri, The Environmental Mercury Problem, Chemical Rubber Co. Press, 1972.
6 R. Hartung and B. D. Dinman, Environmental Mercury Contamination, Ann Arbor Science Publishers, Ann Arbor, Michigan, 1972.
7 D. C. Stuart, Ph.D. thesis, Trace Analysis for Mercury in Biological Material, McMaster University Library, Hamilton, Ont., 1974.
8 A. M. Ure, Anal. Chim. Acta, 76 (1975) 1.
9 D. C. Stuart, Anal. Chim. Acta, submitted.
10 D. C. Stuart, Anal. Chim. Acta, submitted.

11 A. G. Johnels, T. Westermark, W. Berg, P. I. Persson and B. Sjostrand, Oikos, 18 (1967) 323.
12 Report from an Expert Group on Methyl-Mercury in Fish, Nordisk Hyg Tidski, Suppl. 4, Stockholm, 1971.
13 G. Westoo, Acta Chem. Scand., 20 (1966) 2131.
14 G. Westoo, Acta Chem. Scand., 21 (1967) 1790.
15 T. W. Huckabee, C. Feldman and Y. Talmi, Anal. Chim. Acta, 70 (1974) 41.
16 P. C. Stein, B. C. Eutsler and E. E. Campbell, Am. Ind. Hyg. Ass. J., 33 (1972) 71.
17 T. T. Gorsuch, Analyst, 84 (1959) 135.
18 F. R. Barrett, Analyst, 81 (1956) 294.
19 F. Nielsen-Kudsk, Scand. J. Clin. Lab. Invest., 17 (1965) 171.
20 I. M. Weiner and O. H. Muller, Anal. Chem., 27 (1955) 149.
21 M. B. Jacobs and A. Singerman, J. Lab. Clin. Med., 59 (1962) 871.
22 J. Cholak and D. M. Hubbard, Ind. Eng. Chem., Anal. Ed., 18 (1946) 149.
23 D. G. Simonsen, Am. J. Clin. Pathol., 23 (1953) 789.
24 M. Nabrzyski, Anal. Chem., 45 (1973) 2438.
25 D. C. Abbott and E. I. Johnson, Analyst, 82 (1957) 206.
26 J. F. Kopp and R. G. Keenan, Am. Ind. Hyg. Ass. J., 24 (1963) 1.
27 E. E. Campbell and B. M. Head, Am. Ind. Hyg. Qt., 16 (1955) 275.
28 Analytical Methods Committee, Analyst, 90 (1965) 515.
29 G. Lindstedt, Analyst, 95 (1970) 264.
30 S. H. Omang, Anal. Chim. Acta, 53 (1971) 415.
31 G. Lindstedt and I. Skare, Analyst, 96 (1971) 223.
32 K. H. Nelson, W. D. Brown and S. J. Staruch, Int. J. Environ. Anal. Chem., 2 (1972) 45.
33 J. F. Uthe, F. A. J. Armstrong and M. P. Stainton, J. Fish. Res. Bd. Can., 27 (1970) 805.
34 T. Y. Toribara and C. P. Shields, Am. Ind. Hyg. Ass. J., Jan.-Feb. (1968) 87.
35 M. B. Jacobs, S. Yamaguchi, L. J. Goldwater and H. Gilbert, Am. Ind. Hyg. Ass. J., 21 (1960) 475.
36 M. B. Jacobs, L. J. Goldwater and H. Gilbert, Am. Ind. Hyg. Ass. J., 22 (1961) 276.
37 I. Skare, Analyst, 97 (1972) 148.
38 See, e.g. H. J. M. Bowen and P. A. Cawse in Lenihan and Thomson (Eds.), Activation Analysis (Principles and Applications), Academic Press, 1965; H. J. M. Bowen, Analyst, 92 (1967) 124.
39 H. J. M. Bowen, personal communication, June 1973.

Analytica Chimica Acta, 96 (1978) 89—97

SEPARATION OF LOW-MOLECULAR-WEIGHT PURINE ELECTRO-OXIDATION PRODUCTS FROM PHOSPHATE BUFFERS

JAMES L. OWENS, HAZEL H. THOMAS and GLENN DRYHURST*
Department of Chemistry, University of Oklahoma, Norman, Okla. 73019 (U.S.A.)
(Received 24th August 1977)

SUMMARY

Two chromatographic methods have been developed to separate quantitatively a number of organic compounds such as alloxan, urea, allantoin, parabanic acid, oxaluric acid and D-ribose from relatively large amounts of inorganic phosphate. These organic compounds are representative of typical products expected upon electrochemical oxidation of various purine derivatives which may be themselves separated from each other by liquid chromatography with phosphate buffers. The phosphate may subsequently be separated from the organic components either by use of a Sephadex G-10 gel permeation column with water or very dilute hydrochloric acid as the eluant or by use of a methanol-washed column of a strong cation-exchange resin with methanol as the eluant.

Several reports from this laboratory have been concerned with the electrochemical oxidation of biologically important purine derivatives and the relationship between the electrochemical products and mechanisms and the biological oxidations of these compounds [1, 2]. One of the major problems encountered in such studies is the separation and identification of the relatively large number of electrooxidation products that are formed. In the past, several different separations and/or analytical techniques have been utilized for identification and quantification of purine electrooxidation products.

Recently, the electrochemical oxidation of purine nucleosides and nucleotides has been under investigation. It became obvious that the techniques used for qualitative and quantitative analysis of simple purine electrooxidation product mixtures were inadequate for analysis of the products from electrooxidation of the more complex nucleosides, nucleotides and oligonucleotides. Electrooxidation of these latter compounds appears to give more complex product mixtures which require more elegant separation and identification techniques than those used in earlier studies. Accordingly, a series of investigations to develop suitable separation and identification techniques has been initiated. A column chromatographic technique was developed [3] which could quantitatively separate milligram quantities of typical purine electrooxidation products such as alloxan, urea, allantoin, parabanic acid, oxaluric acid and ribose. This procedure utilized series-coupled

Sephadex G-10 and QAE A-25 column packings and aqueous KH_2PO_4 solutions as the eluant. In order to identify properly the products separated, the aqueous phosphate eluant had to be removed from each component. Techniques such as mass, infrared and u.v.—visible spectroscopy, elemental analysis, etc., could then be used to identify the various components.

No methods for adequately separating small quantities of low-molecular-weight organic compounds from relatively large excesses of inorganic phosphate seem to have been reported. However, desalting of high-molecular-weight compounds and biopolymers by gel filtration chromatography has been described [4, 5]. Another method of removing some inorganic salts from organic compounds has employed cation-exchange resins eluted with various mixtures of water and non-aqueous solvents [6, 7].

This report describes two column chromatographic methods which may be used for removal of inorganic phosphate from low-molecular-weight organic compounds.

EXPERIMENTAL

Chemicals

Parabanic acid and allantoin (Eastman), alloxan and oxaluric acid (Nutritional Biochemicals Corporation), urea (Merck), and D-ribose (Calbiochem) were used.

The ion-exchange resins used were: AG11A8 ion retardation, AG 50W-X8 strong cation, AG 501-X8 mixed bed, and AG 21K strong anion (BioRad); Amberlite MB-3 mixed bed, and Amberlite IR-4B weak anion (Mallinkrodt); Dowex 2-X8 strong anion (J. T. Baker); Sephadex QAE-A25 strong anion and Sephadex G-10 gel permeation (Pharmacia).

Thin-layer chromatography was carried out with Brinkman MN-Polygram Polyamide-6-UV_{254} and Eastman Chromogram 6060 silica gel precoated sheets impregnated with fluorescent indicator.

Apparatus

Chromatographic columns for Sephadex G-10 were 75 cm long and 2.75 cm in diameter. A Mariotte flask system was utilized to obtain constant and reproducible flow rates.

Columns for the AG 50W-X8 and the AG11A8 packings were 40 cm long and 2.5 cm in diameter. Most of the other ion-exchange columns ranged from 20 × 1.3 cm to 30 × 2.0 cm.

An ISCO Golden Retriever or an ISCO Model 1200 fraction collector was utilized for sample collection. U.v. spectra and u.v. monitoring of chromatographic fractions utilized a Hitachi-Perkin-Elmer Model 124 Spectrophotometer with 1.00-cm quartz cells.

Column packing conditions

Sephadex G-10. The dry resin (200 g) was allowed to swell in excess of water by heating on a boiling water bath for at least 1 h with constant

stirring. The slurry was then allowed to cool to room temperature (ca. 1.5 h). Excess of water was removed from the gel in order to form a thick slurry. The slurry was then carefully poured down a long glass rod into the column, which contained about 100 ml of water. The column flow was started immediately, because this gave the most even packing. An extension reservoir was placed on the top of the column so that all the required gel could be added at one time, which aids in obtaining an evenly packed bed. The 4—8 cm space above the bed was filled with the eluant and a Mariotte flask fitted to ensure a constant flow rate. Several bed volumes of eluant were passed to stabilize and equilibrate the gel bed. Such columns were operated at room temperature with flow rates of 42.0—54.0 ml h^{-1}, except as otherwise noted.

Methanolic AG 50W-X8. The appropriate amount of dry AG 50W-X8 strong cation-exchange resin necessary to give about 150 ml of swelled resin was hydrated with excess of deionized water for several hours with gentle stirring. After the resin had settled, excess of water was removed by decantation. The slurry was poured into the column in several portions, each portion being allowed to settle before the next was added. The slurry was washed into the column with a little water. This method gave a uniform and reproducible column. If all the packing is added at once, the resin tends to segregate according to size [8]. The space above the resin bed was filled with water and a Mariotte flask system was attached. Several bed volumes of water were passed to equilibrate the resin completely. The column was then washed with 1—2 bed volumes of 1 M HCl to ensure that all the resin was in the hydrogen ion form, and with water until the effluent was free of chloride (as tested with 0.1 M $AgNO_3$). Distilled methanol was then passed through the column (1—2 bed volumes). Owing to some shrinkage of the resin in methanol, significant channeling occurred [6], and the column was inverted several times until the resin settled uniformly. It should be noted that if the cation-exchange resin remains in contact with methanol for extended periods, then a u.v.-absorbing component is dissolved; this causes a large background absorbance which can, on occasion, obscure sample peaks. For this reason, the methanol wash of the column typically preceded the sample application by at most 1—2 h. After sample elution the methanol was washed off the column with several bed volumes of water. This cation-exchange column was operated at room temperature at typical flow rates of 90.0—180.0 ml h^{-1}.

Other ion-exchange resins. Other resins were packed into columns in an analogous manner to that of the AG 50W-X8 resin described above.

Qualitative tests

Thin-layer chromatography. In order to detect alloxan, parabanic acid and urea in column effluents, various thin-layer chromatographic procedures (t.l.c.) were employed. Alloxan was best detected with a polyamide thin-layer plate (see Chemicals) developed with methanol + acetic acid (95:5).

A bright red-brown spot, developed on air drying ($R_F \approx 0.7$ [9]), is characteristic of alloxan. Parabanic acid was detected on silica gel plates developed with n-butanol + acetic acid + water (12:3:5). A blue-black spot ($R_F \approx 0.55$) observed under u.v. light (254 nm) is characteristic of parabanic acid. Urea was detected with the same system as parabanic acid except that it was visualized as a yellow spot ($R_F \approx 0.55$) by spraying the plate with Ehrlich's reagent (10% w/v *p*-dimethylaminobenzaldehyde in 12 M HCl) [10].

Detection of phosphate. Phosphate in the chromatographic effluent was detected by adding a few drops of 3 M nitric acid to ca. 1 ml of test solution followed by 100—200 mg of ammonium molybdate; on gentle heating, a bright yellow precipitate of ammonium molybdophosphate indicated phosphate [11].

Detection of D-ribose. Under the conditions used for detection of phosphate, D-ribose gives a blue color, because of formation of phosphomolybdenum blue [12].

Procedures for removal of phosphate

Sephadex G-10 columns. The test component (typically about 1.7—30 mg) dissolved in 1 ml of 1 M KH_2PO_4 was applied to the column after any eluant above the bed surface had been carefully drained; the bed surface was protected with a disc of Whatman No. 1 paper. The sample was absorbed into the top of the column, and the column walls and gel surface were washed with three 1—2 ml portions of eluant, each of which was allowed to drain into the column. The column was then filled with eluant and connected to a Mariotte flask. Fractions (3-ml) were collected, and monitored at an appropriate wavelength (see Results and Discussion). As a general rule, however, unknown components of purine electrooxidations as they are eluated are best monitored at a wavelength of ca. 200 nm. Every fourth fraction was monitored except in regions where absorbing components were eluted when every second fraction was measured. In the case of each organic compound studied, the first peak eluted was that of phosphate which at high concentrations gives a readily detectable u.v. absorption below ca. 220 nm. The presence of phosphate in this peak was confirmed by testing with ammonium molybdate (see above). Those fractions containing the organic component were combined and freeze-dried. The resulting residue was tested to confirm its identity, usually by its melting point, t.l.c. or u.v. spectrophotometry.

Methanolic AG 50W-X8 columns. The test components, dissolved in 1 ml of 1 M KH_2PO_4, were first freeze-dried. The residue was extracted with the minimum amount of distilled methanol (typically 3—8 ml) and applied to the top of the column in exactly the same way as described for the Sephadex G-10 column except that methanol was employed as the eluant. Again 3-ml fractions of the column effluent were collected and monitored by u.v. spectrophotometry at a suitable wavelength. The fractions containing the

organic component were combined and the methanol removed by evaporation under reduced pressure.

RESULTS AND DISCUSSION

Techniques have already been developed for the chromatographic separation of multicomponent electrooxidation product mixtures from purines [3], in which KH_2PO_4 solutions were used as eluant. Accordingly, methods for quantitative removal of inorganic phosphate from the organic electrooxidation products were sought here. Each component was eluted in a volume of about 40—50 ml of, typically, 0.025 M KH_2PO_4. By freeze-drying these solutions to about 1 ml, each organic component would be present in a solution of ca. 1 M inorganic phosphate. Accordingly, the experiments reported here utilized 1.6—30 mg of the organic species dissolved in 1 ml of 1 M KH_2PO_4.

Sephadex G-10

Some typical chromatograms showing the separation of phosphate and D-ribose, allantoin, and urea with water as the eluant are presented in Fig. 1. Clearly a satisfactory separation of the organic component from inorganic phosphate can be achieved. The yield of the organic component was exactly the same as the amount initially added to the column, i.e., quantitative recovery was possible.

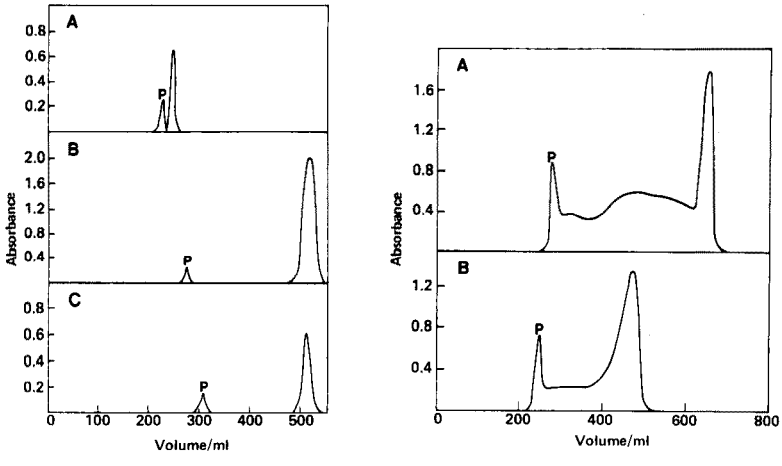

Fig. 1. Chromatograms obtained for 1 ml of 1 M KH_2PO_4 containing (A) 30 mg of D-ribose, (B) 6 mg of allantoin and (C) 10.6 mg of urea, with water as the eluant. Flow rates: (A) 24 ml h^{-1}, (B) 51 ml h^{-1} and (C) 48 ml h^{-1}. Absorbance monitored at (A) 195 nm, (B) 215 nm and (C) 201 nm. P refers to the peak for phosphate.

Fig. 2. Chromatograms obtained for 1 ml of 1 M KH_2PO_4 containing (A) 10 mg of alloxan and (B) 10 mg of parabanic acid with water as the eluant. Flow rate 54 ml h^{-1}. Absorbance monitored at (A) 206 nm and (B) 210 nm. P refers to the peak for phosphate.

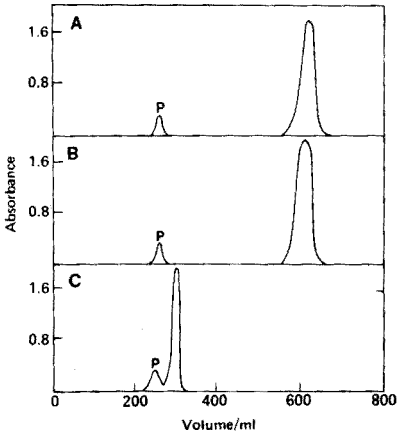

Fig. 3. Chromatograms obtained for 1 ml of 1 M KH_2PO_4 containing (A) 1.8 mg of alloxan, (B) 1.8 mg of parabanic acid and (C) 1.7 mg of oxaluric acid. Flow rate 54 ml h^{-1}. Eluant 0.001 M HCl. Absorbance monitored at (A) 206 nm, (B) 210 nm and (C) 220 nm. P refers to the peak for phosphate.

Chromatograms for alloxan and parabanic acid under identical conditions are shown in Fig. 2; with water as the eluant, an ill-defined peak occurs between the phosphate and alloxan or parabanic acid peaks. The yield of alloxan or parabanic acid that could be recovered after freeze-drying the fractions under the respective peaks, was significantly lower than the original amount of these compounds added to the column. The low yields and the distorted form of the chromatograms suggested that both alloxan and parabanic acid decompose to some extent as the separation proceeds. It is well known that above about pH 4—5 alloxan decomposes to alloxanic acid [13, 14]; at neutral pH parabanic acid decomposes to oxaluric acid [15].

Attempts to separate oxaluric acid from inorganic phosphate on Sephadex G-10 with water as the eluant were unsuccessful; even after passage of more than 1200 ml of water no peak for oxaluric acid could be observed. This behavior suggested that oxaluric acid, which would be in its anionic form at neutral pH [16], is strongly retained on the column.

In order to elute alloxan, parabanic acid or oxaluric acid satisfactorily from a Sephadex G-10 column and to separate these compounds from phosphate, the pH of the eluant has to be significantly lowered. This was accomplished by using dilute HCl (0.001 M, pH 3) as the eluant. Hydrochloric acid was used because it is subsequently easily removed from the organic component by freeze-drying.

Figure 3 shows chromatograms for alloxan, parabanic acid, and oxaluric acid in mixtures with phosphate, with the dilute HCl eluant. In each case, a very good separation is noted with no distortion of the chromatographic peaks.

The chromatograms shown in Figs. 1 and 3 indicate that in most cases the resolution of the phosphate and organic component peaks is excellent.

TABLE 1

Resolution between phosphate and organic component peaks on a Sephadex G-10 column, at a flow rate of 54.0 ml h^{-1}, except where noted

Compound	Eluant	Resolution (R_s)	Compound	Eluant	Resolution (R_s)
D-Ribose	H_2O	0.67	Parabanic acid	0.001 M HCl	4.2
D-Ribose	H_2O	1.0[a]	Urea	H_2O	4.3
Oxaluric acid	0.001 M HCl	1.04	Alloxan	0.001 M HCl	4.6
Allantoin	H_2O	2.0			

[a]Flow rate 24.0 ml h^{-1}.

For comparative purposes, Table 1 shows some peak resolution values (R_s) between each of the six organic components and phosphate based on eqn. (1)

$$R_s = 2(V_p - V_0)/(W_p + W_0) \quad (1)$$

where V_p and V_0 are the retention volumes for the phosphate and organic component peaks, respectively, while W_p and W_0 are their baseline bandwidths [17]. A resolution of 1.5 or greater indicates virtually complete, or baseline, separation. A resolution of 1.0 corresponds to about 98% complete separation [17]. Clearly, four of the compounds exhibit excellent resolution ($\geqslant 1.5$). In the case of D-ribose, a resolution of 0.67 was observed at a flow rate of 54.0 ml h^{-1} (Table 1). However, when the flow rate was decreased to 24.0 ml h^{-1} the resolution increased to 1.0 (Table 1). Accordingly, for D-ribose or oxaluric acid an enhanced resolution between these components and phosphate can, if required, be readily accomplished by appropriate decrease of the eluant flow rate.

All fractions under the component peaks under conditions similar to those shown in Figs. 1 and 3 gave no evidence for the presence of any phosphate.

During this work, the solid organic components after elution and freeze-drying were tested for their authenticity. Typically, melting points were taken and comparative t.l.c. was carried out. Often u.v. spectra were also taken. In each case, the eluted organic compounds were found to be analytically pure and free from inorganic phosphate.

Methanolic AG 50W-X8

After dissolution of the organic component—KH_2PO_4 mixture in methanol and application to the methanolic AG 50W-X8 column, the phosphate formed a white crust at the top of the column and was not eluted. Accordingly, only a single peak, for the organic component, was eluted from the column. Some typical data for allantoin, alloxan, parabanic acid, D-ribose and urea are shown in Table 2. The recovered organic components were pure and free of inorganic phosphate. Oxaluric acid is almost completely insoluble in methanol and hence cannot be desalted by this method.

TABLE 2

Retention volumes for a methanolic AG 50W-X8 column

Compound	Sample weight[a] (mg)	Flow rate (ml h^{-1})	Wavelength monitored (nm)	Retention volume (ml)
Allantoin	4	120	224	55
Alloxan	1.7	90	230	42
Parabanic acid	1.6	90	225	45
D-ribose	30	90	216	42
Urea	12	90	225	51

[a]This weight of sample was dissolved in 1 ml of 1 M KH_2PO_4, freeze-dried, dissolved in 3—8 ml of methanol, and passed through the methanol-washed AG 50W-X8 column.

The white crust of phosphate which forms at the top of the methanolic cation-exchange column may be readily removed during regeneration of the column with water and hydrochloric acid (see Experimental).

Other ion-exchange systems

Several other ion-exchange resins (see Experimental) were also examined as stationary phases for separation of the organic purine electrooxidation products from inorganic phosphate. For each resin several column parameters were examined, e.g., type of eluant, flow rate. Partial success was achieved with Amberlite MB-3 mixed-bed resin. However, generally two or three passes through relatively long, freshly washed columns were required to accomplish a satisfactory separation.

The principal difficulty noted with most separations was the tendency for the organic species to be very strongly retained by the strong anion-exchange resins even though the exchange of phosphate with hydroxide was complete. When weak anion-exchange resins were utilized, however, both the organic sample and phosphate eluted together. The cation-exchange resins exchanged potassium ion very readily for hydrogen ion and the organic sample generally eluted with ease. Because of the strong retention (probably adsorption) of the organic components on all strong anion-exchange resins examined, it was not possible to develop any further suitable separation techniques.

Conclusions

It is possible to separate rapidly and simply highly polar organic compounds of the sort typically formed by electrochemical oxidation of purines, from inorganic phosphate by two chromatographic methods. The first, and most widely applicable method, utilizes a Sephadex G-10 gel permeation column. With water or very dilute hydrochloric acid as the eluting solvent, large excesses of inorganic phosphate (and probably many other inorganic salts) can be separated from small amounts of water-soluble organic compounds

A second method, which can be utilized for organic compounds that are appreciably soluble in methanol, utilizes a methanol-washed column of AG 50W-X8 cation-exchange resin. This method involves eluting a solution of the organic compound/phosphate mixture with methanol. The inorganic phosphate is quantitatively removed as a white insoluble deposit at the top of the column, and only the pure organic material is eluted.

The desalting techniques outlined should provide a basis for removal of inorganic material from a variety of organic compounds. The methods should be particularly useful for desalting solutions formed from electrochemical reactions where reaction products are normally contaminated with large amounts of inorganic buffer/electrolyte materials.

This research was supported by the National Institutes of Health through Grant No. GM-21034.

REFERENCES

1 G. Dryhurst, Top. Curr. Chem., 34 (1972) 47.
2 G. Dryhurst, Electrochemistry of Biological Molecules, Academic, New York, 1977, Chap. 3.
3 M. T. Cleary and G. Dryhurst, Anal. Chim. Acta, 94 (1977) 343.
4 P. Flodin, J. Chromatogr., 5 (1961) 103.
5 M. W. Neal and J. R. Florini, Anal. Biochem., 55 (1973) 328.
6 F. C. Saville, in Comprehensive Analytical Chemistry, Vol. IIB, C. L. Wilson and D. W. Wilson (Eds.), Elsevier, Amsterdam, 1968, p. 241.
7 S. Kato, B. M. Visinski and G. Dryhurst, J. Electroanal. Chem., 66 (1975) 21.
8 Materials, Equipment and Systems for Chromatography, Electrophoresis and Membrane Technology, BioRad Laboratories, Richmond, California, 1975, p. 13.
9 B. M. Visinski and G. Dryhurst, J. Electroanal. Chem., 70 (1976) 199.
10 I. Smith, Chromatographic and Electrophoretic Techniques, 2nd edn., Vol. I, Interscience, New York, 1960.
11 C. H. Sorum, Introduction to Semimicro Qualitative Analysis, 3rd edn., Prentice-Hall, Englewood Cliffs, New Jersey, 1960, p. 200.
12 A. I. Vogel, A Textbook of Macro and Semimicro Qualitative Inorganic Analysis, 4th edn., Longman, London, 1960, p. 577.
13 G. M. Richardson and R. R. Cannon, Biochem. J., 23 (1929) 68.
14 D. Seligson and H. Seligson, J. Biol. Chem., 190 (1951) 647.
15 G. Dryhurst, B. H. Hansen and E. B. Harkins, J. Electroanal. Chem., 27 (1970) 375.
16 J. C. Andrews and I. T. Sell, Arch. Biochem. Biophys., 56 (1955) 405.
17 B. L. Karger, L. R. Snyder and C. Horvath, An Introduction to Separation Science, Wiley, New York, 1973, p. 147.

Analytica Chimica Acta, 96 (1978) 99—106

APPLICATIONS OF ELECTRON SPIN RESONANCE IN THE ANALYTICAL CHEMISTRY OF TRANSITION METAL IONS
Part II. The Determination of Iron(III) in Aqueous Solution [1]

WARREN G. BRYSON

Hugh Adam Cancer Biology Research Unit, Department of Surgery, University of Otago, Dunedin (New Zealand)

(the late) DAVID P. HUBBARD, BARRIE M. PEAKE* and JIM SIMPSON

Department of Chemistry, University of Otago, Dunedin (New Zealand)

(Received 9th July 1977)

SUMMARY

The determination of iron(III) in aqueous solution is investigated by e.s.r. techniques. Hydrated Fe(III) gives rise to a broad spectrum for which the analytical range is 5.0×10^{-1}—5.0×10^{-4} mol dm^{-3} iron(III) with a precision of ± 0.98%. Iron(III) in 2.0 mol dm^{-3} NH_4F solution gives a spectrum with a much narrower line width through the formation of the FeF_6^{3-} complex. The resulting increase in signal amplitude leads to an improved analytical range of 1.0×10^{-2}—6.0×10^{-7} mol dm^{-3} iron(III) with a precision of ± 0.45%. There is also a significant decrease in the time required to determine Fe(III) in this system. The effects of variation in instrumental variables, pH, and stability on the spectra of both systems are considered.

There have been a number of reports [2—4] on the use of electron spin resonance (e.s.r.) techniques to determine iron(III) in aqueous solution as hydrated Fe(III). These attempts have not been particularly successful, as hydrated Fe(III) gives an e.s.r. spectrum consisting of a very broad single line with a relatively weak signal amplitude. Relaxation studies [5—8] suggest that the line width can be reduced considerably, with a resultant increase in the signal amplitude, by changing the environment of the ion by complexation. As a consequence, methods have been developed [2, 4, 9, 10] to improve the limit of detection for Fe(III) by e.s.r. using anionic complexing agents and a combination of other analytical procedures. The problems inherent in using such methods, and the increased time for sample preparation relative to that required for recording the e.s.r. signal, suggested obvious advantages in developing improved methods for determining iron(III) in aqueous media.

This paper reports the use of the instrumental procedures discussed in Part 1 [1] to obtain, for the first time, a limit of detection and analytical range for the e.s.r. determination of hydrated Fe(III) in aqueous solution. The analytical parameters may be improved even further by the formation of the hexa-

fluoroferrate(III) complex which gives rise to spectra with considerably decreased line widths and hence increased signal amplitude.

EXPERIMENTAL

Apparatus

A Varian E-4 spectrometer was used with a standard Suprasil quartz aqueous sample cell (Scanco S-812).

Reagents

Standard Fe(III) solutions were prepared by dissolving AnalaR grade $Fe(NO_3)_3 \cdot 9H_2O$ in deoxygenated, triple glass-distilled water. Fluoride solutions were prepared with AnalaR grade NH_4F. Iron impurities in the fluoride solutions were removed by extraction with purified chloroform and AnalaR 8-hydroxyquinoline as detailed below. AnalaR $HClO_4$ and NaOH were used for pH adjustments.

Procedure

The spectrometer was tuned and operated as described in Part 1 [1].

Hydrated iron(III) solutions. A constant microwave power of 20.0 mW was used together with a scan range of 4000 gauss centred at a field set of 3400 gauss. Before determining an optimum analytical curve for this species, the effect was measured of variation in pH, receiver gain and modulation amplitude on the signal amplitude. The Fe(III) hydrate, $Fe(H_2O)_6^{3+}$, has been reported [11] to undergo a variety of reactions in aqueous solution. These processes have relatively slow reaction rates which may have resulted in slow changes in signal amplitude. Hence the stability of the spectra of this species with time was also investigated.

Iron(III) in aqueous NH_4F solutions. The microwave power was varied over the range 5—100 mW. The scan range was varied from 200 to 4000 gauss centred at a field set of 3400 gauss. The NH_4F was claimed by the manufacturers to contain 0.001% iron impurity and its presence was confirmed by e.s.r. measurements on NH_4F solutions. It has been suggested [12] that Fe(III) ions may be extracted quantitatively from aqueous solutions with 8-hydroxyquinoline in $CHCl_3$. A technique based on this suggestion was developed and the purification steps are summarized in Table 1. Reagent-grade chloroform was purified [13] and then glass-distilled twice. All extractions were performed by vigorous shaking for 10 min. The concentration of Fe(III) was determined at each step by measuring the e.s.r. spectrum of a solution of the NH_4F sample; there was a progressive decrease in the magnitude of this term until no Fe(III) could be determined after the fourth and fifth steps.

The effect of variation in NH_4F concentration, pH, receiver gain, modulation amplitude, microwave power, and signal stability were investigated before determining an analytical curve for Fe(III) in this system.

TABLE 1

Purification steps for the removal of iron(III) from ammonium fluoride solutions

Procedure	Fe(III) concentration (mol dm^{-3})
1. Prepare 2.0 mol dm^{-3} NH_4F solution	3.31×10^{-6}
2. Extract NH_4F solution with 1.0×10^{-2} mol dm^{-3} 8-hydroxyquinoline in $CHCl_3$ (0.5 volume)	6.61×10^{-7}
3. Repeat extraction	2.09×10^{-7}
4. Repeat extraction with 5.0×10^{-4} mol dm^{-3} 8-hydroxyquinoline in $CHCl_3$	$<5 \times 10^{-9}$
5. Degas NH_4F solution in vacuo to remove $CHCl_3$	$<5 \times 10^{-9}$

RESULTS AND DISCUSSION

Hydrated ion(III)

Spectra observed for this species under all conditions consisted of a single broad line of line width ($\Delta B_{pp} \sim 1100$ gauss) as reported in earlier studies [2—4]. A typical spectrum for an iron(III) concentration of 1.0×10^{-2} mol dm^{-3} is shown in Fig. 1(a). Satellite peaks arising from hyperfine interactions with the ^{57}Fe ($I = \frac{1}{2}$) isotope in natural abundance of 2.2% were not observed.

An evaluation of the effect of pH over the range 1.0—13.0 upon the signal amplitude (A) for an iron(III) concentration of 1.0×10^{-2} mol dm^{-3} showed that for pH > 2.2, A decreased to a level which was unsuitable for detection. The decrease was accompanied by precipitation of hydrated iron(III) oxide. The largest value of A was observed at a pH of 1.2 and this decreased gradually for pH values up to 2.2. All solutions used to obtain data for analytical curves were acidic because of hydrolysis of the iron(III) hydrate in aqueous solution and no precipitation effects were observed. Hence no attempt was made to adjust the pH of these solutions.

The variation in A with receiver gain (G) was linear and the ratio of A/G remained constant at a given Fe(III) concentration. The effect of variation in modulation amplitude (M) on the signal amplitude expressed as A/G is shown in Fig. 2; A/G increases linearly with increase in M for $M <$ ca. 10 gauss. For $M > 10$ gauss, the deviation from linearity is predominantly due to the effect of thermal instability of the Varian E-231 cavity [14]. Accordingly, in

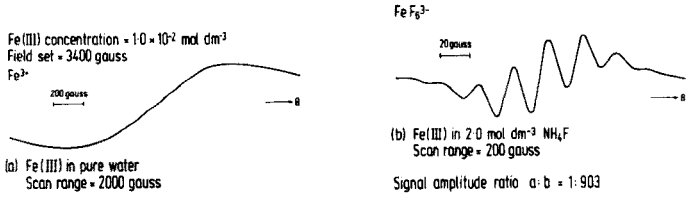

Fig. 1. E.s.r. spectra of the Fe(III) ion.

the subsequent determination of an analytical curve for hydrated Fe(III), M was kept to values <10 gauss. In this way the expression A/GM was found to remain constant for variation in M at a fixed Fe(III) concentration.

No variation in A was observed for spectra of Fe(III) solutions aged in a stoppered flask over 7 d. All solutions were analysed within this time period.

The above conditions were used in the determination of an analytical curve for hydrated Fe(III) in the form of a plot of A/GM versus Fe(III) concentration as shown in Fig. 3. Logarithmic coordinates were used for convenience. The analytical range and precision [1] were calculated to be 5.0×10^{-1}—5.0×10^{-4} mol dm^{-3} Fe(III) and ±0.98%, respectively. The deviation from linearity apparent for Fe(III) concentrations greater than 5.0×10^{-1} mol dm^{-3} may arise from a decrease in A due to relaxation line broadening mechanisms such as intermolecular dipole or exchange interactions [3, 15—17]. Also, oligimerization at high Fe(III) concentrations might lead to a change in A.

The maximum Fe(III) concentration detected was 2.0 mol dm^{-3}, as determined by the solubility of the salt. Although the region from the upper limit of the analytical range of 5.0×10^{-1} mol dm^{-3} to this value is non-linear, it may still be used for analytical purposes. The minimum concentration of Fe(III) detected was 5.0×10^{-4} mol dm^{-3} and this is considered to be the lower limit of the analytical range. The large line width of the Fe(III) signal makes it particularly susceptible to any background effects arising from the spectrometer cavity; this renders the method described [1] inappropriate for the calculation of a detection limit. However, an estimate may be obtained for this quantity by defining it as the concentration of Fe(III) at the point of intersection of the extrapolated portion of the linear analytical curve with the background peak-to-peak noise level, as used in an earlier report [4]. The noise level, represented by the horizontal line shown in Fig. 3, was

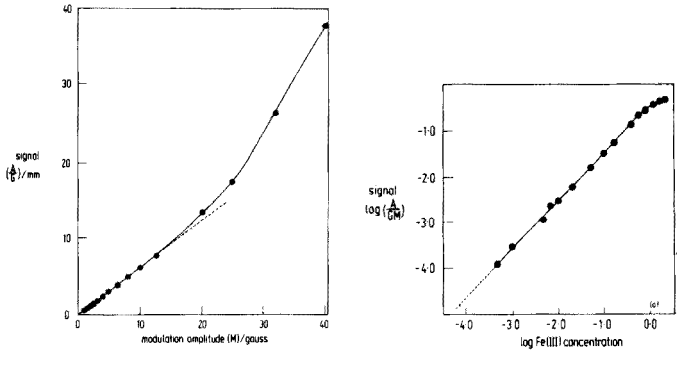

Fig. 2. Variation in signal (A/G) with modulation amplitude (M) for 1.0×10^{-1} mol dm^{-3} Fe(III) in triply distilled water.

Fig. 3. Plot of log (A/GM) versus log Fe(III) concentration for Fe(III) in triply distilled water. Microwave power = 20 mW. Horizontal line (a) represents a noise level plot at a modulation amplitude of 10.0 gauss.

evaluated from the expression $\log_{10}(A_N/G_N M)$, where A_N is the mean amplitude of noise for a time constant value of 10 s and for a receiver gain of G_N. The detection limit calculated in this manner corresponds to an iron(III) concentration of 6.61×10^{-5} mol dm^{-3}.

Iron(III) in aqueous NH_4F solutions

Spectra of Fe(III) in this system were markedly different from those observed in pure aqueous solution. The variation in signal amplitude, expressed as $\log_{10}(A/GM)$, with NH_4F concentration is shown in Fig. 4 for an iron(III) concentration of 1.0×10^{-2} mol dm^{-3}. Spectra showed marked changes in line shape, line width and intensity for NH_4F concentrations in the range 0—2.0 mol dm^{-3}. These changes have been well documented [7, 18] and attributed to spectra arising from the formation of a variety of iron(III)—fluoro complexes superimposed on the spectra of hydrated Fe(III). For these combination spectra the amplitude of the most intense line was used as a measure of A.

At NH_4F concentrations >1.0 mol dm^{-3}, a well-defined seven line spectrum (Fig. 1b) was observed; this has been attributed [7, 18] to fluorine ($I = \frac{1}{2}$) hyperfine coupling in the hexafluoroferrate(III) complex FeF_6^{3-}. As the NH_4F concentration increases from 1.5 to 2.0 mol dm^{-3} the slope of the curve in Fig. 4 tends to zero, and hence this region was chosen for the determination of Fe(III) because variation in NH_4F concentration would have a minimal effect. At NH_4F concentrations above 2.0 mol dm^{-3}, the signal decreases with increasing NH_4F concentration because of the formation of a white crystalline precipitate.

The relative signal intensities in the spectra of the hydrated Fe(III) ion and the FeF_6^{3-} complex are of major quantitative analytical significance. The FeF_6^{3-} spectrum has a signal intensity ca. 900 times greater than that observed for the spectrum of an equal concentration of hydrated Fe(III) ion. This is a result of the much narrower line widths in the FeF_6^{3-} spectrum (centre line has $\Delta B_{pp} \simeq 11.0$ gauss) compared with that of hydrated Fe(III) ($\Delta B_{pp} \simeq 1100$ gauss). The decrease in line width enables the time required to record the central line in the spectrum of FeF_6^{3-} over 20 gauss, with a field set of 200 gauss, to be reduced by a factor of 10 relative to that required for the recording of the hydrated Fe(III) spectrum over 2000 gauss.

The effect of variation in pH over the range 1.5—13.0 on the signal amplitude was investigated for a solution of Fe(III) (1.0×10^{-3} mol dm^{-3}) and NH_4F (1.5 mol dm^{-3}). Maximum signal was observed at the natural pH (7.0—7.3) of this solution. Adjustment of the pH with $HClO_4$ led to a decrease in A with decrease in pH, probably because of the dissociation of the FeF_6^{3-} complex and the formation of HF. When NaOH was added, A decreased rapidly with increasing pH because of the formation of a reddish-brown precipitate, presumably a hydrated iron(III) oxide [11].

The signal amplitude in spectra of a solution of Fe(III) (1.0×10^{-3} mol dm^{-3}) and NH_4F (2.0 mol dm^{-3}) varied linearly with receiver gain (G). In this

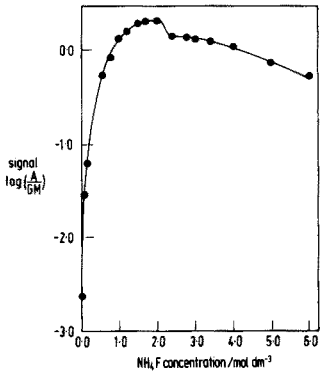

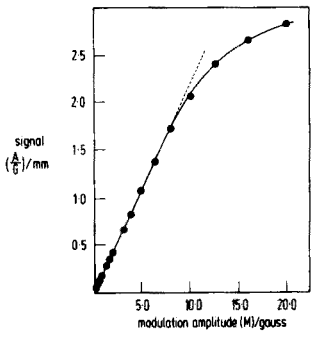

Fig. 4. Variation of log (A/GM) with NH_4F concentration. Fe(III) concentration = 1.0×10^{-2} mol dm^{-3}.

Fig. 5. Variation in signal (A/G) with modulation amplitude (M). Fe(III) concentration = 1.0×10^{-3} mol dm^{-3}. NH_4F concentration = 2.0 mol dm^{-3}.

instance, where relatively narrow line widths are observed, it is important to select a combination of scan time and time constant which avoids distortion of the line shape. The effect of variation in modulation amplitude (M) on the signal amplitude is shown in Fig. 5 for a solution of Fe(III) (1.0×10^{-3} mol dm^{-3}) and NH_4F (2.0 mol dm^{-3}). The magnitude of A/G increases linearly with M for values of $M <$ ca. 8 gauss (Fig. 5). Unlike the situation for the hydrated Fe(III), A/G decreases for M values above 8.0 gauss, presumably through over-modulation effects. To avoid such effects completely, the analytical curve was determined for M values $\leqslant 2.5$ gauss.

Increase in microwave power (P) over the range 5—100 mW led to an increase in A. With the procedure outlined in Part 1 [1] a k value of 0.54 ± 0.02 was determined for a range of concentrations of Fe(III) in 2.0 mol dm^{-3} NH_4F solutions.

With respect to the stability of the signal with time, a freshly prepared solution of Fe(III) (1.0×10^{-3} mol dm^{-3}) and NH_4F (2.0 mol dm^{-3}) showed no variation in signal amplitude over an initial period of 6 h or after 7 d under conditions similar to those used for experiments with iron(III) nitrate solution.

These results were used to establish an analytical curve for a range of concentrations of Fe(III) in 2.0 mol dm^{-3} NH_4F solutions in the form of a plot of A/GMP^k versus Fe(III) concentration as shown in Fig. 6. An analytical range of 1.0×10^{-2}—6.0×10^{-7} mol dm^{-3} with a precision of $\pm 0.45\%$ was calculated for this system; this is a considerable improvement over the values for these parameters obtained earlier for hydrated Fe(III). Precipitation effects determine the upper limit for this range but obviously concentrations of Fe(III) in excess of this value can be determined as hydrated Fe(III) without the use of NH_4F. The narrow width of the FeF_6^{3-}

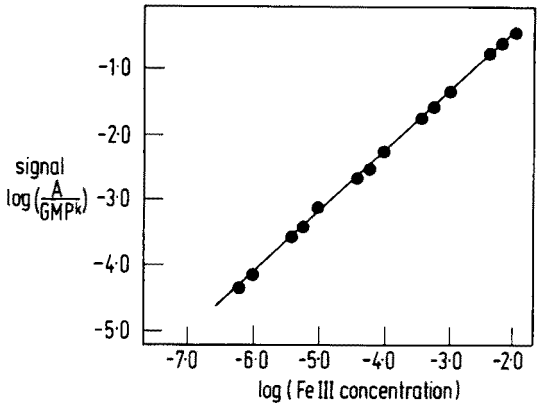

Fig. 6. Plot of log (A/GMP^k) versus log Fe(III) concentration in 2.0 mol dm^{-3} NH_4F aqueous solution.

signal makes it much less susceptible to any background effects arising from the spectrometer cavity compared with the situation for hydrated Fe(III). This enables a limit of detection corresponding to an Fe(III) concentration of 5.0×10^{-8} mol dm^{-3} to be calculated [1] for $P = 20.0$ mW and $M = 2.5$ gauss; this can be improved to 5.1×10^{-9} mol dm^{-3} when P is increased to 100.0 mW and M increased to 10.0 gauss (by accepting slight over-modulation effects).

CONCLUSIONS

By careful control of instrumental variables the analytical range for hydrated Fe(III) by e.s.r. techniques has been calculated to be 5.0×10^{-1} to 5.0×10^{-4} mol dm^{-3} with a precision of ±0.98%. This appears to be the first successful attempt to analyse hydrated Fe(III) by e.s.r. in aqueous solution without complexation. Moyer and McCarthy [4] failed to analyse for Fe(III) quantitatively. Meisel and Guilbault [2] stated that the e.s.r. spectrum of Fe(III) in aqueous solutions "can be used for analytical purposes only with serious limitations". The same authors also attempted [3] to determine Fe(III) in the presence of Cu(II), but concluded that Fe(III) was "practically non-determinable" in aqueous solution. No analytical ranges, precision values or detection limits were given.

However, there still remains the problem of an inherent lack of sensitivity caused by the broad line width in the spectra of hydrated Fe(III). This can be overcome by determining Fe(III) in aqueous 2.0 mol dm^{-3} NH_4F solution, where spectra arising from the formation of FeF_6^{3-} ion have a much narrower line width and hence increased signal amplitude, so that the analytical range is improved. The time required to make a measurement is also significantly less than that required for hydrated Fe(III). The NH_4F system offers advantages over previous techniques [2, 4, 9, 10], including com-

plexation with chloride in a variety of organic solvents [2, 9, 10] or determination in ethanol [4].

The e.s.r. technique is suitable for the determination of a wide range of concentrations of Fe(III) ion in an aqueous environment, and offers advantages over other analytical procedures. The spectrophotometric method involves reduction of Fe(III) to Fe(II) and subsequent complexation with 1,10-phenanthroline to give [19] a limit of detection of ca. 1×10^{-6} mol dm^{-3}. Atomic absorption and atomic fluorescence give [20] a detection limit of 1.8×10^{-6} mol dm^{-3} and determine total iron, rather than Fe(III) specifically.

We thank the Mellor Fund and the New Zealand Universities' Grants Committee for financial support, and Dr. J. K. Grime for useful discussions.

REFERENCES

1 W. G. Bryson, D. P. Hubbard, B. M. Peake and J. Simpson, Anal. Chim. Acta, 77 (1975) 107.
2 T. Meisel and G. G. Guilbault, Anal. Chim. Acta, 50 (1970) 143.
3 G. G. Guilbault and T. Meisel, Anal. Chim. Acta, 50 (1970) 151.
4 E. S. Moyer and W. J. McCarthy, Anal. Chim. Acta, 48 (1969) 79.
5 B. R. McGarvey, J. Phys. Chem., 61 (1957) 1232.
6 L. Burlamacchi, J. Chem. Phys., 55 (1971) 1205.
7 H. Levanon, G. Stein and Z. Luz, J. Am. Chem. Soc., 90 (1968) 5292.
8 A. F. Cotton and G. Wilkinson, Advanced Inorganic Chemistry, 3rd edn., Interscience, New York, 1972, p. 863.
9 G. G. Guilbault and E. S. Moyer, Anal. Chem., 42 (1970) 441.
10 E. S. Moyer, Ph.D. Thesis, University of West Virginia, U.S.A., 1970.
11 J. C. Bailar, H. J. Emeleus, R. S. Nyholm and A. F. Trotman-Dickenson, Comprehensive Inorganic Chemistry, Vol. 3, Pergamon Press, London, 1973, p. 1038.
12 A. K. De, S. M. Khopkar and R. A. Chalmers, Solvent Extraction of Metals, Van Nostrand Reinhold, London, 1970, p. 79.
13 A. I. Vogel, Practical Organic Chemistry, Longmans, London, 1959, p. 174.
14 Technical Manual, E-4 EPR Spectrometer System, 87-125-502 B1271, Varian Analytical Instruments Div., U.S.A., 1973.
15 G. G. Hinckley and L. O. Morgan, J. Chem. Phys., 44 (1966) 898.
16 E. T. Strother, A. Farach and C. P. Poole, Jr., Phys. Rev. A, 4 (1971) 2079.
17 E. S. Moyer and G. G. Guilbault, Anal. Chim. Acta, 52 (1970) 281.
18 H. Levanon, G. Stein and Z. Luz, J. Chem. Phys., 53(3) (1970) 876.
19 J. S. Fritz and G. H. Schenk, Quantitative Analytical Chemistry, Allyn and Bacon, London, 1976, p. 89.
20 G. F. Kirkbright and M. Sargent, Atomic Absorption and Fluorescence Spectroscopy, Academic Press, London, 1974, p. 608.

Analytica Chimica Acta, 96 (1978) 107—115

DETERMINATION OF CHLORINE IN SILICATE ROCKS BY NEUTRON ACTIVATION ANALYSIS

C. K. UNNI* and J.-G. SCHILLING

Graduate School of Oceanography, University of Rhode Island, Kingston, Rhode Island 02881 (U.S.A.)

(Received 20th May 1977)

SUMMARY

A simple radiochemical neutron activation analysis scheme has been developed for the determination of chlorine in silicate rocks. The method involves a 15-min thermal neutron irradiation of rock powder followed by a quick separation of ^{38}Cl as AgCl, and Ge(Li) spectrometry. Chemical yield, normally ranging between 95% and 100%, is monitored gravimetrically through the recovery of AgCl. The procedure has been tested on several geochemical standards to assess its accuracy and precision. The values obtained for standard rocks agree with the literature values. At the 100-ppm level, the analytical precision for chlorine is within ±5% (2σ).

The need to study chlorine-degassing of the earth by volcanism prompted the development of a very sensitive, precise and accurate method for its determination in silicate rocks, particularly basalts. Several analytical methods for chlorine in silicate rocks, based on colorimetry or neutron activation, were found unsatisfactory for this purpose, especially for submarine basalts. Various authors [1—3] have employed colorimetric methods for determining chlorine in geochemical standards and terrestrial rocks, and others [4—7] used neutron activation analysis (n.a.a.) for meteorites, terrestrial rocks, and lunar samples. Colorimetric methods are inherently less sensitive and accurate than n.a.a. in the microgram and sub-microgram ranges and are often subject to the problem of reagent or laboratory contamination.

In spite of its excellent sensitivity, the use of n.a.a. poses certain problems. Of the two stable isotopes, ^{35}Cl and ^{37}Cl, the latter yields the short-lived ^{38}Cl on thermal neutron irradiation (Table 1). The 37.3-min half-life of ^{38}Cl necessitates rapid sample handling and activity determination. Moreover, the ^{24}Na activity produced in irradiated rocks completely masks the γ-ray from ^{38}Cl, thus making it difficult to determine abundances purely by instrumental n.a.a. However, this could be overcome if ^{38}Cl was separated from interfering nuclides, and activity measurements made afterwards. Von Gunten et al. [4] and Reed and Allen [5] used a distillation procedure coupled with chloride precipitation to separate ^{38}Cl from irradiated chondrites before determining its activity through β-counting. Alternatively, Johansen

TABLE 1

Nuclear characteristics of Cl, Na and Fe[a]

Target nuclide	Isotopic abundance (%)	Cross section for n, γ reaction (barn)	Product nuclide	Half-life	γ-ray energy (keV)	γ-ray intensity (%)
$^{37}_{17}Cl$	24.47	0.43	$^{38}_{17}Cl$	37.3 min	1642.7	31
					2167.6	47
$^{23}_{11}Na$	99.99	0.53	$^{24}_{11}Na$	15 h	1368.4	99.999
					2754.1	99.999
$^{58}_{26}Fe$	0.31	1.10	$^{59}_{26}Fe$	45.6 d	1099.3	56.5
					1291.5	43.5

[a]From Filby et al. [8].

and Steinnes [6] and Brunfelt and Steinnes [7] based the separation on silver chloride precipitation and several purification steps before counting the precipitate on NaI(Tl) and Ge(Li) detectors respectively.

This paper describes a fast and reliable thermal neutron activation method involving Ge(Li) spectrometry, after a single chemical separation step of chloride as AgCl, and also an instrumental n.a.a. procedure for chlorine and sodium leached from submarine and sub-aerial basalts. The methods were tested on 8 rock standards supplied by the U.S. Geological Survey, 2 from the Geological Survey of Japan and 2 tholeiitic basalts from Iceland and Reykjanes Ridge.

EXPERIMENTAL

Apparatus

Neutron irradiations were performed at the 2-MW Research Reactor (flux = 4×10^{12} n cm^{-2} s^{-1}) belonging to the Rhode Island Nuclear Science Center. A 35-cm^3 Ge(Li) detector with a resolution of 2.1 keV for the 1332-keV γ-ray of ^{60}Co (efficiency relative to a 3 × 3-in NaI(Tl) detector for the 1332-keV photopeak of ^{60}Co source placed at a distance of 25 cm from the detector was 6.8%) coupled to a 4096-channel Analog—Digital Convertor and magnetic tape readout system was used to acquire the γ-spectra of samples and standards. The activity of the iron wire used for flux monitoring and correction was determined with a 3 × 3-in. well-type NaI(Tl) detector with a resolution of 100 keV for the 1332-keV γ-ray of ^{60}Co (efficiency was 14.5% at 1332 keV in well) attached to a 512-channel analyzer.

Reagents

Chlorine carrier solution (40 mg ml^{-1}). Dry reagent-grade KCl (Baker Analyzed) for 2 h at 110°C and cool in a desiccator. Dissolve 21.031 g in 250 ml of deionized water.

Chlorine standard solution (100 μg ml^{-1}). Dilute 2.5 ml of Cl carrier solution to 1 l with deionized water.

Chlorine standard solution for leachable Cl (16.484 μg ml^{-1}). Dry reagent-grade NaCl (Baker Analyzed) for 2 h at 110°C and cool in a desiccator. Dissolve 1.6484 g in 1 l of water, and further dilute an aliquot 100 times to provide a 10 μg ml^{-1} working standard.

Polythene vials and tubes used for irradiation were washed with alconox—water, soaked in 8 M HNO_3 for 24 h, and rinsed several times with deionized water.

Determination of chlorine in rock powder. Weigh ca. 100 mg of rock powder into a clean 2/5-dram polythene vial and heat-seal. Pipette 1 ml of KCl standard solution (100 μg ml^{-1}) into a clean, thick-walled polythene tube and seal the other end carefully. Attach 6—7 mg of pure iron wire around the sample and standard containers for monitoring neutron flux variations. Irradiate 2 samples and 1 standard simultaneously for 15 min at a thermal flux of 4×10^{12} n cm^{-2} s^{-1} in the rabbit system. Cool for 15—20 min to allow for the decay of ^{28}Al, and separate ^{38}Cl as quickly as possible as follows.

Evaporate 0.5 ml of chlorine carrier in a nickel crucible at 80°C after the addition of 2 drops of 1 M KOH to increase the pH and prevent volatilization of chloride during heating. Transfer the irradiated powder quantitatively from the polythene vial into the nickel crucible, add 5 g of NaOH pellets and fuse over a burner for about 7 min, taking care to avoid spurting. Cool the mixture, add about 15 ml of water, heat, transfer to a 50-ml centrifuge tube and centrifuge to separate the supernatant solution containing chloride, alkalis and silicate from the hydroxide precipitate containing mostly Fe and Mg. Wash the precipitate once with 10 ml of deionized water. Combine the supernatant and wash solutions, add 2 drops of thymol blue indicator (0.04%) and bring the pH to 2 by the addition of concentrated HNO_3 (ca. 8.0 ml). The color changes from blue to pink. Add 2 ml of 1 M $AgNO_3$ solution to the acidified extract and precipitate chloride as AgCl. Filter the precipitate through a pre-treated, tared glass fiber filter (Gelman). Wash several times with 1 M HNO_3, followed by deionized water and acetone. Mount the filter on a petri dish, and count on the Ge(Li) detector for exactly 1000 s. Record γ-spectra on magnetic tape.

To avoid the geometry problem, transfer 0.1 ml of irradiated KCl standard solution from the polythene tube into a centrifuge tube containing 0.5 ml of chlorine carrier solution and precipitate AgCl as before. Count for exactly the same time and in the same position as that of the sample precipitate.

After counting the samples and standards, dry the filters at 110°C for 15 min, cool in a desiccator, and weigh. Monitor the chemical yield in each case from the amount of AgCl recovered. Cool the iron wire flux monitors for 7 d, and record the activity of ^{59}Fe with a NaI detector. Process γ-spectra stored on magnetic tape by the computer program GAMANL [9], which identifies γ-ray photopeaks and integrates their respective areas after subtracting background. Typical γ-spectra of AgCl separated from irradiated KCl standard and rock are given in Fig. 1. Calculate the chlorine content

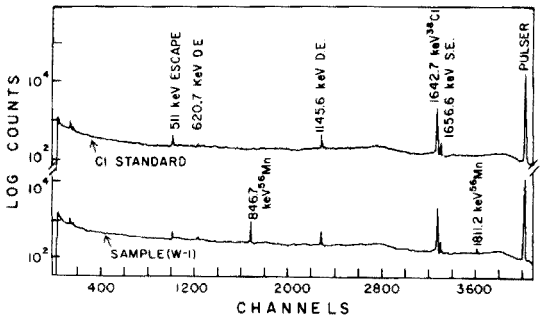

Fig. 1. γ-Spectra of AgCl separated from KCl standard solution and standard rock W-1 irradiated for 15 min and counted for 1000 s. Cl abundances were calculated from the intensity of the 1642.7-keV photopeak.

on the basis of the 1643-keV peak, taking into account decay and dead time corrections, as follows

$$\mathrm{Cl(ppm)} = \frac{A_{\mathrm{sample}}}{A_{\mathrm{std}}} \times \frac{W_{\mathrm{std}}}{W_{\mathrm{sample}}} \times \frac{F_{\mathrm{std}}}{F_{\mathrm{sample}}} \times \frac{E_{\mathrm{std}}}{E_{\mathrm{sample}}} \times \frac{P_{\mathrm{std}}}{P_{\mathrm{sample}}}$$

where,

A_{sample} = decay corrected ^{38}Cl activity of sample, counts/1000 s
A_{std} = decay corrected ^{38}Cl activity of standard, counts/1000 s
W_{sample} = weight of sample (g)
W_{std} = weight of standard (μg)
F_{sample} = specific activity of flux monitor for sample, counts min^{-1} g^{-1}
F_{std} = specific activity of flux monitor for standard, counts min^{-1} g^{-1}
E_{sample} = chemical yield for sample (%)
E_{std} = chemical yield for standard (%)
P_{sample} = pulser counts/1000 s for sample, and
P_{std} = pulser counts/1000 s for standard.

Determination of leachable chlorine

The principal purpose of developing the analytical technique was to determine the concentration of chlorine in submarine basalts. Two components are usually present in submarine basalts: (1) the chlorine content of the magma prior to eruption (intrinsic chlorine), and (2) a component from a subsequent contamination (leachable chlorine) from sea water percolating through the pores and cracks of the rocks after eruption. The procedure for removing leachable chlorine from dredged basalts, described elsewhere [10], involves leaching 0.5 g of rock powder (> 200 mesh) with 15 ml of deionized water, and determining chlorine in the leached residue (intrinsic chlorine) and in the leachate (leachable chlorine). The leachate is also analyzed for sodium to ascertain the sea-water contamination problem. The leaching procedure was also applied to standard rocks even though they were erupted sub-aerially, to find out the amounts of leachable chlorine in them compared with submarine rocks. Leachable Cl and Na are analyzed by the instrumental n.a.a. procedure described below.

Pipette 1 ml of leachate into a clean polythene tube and heat-seal. Pipette 1 ml of NaCl standard solution (10 μg Cl ml^{-1}) into a second polythene tube and seal the other end. Attach 6—7 mg of iron wire as neutron flux monitors to each container. Irradiate 2 samples and 1 standard for 20 min at a flux of 4×10^{12} n cm^{-2} s^{-1}. Cool for 5 min. Pipette 0.5 ml of irradiated standard solution into a 125-ml Erlenmeyer flask, make up the volume to 6.0 ml and count on Ge(Li) detector for exactly 1000 s. Record the γ-spectra on magnetic tape. Transfer the sample solution quantitatively to an Erlenmeyer flask and wash the tube 5 times with 3 M HCl. Make up the volume to 6.0 ml and count on Ge(Li) detector for 1000 s. Typical γ-spectra of irradiated NaCl standard and leachate from rock standard W-1 are given in Fig. 2. Evaporation of standard and sample solutions from the polythene vial during irradiation was not detectable. The transfer of both standard and sample solutions from irradiated vials to clean containers before counting is necessary to reduce the blank problem, as unleached polythene vials contain about 3 ppm chlorine (86% of which is leachable with 8 M HNO_3) [11]. Count and compute the specific activities of the iron wire flux monitors as before. Process the γ-spectra by GAMANL and calculate the amount of leachable chlorine as follows

$$\text{Leachable Cl(ppm)} = \frac{A_{\text{sample}}}{A_{\text{std}}} \times 10 \times \frac{F_{\text{std}}}{F_{\text{sample}}} \times \frac{P_{\text{std}}}{P_{\text{sample}}} \times 30$$

where A denotes decay-corrected activity, F specific activity of flux monitor, and P pulser counts for dead time corrections.

RESULTS AND DISCUSSION

The total and leachable chlorine contents of the standard rocks analyzed, and the literature values, are reported in Table 2. The results are in close agreement with those reported by Johansen and Steinnes [6] by n.a.a. With

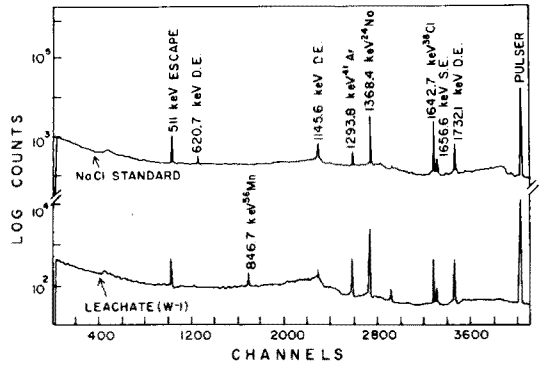

Fig. 2. γ-Spectra of NaCl standard solution and leachate from W-1 irradiated for 20 min and counted for 1000 s. Cl and Na in leachate were determined from the intensities of the 1642.7-keV and 1368.4-keV peaks, respectively.

TABLE 2

Chlorine content of rocks

Sample	Description	Total Cl (ppm)				Intrinsic Cl (ppm)	Leachable Cl (ppm)	Leachable Cl (%)
		Present work	Johansen and Steinnes [6]	Flanagan [12]	Others[a]			
BCR-1	Basalt	59 58	58	50	62 and 120	51	8	14
W-1	Diabase	215 216	206	200	26—270	156	60	28
AGV-1	Andesite	100	115	110	185 and 319	85	15	15
GSP-1	Granodiorite	310 295 298	311	300	342 and 365	257	41	14
DTS-1	Dunite	11 9 10	9.4	11	20 and 33	5	5	50
PCC-1	Peridotite	70 73 72	66	60	65—100	62	10	14
G-1	Granite	55		70	19—130	34	21	38
G-2	Granite	59	53	50	120 and 192	39	20	34
JG-1	Granodiorite	57		200	57 and 200	42	15	26
JB-1	Basalt	172		190	190	147	25	15
IC-58	Icelandic Tholeiite	101 98 98 99				93	6	6
TR41-19D	Reykjanes Ridge Tholeiite	82 80 81				74	7	9

[a]Quoted by Fleischer [13], Flanagan [14] and Ando et al. [15].

the exception of JG-1, our total chlorine values agree with those suggested by Flanagan [12]. For JG-1, our total chlorine content of 57 ppm is in agreement with the 57 ppm found by n.a.a. by Ando et al. [15]. A value of 200 ppm for JG-1 by a colorimetric method [15] appears to be in error. The present results for total chlorine for G-1, W-1, BCR-1, GSP-1 and PCC-1 agree fairly well with the extensive spectrophotometric determinations of Huang and Johns [3] who report, however, very high values for G-2, AGV-1, and DTS-1; high values were also reported for BCR-1, PCC-1, DTS-1, AGV-1, G-2 and JB-1 [14].

The total chlorine values obtained are similar to those obtained by n.a.a. as reported by Flanagan [12] and Ando et al. [15]. Reed and Allen [5] obtained 19 ppm for G-1 and 25 ppm for W-1 by n.a.a. These values appear to in error, and systematically low in comparison with the present values of 55 ppm for G-1 and 216 ppm for W-1 as well as with the values of 70 ppm for G-1 and 200 ppm for W-1 suggested by Flanagan [12]. Johansen and Steinnes [6] also observed this discrepancy in G-1 and W-1 values reported by Reed and Allen. Suspecting that the chlorine content of 210 ppm in W-1 might be due to external contamination, Johansen and Steinnes conducted leaching experiments similar to those of Reed and Allen. As means of 4 runs, they obtained only 30 ± 5% leachable chlorine and concluded that the high value was unlikely to be due to external contamination. Our value of 28% for leachable chlorine is similar to that of Johansen and Steinnes, and confirms their conclusion.

The amount of leachable chlorine varies between 6% and 50% of the total for all the rocks analyzed. In general, slowly-cooled, coarse grained rocks like granites and granodiorites and, to a lesser extent diabase, appear to yield higher leachable chlorine than the rapidly-cooled, fine grained silicates such as basalts. Slow cooling probably results in retention of chloride compounds at interstitial grain boundaries, as most of the chloride is likely to remain in the residual fluids during crystallization. At extremely high chloride concentrations, chloride appears in fluid inclusions as reported for granites from Ascension Island [16]. Leachable chlorine varies between 0 and 23% for Icelandic basalts. In contrast, submarine basalts from Reykjanes Ridge and some Hawaiian basalts exhibit up to 90% leachable chlorine which can be definitely attributed to sea-water contamination [10]. According to Kuroda and Sandell [17], Iwasaki and Katsura [18], and Sugiura [19] the amount of water-soluble chlorine is generally small (<30%), compared with total chlorine, in fresh and uncontaminated rocks.

The precision for replicate analyses falls within ±5% (2σ) for a chlorine content of about 100 ppm, and includes counting statistics. The accuracy of the method is good, as indicated by the previous inter-laboratory comparison of rock standards. The method has a sensitivity as low as 10 ppb. Systematic errors from neutron shielding effects and interfering nuclear reactions such as ^{41}K (n,α) ^{38}Cl are negligible, and are within experimental error. Elements of high neutron absorption cross-sections are not present in significant

concentrations either in the samples or standards, and the contribution from the fast neutron flux in the rabbit system where specimens are irradiated is only about 3%.

In a 15-min irradiation of silicate rocks, ^{28}Al, ^{56}Mn and ^{24}Na are the dominant nuclides which interfere with chlorine analysis. During the 20-min cooling period, ^{28}Al ($t_{\frac{1}{2}}$ = 2.3 min) decays, leaving ^{24}Na and ^{56}Mn. Radiochemical separation removes ^{24}Na completely, whereas small amounts of ^{56}Mn ($t_{\frac{1}{2}}$ = 2.58 h) are adsorbed on to AgCl. This is not a serious problem since the γ-rays from ^{56}Mn (847, 1811 and 2113 keV) do not interfere with the 1643 and 2168-keV γ-rays of ^{38}Cl in the high-resolution (2.1 keV) Ge(Li) spectrometer used. Figure 1 shows the γ-spectra of AgCl separated from Cl standard and W-1. For all calculations the 1643-keV peak was used.

The analytical procedure developed is fast, precise and accurate for chlorine in the ppm and ppb ranges in silicate rocks. It may be applied to other systems with little or no modification. Twelve samples and 6 standards could be irradiated, processed, and counted by a single person in 8—10 h. The method offers an advantage over existing ones in that the sample fusion is followed by only a single separation step before counting of the AgCl precipitate in a Ge(Li) spectrometer. Complete exchange between ^{38}Cl and Cl carrier during sample fusion is assumed on the basis of the observation of Owens and Rowland [20]. Chemical yield of the AgCl recovered normally ranges between 95 and 100%. Yield determinations could be dispensed with if high accuracies are not called for and proper precautions are observed. Most of the n.a.a. methods published consist of sample fusion and several purification steps including double AgCl precipitation before either beta or gamma counting of the precipitate. Chemical yields in these instances are only 60—80% compared with our value of 95—100%. With the advent of high resolution Ge(Li) spectrometers it is not necessary to perform the elaborate chemical separations employed by previous investigators who used β-counting techniques or γ-counting with low resolution NaI(Tl) detectors.

The method described has been successfully applied to a study of basalts from Iceland, Reykjanes Ridge and Hawaii [10].

We thank A. F. DiMeglio and staff of the Rhode Island Nuclear Science Center for providing facilities for this work, and P. R. C. McMahon for typing the manuscript. This research was supported by the National Science Foundation, under NSF Grant OCE 76-01577.

REFERENCES

1 P. K. Kuroda and E. B. Sandell, Anal. Chem., 22 (1950) 1144.
2 I. Iwasaki, S. Utsumi, K. Hayino and T. Ozawa, Bull. Chem. Soc., Jpn., 24 (1956) 860.
3 W. H. Huang and W. D. Johns, Geochim. Cosmochim. Acta, 31 (1967) 597.
4 H. R. Von Gunten, A. Wyttenbach and W. Scherle, Geochim. Cosmochim. Acta, 29 (1965) 475.

5 G. W. Reed, Jr. and R. O. Allen, Jr., Geochim. Cosmochim. Acta, 30 (1966) 779.
6 O. Johansen and E. Steinnes, Geochim. Cosmochim. Acta, 31 (1967) 1107.
7 A. O. Brunfelt and E. Steinnes, Talanta, 18 (1971) 1197.
8 R. H. Filby, A. I. Davis, K. R. Shah, G. G. Wainscott, W. A. Haller and W. A. Cassatt, Gamma-ray energy tables for neutron activation analysis, Washington State University, 1970.
9 J. L. Fasching, private communication, 1971.
10 C. K. Unni, Ph.D. Thesis, University of Rhode Island, 1976, p. 272.
11 R. W. Karin, J. A. Buono and J. L. Fasching, Anal. Chem., 47 (1975) 2296.
12 F. J. Flanagan, Geochim. Cosmochim. Acta, 37 (1973) 1189.
13 M. Fleischer, Geochim. Cosmochim. Acta, 33 (1969) 65.
14 F. J. Flanagan, Geochim. Cosmochim. Acta, 33 (1969) 81.
15 A. Ando, H. Kurasawa, T. Ohmori and E. Takeda, Geochem. J., 5 (1971) 151.
16 E. Roedder and D. S. Coombs, J. Petrol., 8 (1967) 417.
17 P. K. Kuroda and E. B. Sandell, Geol. Soc. Am. Bull., 64 (1953) 879.
18 B. Iwasaki and T. Katsura, Bull. Chem. Soc. Jpn., 37 (1964) 1827.
19 T. Sugiura, Bull. Chem. Soc. Jpn., 41 (1968) 1133.
20 C. W. Owens and F. S. Rowland, J. Inorg. Nucl. Chem., 24 (1962) 133.

Analytica Chimica Acta, 96 (1978) 117—123

SIMULTANEOUS DETERMINATION OF GALLIUM AND GERMANIUM IN IGNEOUS ROCKS BY NEUTRON ACTIVATION

ROBERTO M. ARGOLLO† and J.-G. SCHILLING*

Graduate School of Oceanography, University of Rhode Island, Kingston, Rhode Island 02881 (U.S.A.)

(Received 1st June 1977)

SUMMARY

A neutron activation technique for determining gallium and germanium in igneous rocks is described. After irradiation, germanium is separated from interfering activities by extraction with carbon tetrachloride from 9 M HCl solution. Gallium is extracted from 6 M HCl solution into isopropyl ether. Germanium and gallium activities are determined by counting the radionuclides ^{77}Ge and ^{72}Ga, respectively. Chemical yields are determined by re-irradiation of separated solutions. About 12 man-hours are necessary to process 6 samples, excluding re-irradiation. Precision of the analysis for both elements is ±2—3% for concentrations encountered in typical igneous rocks. The detection limits for a thermal neutron flux of 4×10^{12} n cm^{-2} s^{-1} are about 0.0005 ppm for gallium and 0.01 ppm for germanium with an error of ±50%.

Gallium and germanium are trace elements of great geochemical interest because of their crystallochemical similarity to the major elements Al and Si, respectively. Ga can substitute for Al and Ge for Si in silicate minerals, and the study of the ratios Ga/Al and Ge/Si in igneous rocks may provide important clues regarding the geochemical processes during crust—mantle evolution [1]. Variations in the concentration of Ga and Ge are very small and the abundances of these elements are low relative to those of Al and Si; Ga and Ge concentrations in igneous rocks must therefore be determined with great sensitivity and precision.

Gallium has been determined by neutron activation in igneous rocks [1—6], in meteorites [2, 4, 5, 7, 8] and lunar materials [2], and by spectrometric methods in igneous rocks [9] and terrestrial materials [10, 11]. Germanium has been determined by neutron activation in igneous rocks [1, 2, 4, 5, 12], in meteorites [2, 4, 5, 7, 8] and lunar materials [2], and in terrestrial materials by spectrophotometry [10] or by colorimetry [13].

Methods for the simultaneous determination of Ga and Ge in geological materials and meteorites by neutron activation have been reported [1, 2, 4, 5, 7, 8]. Most of these methods [2, 5, 7, 8] have been developed for iron

†Present address: Programa de Pesquisa e Pós-Graduação em Geofísica Instituto de Física, Universidade Federal da Bahia, 40.000 Salvador Bahia, Brasil.

meteorites and similar materials which require only a short cooling time before handling of the samples and use a short-lived (82 min) ^{75}Ge nuclide for Ge determination; these methods have limited applications in rock analysis because of the high radioactivity (e.g. 2.56-h ^{56}Mn) produced from elements commonly present in these rocks.

A new neutron activation method, developed for simultaneous determination of Ga and Ge in igneous rocks and similar materials, makes use of the long-lived 14.1-h ^{72}Ga and 11.3-h ^{77}Ge nuclides (Table 1).

The samples and standards are irradiated for ca. 7 h in a thermal neutron flux of 4×10^{12} n cm^{-2} s^{-1}. After cooling for 16 h, the samples, consisting of 0.5 g of powdered rock, are dissolved in the presence of gallium and germanium carriers. The solution is transferred to a separatory funnel with 9 M HCl, and germanium is extracted into carbon tetrachloride [14]. The solution is then diluted to 6 M HCl with water and gallium is extracted into isopropyl ether [11]. The γ-ray activity is determined, as soon as the separation is completed, with a well-type NaI(Tl) crystal. The two-step solvent extractions are fast and simple.

The samples analysed are a series of standard igneous rocks kindly provided by the U.S. Geological Survey and by the Geological Survey of Japan. These include the basalts JB-1 and BCR-1, peridotite PCC-1, the andesite AGV-1, and the granites JG-1 and G-2.

EXPERIMENTAL

Apparatus

The γ-spectra were obtained with a 3 × 3-in. well-type NaI(Tl) crystal connected to a Nuclear Data 512-channel analyzer. The activities of the flux monitors were determined with a similar detector connected to a scaler.

Chemicals

Gallium carrier (4.4 mg ml^{-1}) and gallium standard (35 μg ml^{-1}) were prepared by dissolving 99.999% pure gallium metal in a mixture (2 + 1) of concentrated sulfuric acid and 72% perchloric acid heated below the boiling point on a sand bath or temperature-controlled hot plate. Germanium carrier (1.0 mg ml^{-1}) and germanium standard (10.2 μg ml^{-1}) were prepared by dissolving 99.999% pure germanium metal in 3 M nitric acid heated below its boiling point, as above.

TABLE 1

Nuclear data

Element	Activation reaction	Abundance of the active isotope (%)	Cross section (barns)	Half-life (h)	γ-energy used (keV)
Ga	^{71}Ga(n,γ)^{72}Ga	39.80	5.00	14.1	834
Ge	^{76}Ge(n,γ)^{77}Ge	7.67	0.1	11.3	211, 215, 264

Carriers and standards were prepared by dilution of the stock solutions with 3 M doubly distilled HCl.

Treatment of samples and standards for irradiation

About 0.5 g of rock powder was weighed into 2/5 dram polyethylene vials, which were sealed by heating. The Ga and Ge standard solutions (1.0 ml) were pipetted into separate polyethylene tubes (3/8-in. i.d., 6 cm long) and sealed as above. Iron wire flux monitors were used on the vials and tubes. Samples and standards were irradiated together for 7 h at a thermal neutron flux of 4×10^{12} n cm^{-2} s^{-1}.

Radiochemical separation steps

After allowing the irradiated samples to cool for 16 h to eliminate the short-lived activities, mainly 2.56-h ^{56}Mn, they were transferred quantitatively to Teflon beakers together with 0.5 ml of Ga carrier (ca. 2.5 mg) and 1 ml of Ge carrier (ca. 1.0 mg). Samples were decomposed in a hood with lead brick shielding, with a mixture of sulfuric, nitric and hydrofluoric acids [14].

Germanium separation and determination

Germanium was separated by a modification of the methods described by Burton et al. [10] and Schneider and Sandell [14]. After decomposition, the residue was transferred with 9 M hydrochloric acid to a 250-ml separatory funnel. Germanium was extracted twice with 10 ml of carbon tetrachloride and the hydrochloric acid solution was saved for gallium separation. The temperature was kept below 25°C to prevent loss of germanium tetrachloride by volatilization. The organic phase was washed twice with 10 ml of 11 M HCl and germanium was back-extracted from it with 10 ml of water. The aqueous solution was drained into a 100 × 17 mm polypropylene test-tube. The irradiated Ge standard was centrifuged and transferred quantitatively to a similar test-tube. A few drops of concentrated nitric acid were added to the tubes; a fixed volume was kept for the samples and standards. The tubes were stoppered tightly and were γ-counted.

Gallium separation and determination

Gallium was separated by a modification of the methods described by Burton et al. [10] and Culkin and Riley [11]. After germanium separation, the hydrochloric acid solutions were made 6 M in HCl and 2 ml of 20% titanium trichloride were added to reduce all Fe(III) to Fe(II). Gallium was extracted twice with 15 ml of isopropyl ether. The ethereal layer was washed twice, first with a mixture of 1 ml of 7 M HCl and 0.5 ml of titanium trichloride, and secondly with 1 ml of 7 M HCl. Gallium was back-extracted with 15 ml of water, and the aqueous layer was drained into a 100 × 17 mm polypropylene test-tube. The gallium extracts and the irradiated Ga standard were treated as for germanium. An aliquot (0.5 ml) was taken for γ-counting.

Activity measurements

The radioactive nuclides measured are listed in Table 1. The 834-keV γ-peak was integrated to determine the ^{72}Ga activity and decay corrections were made in terms of a 14.1-h half-life. ^{77}Ge activity was obtained by integrating the 211, 215 and 264-keV γ-peaks and decay corrections were made in terms of a 11.3-h half-life. The contribution of 199 and 265-keV γ-peaks from the 82 min. ^{75}Ge was negligible after cooling for 18 h, as can be seen in Fig. 2.

Determination of chemical yield

Chemical yields were determined by re-irradiation. Four days after the original activity measurements, 1 ml of each extract was irradiated in polyethylene tubes with attached flux monitors in a thermal neutron flux of 4×10^{12} n cm^{-2} s^{-1}; irradiation times were 15 min for gallium extracts and standard, and 4 h for germanium extracts and standard. The solutions were transferred to test tubes as described above, and aliquots were taken for γ-counting.

RESULTS AND DISCUSSION

Typical γ-ray spectra of Ga and Ge for sample extracts and standards are shown in Figs. 1 and 2, respectively. In Fig. 1, the two small peaks at 1.10 MeV and 1.29 MeV in the sample spectrum are due to 45-d ^{59}Fe, which remains in very small amount in the gallium extract. Nevertheless, these do not interfere with the ^{72}Ga 834-keV peak used for gallium determination.

The germanium spectrum of the sample (Fig. 2) shows a slight contamination by active sodium, but these activities do not affect the Ge determination with the 211, 215 and 264-keV 11.3-h ^{77}Ge peaks. Germanium spectra of a re-irradiated extract were taken after cooling for 18 and 30 h; a portion of these are shown by spectra 1 and 2 in Fig. 2. The identical shapes of the spectra show that the contribution of 199 and 265-keV γ-peaks from the 82-min ^{75}Ge was negligible. Other interferences may occasionally be encountered. Interference by bromine was found in the analysis of a bromine-containing sediment; bromine is extracted into both carbon tetrachloride and isopropyl ether and the 554, 519, 698-keV 35.3-h ^{82}Br shadowed the ^{72}Ga and ^{77}Ge peaks.

The results obtained for gallium and germanium in the standard rocks are presented in Table 2, which also shows a comparison with Flanagan's recommended values [15] and with the values obtained by other researchers with neutron activation reactions such as ^{72}Ge(n,p)^{72}Ga; ^{75}As(n,α)^{72}Ga and ^{80}Se(n,α)^{77}Ge should be considered when the nuclides ^{72}Ga and ^{77}Ge are used. However, these interferences are small [5] and may be neglected because of the low cross-sections for these reactions in a thermal neutron flux and the low concentration of arsenic and selenium usually found in

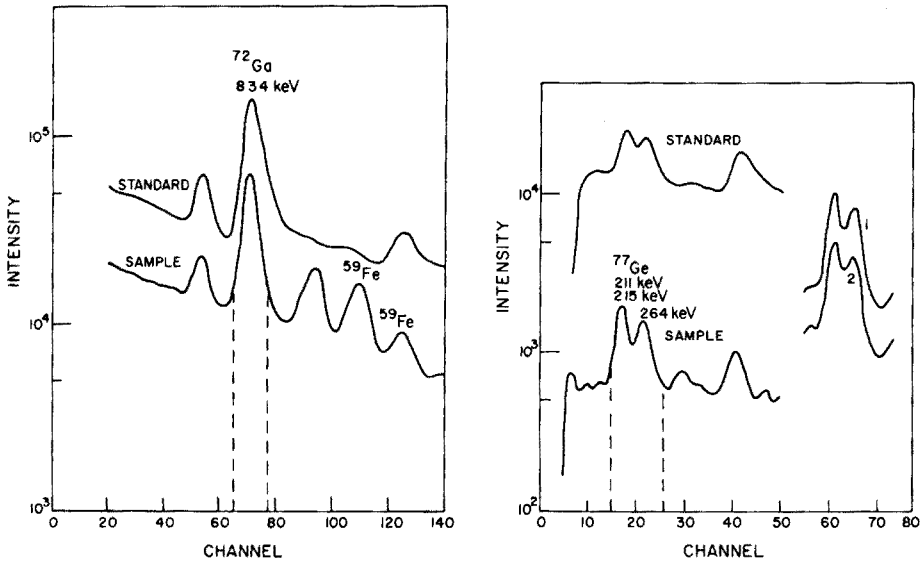

Fig. 1. Gallium spectra for a typical sample (lower) and standard (upper). Dashed lines indicate the channels taken for peak integration.

Fig. 2. Germanium spectra for a typical sample (left lower) and standard (left upper). Dashed lines indicate the channels taken for peak integration. (Right) a portion of the Ge spectra for a typical re-irradiated Ge extract obtained after 18 h (spectrum 1) and 30 h (spectrum 2) of cooling; the peaks are those shown in the sample spectrum. The identical shape of the two spectra shows that only the 11.3-h ^{77}Ge nuclide is involved, with no contribution from ^{75}Ge.

igneous rocks. Other interfering activities (e.g. by bromine) can be detected by careful analysis of the spectra.

The method described is sufficiently sensitive for determining Ga and Ge, not only in igneous rocks, but also, with appropriate modification, in many other terrestrial materials and meteorites. With 0.5 g of igneous rock sample and a 7-h irradiation in a thermal neutron flux of 4×10^{12} n cm^{-2} s^{-1}, the detection limits are estimated to be about 0.0005 ppm for Ga and 0.01 ppm for Ge, with a precision of ca. ±50%. One person is able to analyse 6 samples in 12 h, including extraction and counting of samples and standards; all germanium extractions can be completed in the first 5 h and the gallium extractions in the following 3 h.

TABLE 2

Comparison of present results for USGS and GSJ Standard Rocks with recommended and other values
(All results are given in ppm.)

Element	Standard rock	Present work	Recommended values [15]	Previous n.a.a. values and references
Ga	JB-1	18.1 ± 0.8(7)[a]	17	—
	BCR-1	24.0 ± 0.8(3)[a]	20	24 [6], 20.6 [2], 22.2 [3], 20.7 [4], 16.2 [17]
	PCC-1	0.46, 0.52	0.4	1.3 [6], 0.32 [4], 1.2 [17]
	AGV-1	24.0	20.5	21 [6], 21 [3], 23.6 [4], 16.6 [1
	JG-1	20.0, 20.9	20	—
	G-2	23.4, 22.8	22.9	24 [6], 22.0 [2], 22.5 [3], 24.5 [4], 28 [17]
Ge	JB-1	1.33 ± 0.08(7)[a]	—	—
	BCR-1	1.40 ± 0.08(3)[a]	1.54	1.6 [2], 1.46 [16]
	PCC-1	0.82, 1.03	0.9	—
	AGV-1	1.20	1.3	—
	JG-1	1.34, 1.29	1	—
	G-2	1.10, 1.15	1.15	1.2 [2]

[a]These results are mean values, and the errors quoted correspond to two standard deviations; the number of determinations is given in parentheses.

We thank C. K. Unni and David G. Johnson for assistance in the laboratory work. We are grateful for the use of facilities at Rhode Island Nuclear Sciences Center and the excellent cooperation of F. Di Meglio and his staff for neutron irradiations. We thank David L. Thurber for reading the original manuscript. This work forms part of a thesis submitted by R. M. A. in partial fulfillment of requirements for the M.S. degree, University of Rhode Island. The work was made possible by the award of a fellowship to R. M. A. from UNESCO, through Projects BRA-4 and BR-324, and by support from Universidade Federal da Bahia. The laboratory work was supported by NFS Grant GA 36672X.

REFERENCES

1 R. M. Argollo, Ga—Al and Ge—Si in volcanic rocks, M.S. Thesis (1974), University of Rhode Island.
2 J. T. Wasson and P. A. Baedecker, in Proc. Apollo 11 Lunar Sci. Conf., Geochim. Cosmochim. Acta, Suppl. 1 (1970) 1741.
3 O. Johansen and E. Steinnes, Talanta, 17 (1970) 407.
4 J. C. Laul, D. R. Case, M. Wechter, F. Schmidt-Bleek and M. E. Lipschutz, J. Radioanal. Chem., 4 (1970) 241.
5 K. F. Fouché and A. A. Smales, Chem. Geol., 2 (1967) 5.
6 A. O. Brunfelt, O. Johansen and E. Steinnes, Anal. Chim. Acta, 37 (1967) 172.
7 S. N. Tandon and J. T. Wasson, Geochim. Cosmochim. Acta, 32 (1968) 1087.

8 J. T. Wasson and J. Kimberlin, Radiochim. Acta, 5 (1966) 170.
9 R. J. Goodman, Geochim. Cosmochim. Acta, 36 (1972) 303.
10 J. D. Burton, F. Culkin and J. P. Riley , Geochim. Cosmochim. Acta, 16 (1959) 151.
11 F. Culkin and J. P. Riley, Analyst, 83 (1958) 208.
12 D. F. C. Morris and J. S. P. Batchelor, Geochim. Cosmochim. Acta, 30 (1966) 737.
13 S. A. El Wardani, Geochim. Cosmochim. Acta, 37 (1958) 1189.
14 W. A. Schneider and E. B. Sandell, Mikrochim. Acta, (1954) 263.
15 F. J. Flanagan, Geochim. Cosmochim. Acta, 37 (1973) 1189.
16 U. Krähenbühl, J. W. Morgan, R. Ganaphathy and E. Anders, Geochim. Cosmochim. Acta, 37 (1973) 1353.
17 R. H. Filby, W. A. Haller and K. R. Shah, J. Radioanal. Chem., 5 (1970) 277.

Analytica Chimica Acta, 96 (1978) 125—132

DIAGRAMME POTENTIEL—pO^{2-} DU NEPTUNIUM DANS L'EUTECTIQUE LiCl—KCl A 660°C

R. LYSY[§] et G. DUYCKAERTS*

Laboratoire de Chimie analytique et Radiochimie, Université de Liège au Sart-Tilman, B-4000 Liège (Belgique)

(Reçu le 1 juillet 1977)

RÉSUMÉ

Le produit de solubilité de NpO_2 dans l'eutectique LiCl—KCl a été déterminé à 660°C par titrage potentiométrique au moyen d'une électrode indicatrice en zircone. Sur cette base et en utilisant certaines données plus récentes sur les potentiels normaux des différents couples oxydo—réducteurs, il a été possible d'établir un nouveau diagramme potentiel d'oxydo—réduction (E) du neptunium en fonction de pO^{2-} dans l'eutectique LiCl—KCl à 660°C.

SUMMARY

Potential—pO^{2-} diagram of neptunium in the LiCl—KCl eutectic at 660°C

The solubility product of NpO_2 in the LiCl—KCl eutectic at 660°C has been determined by potentiometric titration with a zircone indicator electrode. With this new value and several other recent values of standard potentials, it became possible to establish the E—pO^{2-} diagram for neptunium in this eutectic.

Le diagramme du potentiel d'oxydo—réduction (E) du neptunium en fonction de la concentration en ions oxyde (pO^{2-}) dans un bain fondu de LiCl—KCl (eutectique) a été publié [1]. Toutefois, une étude ultérieure des propriétés oxydo—réductrices du neptunium dans les bains de chlorures alcalins a mis en évidence un certain nombre de faits en contradiction avec ce diagramme:

1. La valeur du potentiel normal du couple Np(IV)—Np(III) déterminée par Martinot et al. [2] à 450°C dans l'eutectique LiCl—KCl (—1,55 V par rapport à la référence Cl_2—Cl^-) est très différente de celle que l'on obtient par interpolation entre les valeurs correspondantes de l'uranium [3] et du plutonium [4] par la méthode de linéarisation de Nugent et al. [5] (—0,74 V/Cl_2—Cl^-);

2. Contrairement aux prévisions du diagramme en question, il est possible d'étudier l'équilibre NpO_2(V)—Np(IV) à 400°C dans un domaine de pO^{2-} voisin de 13 [6];

[§] Chercheur agréé à l'Institut Interuniversitaire des Sciences Nucléaires.

3. Il est possible d'obtenir, par une méthode indirecte, le produit de solubilité de NpO_2 à partir du potentiel normal du couple $NpO_2(V)—NpO_2\downarrow$ [7], de la constante d'équilibre de la réaction $NpO_2^+ + 4\,HCl \rightleftarrows Np^{4+} + 2H_2O + \frac{1}{2}Cl_2 + 3Cl^-$ [8] et de la constante d'équilibre de la réaction $H_2O + 2Cl^- \rightleftarrows 2HCl + O^{2-}$ [9]. La valeur ainsi calculée vaut $10^{(-24,6\pm2,0)}$ $mol^3\,l^{-3}$ à 400°C [6] alors que la valeur expérimentale déterminée par Martinot et Duyckaerts [1] vaut $10^{-10,5}$. Cette dernière valeur avait été obtenue en mesurant, par voie radiométrique, la teneur en Np(IV) d'une solution saturée en NpO_2.

Dans ces conditions, il nous a paru important de vérifier un certain nombre de données fondamentales pour pouvoir établir un diagramme d'oxydo—réduction versus pO^{2-} plus correct. Nous nous proposons de présenter les résultats d'une nouvelle détermination du produit de solubilité de NpO_2 obtenus par titrage par précipitation et d'établir le nouveau diagramme $E—pO^{2-}$ du neptunium dans l'eutectique LiCl—KCl à 660°C basé sur cette nouvelle valeur et sur d'autres déterminations nouvelles de potentiels normaux.

PARTIE EXPERIMENTALE

Le dispositif de titrage potentiométrique ayant, servi à déterminer le produit de solubilité de NpO_2, est de conception identique à celui mis au point par Combes et al. [10]. Il comprend: une cellule électrochimique composée d'un creuset en alumine frittée contenant une électrode indicatrice en zircone, une électrode de référence (fil d'argent plongeant dans une solution d'AgCl dans l'eutectique LiCl—KCl contenue dans une gaine en alumine), un capillaire d'amenée des gaz réactionnels et un dispositif d'introduction du réactif titrant; ces divers éléments sont enfermés dans une enceinte en quartz permettent le travail en atmosphère contrôlée; une rampe à gaz; un four régulé à ±2°C, et un millivoltmètre Tacussel à haute impédance.

L'installation spectrophotométrique permettant la détermination des potentiels normaux a été décrite de manière détaillée dans plusieurs publications antérieures [8, 11, 12]. Il en va de même pour la préparation des réactif (Cs_2NpCl_6), solvant (LiCl—KCl) et solutions [13].

RESULTATS EXPERIMENTAUX

Détermination du produit de solubilité de NpO_2

Le produit de solubilité de NpO_2 peut être obtenu par titrage potentiométrique d'une solution de Np(IV) dans l'eutectique LiCl—KCl par l'oxyde de lithium, la réaction étant

$$Np^{4+} + 2O^{2-} \rightarrow NpO_2\downarrow \qquad (1)$$

A la solution de concentration connue de Np(IV) introduit sous la forme de Cs_2NpCl_6, on ajoute des quantités croissantes de Li_2O et on suit potentiométriquement l'évolution du pO^{2-}, le potentiel de l'électrode indicatrice de la pile

Ni, NiO // Zircone // O^{2-} + LiCl—KCl // Al_2O_3 // AgCl + LiCl—KCl / Ag

étant donné par les relations suivantes:

$$x < 100, E_1 = A - \frac{2{,}3\,RT}{4F} \log L + \frac{2{,}3\,RT}{4F} \log [Np^{4+}]_0 \left(\frac{100 - x}{100}\right) \quad (2)$$

$$x = 100, E_{\text{équivalent}} = A - \frac{2{,}3\,RT}{6F} \log 2L \quad (3)$$

$$x > 100, E_2 = A - \frac{2{,}3\,RT}{2F} \log 2[Np^{4+}]_0 \left(\frac{x - 100}{100}\right) \quad (4)$$

avec $[Np^{4+}]_0$ = la concentration initiale de la solution titrée, x le taux de titrage exprimé en pourcentage du point équivalent et A étant un terme constant dépendant du potentiel normal de l'électrode à ion oxyde, du potentiel de jonction et du potentiel de la référence.

Les résultats relatifs à différents titrages dans l'eutectique LiCl—KCl à 660°C sont consignés au Tableau 1. Le Tableau 2 montre que les pentes expérimentales des courbes de titrage avant comme après le point équivalent (E en fonction du degré d'avancement du titrage: relations (2) et (4)) satisfont, dans les limites des erreurs, à celles des formules en question.

La valeur du terme A dans les relations (2)—(4) n'est pas connue; dès lors, nous calculons le produit de solubilité $L = [Np^{4+}]\ [O^{2-}]^2$ à partir de la

TABLEAU 1

Titrages potentiométriques dans l'eutectique LiCl—KCl à 660°C

$[Np^{4+}]_0 \cdot 10^2$ (mol l^{-1})	E_1 ind. (V)	$\log [Np^{4+}]_0 \left(\frac{100 - x}{100}\right)$	E_2 ind. (V)	$\log 2[Np^{4+}]_0 \left(\frac{x - 100}{100}\right)$
2,22	0,292	−1,792	−0,316	−2,041
	0,283	−2,059	−0,432	−1,650
	0,113	−2,849	−0,446	−1,420
			−0,458	−1,254
			−0,488	−1,122
1,97	0,257	−1,853	−0,311	−1,895
	0,241	−2,095	−0,349	−1,548
	0,012	−3,172	−0,370	−1,350
			−0,378	−1,217
3,45	0,174	−1,509	−0,479	−2,130
	0,162	−1,730	−0,537	−1,495
	0,150	−2,046	−0,556	−1,276
	0,134	−2,437	−0,568	−1,160
			−0,577	−1,061
			−0,575	−0,869
2,11	0,593	−1,766	−0,100	−1,785
	0,584	−1,959	−0,130	−1,403
	0,557	−2,569	−0,145	−1,228
			−0,158	−1,105

TABLEAU 2

Evolution du potentiel de l'électrode indicatrice en fonction du degré d'avancement du titrage de Np(IV) par (O^{2-})

$[Np^{4+}]_i \cdot 10^2$ (mol l^{-1})	E_1 en fonction de $\log [Np^{4+}]_0 \left(\frac{100-x}{100}\right)$ Pente expérimentale[a]	E_2 en fonction de $\log 2[Np^{4+}]_0 \left(\frac{x-100}{100}\right)$ Pente expérimentale[b]
2,22	0,034	(—0,099 ± 0,048)
1,97	0,066	(—0,089 ± 0,026)
3,45	(0,042 ± 0,006)	(—0,093 ± 0,006)
2,11	(0,045 ± 0,002)	(—0,084 ± 0,011)

[a]Pente théorique = +0,0463.
[b]Pente théorique = —0,0926.

relation suivante, résultant de la différence entre les formules (2) et (4)

$$\log L = \frac{E_2 - E_1}{2{,}3\, RT/4F} + 2\log 2[Np^{4+}]_0 \left(\frac{x-100}{100}\right) + \log [Np^{4+}]_0 \left(\frac{100-x}{100}\right) \quad (5)$$

Le Tableau 3 reprend les valeurs moyennes de $L[NpO_2]$ ainsi calculées. La Fig. 1 montre une courbe de titrage; cette courbe, en traits pleins, a été calculée à partir de la valeur expérimentale de $L[NpO_2]$ déduite de (5). La quantité de Np(IV) de départ étant connue avec précision, il est possible de contrôler la pureté du Li_2O en comparant la position du point équivalent sur la courbe calculée à la position du point équivalent théorique. Dans tous les cas, on observe une correspondance à 2% près entre les points équivalents pratique et théorique. L'une des valeurs de $L[NpO_2] = 10^{-18,0}$ apparaît discordante; cet écart pourrait être attribué à une corrosion oxobasique de l'électrode indicatrice ayant servi dans un premier titrage, corrosion observée par ailleurs dans NaCl—KCl [10]. Pour le calcul du produit de solubilité moyen, cette valeur douteuse n'a pas été prise en considération et on obtient ainsi la valeur moyenne proposée (pour un taux de confiance de 95%)

$$L[NpO_2] = 10^{(-20,3\pm0,8)}\ mol^3\ l^{-3}$$

Diagramme E—pO^{2-} *du neptunium dans l'eutectique (LiCl—KCl) à 660°C*

Ce diagramme (Fig. 2) est établi en adoptant comme unités les molarités et les atmosphères; les potentiels sont rapportés à l'électrode normale à chlore et les concentrations des espèces solubles sont prises égales à 10^{-2} mol l^{-1}. La valeur du potentiel normal du couple NpO_2(VI)—NpO_2(V) à 660°C est obtenue par calcul en extrapolant les mesures de $E^0_{NpO_2(VI)—NpO_2(V)}$

TABLEAU 3

Produit de solubilité du dioxyde de neptunium dans l'eutectique LiCl—KCl à 660°C

$[Np^{4+}]_0 \cdot 10^2$ (mol l^{-1})	2,22	1,97	3,45	2,11
$-\log L_{NpO_2}$	20,7	18,0	19,9	20,2

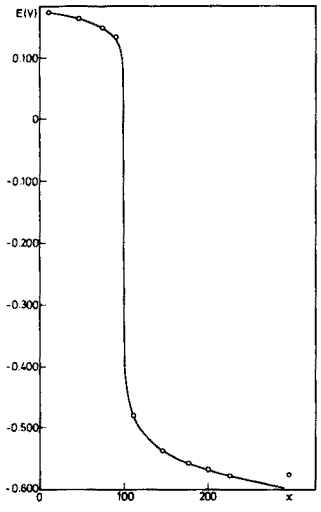

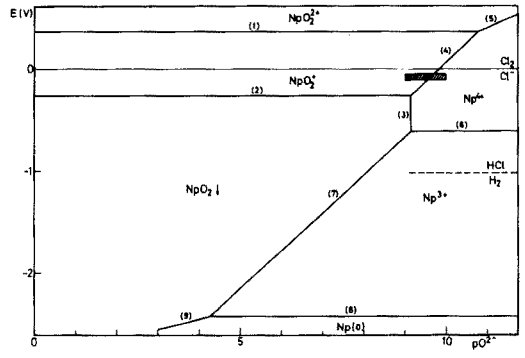

Fig. 1. Courbe de titrage potentiométrique de Np(IV) par Li_2O dans l'eutectique LiCl—KCl à 660°C; $[Np^{4+}]_0 = 3{,}45\ 10^{-2}$ mol l^{-1}.

Fig. 2. Diagramme E—pO^{2-} relatif au neptunium dans l'eutectique LiCl—KCl. T = 660°C; $[Np^{3+}] = [Np^{4+}] = [NpO_2^+] = [NpO_2^{2+}] = 10^{-2}$ mol l^{-1}. La zone hachurée indique le domaine tampon E—pO^{2-} balayé lors de l'étude du système oxydo—réducteur NpO_2(V)—Np(IV).

effectuées dans un domaine de température allant de 400 à 500°C [6]; on obtient

$E^0_{NpO_2(VI)—NpO_2(V)} = 0{,}36 \pm 0{,}13$ V (droite 1)

Si l'on possède la valeur de la constante d'équilibre de la réaction: $NpO_2^+ + Cl^- \rightleftarrows NpO_2\downarrow + \frac{1}{2}Cl_2$, à savoir $K_1 = P^{\frac{1}{2}}_{Cl_2}/[NpO_2^+]$, on détermine aisément $E^0_{NpO_2(V)—NpO_2\downarrow} = (2{,}3\ RT/F) \log K_1$.
Or, K_1 peut être obtenu à partir de valeurs suivantes provenant de diverses déterminations:

(a) La constante d'équilibre de la réaction $NpO_2^+ + 4HCl \rightleftarrows Np^{4+} + 2H_2O + \frac{1}{2}Cl_2 + 3Cl^-$, $K_2 = [Np^{4+}]P^2_{H_2O}P^{\frac{1}{2}}_{Cl_2}/[NpO_2^+]P^4_{HCl}$ déterminée par spectrophotométrie [8] dans un domaine de température allant de 450 et 600°C et extrapolée à 660°C.

(b) La constante d'équilibre de la réaction $H_2O + 2Cl^- \rightleftarrows 2HCl + O^{2-}$, $K_3 = P^2_{HCl}[O^{2-}]/P_{H_2O}$ déterminée par mesure d'équilibres oxoacido—basiques [9] dans un domaine de température allant de 642 à 742°C.

(c) $L[NpO_2]$. A 660°C, $K_2 = 10^{(-5{,}9\pm0{,}9)}$ atm$^{(-\frac{3}{2})}$, $K_3 = 10^{(-7{,}0\pm0{,}4)}$ mol l^{-1} atm et $L[NpO_2] = 10^{(-20{,}3\pm0{,}8)}$ mol^3 l^{-3}; dans ces conditions, $K_1 = K_2K_3^2/L[NpO_2]$ $= 10^{(0{,}6\pm1{,}3)}$ atm$^{\frac{1}{2}}$ l mol^{-1}, par suite

$E^0_{NpO_2(V)—NpO_2\downarrow} = 0{,}11 \pm 0{,}24$ V et $E = -0{,}26$ V (droite 2).

La précipitation de NpO_2 a lieu pour $[O^{2-}] \geqslant \left(\frac{10^{-20,3}}{10^{-2}}\right)^{\frac{1}{2}}$, c'est-à-dire $pO^{2-} \leqslant 9,15$. Les valeurs de K_2 et K_3 permettent le calcul de $E^0_{NpO_2(V)-Np(IV)}$; on a, en effet:

$$E^0_{NpO_2(V)-Np(IV)} = 2,3\ (RT/F) \log ([Np^{4+}]\ [O^{2-}]^2 P^{\frac{1}{2}}_{Cl_2}/[NpO_2^+])$$
$$= 2,3\ (RT/F) \log K_2 K_3^2 = -3,65\ V$$

ce qui conduit, pour l'équilibre NpO_2(V)—Np(IV) à l'équation

$$E = -3,65 + 2 \times 2,3\ (RT/F)\ pO^{2-} \qquad \text{(droite 4)}$$

L'intersection des droites (1) et (4) se produit à $pO^{2-} = 10,8$; pour $pO^{2-} > 10,8$, on a, pour le couple NpO_2(VI)—Np(IV)

$$E = -1,65 + 2,3\ (RT/F)\ pO^{2-} \qquad \text{(droite 5)}$$

La valeur de $E^0_{Np(IV)-Np(III)}$ à 660°C est obtenue par interpolation entre les valeurs de $E^0_{Pu(IV)-Pu(III)}$ [4] et $E^0_{U(IV)-U(III)}$ [3] par la méthode de Nugent et al.; ces valeurs déterminées dans un domaine de température allant de 400 à 550°C ont été extrapolées à 660°C. On obtient ainsi:

$$E^0_{Np(IV)-Np(III)} = E = -0,61 \pm 0,20\ V \qquad \text{(droite 6)}$$

Pour $pO^{2-} < 9,15$, on a l'équilibre $NpO_2\downarrow$—Np(III) avec

$$E = -4,00 + 2 \times 2,3\ (RT/F)\ pO^{2-} \qquad \text{(droite 7)}$$

L'extrapolation des valeurs de $E^0_{Np(III)-Np(0)}$ déterminées par Martinot et Duyckaerts [14] de 400 à 550°C, donne à 660°C $E^0_{Np(III)-Np(0)} = -2,30 \pm 0,02$ V, soit pour le système Np(III)—Np(0), $E = -2,42$ V (droite 8). L'intersection des droites (7) et (8) se produit à $pO^{2-} = 4,27$; pour $pO^{2-} < 4,27$, on obtient:

$$E = -2,82 + 2,3\ (RT/2F)\ pO^{2-} \qquad \text{(droite 9)}$$

DISCUSSION

Nous avons étudié précédemment [8] l'équilibre de la réaction $NpO_2^+ + 4HCl \rightleftarrows Np^{4+} + 2H_2O + \frac{1}{2}Cl_2 + 3Cl^-$ par la méthode spectrophotométrique; connaissant d'autre part la constante d'équilibre K_3, il est possible de délimiter, dans le diagramme de la Fig. 2, le domaine de E—pO^{2-} couvert par les mélanges gazeux (N_2, H_2O, HCl, Cl_2) utilisés lors de cette étude (zone hachurée). On peut constater que ce sont là les conditions les meilleures pour l'étude du couple NpO_2(V)—Np(IV).

De même, en considérant sur la Fig. 2 le potentiel du système H(I)—H_2 déterminé par Laitinen et Plambeck [15], on comprend que la réduction de Np(IV) par H_2 soit aisée dans LiCl—KCl à 660°C; ce fait ne pouvait être expliqué d'après la valeur de $E^0 = -1,48$ V/Cl_2—Cl^- à 660°C [2], par ailleurs

voisine de celle de $E^0_{U(IV)-U(III)} = -1{,}45$ V/Cl_2—Cl^- à 660°C [3], l'U(IV) n'étant réduit que partiellement par H_2 [16].

Influence de la température

La comparaison des valeurs de $L[NpO_2]$ calculée à 400°C et déterminée expérimentalement à 660° C indique que la solubilité augmente avec la température; on retrouve, par ailleurs, une évolution similaire pour d'autres oxydes dans les chlorures fondus, notamment TiO_2 [17], Cu_2O [18] et NiO [19]. En considérant, en outre, les résultats obtenus antérieurement [6] en ce qui concerne l'évolution des potentiels normaux avec la température, on peut conclure à un déplacement du diagramme vers les potentiels plus négatifs et vers les plus grandes valeurs de pO^{2-}, lorsque la température diminue.

Influence de la nature du solvant

Il est également intéressant d'examiner l'évolution du diagramme E—pO^{2-} avec la composition en cations alcalins des bains de chlorures fondus. Plusieurs couples oxydo—réducteurs du neptunium ont, en effet, été étudiés dans d'autres solvants, notamment les mélanges LiCl—KCl (70—30% mol) [20] LiCl—CsCl (55—45% mol) [21, 22] et RbCl—CsCl (25—75% mol) [6] Néanmoins, toutes les données nécessaires n'étant pas disponibles, on doit se contenter de montrer une tendance dans l'évolution de ce diagramme avec la nature du solvant.

Les potentiels normaux $E^0_{NpO_2(VI)-NpO_2(V)}$ et $E^0_{Np(IV)-Np(III)}$ diminuent suivant la séquence: LiCl—KCl (70—30% mol) > LiCl—KCl (eutectique) > LiCl—CsCl > RbCl—CsCl. On observe aussi que NpO_2(V) en solution dans LiCl—KCl sous balayage d'azote donne un précipité de NpO_2 alors que cette réaction ne se produit pas dans LiCl—CsCl et RbCl—CsCl. Ce fait semble également indiquer que le potentiel normal du couple NpO_2(V)/NpO_2 diminue suivant la même séquence ci-dessus.

En conclusion, le diagramme (Fig. 2) a tendance à se déplacer vers les potentiels plus négatifs en augmentant le rayon ionique des cations du bain.

Nous remercions vivement l'Institut Interuniversitaire des Sciences Nucléaires pour l'intérêt constant apporté à nos travaux et le soutien financier accordé à notre laboratoire.

BIBLIOGRAPHIE

1 L. Martinot et G. Duyckaerts, Anal. Chim. Acta, 66 (1973) 474.
2 L. Martinot, G. Duyckaerts et F. Caligara, Bull. Soc. Chim. Belg., 77 (1968) 77.
3 F. Caligara, L. Martinot et G. Duyckaerts, Bull. Soc. Chim. Belg., 76 (1967) 5.
4 G. Landresse et G. Duyckaerts, Inorg. Nucl. Chem. Lett., 10 (1974) 675.
5 L. J. Nugent, R. D. Baybarz, J. L. Burnett et J. L. Ryan, J. Phys. Chem., 77 (1973) 1528.
6 R. Lysy, thèse de doctorat, Liège, 1977.
7 L. Martinot et G. Duyckaerts, Inorg. Nucl. Chem. Lett., 5 (1969) 909.
8 R. Lysy, G. Landresse et G. Duyckaerts, Anal. Chim. Acta, 72 (1974) 307.
9 R. Lysy et R. Combes, J. Electroanal. Chem., (sous presse).

10 R. Combes, J. Vedel et B. Trémillon, Electrochim. Acta, 20 (1975) 191.
11 R. Lysy, G. Landresse et G. Duyckaerts, Inorg. Nucl. Chem. Lett., 10 (1974) 685.
12 G. Landresse, Anal. Chim. Acta, 56 (1971) 29.
13 R. Lysy, G. Landresse et G. Duyckaerts, Bull. Soc. Chim. Belg., 83 (1974) 227.
14 L. Martinot et G. Duyckaerts, Bull. Soc. Chim. Belg., 78 (1969) 495.
15 H. A. Laitinen et J. A. Plambeck, J. Am. Chem. Soc., 87 (1965) 1202.
16 G. Landresse, thèse de doctorat, Liège, 1972.
17 T. L. Inyushkina, I. N. Marenkova et L. N. Dzyubo, Russ. J. Phys. Chem., 49 (1975) 1446.
18 R. Combes, thèse de doctorat, Paris, 1973.
19 J. P. Wiaux, thèse de doctorat, Louvain, 1976.
20 R. Lysy et G. Duyckaerts, Inorg. Nucl. Chem. Lett., 12 (1976) 205.
21 R. Lysy et G. Duyckaerts, Inorg. Nucl. Chem. Lett., 11 (1975) 79.
22 R. Lysy et G. Duyckaerts, Rev. Chim. Minérale, 14 (1977) 119.

Analytica Chimica Acta, 96 (1978) 133—142

STABILITE DE COMPLEXES ORGANOMETALLIQUES DANS LE CARBONATE DE PROPYLENE SATURE D'EAU
I. Complexes Hydroxy-8 quinoléine-Cuivre(II), Cadmium(II), Zinc(II) et Plomb(II)

F. QUENTEL, J. Y. CABON, M. L'HER et J. COURTOT-COUPEZ*

Laboratoire de chimie analytique, E.R.A. CNRS 677, Université de Brest, 6, Avenue Victor Le Gorgeu, 29283 Brest-Cedex (France)

(Reçu le 8 juin 1977)

RÉSUMÉ

Dans le but d'utiliser le carbonate de propylène comme milieu d'extraction, la formation de complexes entre l'hydroxy-8 quinoléine et différents cations métalliques {cuivre(II), cadmium(II), zinc(II) et plomb(II)} a été étudiée dans ce solvant saturé d'eau. Ces études ont été effectuées par spectrophotométrie, polarographie et potentiométrie. Les complexes formés sont mononucléaires de type 1:1 et 1:2 pour le plomb(II) et le zinc(II); des composés de type 1:3 ont été en outre mis en évidence dans le cas du cuivre(II) et du cadmium(II). Les constantes de stabilité de ces différentes espèces à 25°C et à force ionique 0,1 M ont été déterminées.

SUMMARY

The stability of organometallic complexes in propylene carbonate saturated with water. Part 1. Copper(II), cadmium(II), zinc(II) and lead(II) hydroxyquinolinates

Complex formation between 8-hydroxyquinoline and several cations {copper(II), cadmium(II), zinc(II) and lead(II)} has been studied in water-saturated propylene carbonate. Measurements have been made by spectrophotometry, polarography and potentiometry. Type 1:1 and 1:2 mononuclear complexes for lead(II) and zinc(II) are formed; type 1:3 complexes are also detected with copper(II) and cadmium(II). Stability constants for these species at 25°C and 0.1 M ionic strength have been determined.

Nous nous sommes antérieurement intéressés à l'évolution des propriétés physiques et des propriétés solvatantes à l'égard des ions simples des mélanges eau—carbonate de propylène à 25°C [1—3]. A cette température, le solvant organique n'est pas miscible à l'eau en toutes proportions; il existe une importante zone de démixion pour des fractions molaires en carbonate de propylène comprises entre 0,03 et 0,7. Ce phénomène a été mis à profit par certains expérimentateurs qui utilisent le carbonate de propylène comme agent d'extraction à partir de solutions aqueuses de divers complexes organométalliques [4]. Les caractéristiques du carbonate de propylène qui sont celles d'un solvant moléculaire dissociant seraient intéressantes à exploiter

en vue de l'analyse des traces; elles permettraient d'atteindre grâce à la mise en oeuvre de méthodes électrochimiques au sein de la phase organique, une plus grande sensibilité dans l'analyse par extraction qu'avec les solvants actuellement employés. C'est en poursuivant ce but que nous avons été conduits à examiner le comportement de différents cations métalliques en présence de ligands types classiquement utilisés en extraction. Nous avons dans un premier temps étudié le pouvoir complexant de l'hydroxy-8 quinoléine.

Dans un travail précédent nous avons montré [5] que le carbonate de propylène saturé d'eau offre un domaine d'acidité pratique de 14 unités de pH. Ce domaine est limité vers les milieux alcalins par la basicité de l'ion hydrogénocarbonate provenant de l'hydrolyse de l'ester. Dans le mélange hydro-organique, l'électrode de verre aussi bien que l'électrode à hydrogène permettent la mesure du pH.

PARTIE EXPERIMENTALE

Appareillage

Les spectres d'absorption électronique ont été obtenus à l'aide d'un appareil Beckman DK-2A. Les titrages spectrophotométriques ont été réalisés dans une cuve à circulation montée dans un spectrophotomètre Prolabo type Jean et Constant.

Toutes les mesures de pH ont été effectuées avec un millivoltmètre Tacussel type ISIS 20000 en utilisant une électrode de verre Radiometer type G.202B et une électrode de référence constituée d'un fil d'argent recouvert de chlorure d'argent plongeant dans une solution de chlorure de tétraéthylammonium 0,1 M. Cette dernière électrode est séparée du milieu à étudier par un pont liquide comportant un disque de verre fritté de porosité 4 à chacune de ses extrémités et contenant une solution de perchlorate de tétraéthylammonium 0,1 M. Avant chaque série de mesures, l'électrode de verre a été étalonnée à partir de solutions d'acide perchlorique de titre connu et de force ionique 0,1 M (Et_4NClO_4).

Le polarographe à trois électrodes utilisé comprend un potentiostat PRT-20-2 et une unité d'adaptation UAPI Solea Tacussel ainsi qu'un enregistreur graphispot GRSO Sefram.

Les mesures potentiométriques et polarographiques ont été effectuées dans des cellules classiques à double paroi reliées à un thermostat à circulation Haake type FE maintenant la température à 25 ± 0,1°C.

Réactifs et solutions

Les différents perchlorates métalliques (cuivre, zinc, cadmium, plomb) et le perchlorate de tétraéthylammonium sont des produits G. F. Smith. L'hydroxyde de tétrabutylammonium est un produit Fluka. Tous les autres produits utilisés sont des réactifs pour analyse.

Le carbonate de propylène (produit Hulls) est distillé sous pression réduite (environ 1 mm Hg) avant utilisation. Les mélanges eau—carbonate

de propylène (fraction molaire en solvant organique 0,7) sont préparés par pesée. L'eau utilisée est désionisée par échange d'ions après avoir subi une première purification par distillation.

Le titre des solutions d'hydroxy-8 quinoléine a été déterminé par acidimétrie. Les titres des solutions des différents cations étudiés ont été déterminés par complexométrie à l'EDTA.

RESULTATS ET DISCUSSION

L'étude de la complexation proprement dite a été précédée par celle de l'influence de l'acidité du milieu sur les formes du ligand et des différentes espèces métalliques.

Comportement acido—basique de l'hydroxy-8 quinoléine

Suivant l'acidité du milieu, l'hydroxy-8 quinoléine ou oxine HOx peut soit fixer un proton sur l'atome d'azote soit perdre un proton phénolique. Les deux équilibres acido—basiques suivants sont facilement mis en évidence dans le solvant

$$HOx \rightleftarrows Ox^- + H^+ \ (K_{A_1}) \quad \text{et} \quad HOx + H^+ \rightleftarrows H_2Ox^+ \ (K_{A_2})$$

L'ion Ox^- est fortement basique dans le carbonate de propylène saturé d'eau; la courbe de neutralisation de HOx par de l'hydroxyde de tétrabutylammonium ne présente pas de point équivalent. La valeur de K_{A_1} a été déterminée par exploitation mathématique de la courbe de début de titrage d'une solution concentrée d'hydroxy-8 quinoléine (0,1 M) par de l'hydroxyde de tétrabutylammonium.

La courbe de neutralisation de l'hydroxy-8 quinoléine par une solution d'acide perchlorique est typiquement celle d'une base faible par un acide fort. Les titrages ont été effectués sur des solutions 0,01 M en HOx et 0,1 M en Et_4NClO_4; leur exploitation au moyen de la méthode classique de Bjerrum et Anderson [6] conduit à la valeur de la constante d'acidité K_{A_2}.

Dans le Tableau 1 figurent les pK_A de l'hydroxy-8 quinoléine dans l'eau [7], le mélange eau—dioxanne (1 + 1) [8] et le carbonate de propylène saturé d'eau. La valeur de la constante d'acidité K_{A_2} est peu modifiée lorsque l'on passe de l'eau au carbonate de propylène saturé d'eau. Nous avons déjà montré sur d'autres exemples [5] que les valeurs de pK_A des couples HB^+/B

TABLEAU 1

Constantes d'acidité de l'oxine

	H_2O	C.P. saturé d'eau	Eau—dioxanne 1 + 1
pK_{A_1}	9,81	12,9	11,20
pK_{A_2}	4,91	4,7	4,16

sont peu différentes pour ces deux solvants. Dans le milieu mixte eau—dioxanne (1 + 1), l'acide H_2Ox^+ est plus fort que dans le milieu hydro-organique étudié et dans l'eau. Par contre, l'anion Ox^- est une base plus forte dans le carbonate de propylène saturé d'eau que dans l'eau et le mélange eau—dioxanne (1 + 1), ce qui correspond à une différence importante de la solvatation de l'anion par ces différents milieux.

Hydrolyse des ions métalliques

Les expériences effectuées n'avaient pour but que de déterminer la zone de pH dans laquelle la formation des complexes cation—hydroxyle peut être considérée comme négligeable. Des titrages de solutions acides de cation métallique par l'hydroxyde de tétrabutylammonium ont été effectuées pour deux concentrations en métal: 0,001 et 0,005 M. Dans les deux cas, il y a addition de deux ions hydroxyle sur chaque cation; lorsque la concentration en métal est de l'ordre de 0,005 M, tous les hydroxydes correspondants précipitent dès le début de la réaction. Pour une teneur en métal de 0,001 M (Fig. 1) l'on n'observe pas de précipitation pour le cuivre(II) et le zinc(II), il y a seulement formation de complexes solubles; l'hydroxyde de cadmium(II) précipite dès la neutralisation des protons tandis que dans le cas du plomb(II), il se forme d'abord des complexes solubles avant que l'hydroxyde ne précipite en fin de titrage.

En comparant ces résultats à ceux obtenus dans le mélange eau—dioxanne (1 + 1) [9], on peut remarquer une nette différence dans le comportement du plomb(II) qui précipite dans ce milieu sous la forme $Pb(ClO_4)_2$, $3Pb(OH)_2$, l'ordre d'acidité des cations étant Cu^{2+}, Pb^{2+}, Zn^{2+} et Cd^{2+}. Dans le carbonate de propylène saturé d'eau, le cadmium(II) est hydrolysé en milieu plus acide que le zinc(II); pour des concentrations 0,001 M environ, il est légitime de négliger l'hydrolyse des différents cations considéres en travaillant en dessous de pH 6.

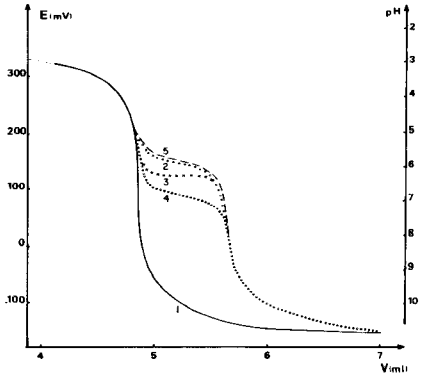

Fig. 1. Titrage potentiométrique de solutions d'acide perchlorique $1{,}27\ 10^{-2}$ M et de perchlorate métallique 10^{-3} M par de l'hydroxyde de tétrabutylammonium 0,1 M; courbe 1: acide seul; courbe 2: $Cu(ClO_4)_2$; courbe 3: $Cd(ClO_4)_2$; courbe 4: $Zn(ClO_4)_2$; courbe 5: $Pb(ClO_4)_2$.

Etude spectrophotométrique

Le spectre d'absorption électronique de l'hydroxy-8 quinoléine est modifié aussi bien en présence d'acide perchlorique qu'en présence de perchlorate de cuivre(II), de plomb(II), de cadmium(II) et de zinc(II) (Tableau 2).

La spectrophotométrie d'absorption met donc en évidence la formation de complexes stables métal—hydroxy-8 quinoléine en milieu neutre mais la forme protonée du ligand absorbant à des longueurs d'onde voisines de celles des complexes métalliques, la méthode spectrophotométrique ne peut être utilisée pour analyser les réactions de complexation en milieu acide.

Seule la formation des complexes du cuivre(II) a pu être étudiée par spectrophotométrie en milieu neutre. En effet, les complexes du plomb(II), du cadmium(II) et du zinc(II) étant moins stables que ceux du cuivre(II), les titrages de ces cations sont perturbés par la précipitation d'espèces hydroxylées. La Fig. 2 présente un titrage spectrophotométrique de perchlorate de cuivre(II) 0,0006 M par de l'hydroxy-8 quinoléine, titrage suivi à 383 nm correspondant au maximum d'absorption de l'un des complexes formés. Trois points équivalents bien définis correspondant respectivement à des rapports ligand/métal égaux à 1, 2 et 3 mettent en évidence l'existence des trois complexes $CuOx^+$, $CuOx_2$ et $CuOx_3^-$. La méthode des variations continues de Job [10] effectuée sur des solutions de concentration totale 0,0006 M (Tableau 3) permet de conclure à la formation d'un complexe 1:3 n'excluant pas pour autant celle d'autres composés.

TABLEAU 2

Spectres d'absorption de l'oxine et des oxinates métalliques

Complex	HOx	H_2Ox^+	Cu—Ox	Pb—Ox	Zn—Ox	Cd—Ox
λ_m (nm)	241	252	258	258,5	259	259
λ_m (nm)	308	361	383	367,5	371	367,5

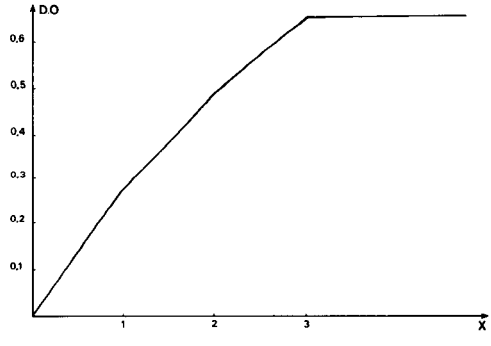

Fig. 2. Titrage spectrophotométrique à 383 nm d'une solution de perchlorate de cuivre $6{,}25\ 10^{-4}$ M par une solution d'oxine $6{,}25\ 10^{-3}$ M.

TABLEAU 3

Méthode des variations continues. Complexation du cuivre(II)

% $Cu(ClO_4)_2$	7,5	10	15	20	25	30	40	50	60	70	80	85
% HOx	92,5	90	85	80	75	70	60	50	40	30	20	15
Absorbance	0,277	0,364	0,538	0,686	0,820	0,821	0,746	0,632	0,515	0,392	0,274	0,1

Etude polarographique

Dans la mesure où le cation métallique est réductible réversiblement et le ligand non électroactif, la polarographie permet d'étudier les réactions de formation de complexe. La méthode polarographique impose d'opérer en présence d'un excès de complexant ce qui en règle générale favorise la formation des complexes supérieurs. Nos résultats ont été exploités par la méthode de Lingane [11] ou celle de DeFord et Hume [12], cette dernière étant applicable à la formation de plusieurs complexes de stabilité voisine.

La réduction polarographique de solutions 0,0001 M des différents cations métalliques a été étudiée en milieu acide perchlorique 0,1 M. La réduction du cuivre(II) ne correspond pas à un échange électronique réversible, la pente de la transformée logarithmique de la vague étant de 0,071 V/unité de log. Les réductions du cadmium(II) et du plomb(II) en amalgame sont en revanche réversibles, les pentes étant respectivement de 0,030 et 0,031 V log^{-1}; les potentiels de demi-vague mesurés par rapport a la référence Ag(s)/AgCl(s) $Et_4N^+Cl^-$ 0,1 M [5] sont —0,336 V pour $Cd^{2+}/Cd(Hg)$ et —0,174 V pour $Pb^{2+}/Pb(Hg)$. La vague de réduction du zinc(II) ne peut être correctement analysée car elle est trop voisine de celle correspondant à la décharge des protons.

Nous n'avons donc pu mener par polarographie que l'étude des complexes du cadmium(II) et du plomb(II). Afin d'éviter la formation conjointe d'espèces hydroxylées d'une part et de maintenir constant le pH du milieu d'autre part, nous avons choisi de travailler à pH 4,5 en utilisant comme mélange tampon le couple H_2Ox^+/HOx et comme électrolyte destiné à ajuster la force ionique à la valeur 0,1 M le perchlorate de tétraéthyl-ammonium. En présence de ligand, les systèmes électrochimiques correspondant à la réduction des complexes du cadmium(II) et du plomb(II) sont pratiquement réversibles (pentes respectives de 0,029 et 0,032 V log^{-1}). En ce qui concerne le plomb(II), pour une concentration en ligand variant de 0,0025 à 0,04 M, la courbe représentant les variations de $E_{1/2}$ en fonction de log [HOx] est une droite de pente —0,026 V/ unité de log, ce qui correspond à la formation d'un complexe 1:1. Lorsque la teneur en hydroxy-8 quinoléine varie de 0,04 à 0,1 M, la pente obtenue est de —0,059 V log^{-1}, le complexe majoritaire étant de type 1:2.

Dans le cas du cadmium(II), quel que soit l'excès de ligand présent en solution, nous avons obtenu une droite de pente 0,095 V log^{-1} pour rendre compte des variations de $E_{1/2}$ en fonction de log [HOx] ce qui correspond à l'existence d'un complexe 1:3. Les constantes de stabilité correspondant à ces différents complexes sont $\log \beta_1 = 12,7$ et $\log \beta_2 = 23,0$ pour Pb—Ox, et

$\log \beta_3 = 32{,}6$ pour Cd—Ox. Les valeurs obtenues doivent être considérées avec prudence; en effet, une légère adsorption du ligand à l'électrode conduisant à des résultats trop élevés [13] n'est pas à exclure.

Etude potentiométrique

Les méthodes potentiométriques d'étude des réactions entre un cation métallique et un coordinat basique sont fondées sur l'exploitation de la différence d'affinité du proton et du cation à l'égard du ligand, caractérisée par un équilibre du type

$$M^{2+} + n\ HL \rightleftarrows ML_n^{(2-n)+} + n\ H^+$$

On peut analyser cet équilibre en suivant la neutralisation par une base d'un mélange cation—ligand en proportions variables. Le paramètre mesuré est le pH du milieu, ce à l'aide d'une électrode de verre. A partir de la connaissance des pK_A du ligand, des concentrations totales des produits mis en oeuvre et du pH, il est alors possible de calculer $\overline{n}$ la fonction de formation de Bjerrum [14] égale au nombre moyen de ligands liés par un atome métallique. L'analyse des variations de $\overline{n}$ au cours du titrage par la méthode de Rossotti et Rossotti [15] conduit alors à la formule des complexes et à la valeur des constantes de stabilité correspondantes. Sur la Fig. 3 ont été représentées les courbes de titrage potentiométrique par l'hydroxyde de tétrabutylammonium de solutions contenant du perchlorate de cuivre(II) et du perchlorate d'oxinium dans les rapports un, deux et quatre. Dans le

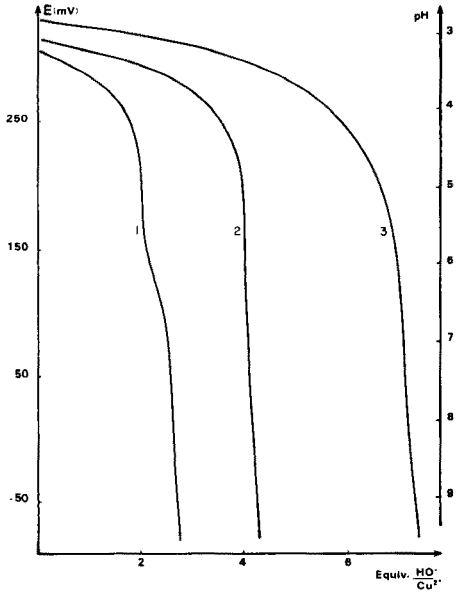

Fig. 3. Titrage potentiométrique de mélanges Cu^{2+}—H_2Ox^+ par de l'hydroxyde de tétrabutylammonium 6,67 10^{-3} M; courbe 1: $[HOx] = [Cu^{2+}] = 2 \cdot 10^{-4}$ M; courbe 2: $[Hox] = 2[Cu^{2+}] = 4 \cdot 10^{-4}$ M; courbe 3: $[HOx] = 4[Cu^{2+}] = 8 \cdot 10^{-4}$ M.

premier cas (courbe 1), on dose deux équivalents d'acide fort, ce qui correspond à la formation d'un complexe contenant le cation et le ligand en égale proportion. Les deux autres expériences (courbes 2 et 3) mettent respectivement en évidence la formation de complexes de type $(CuOx_2)_n$ et $(CuOx_3^-)_n$. Les courbes représentatives de l'évolution de la fonction de formation $\overline{n}$ en fonction colog$[Ox^-]$ au cours de ces différents titrages sont confondues, ce qui permet de conclure que les complexes formés sont mononucléaires soit respectivement $CuOx^+$, $CuOx_2$ et $CuOx_3^-$. Dans le mélange eau—dioxanne (1 + 1), seule l'existence des complexes $CuOx^+$ et $CuOx_2$ a été mentionnée [8, 16].

Dans le cas du plomb(II), du cadmium(II) et du zinc(II), nous n'avons observé que la formation des complexes MOx^+ et MOx_2. En présence d'un grand excès de ligand par rapport au métal correspondant à des conditions d'extraction, Freiser et coll. [17] ont cependant observé la formation du composé $ZnOx_2$, HOx dans le chloroforme.

La méthode potentiométrique confirme les résultats obtenus par spectrophotométrie en ce qui concerne les différents complexes du cuivre(II); elle confirme également les résultats obtenus par polarographie dans le cas du plomb(II); par contre, l'existence du complexe $CdOx_3^-$ mis en évidence par polarographie en présence d'un fort excès de ligand n'a pu être confirmée par la méthode de Bjerrum.

Les constantes de stabilité des complexes ont été déterminées en appliquant la méthode graphique de Rossotti et Rossotti [15], c'est-à-dire en considérant dans le cas de la coexistence des complexes 1:1 et 1:2 l'évolution de la fonction G_1 (Fig. 4)

$$G_1 = \overline{n}/(1 - \overline{n}\,[Ox^-]) = \beta_1 + \beta_2\,(2 - \overline{n})\,[Ox^-]/(1 - \overline{n})$$

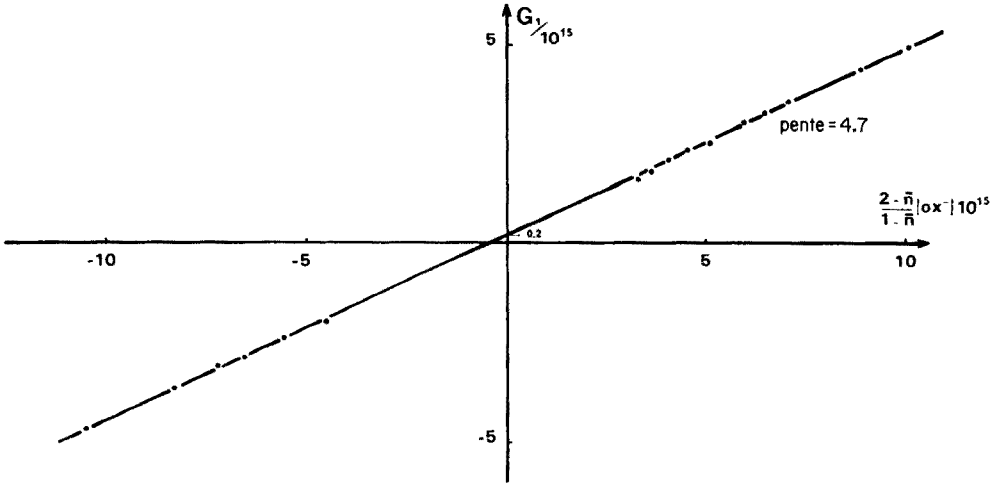

Fig. 4. Application de la méthode de Rossotti et Rossotti [15] aux complexes $CuOx_n$.

et dans le cas de la coexistence des complexes 1:2 et 1:3 l'évolution de fonction G_2

$$G_2 = \frac{G_1\beta_1}{[Ox^-]}\,\frac{1-\overline{n}}{2-\overline{n}} = \beta_2 + \beta_3\,\frac{3-\overline{n}}{2-\overline{n}}\,[Ox^-]$$

Les résultats obtenus sont rassemblés dans le Tableau 4 où figurent également les valeurs publiées par Gutnikov et Freiser dans le cas des mélanges eau—dioxanne à 25°C et à force ionique 0,1 M [18].

Dans les deux solvants l'ordre de stabilité des complexes est le même à savoir $Cu^{2+} > Pb^{2+} > Zn^{2+} > Cd^{2+}$ pour les complexes 1:1 et $Cu^{2+} > Zn^{2+} > Pb^{2+} > Cd^{2+}$ pour les complexes 1:2. En ce qui concerne le cuivre(II), le zinc(II) et le cadmium(II), l'ordre d'affinité est celui proposé par Irving et Williams [19]. Il est intéressant de remarquer que tous les complexes étudiés sont plus stables dans le carbonate de propylène saturé d'eau que dans le mélange eau—dioxanne (1 + 1).

La connaissance des constantes de stabilité des différents oxinates permet de calculer le diagramme de répartition des espèces en solution en fonction de la concentration du ligand libre dans le milieu. Si on note α_i la proportion du complexe MOx_i la grandeur $\alpha_i = [MOx_i]/[M^{2+}]_t$ peut être facilement exprimée en fonction de la concentration en Ox^- qui elle-même dépend du pH et des concentrations totales des produits mis en oeuvre. Ces courbes de répartition données ici dans le cas du cuivre(II) et du zinc(II) (Figs. 5 et 6) permettent de connaître les différentes formes susceptibles d'intervenir lors d'une extraction; elles peuvent être en particulier utilisées pour prévoir les conditions les plus favorables à la présence quasi exclusive du complexe moléculaire dans le solvant.

TABLEAU 4

Constantes de stabilité des complexes de l'oxine

Ion métallique	H_2O—dioxanne (1 + 1) $pK_{A_1} = 10{,}96$ $pK_{A_2} = 4{,}13$			Carbonate de propylène saturé d'eau $pK_{A_1} = 12{,}9$ $pK_{A_2} = 4{,}7$				
	$\log \beta_1 = \log K_1$	$\log \beta_2$	$\log K_2$	$\log \beta_1 = \log K_1$	$\log \beta_2$	$\log K_2$	$\log \beta_3$	$\log K_3$
Cu^{2+}	13,29	25,90	12,61	14,3	29,8	15,5	42,5	12,7
Zn^{2+}	9,45	18,15	8,70	10,8	20,5	9,7		
Pb^{2+}	10,03	17,34	7,31	$11{,}4_5$	21,0	$9{,}5_5$		
Cd^{2+}	8,22	15,22	7,00	10,7	20,2	9,5		

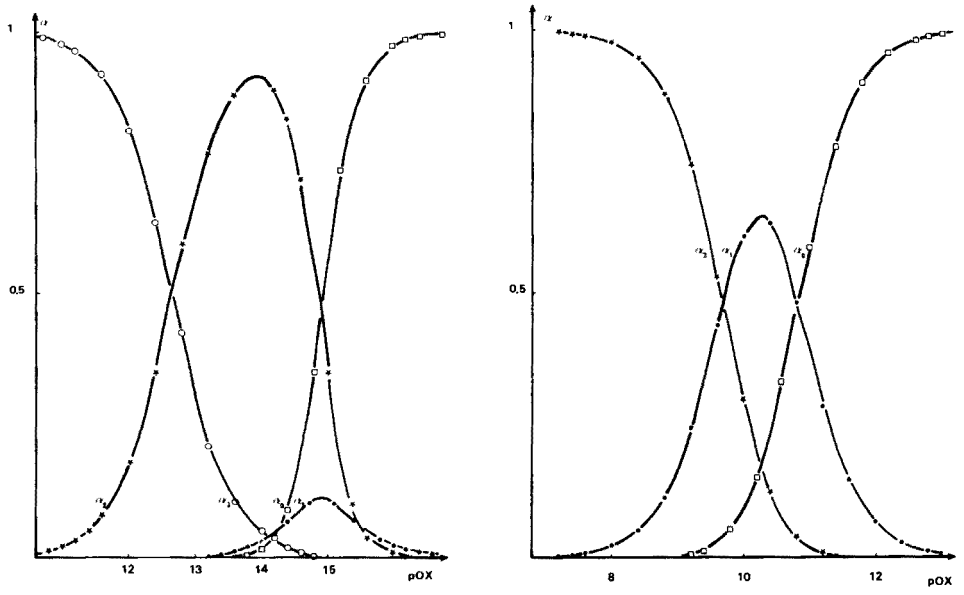

Fig. 5. Répartition des espèces Cu^{2+} (α_0), $CuOx^{+}$ (α_1), $CuOx_2$ (α_2) et $CuOx_3^{-}$ (α_3) en fonction de la concentration en oxinate.

Fig. 6. Répartition des espèces Zn^{2+} (α_0), $ZnOx^{+}$ (α_1) et $ZnOx_2$ (α_2) en fonction de la concentration en oxinate.

Nous tenons à remercier la Délégation générale à la recherche scientifique et technique pour l'aide dont elle nous a fait bénéficier.

BIBLIOGRAPHIE

1 (a) J. Courtot-Coupez et M. L'Her, C.R. Acad. Sci. Ser. C, 275 (1972) 103.
(b) J. Courtot-Coupez et M. L'Her, C.R. Acad. Sci. Ser. C, 275 (1972) 195.
2 M. L'Her, D. Morin-Bozec et J. Courtot-Coupez, J. Electroanal. Chem., 55 (1974) 133.
3 M. L'Her, D. Morin-Bozec et J. Courtot-Coupez, J. Electroanal. Chem., 61 (1975) 99.
4 B. G. Stephens et H. L. Felfel, Anal. Chem., 47 (1975) 1676.
5 F. Quentel, J. Y. Cabon, M. L'Her et J. Courtot-Coupez, C.R. Acad. Sci. Ser. C, 284 (1977) sous presse.
6 J. Bjerrum et P. L. Anderson, Kgl. Danske. Vid., 7 (1945) 1.
7 L. G. Sillen et A. E. Martell, Stability of metal—ion complexes, The Chemical Society, London, 1964.
8 R. L. Stevenson et H. Freiser, Anal. Chem., 39 (1967) 1354.
9 H. Freiser, R. G. Charles et W. D. Johnson, J. Am. Chem. Soc., 74 (1952) 1383.
10 P. Job, Ann. Chim., 9 (1928) 113.
11 J. J. Lingane, Chem. Rev., 29 (1941) 1.
12 D. DeFord et D. N. Hume, J. Am. Chem. Soc., 73 (1951) 5321.
13 A. M. Bond et G. Hefter, J. Electroanal. Chem., 68 (1976) 203.
14 J. Bjerrum, Metal ammine formation in aqueous solution, Haase and Son, Copenhagen, 1941.
15 F. J. C. Rossotti et H. S. Rossotti, Acta Chem. Scand., 9 (1955) 1166.
16 W. D. Johnson et H. Freiser, J. Am. Chem. Soc., 74 (1952) 5239.
17 F. A. Chun Chou, Q. Fernando et H. Freiser, Anal. Chem., 37 (1965) 361.
18 G. Gutnikov et H. Freiser, Anal. Chem., 40 (1968) 39.
19 H. Irving et R. J. P. Williams, J. Chem. Soc., (1953) 3192.

Analytica Chimica Acta, 96 (1978) 143—151

COMPARATIVE STUDIES OF TEMPORAL CHANGES IN POLAROGRAPHIC CURRENTS AND ULTRAVIOLET ABSORPTION OF BENZYLPENICILLENIC ACID

MOHAMMED JEMAL and ADELBERT M. KNEVEL*

Department of Medicinal Chemistry and Pharmacognosy, School of Pharmacy and Pharmacal Sciences, Purdue University, West Lafayette, IN 47907 (U.S.A.)

(Received 1st June 1977)

SUMMARY

The time behavior of the polarographic current and u.v. absorbance of benzylpenicillenic acid in buffers at different pH values are compared. The rate of decrease of current with time is the same as the rate of decrease of absorbance in the intermediate pH region but is slower in the alkaline and acidic regions. The slower rate in these regions is explained by the transformation of the thiazolidinyl—oxazolone isomer to the u.v.-absorbing and polarographically active isomer at the electrode.

Among the degradation products of benzylpenicillin, benzylpenicillenic acid has been given a significant role in penicillin allergy [1, 2]. It has also been proposed that benzylpenicillenic acid is an intermediate in the formation of benzylpenillic acid from benzylpenicillin in acidic solutions [3] and in the formation of benzylpenicilloic acid from penicillin at a neutral pH [4].

Longridge and Timms [5, 6] studied the hydrolysis of benzylpenicillenic acid at different pH values and proposed that benzylpenicillenic acid is found in equilibrium with thiazolidinyl—oxazolone isomer, which does not absorb at 322 nm (Fig. 1). The existence of this equilibrium was also proposed by Dudley et al. [7] based on the rate of fall of the absorbance at 322 nm by benzylpenicillenic acid in aqueous buffers, and by Bundgaard [8] based on the kinetics of the formation of benzylpenicillenic acid from benzylpenicillin in acidic solutions.

Although benzylpenicillenic acid is such an important compound and possesses polarographically active functional groups, there has been no systematic study of its electrochemical properties. However, during polarographic studies of benzylpenicillin solution, some waves were observed and these were attributed to benzylpenicillenic acid formed from benzylpenicillin. In acidic solutions of benzylpenicillin, the two cathodic waves were attributed to electroreduction of the conjugated oxazolone group of benzylpenicillenic acid [9, 10]. Oscillograms of benzylpenicillin solutions in acidic media exhibited several signals, two of which were assigned to the oxazolone

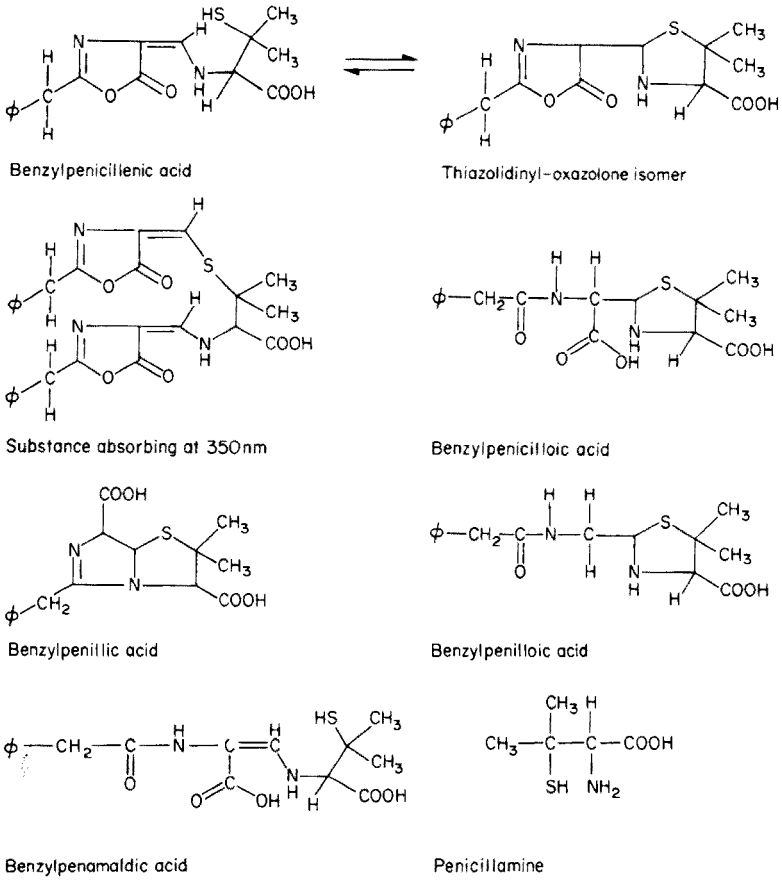

Fig. 1. Structures of benzylpenicillenic acid and related compounds.

system of benzylpenicillenic acid [11]. Study of the polarography of commercial samples of sodium benzylpenicillin in a solution of ammonium chloride, ammonium hydroxide and cobalt(II) chloride (Brdicka solution) showed the presence of catalytic waves [12]. The catalytic waves were thought to be due to the sulfhydryl group of benzylpenicillenic acid formed from benzylpenicillin.

As part of a study of the electrochemical properties of benzylpenicillenic acid, the temporal changes in the polarographic currents of benzylpenicillenic acid in buffers of different pH values are reported in this paper. The polarographic studies are based on the electrode reaction of the sulfhydryl group of benzylpenicillenic acid. The polarographic results are compared with the temporal changes in the u.v. absorption of benzylpenicillenic acid at 322 nm. The significance of the existence of benzylpenicillenic acid in equilibrium with a thiazolidinyl—oxazolone isomer in aqueous buffers to the interpretation of its polarographic behavior is discussed.

EXPERIMENTAL

Chemicals

Benzylpenicillenic acid was obtained commercially as an amorphous product (Sigma Chemical Company, St. Louis, Mo., U.S.A.). It was prepared from benzylpenicillin by Levine's method [13]. Benzylpenicillenic acid is unstable in aqueous solutions as shown by the decrease of the band at 322 nm [6, 7]. Solid benzylpenicillenic acid is also unstable and must be kept in the freezer. Dudley et al. [7] synthesized stable derivatives of this compound in which the sulfhydryl group was either converted to a stable sulfide or removed from the molecule entirely. The molar absorptivities (ϵ) of these compounds at 322 nm in ethanol were about 30 500, and this value was assigned to benzylpenicillenic acid. The value is higher than the molar absorptivities reported previously [13, 14], but ϵ = 30 500 l mol^{-1} cm^{-1} was used in the present work. The commercial product used gave a molar absorptivity of 21 000; this low value is attributed in part to the presence of water of hydration. Benzylpenicilloic acid is known to be a common degradation product of benzylpenicillenic acid, and its presence in the commercial product was identified by t.l.c. on silica gel (EM Laboratories, Elmsford, New York) with n-butanol–water–acetic acid (66:17:17); the R_F values were 0.39 for benzylpenicilloic acid and 0.70 for benzylpenicillenic acid. Solutions of the benzylpenicillenic acid product in buffers of low or high pH values (e.g. McIlvaine buffer pH 2.30 or Sorensen glycine buffer pH 8.60) exhibited a rapid decrease of the band at 322 nm leaving a stable absorbance maximum at 350 nm. The stable absorbance was assigned to a compound proposed by Longridge and Timms [6] and the proposed structure for the u.v.-absorbing derivative is shown in Fig. 1. The absorbance caused by this compound in the commercial product was estimated as 6% of the total absorbance at 322 nm.

Benzylpenillic acid was prepared by the procedure of Cook [15]. Benzylpenilloic acid was prepared by a standard procedure [16]. Benzylpenicilloic acid was prepared fresh as needed [17].

DL-Penicillamine was obtained commercially (99 + %; Aldrich Chemical Company). Polarography of freshly prepared penicillamine solution did not show any penicillamine disulfide.

Apparatus

A PAR polarographic analyzer model 174A was used in conjunction with PAR model 174/70 drop timer (Princeton Applied Research Corporation, Princeton, N.J.). The cell was a PAR model 9301 cell bottom with a PAR Model 9300 cell top. A three-electrode system was used: a dropping mercury working electrode, a saturated calomel reference electrode (model 3-712; Coleman Instruments, Oak Brook, Illinois), and a platinum wire counter (auxiliary) electrode. The mercury capillary had the following characteristics: in 0.056 M citrate buffer pH 6.45 (with 5% ethanol) at open circuit, the

mercury flow rate was 2.57 mg s^{-1} and the natural drop time was 3.0 s at a mercury reservoir height of 78.6 cm. Except for the study of the effect of mercury pressure on wave heights, a mercury column of 78.6 cm was used. Natural drop time was employed throughout. Polarographic waves were recorded with an Omnigraphic model 2000 x—y recorder (Houston Instruments, Bellaire, Texas).

Ultraviolet studies were performed with a Cary 17 spectrophotometer (Cary Instruments, Monrovia, California). The u.v. cells were provided with ground-glass stoppers (model 193-QS; Hellma Cells Inc., Jamaica, New York).

Solution

Common buffer solutions were prepared in a standard way [18]. Citrate buffer (0.056 M; pH 6.45) was prepared from 16.0 g of trisodium citrate dihydrate and 0.51 g of citric acid monohydrate per liter.

Because benzylpenicillenic acid is readily soluble and sufficiently stable in alcohol, stock solutions were made in ethanol. The concentrations were checked before use by measuring the absorbance at 322 nm. Stock solutions of the order of 5×10^{-3} M deteriorated at the rate of about 1% per h at room temperature.

Procedures

All polarographic and u.v. data were obtained at 22 ± 1°C. For the polarographic studies, exactly 9.5 ml of the appropriate buffer was transferred to the polarographic cell. Sufficient ethanol was added to make the final solution 5% in ethanol, i.e. 0.5 ml minus the volume of benzylpenicillenic acid stock solution to be added. A stream of pre-purified nitrogen was bubbled through the solution for 5 min (the nitrogen was pre-saturated by passing through distilled water). Then the appropriate volume of benzylpenicillenic acid stock solution was introduced into the cell, which was gently deaerated with nitrogen for about 1 min, after which the nitrogen stream was directed so that it formed a blanket over the solution. Recording of the polarogram was begun at exactly a known time after the benzylpenicillenic acid sample had been placed in the cell. To follow the temporal changes in the polarographic waves, recording was repeated as required with the solution kept under a nitrogen blanket throughout the period.

Benzylpenicillenic acid solutions for u.v. studies were prepared in 10-ml volumetric flasks. Deaerated buffer was mixed with sufficient deaerated alcohol to produce a solution 5% in alcohol and a sample of deaerated benzylpenicillenic acid stock solution was added to the mixture. The resulting solution was immediately transferred under a nitrogen atmosphere to a u.v. cell. Recording was started at exactly a known time after the addition of benzylpenicillenic acid sample.

The concentrations of benzylpenicillenic acid solutions were calculated on the basis that the molar absorptivity of pure benzylpenicillenic acid was 30 500 at the λ_{max} at 322 nm in ethanol. A correction for the impurity

absorbing at 350 nm was made by subtracting 6% of the total absorbance at 322 nm in ethanol. For the study of change of absorbance with time in aqueous buffers, 6% of the absorbance at zero time (which is equal to the absorbance in the ethanol) was subtracted from each absorbance at a given time. This was because the substance absorbing at 350 nm was stable during the period of the kinetic runs.

RESULTS AND DISCUSSION

The d.c. polarography of benzylpenicillenic acid was investigated in acidic, neutral and alkaline buffer solutions. It gave anodic waves in all solutions investigated. One or two waves were obtained depending on the concentration of benzylpenicillenic acid and the height of the mercury reservoir. The first wave (the more negative) showed the characteristics of an adsorption-controlled pre-wave. The half-wave potential of the second wave was very close to the half-wave potential of penicillamine in a given buffer. Since penicillamine is produced from benzylpenicillenic acid in buffers of certain pH values, the overlap would make it impossible to follow the change of the benzylpenicillenic acid giving two waves with time. Therefore, for the study involving the decrease of the benzylpenicillenic acid wave height with time, the concentrations employed were such that only one wave was obtained for benzylpenicillenic acid. In this paper, reference to the benzylpenicillenic acid wave means this single wave. There was a linear relationship between concentration and wave height in the pH regions investigated.

The half-wave potential ($E_{\frac{1}{2}}$) of the first wave of benzylpenicillenic acid changed with pH as shown in Fig. 2. The plot gives a straight line in the low pH region and then a curve of decreasing slope as the pH becomes higher. The slope of the straight line is 0.055 V/pH. This type of behavior of half-wave potential versus pH is characteristic of anodic waves of the sulfhydryl group [19—23].

In the intermediate pH region 4.0—8.0, the rate of fall of benzylpenicillenic acid current increased as the pH was lowered or raised. The pH-rate profile observed for the decrease of current was in agreement with the pH-rate profile for the decrease in u.v. absorbance of benzylpenicillenic acid [6, 7]. The rate of decrease of absorbance is at a minimum around pH 6.0 and increases as the pH is raised or lowered. The similarity between the rate of fall of current and the rate of fall of absorbance in this pH region can be seen by comparing the two rates in 0.056 M citrate buffer pH 6.45 (Fig. 3). The small difference between the two curves is possibly due to oxidation of benzylpenicillenic acid to its disulfide by traces of oxygen in the spectral studies. Benzylpenicillenic acid disulfide absorbs at 322 nm but is much more stable than benzylpenicillenic acid itself [5, 7]; hence, the rate of fall of absorbance of a benzylpenicillenic acid solution forming some benzylpenicillenic acid disulfide will appear to be slower.

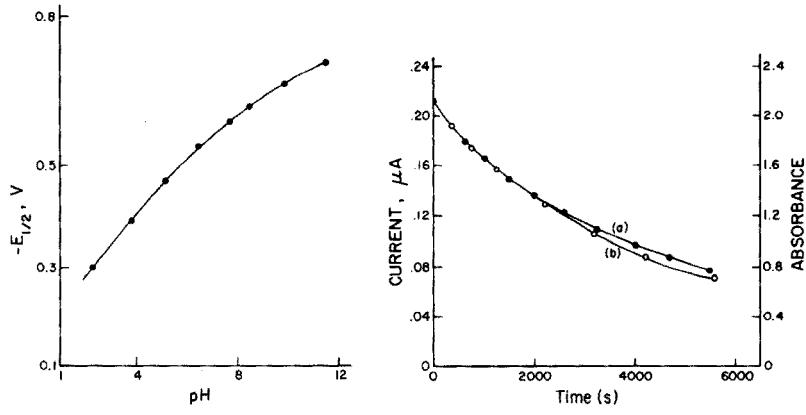

Fig. 2. Half-wave potential of benzylpenicillenic acid versus pH.

Fig. 3. Absorbance—time (a) and current—time (b) plots of 7.0×10^{-5} M benzylpenicillenic acid in citrate buffer pH 6.45. Current measured at —0.4 V. Absorbance at $t = 0$ was taken to be equal to the absorbance in ethanol. Current at $t = 0$ was calculated by using the ratio of absorbance to current at $t = 300$ s and the absorbance at $t = 0$. The scale on the y-axis was chosen so as to make current at $t = 0$ equivalent to absorbance at $t = 0$.

This apparent effect made it necessary to determine, and correct for, the u.v.-absorbing impurity (λ_{max} at 350 nm) found in the product used. The substance does not possess a sulhydryl group (see Fig. 1) and does not give an anodic wave, so that it does not interfere polarographically.

In the low and high pH regions, the rate of decrease of benzylpenicillenic acid current was different from the rate of decrease of its absorbance. In Fig. 4, the absorbance—time and current—time profiles in Sorensen glycine buffer pH 9.70 are compared. Long after the absorbance has disappeared, the benzylpenicillenic acid wave is still present. To determine if the degradation products of benzylpenicillenic acid wave contributed to the benzylpenicillenic acid wave, the polarographic behavior of these substances was investigated. The major degradation product in the alkaline region is

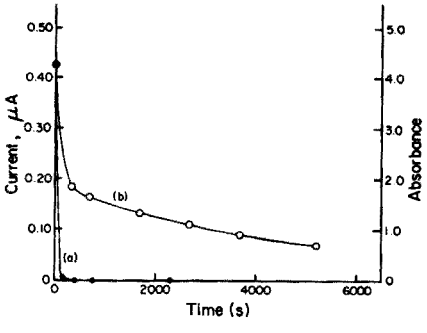

Fig. 4. Absorbance—time (a) and current—time (b) plots of 1.40×10^{-4} M benzylpenicillenic acid in Sorensen glycine buffer pH 9.70. Current measured at —0.5 V.

benzylpenicilloic acid [6]. Benzylpenicilloic acid gave a wave of the positive side of the benzylpenicillenic wave with a half-wave potential of —0.30 V (possibly a capacitive effect). Penicillamine, another possible degradation product, gave a wave between the waves of benzylpenicillenic acid and benzylpenicilloic acid, but was found not to be a degradation product in the alkaline pH region. Thus it was concluded that none of the degradation products contributed to the persisting benzylpenicillenic acid wave. Because the rate of fall of current is different from the rate of fall of absorbance, the ratio of absorbance to current is not independent of time, and the current at zero time cannot be determined. The current in glycine buffer pH 9.70 at zero time was taken as equal to the current of an identical solution of benzylpenicillenic acid in 0.056 M citrate buffer pH 6.45. This was done because d.c. currents of sulfhydryl compounds are normally independent of pH.

Below pH 4.0, a slower decrease in the height of anodic wave than that of absorbance was again observed. Typical polarograms of 1.40×10^{-4} M benzylpenicillenic acid in McIlvaine buffer at pH 2.90 are presented in Fig. 5. The decrease of the original anodic wave (at —0.33 V) is accompanied by formation of a smaller anodic wave at —0.38 V. As benzylpenillic, benzylpenicilloic, and benzylpenilloic acids do not possess a free sulfhydryl group and do not yield anodic waves in this potential range, they can be excluded as the electroactive product formed. Similarly it is possible to exclude penicilamine (Fig. 1), because it gives an anodic wave at a more positive potential than benzylpenicillenic acid. The new anodic wave (at —0.38 V) can be tentatively ascribed to benzylpenamaldic acid (Fig. 1), whose formation was mentioned by Longridge and Timms [6].

Because of the appearance of the poorly resolved wave just before the benzylpenicillenic acid wave, it is difficult to measure the heights of the benzylpenicillenic acid waves at different ages of the solution. However, by

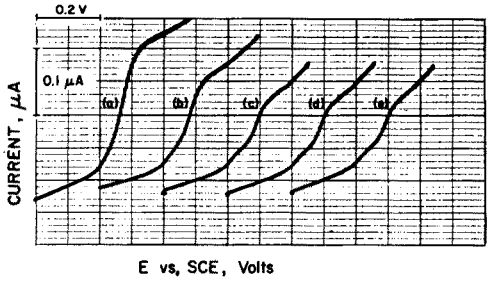

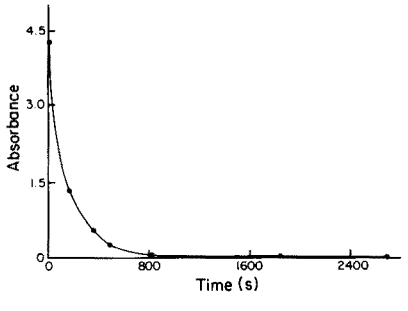

Fig. 5. Temporal changes in polarograms of 1.40×10^{-4} M benzylpenicillenic acid in McIlvaine buffer pH 2.90. Age of solution (in s) when recording started: (a) 150, (b) 450, (c) 1500, (d) 2500, (3) 3850. Initial potential, —0.6 V, Scan rate, 2 mV s^{-1}. Potential increases in the positive sense to the right.

Fig. 6. Absorbance—time plot of 1.40×10^{-4} M benzylpenicillenic acid in McIlvaine buffer pH 2.90.

comparing Figs. 5 and 6, it can be seen that the benzylpenicillenic acid wave is still present even when absorption is practically zero.

The pattern of decrease of benzylpenicillenic acid current with time in different pH regions, can be explained by the fact that benzylpenicillenic acid in an aqueous solution exists in two isomeric forms in equilibrium [6, 7]. Isomer A exists in the solid form, possesses a sulfhydryl group and is u.v.-absorbing, whereas isomer B lacks the sulfhydryl group and is not u.v.-absorbing. When isomer A is dissolved in an aqueous buffer, it isomerizes to B and, at the same time, either A or B (depending on pH) is converted irreversibly to other compounds, e.g. at pH 8.60, B is converted to benzylpenicilloic acid but A does not react except for isomerization to B [6]. Since only A absorbs at 322 nm, the fall of absorbance represents the disappearance of A. Polarography also shows the disappearance of A, because only A is electroactive at the potential region employed. But, in the case of polarography, B may be converted to A at the electrode. The pattern of decrease of current with time in the intermediate pH region may be explained as follows. Because A isomerizes to B, the ratio of B to A increases with time until equilibrium is reached. Since the ratio of current to absorbance is independent of time, the current obtained must be due to A as it exists in the bulk of the polarographic solution. Thus there is no transformation of B to A at the electrode. In the alkaline and acidic pH regions, the sequence of events is the same as above except that there is transformation of B to A at the electrode. The current obtained is due to the kinetic reaction B → A plus the concentration of A which is found in the bulk of the solution, i.e. the current measured is a combination of kinetic and diffusion-controlled currents. Under these conditions the rate of fall of current will be slower than the rate of fall of absorbance. In glycine buffer pH 9.70 (Fig. 4), absorbance is virtually zero after 500 s. Therefore, the current obtained beyond this time must be entirely due to A obtained by isomerization of B at the electrode. Consequently, the rate of fall of current in this period represents the rate of irreversible destruction of B to benzylpenicilloic acid. In the period between zero and 500 s, the current measured is due to the concentration of A in the bulk solution plus that obtained by isomerization of B at the electrode. If the transformation of B to A at the electrode were 100%, the current obtained at any age of the solution would be proportional to the total concentrations of A plus B. But the current after 500 s is only 40% of the current at zero time. This is too large a decrease to be accounted for by irreversible destruction of B to benzylpenicilloic acid during this short period, because hydrolysis of B to benzylpenicilloic acid is relatively slow as evidenced by the later portion of the current curve. Therefore, it can be concluded that there is not a 100% conversion of B to A at the electrode, but that the conversion is at least 40%. Study of the effect of mercury pressure on wave height at t = 500 s showed that the wave height increased with increase in mercury pressure (the wave-height change was nearly proportional to

$h^{\frac{1}{2}}$). Since the current would behave as a diffusion-controlled current if B → A were 100%, the result indicated that a large portion of B is converted to A at the electrode. The current—time behavior in the acidic region can also be explained similarly.

Thus, the results obtained show that the current obtained from benzylpenicillenic acid is a function of several factors: rate of isomerization of A to B, rate of transformation of B to A at the electrode, and rate of destruction of A or B irreversibly to form degradation products.

REFERENCES

1 B. B. Levine, Fed. Proc. Fed. Am. Soc. Exp. Biol., 24 (1965) 45.
2 M. A. Schwartz, J. Pharm. Sci., 58 (1969) 643.
3 M. A. Schwartz, J. Pharm. Sci., 54 (1965) 472.
4 B. B. Levine, Nature, 187 (1960) 939.
5 J. L. Longridge and D. Timms, J. Chem. Soc. B, (1971) 848.
6 J. L. Longridge and D. Timms, J. Chem. Soc. B, (1971) 852.
7 K. H. Dudley, T. C. Butler and D. Johnson, J. Pharmacol. Exp. Ther., 179 (1971) 505.
8 H. Bundgaard, J. Pharm. Sci., 60 (1971) 1273.
9 V. Hanus and E. Krejci, Chem. Listy, 46 (1952) 52.
10 E. Krejci, Collect. Czech. Chem. Commun., 21 (1956) 707.
11 J. Heyrovsky, Collect. Czech. Chem. Commun., 18 (1953) 739.
12 N. Narasimhachari, G. R. Rao and K. S. V. Santhanam, Curr. Sci., 34 (1965) 309.
13 B. B. Levine, Arch. Biochem. Biophys., 93 (1961) 50.
14 A. H. Livermore, F. H. Carpenter, R. W. Holley and V. Du Vigneaud, J. Biol. Chem., 175 (1948) 721.
15 A. H. Cook in H. T. Clarke, J. R. Johnson and B. Robinson (Eds.), The Chemistry of Penicillin, Princeton University Press, Princeton, N.J., 1949, pp. 106—143.
16 R. Mozingo and K. Folkers, in H. T. Clarke, J. R. Johnson and B. Robinson (Eds.), The Chemistry of Penicillin, Princeton University Press, Princeton, N.J., 1949, pp. 535—656.
17 M. A. Schwartz and A. J. Delduce, J. Pharm. Sci., 58 (1969) 1137.
18 K. Diem and C. Lentner (Eds.), Scientific Tables, 7th edn., Ciba-Geigy, Switzerland, 1970, pp. 280—282.
19 W. Stricks and I. M. Kolthoff, J. Am. Chem. Soc., 74 (1952) 4646.
20 C. A. Mairesse-Ducarmois, G. J. Patriarche and J. L. Vandenbalck, Anal. Chim. Acta, 71 (1974) 165; 76 (1975) 299.
21 F. Peter and B. Rosset, Anal. Chim. Acta, 79 (1975) 47.
22 G. Saratori and A. Liberti, J. Electrochem. Soc., 97 (1950) 20.

Analytica Chimica Acta, 96 (1978) 153—163

SPECTROPHOTOMETRIC DETERMINATIONS OF ARYLDIAZONIUM SALTS OF COMPLEX HALIDES USED AS PHOTOINITIATORS IN U.V.-CURED EPOXIDE SYSTEMS

H. POBINER

American Can Company, Princeton Research Center, P.O. Box 50, Princeton, NJ 08540 (U.S.A.)

(Received 27th June 1977)

SUMMARY

Methods for the determination of aryldiazonium salts of complex halides are reported. These salts serve as photoinitiators of polymerization in thin films of u.v.-cured epoxides and in coating solutions. The methods can be applied at the 0.5—4.0 wt.-% level, for determining the quantum yields of photolyses of initiators such as aryldiazonium hexafluorophosphate and tetrafluoroborate. Thin films on reflective substrates are analyzed by spectroreflectometry and films on transparent substrates are analyzed by transmission. An absorbance ratio calculation is used so that the methods are independent of variations in film thickness. Significant analytical bands are the diazonium band at 280—403 nm, depending on the specific initiator, and a series of internal reference bands of the polymer which absorb in different regions of the u.v. and i.r. spectra. The coating solutions are monitored by a differential i.r. method sensitive to less than 0.04 wt.-% of the initiator in a multicomponent system.

Some of the current developments [1—3] in u.v.-cured, solventless coatings are based on a photopolymerization of epoxide via a Lewis acid precursor, namely, the aryldiazonium complex halide salts. For example, an aryldiazonium hexafluorophosphate, of the general formula, $Ar—N{=}NPF_6$, when photolyzed by ultraviolet radiation, will decompose into PF_5, Ar—F, and N_2. PF_5 is actually the Lewis acid catalyst for the cationic photopolymerization of epoxides. Either PF_5, or BF_3 if the $Ar—N{=}NBF_4$ is used, can be detected. One method for determining PF_5 or BF_3 is based on the u.v. spectrum of a complex of the liberated Lewis acid with cyclic ethers [4]. The photochemistry of the entire process has been described elsewhere [5].

This paper describes the analytical methods that were developed to follow the photolysis of the aryldiazonium complex halide salts used as photoinitiators in u.v.-cured epoxide systems. The analytical information was necessary to determine the quantum efficiencies of photolyses of these photoinitiators in thin films of epoxides and for stability studies of coating solutions. Quantitative analysis for the diazonium complex halide in a thin film is based on an absorbance ratio method in both the spectroreflectometric and transmission modes, which readily follow the u.v.-induced

decomposition of the photoinitiator. The ratio method is independent of the variations in film thickness which can occur. The diazonium band is in the u.v. or visible spectrum, depending on the specific photoinitiator, and the internal reference band is in the u.v. or i.r. spectrum. For the determination of the photoinitiator in coating solutions, as opposed to films and panels, a differential i.r. technique is suitable. This method allows rapid determination of the concentration of the diazonium halide in solvent systems for imaging applications.

The literature describes individual methods for the hexafluoro anions and the diazonium group. Archer and Twelves [6] reviewed the analytical chemistry of the hexafluoro anion group. They used a direct gravimetric determination of the hexafluoroantimonate anion, SbF_6^-, with tetraphenylarsonium chloride and nitron as precipitants. They also developed a spectrophotometric method for the anion with ferroin reagents which previously had been described for hexafluorophosphate [7]. Behrends [8] described a direct partition titration for extractable ions, including PF_6^-, with tetraphenylarsonium hydroxide as the titrant and $KMnO_4$ as the indicator. These methods were not applied to the thin epoxide films described here, containing diazonium hexafluorophosphate and tetrafluoroborate photoinitiators at levels as low as 0.03%, because of considerations of sensitivity and selectivity. In addition, the intense color of the coating solutions precluded a direct colorimetric analysis.

Rosenberger and Shoemaker [9] reported a spectrophotometric determination of the diazonium chromophore at 380 nm and its correlation with nitrometer values. The range of analytical wavelengths of the diazonium compounds reported here encompasses this region of the spectrum. Other methods for the diazonium group involve non-aqueous titrimetry [10], and differential kinetics in measuring liberated nitrogen [11], but these methods were not applicable for the study of these photoinitiators at low concentrations in thin films and in complex coating solutions.

A recent paper [12] by Geary dealt with the determination of the aromatic ketone-type photoinitiators used in the free radical polymerization of acrylates for u.v.-cured coatings; the procedure involved extraction followed by u.v.-absorption spectrophotometry. An extraction step was not selected for the present work on the diazonium acid salt photoinitiators because of a lack of unreactive solvents. Furthermore, a non-destructive method was needed to analyze coatings on reflective substrates before and after u.v. exposure, followed by photometric measurements for quantum yield data. In addition, the analytical methods were used to monitor the shelf-lives of photosensitized plates in storage. Analytical methods are described below for the different aryldiazonium salts of complex halides which are used in photopolymerizable epoxy systems [1—3, 5].

EXPERIMENTAL

Instrumentation

An u.v.—visible—near-i.r. spectrophotometer, equipped with an integrating sphere reflectance attachment, e.g. the Beckman DK-2A Spectroreflectometer, and an infrared spectrophotometer, e.g. the Perkin-Elmer Model 521, equipped with a specular reflectance attachment, are required. The laboratory is illuminated by yellow safelights for the preparation of panels and films and the subsequent spectral examinations.

Preparation of panels for reflectance

Prepare a series of solutions each containing 50.0 g of commercial epoxide, such as CIBA, ECN No. 1299, an epoxidized cresol novolac, in 500 ml of butyronitrile (Fisher Sci. Co., No. 741). To each, add an amount of a diazonium photoinitiator, e.g. 2,5-diethoxy-4-(*p*-tolylmercapto)benzenediazonium hexafluorophosphate [1—3, 5], so that the following concentrations, expressed as weight percentage of the epoxide resin, result: 0, 0.1, 0.5, 1.0, 1.5, 2.0, 2.5, 3.0, 3.5, 4.0%. Whirl-coat each solution onto the surface of a 10-in. square of reflective aluminum at about 38°C. Control the coating conditions so that a film of about 0.1 mil is deposited. Use this series for the spectroreflectometric calibration.

Analysis by spectroreflectometry

Reduce the panels to 2 × 3 in. sections. Obtain the visible spectrum for 700—350 nm in the reflectance mode for each panel vs. an uncoated panel. Then obtain the u.v. spectrum in the reflectance mode for 360—210 nm. (With the Beckman DK-2A Spectroreflectometer, it may be necessary to increase the sensitivity from 12 for the visible spectrum to 50 for the u.v. spectrum. For both regions, run at a time constant of 0.1 and a photomultiplier setting at 20×). Read absorbances at the diazonium band at 405 nm, the aromatic band at 280 nm, and the reference point at 700 nm. Representative spectra are shown in Fig. 1. Calculate the absorbance ratio $A_{405\,nm} - A_{700\,nm}/A_{280\,nm} - A_{700\,nm}$. Prepare a calibration plot of absorbance ratio vs. percent diazonium catalyst (Fig. 2). Once the calibration has been completed, analyze the samples similarly. A given sample is analyzed before and after photolysis, so that the extent of decomposition, under specific conditions, is measured. Evaluation of radiation sources and quantum efficiency studies can thus be accomplished.

Preparation of films for absorbance

If the diazonium band of a given photoinitiator occurs in the u.v. spectrum, near the aromatic band of the epoxide resin, then the photolysis can be studied by substituting an aliphatic epoxide, thereby eliminating any possible interference. This is illustrated, together with an absorbance method, in studying transparent films.

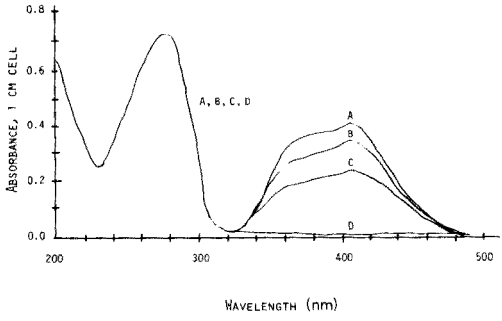

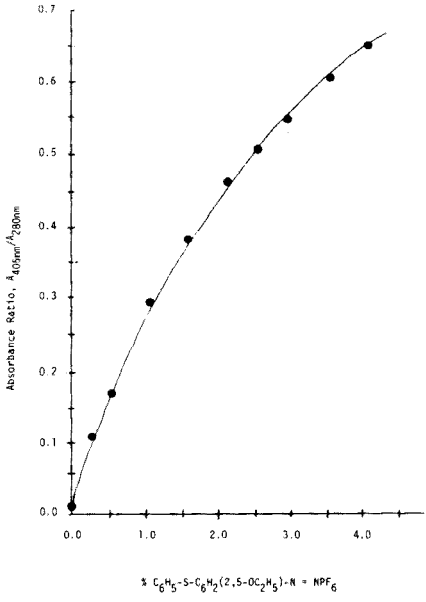

Fig. 1. Progressive photolysis of an aryldiazonium halide photoinitiator in an epoxidized cresol novolac resin on aluminum panels determined by spectroreflectometry. A, 3.00% 2,5-diethoxy-4-(*p*-tolylmercapto)-benzenediazonium hexafluorophosphate, unirradiated. B, irradiated for 2.5 s by xenon lamp; 2.35% residual initiator. C, irradiated for 10 s, 1.35% residual initiator. D, irradiated for 120 s, photolysis complete.

Fig. 2. Calibration curve obtained by spectroreflectometry for 2,5-diethoxy-4-(*p*-tolylmercapto)benzenediazonium hexafluorophosphate in epoxidized cresol novolac film on aluminum.

Prepare a series of solutions, each containing 50.0 g of a non-aromatic epoxide, such as an aliphatic glycidyl ether in 500 ml of butyronitrile. To each, add an amount of *p*-chlorobenzenediazonium hexafluorophosphate, to give concentration levels of 0.0—4.0 wt.-% expressed as a percentage of the resin. Whirl-coat each solution onto the surface of 1-mil polypropylene. Control coating conditions so that a 0.1-mil epoxide film is deposited. Use this series for an absorbance calibration.

Analysis by absorbance measurements

Obtain the absorbance spectrum from 360 nm to 230 nm for each film vs. an uncoated polypropylene film. Similarly obtain the near-i.r. spectrum from 3400 to 3000 nm. (With the Beckman DK-2A, in absorbance configuration, it may be necessary to increase the sensitivity from 12 for the u.v. spectrum to 312 for the near-i.r. spectrum.) Representative spectra are shown in Fig. 3. Read the absorbance of the diazonium band at 283 nm relative to a reference point at 360 nm. Read the absorbance of the aliphatic C—H stretching vibration at 3330 nm relative to a baseline drawn tangentially

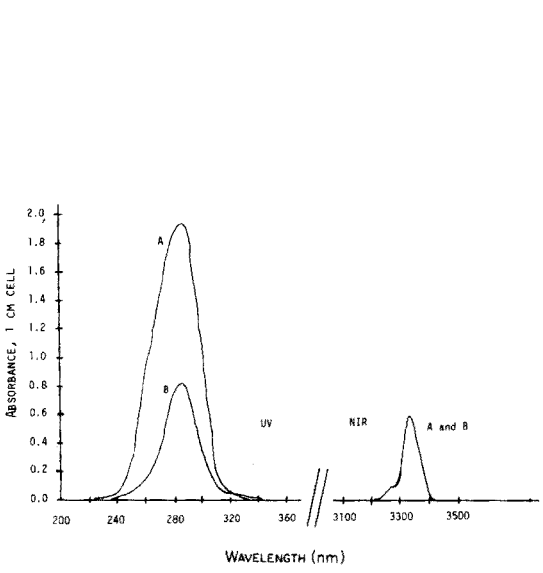

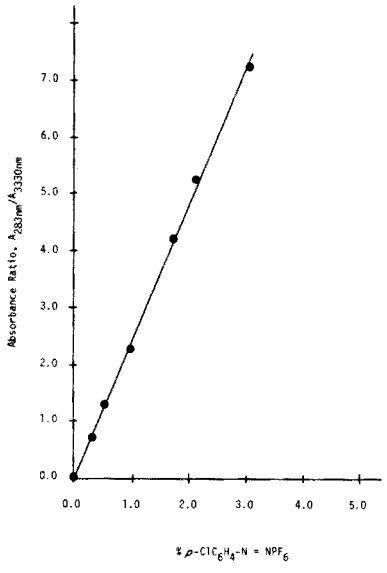

Fig. 3. Photolysis of *p*-chlorobenzenediazonium hexafluorophosphate in an aliphatic epoxide resin on polypropylene film. A, 1.50% photoinitiator, unirradiated. B, after photolysis by xenon lamp; 0.63% residual photoinitiator remaining.

Fig. 4. Calibration curve obtained by absorbance method for *p*-chlorobenzenediazonium hexafluorophosphate in an aliphatic glycidyl ether film on polypropylene.

to the minima at 3280 and 3440 nm. Calculate the absorbance ratio $A_{283\,nm}/A_{3330\,nm}$. Prepare a calibration plot of absorbance ratio vs. % *p*-chlorobenzenediazonium hexafluorophosphate (Fig. 4). The extent of photolysis of irradiated samples for quantum efficiency studies can then be determined.

An alternative internal reference band of the epoxide resin can be used in the i.r. spectrum. For example, if the epoxy resin is of the glycidyl methacrylate type, then the carbonyl band at 1725 cm^{-1} is used. Obtain the i.r. spectrum of the sample film from 1900 cm^{-1} to 1400 cm^{-1} vs. an uncoated polypropylene. Read the absorbance at 1725 cm^{-1} relative to a baseline drawn tangentially to the minima at 1765 cm^{-1} and 1540 cm^{-1}. Calculate the absorbance ratio $A_{283\,nm}/A_{1725\,cm^{-1}}$ and prepare a calibration plot.

Analysis of coating solutions

Prepare a 4% master solution containing the following components of a coating solution: 10.0 g of commercial epoxide, such as epoxy cresol novolac, 197.0 g of chlorinated solvent, such as trichloroethylene, and 0.4 g of aryldiazonium halide photoinitiator. Weigh components accurately so that the photoinitiator represents 4.0 wt.-% of the epoxide resin and 0.19 wt.-% of the entire solution. Prepare a reference solution containing all of these components, except the photoinitiator. Deliver by buret the following aliquots

of the master solution into 25-ml volumetric flasks: 5, 10, 15, 20, 22, 23, 24 ml. Dilute to the mark with reference solution. Obtain the differential i.r. spectra of the master and the diluted solutions vs. the reference solution in 1-mm matched KBr cells from 2400 cm^{-1} to 2100 cm^{-1} (Fig. 5). Measure the diazonium absorption at 2195 cm^{-1} relative to a baseline drawn tangentially to the absorption minima at about 2260 cm^{-1} and 2140 cm^{-1}. Plot a calibration curve of % (w/w) initiator, at the 0.035—0.19% level in solution, vs. the absorbance at 2195 cm^{-1}. For samples, obtain the i.r. spectrum of the coating solution vs. the reference solution, as in the calibration. Calculate the % diazonium level, as a percentage of the solution and as a percentage of the resin.

RESULTS AND DISCUSSION

The photolysis of the diazonium chromophore is readily followed by spectrophotometry. This decomposition is evident in one or more of three spectral regions (ultraviolet, visible, and infrared), and becomes the basis of specific determinations of diazonium photoinitiators in panels, films, and coating solutions. The literature of the photodissociation process in diazo compounds is extensive [13, 14]. In some commercial processes based on the coupling reaction, the direct analysis of the diazonium compound in exposed and unexposed areas is possibly complicated by the presence of

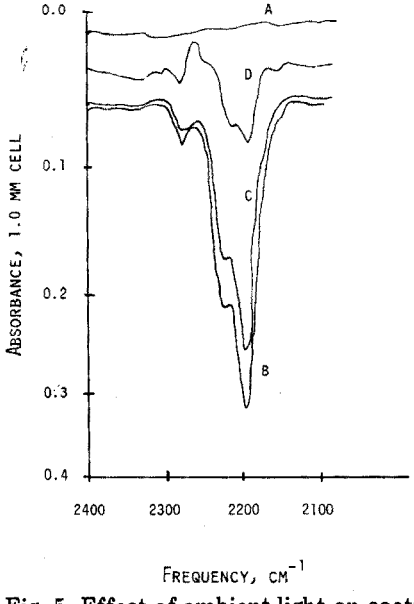

Fig. 5. Effect of ambient light on coating solutions containing diazonium hexafluorophosphate photoinitiators. A, differential I_0, solvent cancellation. B, 3.00% photoinitiator after 64 h in actinic glassware (no change in concentration). C, after 17.5 h in clear glassware (2.32% residual photoinitiator). D, after 64 h in clear glassware (0.72% residual photoinitiator). (All concentrations expressed as a percentage of the resin in the mixed solvents.)

other spectral absorbers. In the exposed and unexposed areas of the films and panels of the photochemical systems described here, direct analyses are facilitated by monitoring the disappearance of the diazonium band at a wavelength independent of the spectral absorptions of other components.

Absorbance ratio method

The deposition of photosensitive epoxide films, at the 0.05—0.1-mil level, on a substrate by the whirl coating technique is reproducible to within 5% of the desired thickness. Since this variation in film thickness can lead to a variation in a direct absorbance calculation, an absorbance ratio method was chosen. By ratioing the absorbance of the photoinitiator, at the 0—4 wt.-% level, at a given analytical wavelength, to that of the epoxide matrix at another analytical wavelength, a suitable quantitative method can be established (Figs. 2 and 4). The data in Table 1 show the absorbance ratios of a series of epoxide films, each containing 3% aryldiazonium hexafluorophosphate, deposited on reflective panels at different times during a 2-month period. Both the absorbances of the photoinitiator and the resin are given to reflect the variations expected in the method. The relative error is 1.7% of the amount present at the 3.0% photoinitiator level.

The recent patent and technical literature [1—3, 5] describe an extensive group of diazonium complex halide salts which are effective initiators of photopolymerization catalysts. Any of these can be determined by selecting the band associated with the diazonium chromophore and ratioing it to a suitable band of the resin. There is a considerable spectral range in which the diazonium band appears and this is, of course, dependent on the aromatic substituents and the type of halide salt [5]. Nevertheless, the analytical wavelength for monitoring the diazonium becomes evident with progressive decrease in absorbance as the sample is irradiated by the u.v. source used in the photopolymerization process. The resins and photoinitiators of some typical photosensitive systems, together with analytical wavelengths, are shown in Table 2.

For these systems, u.v. and visible spectroreflectometry are used to resolve the diazonium band of the photoinitiator, and, if necessary, another reflective technique, such as i.r. specular reflectance, can be used to resolve the internal reference band, such as the carbonyl band of the resin matrix.

TABLE 1

Analysis as a function of the reproducibility of the absorbance ratio data

Ratio $A_{405\,nm}/A_{270\,nm}$	% Photoinitiator found	Ratio $A_{405\,nm}/A_{270\,nm}$	% Photoinitiator found
0.422/0.747 = 0.565	3.06	0.404/0.713 = 0.567	3.08
0.416/0.748 = 0.556	2.98	0.390/0.698 = 0.559	3.00
0.415/0.727 = 0.571	3.13	0.410/0.726 = 0.565	3.06
		Average	3.05

TABLE 2

Representative analytical wavelengths of some photosensitive systems

Photoinitiator/epoxy resin	Analytical wavelength, nm	
	Diazonium band of initiator	Internal referen band of epoxid resin
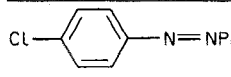 / Aliphatic polyglycidyl ether	283	3330
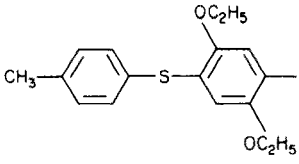 / Aromatic polyglycidyl ether	405	280
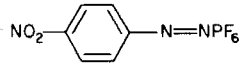 / Polyglycidyl methacrylate	310	5800

Photolysis from spectral source

It is known that the energy requirements for photolysis of some diazonium compounds [15] are sufficiently stringent to warrant the use of high pressure mercury sources and xenon lamps. Nevertheless, it was necessary to demonstrate that the use of an ultraviolet source in the spectrophotometric analysis does not contribute additional photolysis. This is shown by the data of Table 3; clearly the hydrogen and tungsten lamps of the Beckman DK-2A spectrophotometer do not induce measurable photolysis of the diazonium salt of the complex halide being monitored.

TABLE 3

Stability of diazonium complex halides to photolysis induced by spectral energy sources

U.v. and near-i.r. sources			U.v. and vis. sources	
Exposure time (min)	Ratio[a] $A_{310\,nm}/A_{5800\,nm}$	Diaz. halide % found	Ratio[b] $A_{405\,nm}/A_{280\,nm}$	Diaz. halide % found
0	1.085	1.93	0.198	4.00
5	1.085	1.93	0.199	4.02
15	1.085	1.93	0.199	4.02
40	1.089	1.94	0.199	4.02
90	1.082	1.92	0.199	4.02

[a]For an initiator such as *p*-nitrobenzenediazonium hexafluorophosphate.
[b]For an initiator such as 2,5-diethoxy-4-(*p*-tolylmercapto)benzenediazonium hexafluorophosphate. (Both in epoxy films on polypropylene, and determined by the absorbance method.)

Applications of the methods

The spectroreflectometric and absorbance methods are useful in following the shelf-life of photosensitive films or plates based on the cationic polymerization of epoxides initiated by the in situ photolytic generation of Lewis acids. The quantum efficiencies of different initiators can be determined and compared and the relative exposure requirements of test panels in a solventless coatings process can be established [5]. The effect of the number of the exposure units on the photolysis can be studied. For example, in Table 4, the concentrations of residual aryldiazonium hexafluorophosphate initiator, determined by spectroreflectometric absorbance ratios, are tabulated as a function of the time of exposure to a 2000-W xenon lamp. From these data, an optimal exposure time can be selected for the photolysis of the diazonium compound to initiate formation of the Lewis acid catalyst for polymerization. The progressive photolysis of a series of panels is shown in the spectroreflectometric curves of Fig. 1. Photolysis, as measured by the absorbance method, is shown in Fig. 3. Other applications involved correlation of the photodecomposition with process parameters such as u.v. intensity, conveyor or belt speed, temperature and the nature of the coating and the substrate.

The method is sensitive to subtle differences in residual levels of the photoinitiator. Residual concentrations of 0.35, 0.20, 0.10 and less than 0.05% were found after a series of four panels, containing respectively 12, 9, 6 and 3% of the photoinitiator, were exposed to a constant irradiation for 100 s.

The differential i.r. method is used to monitor the concentration of the photoinitiator in coating solutions to be used in imaging and in lithography. Since the method is based on the diazonium frequency, this permits direct analytical control of any undesired photolysis of the initiator. Actinic

TABLE 4

Concentration of aryldiazonium hexafluorophosphate photoinitiator as a function of exposure time

Exposure (s)	Spectroreflectometric absorbance ratio $A_{405\,nm}/A_{280\,nm}$	Concn. of initiator (%)
0	0.560	3.00
2.5	0.485	2.35
5	0.430	1.95
10	0.335	1.35
15	0.257	0.93
30	0.125	0.35
50	0.085	0.20
70	0.030	0.05
120	0.000	0.00
240	0.000	0.00

TABLE 5

Stability of the photoinitiator measured by the i.r. method

Time (h)	Aryldiazonium hexafluorophosphate (%)	
	Storage in actinic glassware	Storage in clear glassware
0	3.05	2.96
17.5	2.96	2.32
41	2.96	1.32
64	2.96	0.72

glassware normally provides sufficient protection against decomposition of the photosensitive agent [13]. The data of Table 5, obtained by the i.r. method show the stability of the aryldiazonium complex halide in actinic glassware, compared with a progressive decrease in concentration, as a result of photolysis, in clear glassware. In clear glassware, the solution finally polymerizes to a gel. The progressive photolysis of the unprotected coating solution is shown in the spectra of Fig. 5.

Precision, sensitivity and relative error

The detection limit for an aryldiazonium complex halide, such as *p*-chlorobenzenediazonium hexafluorophosphate, in a 0.1-mil polymer film on a reflective panel by the method described, is 0.05 wt.-%. In a transparent polypropylene film, the detection limit by the absorbance method is also 0.05 wt.-%, although this limit can be extended, if necessary, by the use of multiple films in a sandwich arrangement or by ordinate scale expansion. At a concentration of 4.0%, the standard deviation for a series of 20 replicate determinations by the absorbance method is 0.019% or 0.48% of the initiator present.

For the i.r. determination of the photoinitiator in a coating solution, the detection limit is 0.02 wt.-%, based on the weight of solution. At a photoinitiator concentration of 0.19%, based on the weight of solution, equivalent to 4.0% based on the weight of resin, the standard deviation for a series of 10 replicate determinations is 0.05% based on the weight of resin, or 1.3% of the initiator present.

As described earlier, the relative error in the spectroreflectometric method is 1.7% of the amount present at the 3.0 wt.-% initiator level in the epoxide film on aluminum. The relative error in the i.r. method for the analysis of the coating solution is 3.3% of the amount present at the 4.0 wt.-% concentration, relative to the resin in solution. This is based on analyses of synthetic blends and newly prepared coating solutions.

The technical advice and cooperation of Sheldon I. Schlesinger, George Hardick, Jr. and (the late) Trevor Blake are respectfully acknowledged.

REFERENCES

1 S. I. Schlesinger, U.S. Patent 3,708,296 (1973).
2 J. H. Feinberg, U.S. Patents 3,711,390 and 3,711,391 (1973).
3 W. R. Watt, U.S. Patents 3,721,616 and 3,721,617 (1973).
4 H. Pobiner, Anal. Chim. Acta, 67 (1973) 448.
5 S. I. Schlesinger, Photogr. Sci. Eng., 18 (1974) 387.
6 V. S. Archer and R. B. Twelves, Talanta, 15 (1968) 47.
7 V. S. Archer and F. G. Doolittle, Anal. Chem., 39 (1967) 371.
8 K. Behrends, Z. Anal. Chem., 250 (1970) 246; Anal. Abstr., 20 (1971) 2996.
9 H. M. Rosenberger and C. J. Shoemaker, Anal. Chem., 31 (1959) 204.
10 T. Jasinski, R. Korewa and H. Smagowski, Chem. Anal. (Warsaw), 9 (1964) 655; Anal. Abstr., 12 (1964) 6551.
11 S. Siggia, J. G. Hanna and N. M. Serencha, Anal. Chem., 35 (1963) 575.
12 J. T. Geary, J. Coatings Technol., 49 (1977) 25.
13 H. Zollinger, Azo and Diazo Chemistry—Aliphatic and Aromatic Compounds, Interscience, 1961, Ch. 7.
14 J. G. Calvert and J. N. Pitts, Jr., Photochemistry, Wiley, 1966, p. 466.
15 J. Kosar, Light-Sensitive Systems: Chemistry and Applications of Nonsilver Halide Photographic Processes, Wiley, 1965, Ch. 6.

Analytica Chimica Acta, 96 (1978) 165—170

THE USE OF HYDROXYNAPHTHOL BLUE IN THE ULTRAMICRO-DETERMINATION OF ALKALINE EARTH AND LANTHANIDE ELEMENTS: AN IMPROVED METHOD

HARRY G. BRITTAIN

Department of Chemistry, Ferrum College, Ferrum, Virginia 24088 (U.S.A.)

(Received 4th April 1977)

SUMMARY

An improved spectrophotometric method for the ultramicrodetermination of alkaline earth and lanthanide elements is reported. Uranyl ion may also be determined. Hydroxynaphthol blue (HNB) dissolved in ammonia buffer (8.5 M in NH_4OH and 1.25 M in NH_4Cl), enables lanthanide elements to be detected at levels of 2.3×10^{-7} M—6.5×10^{-7} M, depending on the particular element. For the Group IIa elements, the lower limits of detection are 3.0×10^{-7} M for Be^{2+}, 4.9×10^{-7} M for Mg^{2+} and 2.0×10^{-6} M for Ca^{2+}. The sensitivity for Sr^{2+} and Ba^{2+} is less, with limits of 8.9×10^{-6} M and 1.8×10^{-5} M, respectively. Uranyl ion can be determined down to 3.3×10^{-7} M. In all cases, a 1:1 metal—dye complex is formed; formation constants were calculated for all metals involved.

o,o'-Dihydroxyazobenzene dyes have found widespread use as metallochromic indicators for calcium and magnesium [1]. A wide variety of substituents and subgroups has been introduced on azobenzene and azonaphthalene derivatives in attempts to obtain more favorable metal-binding and colorimetric behavior. For lanthanide elements, arsenazo-III [2] and xylenol orange [3] seem to have found the most widespread use as spectrophotometric reagents. However, atomic absorption and atomic emission techniques are vastly superior to any of the spectrophotometric procedures described to date, so it is clear that further work is indicated.

1-(2-Naphtholazo-3,6-disulfonic acid)-2-naphthol-4-sulfonic acid, commonly known as hydroxynaphthol blue (HNB), has not received as wide application as other azodyes, and its properties are not well documented. It was first used as an indicator in the EDTA titration of calcium [4], and subsequently applied to the determination of Ca^{2+} in serum and urine [5, 6]. HNB has also been used in successive titration of Mg^{2+} and Ca^{2+} in river and lake waters [7]. More recently, HNB has been used in the spectrophotometric and fluorimetric determination of the uranyl ion [8], and in spectrophotometric analysis for alkaline earth and lanthanide elements [9].

The previous work carried out in this laboratory [9] employed a solution pH of 6.0 and involved the formation of a HNB—EDTA complex to chelate metal ions. Alkaline earth elements could only be determined to levels as low

as 6.0 μg ml^{-1} for Mg^{2+} and even higher levels for the other alkaline earths. Likewise, Sm^{3+} could be determined to levels as low as 1.6 μg ml^{-1}, but other lanthanides could not be measured except at even higher levels. In this present study, the spectrophotometric procedure has been modified, and a resultant 100-fold or better improvement in the metal ion sensitivity obtained. In addition, the new method allows the determination of Be^{2+}, which the older method did not.

EXPERIMENTAL

HNB solution

Hydroxynaphthol blue was obtained (Mallinckrodt Chemical Works) as a 0.5% dispersion in inert salt. Dissolve 0.175 g of this material in 25 ml of ammonia buffer (16.9 g of NH_4Cl in 143 ml of ammonia liquor diluted to 250 ml with distilled water). This solution, which is at pH 10, contains 8.75×10^{-4} g of HNB dye, i.e., 5.85×10^{-5} M. HNB solutions are stable at pH 10 for only one week. They should be allowed to stand in a polyethylene bottle for at least 1 h before use, as there is a rapid initial decomposition (amounting to as much as 10% of the total dye concentration) of the dye, but after this period the rate becomes much slower and will not affect results. The decomposition products do not interfere with the analysis.

Apparatus

A Beckman 25 UV/VIS recording spectrophotometer equipped with various absorbance scales was used for all work (which was carried out at a room temperature of 20°C). The instrument was used in the normal absorption mode (0—1 absorbance scale) for concentrated metal ion solutions (greater than 1 μg ml^{-1}) and in the differential absorption mode (0—0.1 absorbance scale) for concentrations less than 1 μg ml^{-1}.

Stock solutions

Prepare solutions of Group IIa elements from the nitrate salts in doubly distilled water, and standardize by gravimetric procedures. Prepare solutions of lanthanide elements by dissolving the hydrated chlorides (obtained by dissolving the 99.9% oxides in 12 M HCl and evaporating to dryness) in distilled water; prepare uranyl ion stock solutions from uranyl nitrate. Stock solutions of 10^{-5}—10^{-3} M concentration were used to cover the useful concentration ranges, and all were made up in class A accuracy glassware.

Procedure

Pipette small quantities (0.01—0.10 ml) of metal ion solution directly into the spectrophotometer cuvette, and then add 3.0 ml of the HNB stock solution by pipette. Mix, allow to stand for about 5 min (which permits equilibrium to be established), and then scan over the 450—800-nm spectral region. If the metal ion concentration to be determined is above 10^{-5} M,

record the absorbances (λ_{max} = 650 nm) of the metal-free dye and of the dye with metal ions added, and subtract the values to find the absorption change effected by the metal ions (the change being greater than 0.02 absorbance units). If lower concentrations are to be determined, use the differential technique. Place a solution of metal-free dye in the reference beam and read the absorbance of the sample solution in the normal manner. Both solutions must contain exactly the same concentration of HNB; any dilutions of samples must be duplicated in the reference. With the recorder adjusted so that instrumental zero is located in the center of the chart, the change in HNB concentration caused by complexation appears as a negative peak centered around 650 nm. Maximum sensitivity is attained with this method by setting the spectrophotometer on a 0 to 0.1 absorbance scale.

Calibration curves

Linearity in the calibration curves is maintained until the total metal ion concentration reaches approximately that of the HNB dye. Higher concentrations may be determined, but the calibration curves will not be linear. Calibration curves for the change in HNB absorbance with metal ion concentration were constructed (each consisting of 10 points), and the data fitted by standard least squares analysis: $\Delta A = a_0 + a_1[M]$. Lower limits of detection for the various metal ions were obtained by substituting the smallest ΔA measurable for the given spectrophotometer (0.001 absorbance units for the Beckman 25) and then finding the resulting metal ion concentration.

RESULTS AND DISCUSSION

Three states of hydroxynaphthol blue have been identified in the absorption spectra of the dye as solution pH is varied. HNB exists in a red (H_2B) form below pH 4 (λ_{max} = 530 nm) undergoes a red-to-blue transition at pH 4—5, exists in a blue (HB^-) form at pH 5—12 (λ_{max} = 650 nm), undergoes a blue-to-blue-green transition at pH 12—13, and finally exists in the blue-green (B^{2-}) form above pH 13 (λ_{max} = 600 nm). Figure 1 shows the absorption spectra that result from these three forms. The equilibria may be interpreted in terms of the removal of the hydroxy protons that are located ortho to the azo bridge connecting the naphthalene rings:

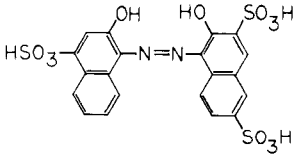

Figure 1 indicates that there is little (if any) overlap between the absorption of the red (H_2B) and blue (HB^-) forms of the HNB dye, so if the solution pH is maintained at 10.0, then the change in HNB absorbance at 650 nm is directly proportional to the change in metal-free dye concentration.

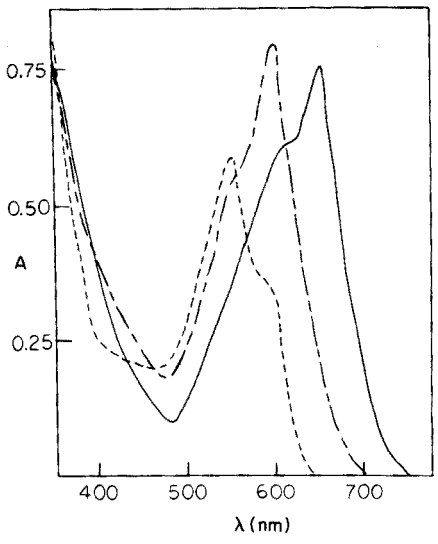

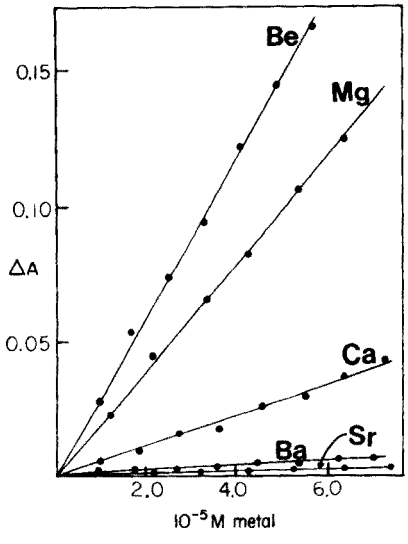

Fig. 1. Absorption spectra of hydroxynaphthol blue at various solution acidities. Spectra are taken at pH 4.0 (— — —), 10.0 (——), and 13.5 (— · —).

Fig. 2. Change in absorbance of hydroxynaphthol blue as a function of Group IIa element concentration.

At pH 10, the blue HNB (HB^-) can be converted to the red metal complex (whose absorption spectrum is identical to the red H_2B form of HNB) by addition of alkaline earth elements, lanthanide elements, or uranyl ions. Previous work [9] with a HNB—EDTA reagent (at pH 6.0) indicated that Be^{2+} could not be determined, but that all other Group IIa elements could be. Under the conditions described here, Be^{2+} can be determined, and HNB is more sensitive to Be^{2+} ions than to any other element in the group. This behavior is illustrated in Fig. 2, in which typical calibration curves for all these elements are presented. HNB sensitivity to alkaline earths decreases as the atomic number (and the ionic radius) of the metal ion increases. Values for the lower limits of detection are given in Table 1.

Lanthanide ions also form complexes with the blue (HB^-) form of HNB. Unlike the Group IIa elements which show varying degrees of sensitivity toward HNB at pH 10.0, the lanthanides all exhibit approximately the same sensitivity. This behavior is not unexpected, considering their similar chemical properties. Table 1 shows that the lower limits range from 2.3×10^{-7} M for Nd^{3+} to 6.5×10^{-7} M for Yb^{3+}. The HNB—EDTA reagent at pH 6.0 [9] showed more variation in metal ion sensitivities than does HNB at pH 10.0; with the former method, determination of Er^{3+} and Yb^{3+} was deemed inadequate. Like arsenazo-III [2] and xylenol orange [3], hydroxynaphthol blue at pH 10 appears to complex the entire series equally well and thus enables the determination of total lanthanide content. This type of analysis

TABLE 1

Lower limits of detection and formation constants obtained in the reaction of hydroxynaphthol blue and various metal ions

Metal	Limit (M)	Limit (μg ml^{-1})	log K	Metal	Limit (M)	Limit (μg ml^{-1})	log K
Be^{2+}	3.0×10^{-7}	0.0027	3.63	Eu^{3+}	2.7×10^{-7}	0.041	4.10
Mg^{2+}	4.9×10^{-7}	0.012	3.43	Gd^{3+}	3.1×10^{-7}	0.049	3.76
Ca^{2+}	2.0×10^{-6}	0.081	2.82	Tb^{3+}	3.7×10^{-7}	0.059	3.77
Sr^{2+}	8.9×10^{-6}	0.78	2.05	Dy^{3+}	4.0×10^{-7}	0.065	3.71
Ba^{2+}	1.8×10^{-5}	2.43	1.75	Ho^{3+}	4.5×10^{-7}	0.073	3.68
La^{3+}	3.4×10^{-7}	0.047	3.57	Er^{3+}	5.4×10^{-7}	0.090	3.60
Pr^{3+}	2.5×10^{-7}	0.035	4.03	Yb^{3+}	6.5×10^{-7}	0.112	3.50
Nd^{3+}	2.3×10^{-7}	0.033	4.13	UO_2^{2+}	3.3×10^{-7}	0.089	4.10
Sm^{3+}	2.5×10^{-7}	0.038	4.09				

is of interest in the analysis of monazite sands. If individual rare earths are to be determined with HNB, they must first be separated from each other.

Uranyl ion forms a complex with HNB at pH 4.0 (in phthalate buffer), and can be determined spectrophotometrically down to 1.1×10^{-6} M (0.30 μg ml^{-1}) [8]. A fluorimetric method was also described in which uranyl ion could be measured down to 3.2×10^{-6} M (0.86 μg ml^{-1}) [8]. With the present conditions, uranyl ion may be determined down to 3.3×10^{-7} M (0.089 μg ml^{-1}), which is a significant improvement. Work is now proceeding to learn if other actinides may be determined with HNB at pH 10.

Job's method of continuous variations was used to determine the stoichiometry of the metal—HNB complex. In all the cases studied here, a 1:1 type of complex was formed; equilibrium constants for the metal complexes were therefore calculated (Table 1). As is usual, the strength of the metal—HNB complex (as measured by log K) is directly related to the sensitivity of the analytical method.

A few potential interferences were studied with the ultimate intent of applying the HNB reagent to a study of natural waters. Fe^{2+} ions strongly complex the HNB (forming a red compound) and must be excluded; Fe^{3+} provides a much smaller interference but should also be excluded, unless the total hardness of a water sample is to be determined (alkaline earths plus iron). Cu^{2+} and Ni^{2+} both form colored ammines with the buffer and must be avoided. Finally, Al^{3+} interferes slightly and should be removed.

Analysis for lanthanide ions with HNB is about one order of magnitude more sensitive than that with arsenazo-III [2]. Analysis with xylenol orange [3] yields approximately the same sensitivity as the HNB method described here, but requires the presence of additional reagents to attain the optimum results. It is clear that hydroxynaphthol blue makes an excellent spectrophotometric reagent for the determination of Group IIa and lanthanide elements and that it will find wider use in the future.

REFERENCES

1 See, for example, H. Diehl, Calcein, Calmagite, and *o,o'*-dihydroxyazobenzene. Titrimetric, Colorimetric, and Fluorometric Reagents for Calcium and Magnesium, G. Frederick Smith Chemical Company, Columbus, Ohio, 1964.
2 S. B. Savvin, Talanta, 8 (1961) 673; H. Onishi and C. V. Banks, Talanta, 10 (1963) 399.
3 V. Svoboda and V. Chromy, Talanta, 13 (1966) 237; W. J. de Wet and G. B. Behrens, Anal. Chem., 40 (1968) 200.
4 R. W. Goettsch, J. Pharm. Sci., 54 (1965) 317.
5 G. Catledge and H. Biggs, Clin. Chem., 11 (1965) 521.
6 O. E. Newfield, Med. J. Aust., 1 (1967) 257.
7 A. Ito and K. Ueno, Bunseki Kagaku, 19 (1970) 393.
8 H. G. Brittain, Anal. Lett., 10 (1977) 263.
9 H. G. Brittain, Anal. Chem., 49 (1977) 969.

Analytica Chimica Acta, 96 (1978) 171—175

Short Communication

AN EVALUATION OF PVC MATRIX MEMBRANE CALCIUM-SELECTIVE ELECTRODES BASED ON NITRATED (OCTYLPHENYL)PHOSPHATE SENSORS AND PHOSPHONATE MEDIATORS

L. KEIL, G. J. MOODY and J. D. R. THOMAS*

Chemistry Department, UWIST, Cardiff CF1 3NU (Wales)

(Received 18th July 1977)

Calcium salts of dialkylphosphoric acids, $(RO)_2P(O)OH$, e.g. di-n-decylphosphoric acid in conjunction with di-n-octylphenylphosphonate as a solvent mediator, constitute the basis of the classical Orion liquid ion-exchanger calcium electrode [1, 2]. This electrode is, however, subject to pH interference to an extent depending on the calcium levels in samples. Růžička et al. [3] suggested that increasing the electrophilic character of the alkyl chain, R, in such sensors would give a more labile hydrogen atom, thereby shifting the region of the existence of the acid form to lower pH values, and so would enhance the pH selectivity range. Replacing both the decyl groups of di-n-decylphosphoric acid with either two n-octylphenyl [3], or two 4-(1,1,3,3-tetramethylbutyl)phenyl [4, 5] groups does indeed provide calcium ion-selective electrodes for which the characteristic dips [2] in the pH vs. calcium activity plots shift from about pH 5 to 4 (see also Table 1). A further increase in electrophilic character of the octylphenyl group, for example, by incorporating one or more nitro groups, might confer even better pH response. In this respect, Jagner and Østergaard-Jensen [6] recorded a pH shift of about 0.4 towards the alkaline region for a calcium-selective electrode with a membrane of calcium di(4-n-octyl-2-nitrophenyl)-phosphate sensor plus di-n-octylphenylphosphonate solvent mediator. Membranes based on calcium di(4-n-octyl-2-bromophenyl)phosphate sensor with di-n-octylphenylphosphonate solvent mediator gave electrodes that closely resembled those employing calcium di(4-n-octylphenyl)phosphate sensor with di-n-octylphenylphosphonate solvent mediator in the membrane [6]. Nitration of the much-used di-n-octylphenylphosphonate solvent mediator could be beneficial.

This communication describes an evaluation of the calcium salts of di[4-(1,1,3,3-tetramethylbutyl)-2-nitrophenyl] phosphoric acid, di[4-(1,1,3,3-tetramethylbutyl)-2,6-dinitrophenyl] phosphoric acid, and di(4-nitrophenyl)phosphoric acid as sensors together with di-n-octyl-(3-nitrophenyl)-phosphonate as solvent mediator.

Experimental

Chemicals. Except in cases where membrane materials were synthesized, the chemicals used were generally of analytical-reagent grade or reagent grade. Di(4-nitrophenyl)phosphoric acid was obtained from Aldrich Chemical Co. Ltd.

Preparation of sensor materials. Di-n-octylphenylphosphonate and calcium di-n-decylphosphate were synthesized as previously described [7, 8]. Di-n-octyl(3-nitrophenyl)phosphonate was obtained [9] by nitrating di-n-octylphenylphosphonate with 10 M nitric acid in conjunction with 18 M sulphuric acid. Di[4-(1,1,3,3-tetramethylbutyl)phenyl] phosphoric acid was prepared [10] by reacting phosphoryl chloride with 4-(1,1,3,3-tetramethylbutyl)phenol. The calcium salt was prepared by reacting an aqueous methanolic solution of the acid with calcium hydroxide [10]. Di[4-(1,1,3,3-tetramethylbutyl)-2-nitrophenyl] phosphoric acid was prepared by reacting phosphoryl chloride with 4-(1,1,3,3-tetramethylbutyl)-2-nitrophenol obtained by nitrating 4-(1,1,3,3-tetramethylbutyl)phenol with dilute nitrous acid [9]. Di[4-(1,1,3,3-tetramethylbutyl)-2,6-dinitrophenyl] phosphoric acid was similarly prepared [9] from phosphoryl chloride and 4-(1,1,3,3-tetramethylbutyl)-2,6-dinitrophenol obtained by nitrating 4-(1,1,3,3-tetramethylbutyl)-phenol with fuming nitric acid in glacial acetic acid at -15° C. The calcium salts of each of the nitrated acids were prepared [9] by reacting an aqueous methanolic solution of the appropriate acid with calcium hydroxide.

Electrodes. Ion-selective electrodes with membranes containing the calcium liquid ion-exchanger (solvent mediator (0.36 g) plus sensor (0.036 g)) trapped in PVC were prepared as previously described [7, 11]. Membrane II (Table 1) based on calcium di(4-n-octylphenyl)phosphate sensor and di-n-octylphenylphosphonate mediator trapped in PVC was a gift from Dr. J. Růžička (The Technical University of Denmark).

Procedures. All e.m.f. measurements were made relative to a Corning model 476 109 ceramic plug-type calomel reference electrode containing 4 M potassium chloride solution. A Corning-EEL Model 112 or Radiometer Model PHM 64 digital millivoltmeter-pH meter was used in conjunction with a Servoscribe potentiometric recorder. Selectivity coefficients, k_{CaB}^{pot}, were determined by the mixed solution method [12] with a fixed level of interferent B. pH interference was assessed by the mixed solution method [12] where the calcium ion level was fixed at 10^{-3} M and pH varied.

Results and discussion

The superiority (Table 1) of electrodes of both the di(octylphenyl)-phosphate membranes (II and IIIA) over an electrode of the didecylphosphate membrane (IA) is indicated not only by the pH range but more so by the remarkable lack of sodium ion interference, a feature that extends even to mixed solutions containing calcium ions in 0.15 M sodium chloride [5]. In this respect, it is also interesting that PVC calcium microelectrodes based on the branched chain di[4-(1,1,3,3-tetramethylbutyl)phenyl] phosphate

Some specifications of PVC calcium-selective electrodes based on various sensors and mediators at 25°C
(In all cases, the lifetimes of the electrodes exceed 2 weeks.)

Membrane No.	Liquid ion-exchanger System		Detection limit[a]	Slope (mV/ decade)	Interferences		
	Sensor	Mediator			pH range[b]	k^{pot}_{CaNa} [c]	k^{pot}_{CaMg} [d]
IA	$[n\text{-}(C_{10}H_{21}O)_2\ P(O)O]_2Ca$ + $(n\text{-}C_{10}H_{21}O)_2\ P(O)OH$ (1:1 w/w)	DOPP (ϵ = 6.2)	6.5×10^{-6}	29.5	5 → 8	0.016	0.21
IB		3-NO_2.DOPP (ϵ = 11.4)	7×10^{-6}	29	5 → 8	0.018	0.06
II	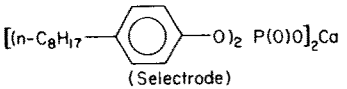 (Selectrode)	DOPP	6×10^{-6}	30	4 → 9.5	Nil	0.03
IIIA	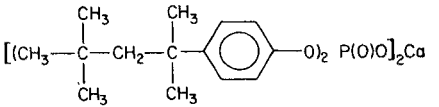	DOPP	4.6×10^{-6}	30	4 → 9.5	Nil	0.03
IIIB		3-NO_2.DOPP	5×10^{-6}	30	4 → 9.5	Nil	0.03
IVA	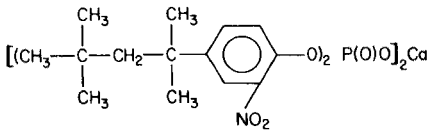	DOPP	1.5×10^{-5}	29.5	3.5 → 7.5	0.04	0.07
IVB		3-NO_2.DOPP	8×10^{-6}	28.5	5 → 8	0.1	0.055
VA	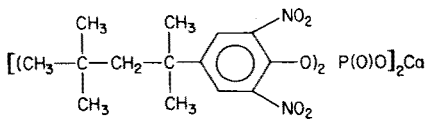	DOPP	8×10^{-6}	30	5 → 10	0.02	0.07
VB	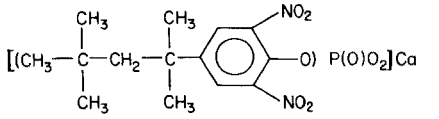	3-NO_2.DOPP	9.5×10^{-6}	29.5	5 → 10	0.03	0.09
VIA	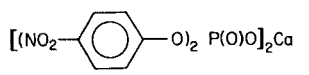	DOPP	3.5×10^{-5}	35	No useful range	—	—
VIB		3-NO_2.DOPP	6×10^{-6}	29.5	3.5 → 8.5	0.6	0.05

[a]Lower detection limit based on $18/z$ mV deviation from the linear calibration plots for calcium chloride standards. [b]In 10^{-3} M $CaCl_2$. [c]NaCl = 5×10^{-2} M. [d]$MgCl_2$ = 5×10^{-3} M.

sensor of membranes III have been reported [4] to have less sodium, potassium and magnesium interference than their macro counterparts.

The general performance of calcium(II) electrodes made from membranes containing di-n-octylphenylphosphate [3] and di[4-(1,1,3,3-tetramethylbutyl)phenyl] phosphate sensors [4] (membranes II and IIIA) is such that they are virtually identical (Table 1). This characteristic is fortuitous in view of the greater ease of preparation of the branched isomeric octylphenylphosphate sensor [9] and also bearing in mind that selectivity coefficients can vary between similar sensor systems. Thus, while k^{pot}_{CaMg} values are similar for PVC calcium-selective electrodes based on membranes containing di-n-decylphosphate or di-2-ethylhexylphosphate with di-n-octylphenylphosphonate solvent mediator, the k^{pot}_{CaNa} values are quite different [13].

Nitrating the di-n-octylphenylphosphate solvent mediator considerably raises the permittivity, but here this has had little effect on selectivity coefficients. Thus, the values of k^{pot}_{CaMg} are similar for all the electrodes studied except for that made from membrane IA (Table 1). Also, the virtual absence of sodium interference and the similar pH profiles of membranes IIIA and IIIB seem independent of the solvent mediator employed.

Membrane IVA, comprising the mononitrated sensor corresponding to the reference membrane III system, gives a calcium electrode that exhibits the further anticipated shift of pH interference to lower pH values, but this feature is not characteristic of the electrode when the membrane (IVB) contains the nitrated solvent mediator, nor when it contains the di-nitrated sensor (membranes VA and VB). Indeed, in these instances the pH interference sets in at pH ca. 5 and nullifies predicted trends.

Despite the slight improvement with respect to pH interference for calcium electrodes with certain membranes (II, IIIA, IIIB, IVA and VIB), which permits their use for calcium(II) measurements under slightly more acidic conditions, the serious dip features characteristic of calcium-selective electrodes based on dialkylphosphate sensors and phosphonate solvent mediators were seen in all except for the electrode (Fig. 1) from membrane VIB. In this respect, membrane VIB is similar in behaviour to a system based on a sensor composed of the tetraphenylborate salt of a polypropylene glycol complex of calcium used in association with di-n-octylphenylphosphonate or its nitrated analogue as solvent mediator [14].

Di(4-nitrophenyl)phosphoric acid and its calcium salt are relatively water-soluble and electrodes with membranes (VI) containing these materials impart a yellow tinge to aqueous calcium chloride standards.

Conclusion. Calcium-selective electrodes based on PVC matrix membranes containing di(n-octyl)phenylphosphate or di[4-(1,1,3,3-tetramethylbutyl)-phenyl] phosphate are confirmed to be superior to their didecylphosphate counterparts with respect to pH interference and selectivity over sodium and magnesium. No further advantage is gained by nitrating the phenyl groups either of the sensor or of the di-n-octylphenylphosphonate solvent mediator.

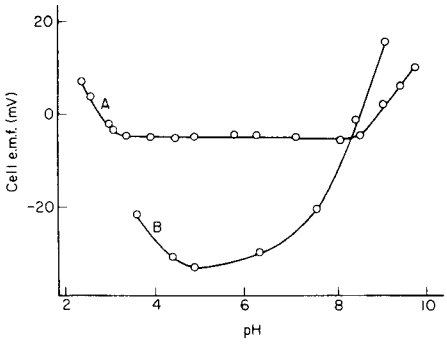

Fig. 1. The effect of pH on the response to 10^{-3} M calcium chloride solutions of calcium-selective electrodes prepared from PVC matrix membranes based on calcium di(4-nitrophenyl)phosphate sensor with di-n-octyl-(3-nitrophenyl)-phosphonate (curve A) or di-n-octylphenylphosphonate (curve B) solvent mediator.

The authors thank the University of Wales for a research studentship (L. K.).

REFERENCES

1 J. W. Ross, Science, 156 (1967) 1378.
2 J. W. Ross, in R. A. Durst (Ed.), Ion-selective Electrodes, Special Publication, 314, National Bureau of Standards, Washington, D.C., 1969, p. 57.
3 J. Růžička, E. H. Hansen and J. Chr. Tjell, Anal. Chim. Acta, 67 (1973) 155.
4 H. M. Brown, J. P. Pemberton and J. D. Owen, Anal. Chim. Acta, 85 (1976) 261.
5 A. Craggs, L. Keil, G. J. Moody, N. S. Nassory and J. D. R. Thomas, unpublished work.
6 D. Jagner and J. P. Østergaard-Jensen, Anal. Chim. Acta, 80 (1975) 9.
7 G. J. Moody, R. B. Oke and J. D. R. Thomas, Analyst, 95 (1970) 910.
8 A. Craggs, L. Keil, G. J. Moody and J. D. R. Thomas, J. Inorg. Nucl. Chem., 37 (1975) 577 (and references therein).
9 A. Craggs, P. G. Delduca, L. Keil, G. J. Moody and J. D. R. Thomas, to be published.
10 A. Craggs, P. G. Delduca, L. Keil, B. J. Key, G. J. Moody and J. D. R. Thomas, to be published.
11 A. Craggs, G. J. Moody and J. D. R. Thomas, J. Chem. Educ., 51 (1974) 541.
12 G. J. Moody and J. D. R. Thomas, Lab. Pract., 20 (1971) 307; Talanta, 19 (1972) 623; Sel. Ann. Rev. Anal. Sci., 3 (1973) 59.
13 A. Craggs, L. Keil, G. J. Moody and J. D. R. Thomas, Talanta, 22 (1975) 907.
14 A. M. Y. Jaber, G. J. Moody and J. D. R. Thomas, Analyst, in press.

Analytica Chimica Acta, 96 (1978) 177—181

Short Communication

SUBTRACTIVE ANODIC STRIPPING VOLTAMMETRY AT TWIN MERCURY FILM ELECTRODES

E. STEEMAN, E. TEMMERMAN* and R. VERBINNEN

Laboratory of Analytical Chemistry, Ghent University, J. Plateaustraat 22, B-9000 Ghent (Belgium)

(Received 12th July 1977)

Anodic stripping voltammetry (a.s.v.) is a valuable technique for the determination of traces of metals [1]. A.s.v. at solid electrodes is frequently complicated by the appearance of multiple stripping peaks, which explains the widespread use of mercury electrodes when possible. Thin-film mercury electrodes and especially the in situ plated electrode proposed by Florence [2] offer distinct advantages over the classical mercury drop electrode [3] in d.c. stripping voltammetry. One of the advantages of in situ plating is that the amalgam concentration does not vary significantly with deposition time so that amalgam saturation problems are minimized. Problems encountered in a.s.v. are often associated with the large capacitive background current in conventional linear scan techniques and the occurrence of reagent blanks of the elements to be determined. When voltammetric methods are used, the addition of supporting electrolyte is mandatory for most samples.

In order to increase the signal-to-background ratio, various voltammetric techniques have been employed. These include derivative [4], phase-selective a.c. [5], ring-disk [6], staircase [7] and the more and more frequently used pulse techniques [8].

In addition to the capacitive current, the background processes also include electrochemical reactions of the electrode itself and reduction or oxidation of impurities in the solution or adsorbed at the surface of the electrode. This communication reports the use of a subtractive technique with a twin-cell, twin-mercury film electrode system in linear-scan stripping voltammetry to minimize the background current. One cell contains a blank solution while the other contains the solution under test. The same potential scan is applied to both electrodes and the difference between the cell currents is measured.

Experimental

Instrumentation. A model A 1660 Davis Differential Cathode Ray Polarograph (Southern Analytical Ltd.) was modified to permit the voltage scan to be started manually. The current—potential curves, registered on the built-in

oscilloscope, were also recorded on a Hewlett-Packard x—y recorder (Model 7004 B) to make the measurement of the current easier and more accurate. As the instrument is a two-electrode polarograph, the resistance of the reference electrode, which also serves as the counter electrode, should be as low as possible. Therefore a mercury pool was used as reference electrode in a 0.1 M hydrochloric acid supporting electrolyte. Small differences (< 10 mV) of the pool potentials of the two cells can be compensated by means of the potential balance control of the polarograph.

The construction of the glassy carbon electrodes (Tokai Electrode Mfg. Co., Tokyo; grade GC-30S, code RA-3, surface area 6.1 mm^2) serving as substrate for the mercury film has been described previously [9]. In order to match optimally the characteristics of the two carbon surfaces, a piece of carbon rod was cut into two. The newly cut faces were used as the working surfaces after polishing with a succession of silicon carbide grits and diamond compounds (Engis Hyprez 6, 3, 1, 0.25 and 0.1 μm) on a polishing cloth with an Engis Kent Mk 2 polishing machine. Finally, the electrodes were cleaned by ultrasonic vibration in 0.1 M nitric acid for 5 min. Standard Metrohm 25-ml cell assemblies and Beckman rotators (Model 1885) were used.

Reagents. Water was double-distilled in quartz apparatus and stored in polyethylene bottles. Nitric and hydrochloric acid were Merck Suprapur. Lead and cadmium standards were prepared from high-purity metals dissolved in nitric acid. Solutions more dilute than 10^{-3} M were freshly prepared immediately before use. A mercury stock solution was prepared by dissolving very pure, electrolytically refined mercury in 7 M nitric acid. High-purity nitrogen (Oxhydrique, type E, containing less than 1 ppm of oxygen) was used to deoxygenate the sample solutions.

Procedure. Prepare two cells, one containing the solution under test, and the other containing a blank solution (supporting electrolyte, reagents used). Add 2.5×10^{-5} M mercury(II) to both cells, and deaerate the solutions at the same rate to prevent differential evaporation; then maintain a nitrogen atmosphere above the solutions. Start the electrode rotation and deposit mercury at —1 V vs. mercury pool for 3 min. Set the plating potential (—0.9 V for lead) and switch one or both of the cells, as appropriate, into the circuit. Mercury is also plated during the pre-electrolysis. Stop the rotation after 2 or 3 min. After a delay of 30 s, start the anodic voltage scan and record the current—voltage curve of one of the cells or the subtractive curve of both cells.

Results and discussion

Figure 1 shows the single-cell (curves a and b) and the subtractive (curve c) voltammetric curves obtained under identical experimental conditions after a 2-min pre-electrolysis at 750 rpm of the 0.1 M supporting electrolyte. The peaks at about —0.5 V are due to lead, and at ca. —0.68 V, much smaller cadmium peaks can be detected. A lead(II) concentration of 2.75×10^{-8} M

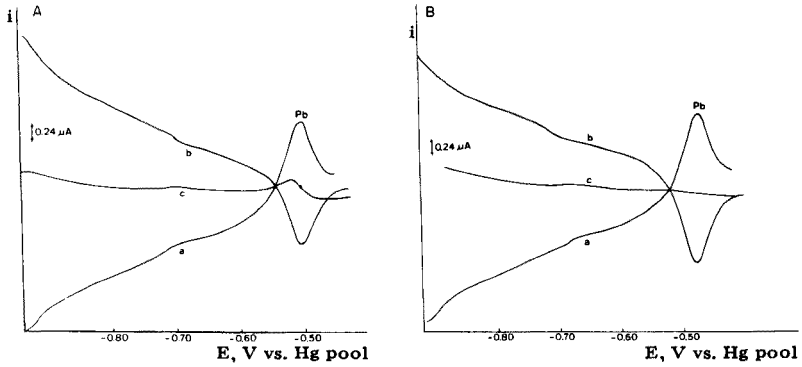

Fig. 1. Anodic stripping curves obtained in 0.1 M HCl. Curves a and b are single-cell curves; c is the subtractive curve. (A) Solutions: 2.5×10^{-5} M Hg(II) and 2.75×10^{-8} M Pb(II) blank in 0.1 M HCl. 2-min pre-electrolysis at −0.95 V and 750 rpm; delay time, 30 s; scan rate, 15 V min^{-1}. (B) Conditions are the same as for A except that the rotation rate of electrode *b* was 970 rpm during the deposition step.

was determined from curve (a) by standard addition analysis. This is almost entirely due to lead present in the double-distilled water, as no significant increase in peak height was obtained after doubling the hydrochloric acid concentration.

The two cells contain identical solutions, and if the conditions of operation of the two electrode systems were also identical one would expect the resulting subtractive trace (curve c) to be a flat line since the opposing currents would cancel. Obviously this is not the case: the lead peak of curve (b) is 12.5% lower than the corresponding peak of curve (a), and the base lines do not cancel each other perfectly. This results from the almost inevitably imperfect match of the conditions of operation of two mercury-film electrode systems. There are many possible causes: differences of surface areas, surface condition (e.g. oxidation of some mercury to calomel by oxygen, mechanical disturbance of the electrode surface), pretreatment (polishing), rotation rate and mercury deposition potential between the two film electrodes; differences of cell-electrode geometries and efficiency of stirring; dissimilar mercury pool potentials; differences in deaeration of both cells; and inequality of the concentration of lead in the two cells because of contamination.

Matching the conditions of operation of two-electrode systems is the chief difficulty in all polarographic or voltammetric subtractive techniques. In the case of rotating disk electrodes, however, currents from convective diffusion-controlled reactions can be matched rather easily by adjusting the rotation rate of one of the electrodes.

According to the Levich equation, currents limited by convection and thus the amounts of material deposited during the plating period, are proportional to the square root of the electrode rotation rate. Thus one would expect to obtain equal lead peaks for the two cells of Fig. 1A (curves a and b)

when the square root of the rotation rate of electrode *b* during the deposition step is increased by 12.5%, or the rotation rate is increased from 750 to 941 rpm. Actually, the best cancelling of the single-cell lead peaks was obtained by increasing the rotation rate slightly more to 970 rpm (Fig. 1B). This may have been due to deviations of the rotation rates, which were not externally monitored, from the preset nominal values.

Comparison of Fig. 1A and Fig. 1B indicates that the base line of the subtractive curve is not affected by changing the rotation rate of one of the electrodes during deposition. Thus the base line does not contain any significant contribution from a transport-controlled process during the deposition step, and any deviation from the flat line is caused mainly by imperfect matching of the processes (capacitive current, oxidation or reduction of impurities in solution) at the two electrodes during the anodic scan. In this investigation, a sufficiently flat base line in the potential region of interest of the subtractive voltammetric curve was obtained by carefully matching the potentials of the two electrodes by means of the potential balance control. If this is not possible even after replating the mercury film or repolishing the glassy carbon substrates, the pool potentials being less than 10 mV apart, a new pair of electrodes must be prepared.

After an optimal base line had been obtained in the potential region of the lead and cadmium peaks, one of the cell solutions was spiked with lead(II) and cadmium(II) and subtractive current—potential curves were recorded. A linear calibration curve was obtained in the concentration range 4×10^{-10}—10^{-7} M. Figure 2 shows the stripping curve obtained after the addition of 8.9×10^{-10} M lead(II) and 7.2×10^{-9} M cadmium(II). The width of the lead peak at half height is 40 mV, which is identical to the value obtained in single-cell d.c. stripping. The sensitivity of the subtractive method, defined as the current increase per unit increment of concentration, is obviously the same as for the single-cell, linear-scan technique but the subtractive curve exhibits an improved signal-to-background response. For repeated cycles of plating (3 min) and stripping of this sample, the relative standard deviation of the lead peak was 10%. According to Gabriels [10] this gives a detection limit of 1.6×10^{-10} M lead or 0.03 ng Pb ml^{-1}. It is difficult to compare this value with a detection limit for the single-cell, linear-scan method

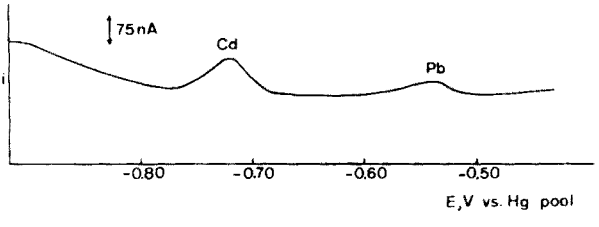

Fig. 2. Anodic stripping curve. The conditions were the same as for Fig. 1B except that solution b was spiked with 8.9×10^{-10} M Pb(II) and 7.2×10^{-9} M Cd(II) and the pre-electrolysis was for 3 min.

when a blank is present and where the scan rate of 15 V min^{-1} used in this investigation normally results in high background currents. Eight replicate single-cell analyses of lead were carried out by standard addition procedures on a 0.1 M HCl solution containing a relatively low lead blank value of 2.75×10^{-8} M and on the same solution spiked with 5×10^{-8} M of lead(II). With a scan rate of 2 V min^{-1} the detection limit [10] was 4×10^{-9} M. In practical analysis when blanks are present, these statistically defined limits may be of little value. Detection limits of elements frequently determined by a.s.v. such as zinc, cadmium, lead and copper, are often limited by the blank values, which may be several orders of magnitude larger than the detection limits defined from results obtained in pure supporting electrolytes.

It can be concluded that the subtractive technique obviously has its merits when large non-capacitive background currents are present, because discrimination against double-layer charging currents is more easily achieved when a single cell is combined with a technique such as differential pulse stripping [8], which also has high sensitivity and good resolving power. The non-capacitive background currents may be due to blanks and sloping or irregular base lines caused by reduction of hydrogen ions, the oxidation of mercury or reactions of other interfering compounds. These interferences pose problems in all single-cell voltammetric techniques. Even matrix effects can be minimized when the approximate concentration of the interfering compounds is known or can be determined, so that a similar concentration can be added to the reference cell. It is clear that the capacitive current is minimized, and high scan rates can therefore be employed. Of course, the use of the subtractive method adds some complexity to the mercury-film stripping technique but may prove valuable if, for example, the alternatives were elaborate separation procedures or purification of reagents.

REFERENCES

1 E. Barendrecht, in A. J. Bard (Ed.), Electroanalytical Chemistry, Vol. 2, M. Dekker, New York, 1967.
2 T. M. Florence, J. Electroanal. Chem., 27 (1970) 273.
3 G. E. Batley and T. M. Florence, J. Electroanal. Chem., 55 (1974) 23.
4 S. P. Perone and J. R. Birk, Anal. Chem., 37 (1965) 9.
5 W. L. Underkofler and I. Shain, Anal. Chem., 37 (1965) 218.
6 D. C. Johnson and R. E. Allen, Talanta, 20 (1973) 305.
7 U. Eisner, J. A. Turner and R. A. Osteryoung, Anal. Chem., 48 (1976) 1603.
8 T. R. Copeland, J. H. Christie, R. A. Osteryoung and R. K. Skogerboe, Anal. Chem., 45 (1973) 2171.
9 E. Temmerman and F. Verbeek, Anal. Chim. Acta, 58 (1972) 263.
10 J. R. Gabriels, Anal. Chem., 42 (1970) 1439.

Analytica Chimica Acta, 96 (1978) 183—184

Short Communication

THE CONDUCTOMETRIC TITRATION OF THIOUREA BY MERCURY(II) CHLORIDE

H. L. KIES

Laboratory for Analytical Chemistry, University of Technology, Delft (The Netherlands)

(Received 22nd July 1977)

The available information on mercury(II) complexes of thiourea (TU) and thiosemicarbazide indicates that the conductometric titration of these compounds with mercury(II) chloride should be feasible. The reaction, which is fast, can be represented by $2TU + HgCl_2 = (Hg(TU)_2)^{2+} + 2Cl^-$. Complexes of this kind are well known, and have been applied in chemical analysis for masking of mercury(II) [1], determination of thiourea and some derivatives, and thiosemicarbazide [2—4]. Though the effect observed is somewhat reminiscent of the formation of certain charge-transfer complexes [5], the types of complexes are different.

When thiourea is titrated with mercury(II) chloride, a steep rise in conductivity is observed until the equivalence point has been reached; beyond this point the conductivity does not change significantly (apart from the small dilution effect) because of the strongly covalent character of mercury(II) chloride.

A slight deviation from rectilinearity is shown by the calibration plot, especially at higher concentrations, which is certainly due to the formation of the higher complexes $[Hg(TU)_3]^{2+}$ and especially $[Hg(TU)_4]^{2+}$ [6, 7]. In this context, the construction of the titration curve and the calculation of the intersection point should be based on data obtained after the titration has been half-completed; or the sample solution should be diluted sufficiently. With respect to the latter recommendation, experiments showed that optimum results are obtained in the range 0.5—30 mg of thiourea dissolved in 35 ml of de-ionized water. A typical titration curve is shown in Fig. 1; the standard deviation for graphical estimation of the equivalence point ($n = 14$) was 0.35%.

Conductometric titrations of this type always guarantee a good difference in slope between the two branches of the curve. Broadening of the field of application is possible if the titrand and titrant are both undissociated, if the reaction product(s) are almost completely dissociated and are soluble in the medium chosen (if they contribute to the conductivity), and if a solvent inert with respect to the reagent and to the sample is available.

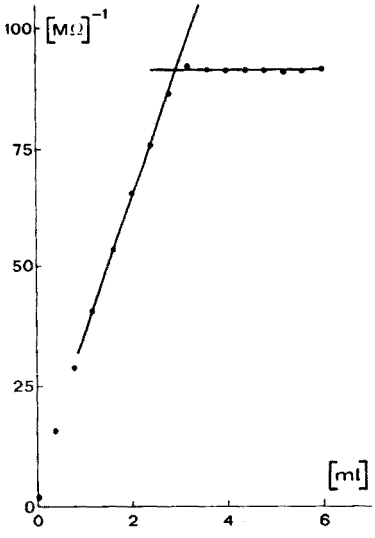

Fig. 1. The titration curve for 4.50 mg of thiourea with 0.0103 M $HgCl_2$ in aqueous medium.

REFERENCES

1 H. A. Flaschka and A. J. Barnard, Chelates in Analytical Chemistry, Vol. 1, M. Dekker, New York, 1967, p. 327.
2 H. L. Kies, Fresenius' Z. Anal. Chem., 145 (1955) 5.
3 H. L. Kies and G. J. van Weezel, Fresenius' Z. Anal. Chem., 161 (1958) 348.
4 H. L. Kies, Fresenius' Z. Anal. Chem., 183 (1961) 194.
5 F. Gutman and H. Keyzer, Electrochim. Acta, 12 (1967) 1255.
6 K. B. Yatsimirsky and A. A. Astosheva, Zh. Fiz. Khim., 27 (1953) 1539.
7 A. Rosenheim and V. Meyer, Z. Allg. Anorg. Chem., 49 (1906) 13.

Analytica Chimica Acta, 96 (1978) 185—188

Short Communication

THE DETERMINATION OF SILICON IN FLUORIDE-BEARING MATERIALS BY ATOMIC ABSORPTION SPECTROMETRY

R. J. GUEST*, D. R. MacPHERSON and R. J. PUGLIESE

Solution Chemistry Section, Chemical Laboratory, Canada Centre for Mineral and Energy Technology, Ottawa (Canada)

(Received 4th May 1977)

Because of the special precautions which are necessary when determining silicon gravimetrically in fluoride-bearing materials [1, 2], the use of alternative and, preferably, faster techniques such as atomic absorption spectrometry, is especially attractive for such materials. This communication describes an extension of an earlier method for the atomic absorption determination of silicon in minerals, ores and slags [3] to the analysis of fluoride-bearing materials. Several Standard Reference Materials and a sulphide ore concentrate of unusual complexity were analysed for silicon and various mixtures of sample materials were prepared to simulate typical complex samples. Sample dissolution was effected by Teflon bomb and sodium peroxide fusion as described previously [3]. The procedure was applied to process solution samples from fluorosilicic acid leaching of anorthosite.

Experimental

Apparatus and reagents. The apparatus and reagents used were essentially as described previously [3]. The Jarrell-Ash atomic absorption spectrophotometer dual double-beam fully compensated unit, model 810, with a pre-mix burner with laminar-flow head, and a Techtron atomic absorption spectrophotometer, model AA-6, were used.

When comparison solutions of silicon plus concomitants were required, the concomitants were added to the diluted silicon standard just before dilution of the standard in the volumetric flask. Plastic volumetric flasks, pipettes and beakers were used.

Dissolution of solid sample material. Weigh out 0.5—2 g of sample for sodium peroxide fusion, or 0.2—0.5 g for Teflon bomb dissolution, and follow the procedure described previously [3].

Solution samples. Place an aliquot of the sample solution in an appropriate volumetric flask. Add enough 5% sodium solution (NaCl) so that the final solution for atomization will contain about 3000 ppm sodium, making sure that the sample solution contains 1—5% hydrochloric acid. Dilute to the mark with water. This solution should contain 10—200 ppm of silicon.

If the ratio of concomitants to silicon is very high, dilute the sample to establish whether or not suppression of silicon values occurs, i.e., take different aliquots and dilute, maintaining the sodium content at 3000 ppm and keeping the solution acidic. Alternatively, use a standard addition technique, or add major concomitants to the comparison standards in the same ratio as found in the sample.

Atomic absorption. Atomize the sample directly as described previously [3].

Results

Several Standard Reference Materials containing fluoride, and a complex fluoride-bearing ore concentrate, were analysed for silicon as described. The results obtained showed good agreement with certified and other values (Table 1). Some of these materials were then mixed with other reference

TABLE 1

Comparison of atomic absorption results with certified and other results for silicon

Sample type	Si present (%)	Fusion		Teflon bomb	
		Si found (%)	Deviation (%)	Si found (%)	Deviation (%)
NBS Phosphate Rock-56B (3.4% F)	4.72[a]	4.62	−2.12	4.82	+2.12
NBS Fluorspar-79 (46.2% F)	0.88[a]	0.90	+2.27	0.90	+2.27
NBS Opal Glass-91 (5.7% F)	31.55[a]	31.00	−1.74	31.57	+0.06
NBS Phosphate Rock-120 (3.8% F)	3.55[a]	3.66	+3.10	3.75	+5.63
NBS Flint Clay-97	20.03[a]	19.74	−1.45	20.25	+1.10
NBS Soda Feldspar-99	32.08[a]	31.83	−0.78	32.25	+0.53
Tin Concentrate-F14[b]	8.54[c]	8.50	−0.47	7.64[d]	—
Composite process solution[e]		Standard addition 0.099 g l^{-1}			Direct 0.098 g l^{-1}

[a]NBS Certified results.
[b]Contains 1.90% F, 6.00% As, 12.5% Zn, 5.44% MoS_2, 1.1% WO_3, 8.16% Pb, 2.16% Bi, 0.90% Cu, 0.13% Sn.
[c]Gravimetric result.
[d]Incomplete dissolution of sample.
[e]Contains 31.5 g Al l^{-1}, 17.0 g Ca l^{-1}, 7.63 g Na l^{-1}, 5% HCl (est.), 1% HF (est.).

TABLE 2

Composition of the prepared fluoride-bearing mixtures for atomic absorption determination of silicon

Sample mixture	Sample composition (%)								
	Si	F	CaO	P_2O_5	Na_2O	K_2O	Al_2O_3	Fe_2O_3	Other
1[a]	10.46	23.1	34	<0.1	0.2	0.3	19.4	0.5	1.2 TiO_2
2[b]	16.48	23.1	34	<0.1	5.4	0.2	9.6	0.1	—
3[c]	2.80	24.8	56	15.8	—	—	—	—	—
4[d]	14.43	12.4	28	7.96	2.76	0.2	14.5	0.3	0.6 TiO_2
5[e]	0.44	23.1	34	—	—	—	—	—	50 U_3O_8
6[f]	0.22	11.5	17	—	—	—	—	—	75 U_3O_8
7[g]	4.71	24.0	As 3.0	MoS_2 2.7	Zn 6.3	WO_3 0.6	Bi 1.08	Pb 4.08	Cu 0.45
8[h]	0.16 g l^{-1}	1%	Ca 17 g l^{-1}	Al 30 g l^{-1}	Na 7.6 g l^{-1}	HCl 15—20%			

[a] One part each of NBS Flint Clay-97 and NBS Fluorspar-79.
[b] One part each of NBS Soda Feldspar-99 and NBS Fluorspar-79.
[c] One part each of NBS Phosphate Rock-56B and NBS Fluorspar-79.
[d] One part each of NBS 97, NBS 99, NBS 56B and NBS 79.
[e] One part each of NBS Uranium Oxide-950 and NBS Fluorspar-79.
[f] Three parts NBS Uranium Oxide-950 and one part NBS Fluorspar-79.
[g] One part NBS Fluorspar-79 and one part Tin Concentrate-F14.
[h] Solution sample mixture prepared from reagent chemicals.

TABLE 3

Comparison of atomic absorption with certified and other results in prepared fluoride-bearing mixtures

Prepared[a] sample mixture	Si[b] present (%)	Fusion		Teflon bomb	
		Si found (%)	Deviation (%)	Si found (%)	Deviation (%)
1	10.46	10.35	−1.05	10.26	−1.91
2	16.48	16.58	+0.61	15.84	−3.88
3	2.80	2.72	−2.86	2.93	+4.64
4	14.43	14.46	+0.21	14.22	−1.46
5	0.44	0.49 0.46[d]	+11.4 +4.54	0.45[d]	+2.27
6	0.22	0.23 0.22[d]	+4.5 0.0	0.22	0.0
7	4.71[c]	4.71	0.0	4.00[e]	—
8		Standard Addition		Direct	
	0.160 g l^{-1}	0.160 g l^{-1}	0.0	0.156 g l^{-1}	−2.50

[a] For sample composition, see Table 2.
[b] Calculated from certified analyses.
[c] Calculated from certified and other analyses.
[d] Uranium and fluoride added to comparison standards.
[e] Sample decomposition incomplete.

materials to simulate typical complex samples (Table 2). The results obtained agreed with the calculated values, and the deviations were similar to those found for individual samples (Table 3).

The procedure was applied to process control samples from leaching of anorthosite with fluorosilicic acid; these samples contained very high ratios of calcium and aluminum to silicon (>100:1) and smaller quantities of many other concomitants, i.e., Na, Fe, Mg, F, HCl. As no similar standard samples were available for comparative purposes, a synthetic sample was prepared containing the major constituents of the samples, and this was analysed for silicon by the recommended procedure with and without standard addition. Also, from the process samples being analysed routinely, a composite solution of high concomitant content was chosen and this was also analysed with and without standard addition. The results obtained for silicon in both the synthetic and composite solutions with and without standard addition were in good agreement (Tables 1 and 3). The result found on the synthetic sample agreed well with the calculated value (Table 3). Recovery of added silicon was satisfactory; the average deviation found from the added silicon was +2.4% for the composite process solution and −4.5% for the prepared synthetic sample.

Conclusions

Results were satisfactory in all cases except where sample dissolution was incomplete, as in Teflon bomb attack of the tin ore concentrate and of Prepared Mixture No. 7 (Table 3). In the case of process control solutions, from leaching of anorthosite, where the ratio of contaminants to silicon was very high, low results were found unless a sample dilution of at least fivefold was made before the final a.a.s. step. Where the silicon content is so low that a large dilution is impossible, either a standard addition technique should be used, or the major contaminants should be added to the comparison standard in the same ratios as are present in the sample.

The effective range of the procedure was at least 0.1—30% for solid samples. The analysis time with the a.a.s. procedure was much less than that required by gravimetric procedures. The average deviation found between atomic absorption and certified and other results was ± 1.8% both on the actual samples and on the prepared mixtures.

REFERENCES

1 W. F. Hillebrand and G. E. F. Lundell, H. A. Bright and J. I. Hoffman, Applied Inorganic Analysis, 2nd edn., J. Wiley, New York, 1953, pp. 672—3.
2 W. T. Schrenk and W. H. Ode, Ind. Eng. Chem., Anal. Ed., 1 (1929) 200.
3 R. J. Guest and D. R. MacPherson, Anal. Chim. Acta, 71 (1974) 233.

Analytica Chimica Acta, 96 (1978) 189—194

Short Communication

INFLUENCE DE L'AMERICIUM-241 SUR LA DETERMINATION DU PLUTONIUM PAR LA METHODE A L'OXYDE D'ARGENT(II)

V. SPEVACKOVA†, C. GUICHARD et P. CAUCHETIER*

Centre d'Etudes Nucléaires de Fontenay-aux-Roses, Département de Recherche et Analyse/ Scape, BP n° 6, F 92260, Fontenay-aux-Roses (France)

(Reçu le 8 juin 1977)

The effect of americium-241 on the determination of plutonium by the silver(II) oxide method

L'américium est produit suivant les réactions nucléaires

$$^{239}Pu(n, \gamma)\ ^{240}Pu(n, \gamma)\ ^{241}Pu \xrightarrow[15\ ans]{\beta^-}\ ^{241}Am$$

La période relativement courte de ^{241}Pu entraîne l'apparition de quantités appréciables d'américium dans les plutonium riches en isotopes supérieurs. L'influence de l'américium sur la détermination du plutonium par la méthode à l'oxyde d'argent(II) [1] a été estimée pour des rapports Pu/Am de l'ordre de 100 [2]. Le même titrage appliqué à des solutions synthétiques d'américium donne des résultats dispersés et non quantitatifs.

L'oxyde d'argent(II) peut oxyder partiellement l'américium à des états de valence supérieurs et nous avons envisagé, d'autre part, la formation de peroxyde d'hydrogène par radiolyse des solutions.

Partie expérimentale

La solution de plutonium en milieu nitrique 1 M, préparée et dosée 16 mois avant cette étude, avait une teneur en plutonium de 5,425 mg g^{-1}. Le rapport Am/Pu était de 0,5%: compte tenu de l'abondance de l'isotope 241 (8,6%), ce rapport est voisin de 1%, au moment de l'étude.

Les solutions d'américium en milieu perchlorique 1 M ont été préparées à partir d'un oxyde fraîchement purifié (exempt de neptunium). Leurs concentrations, déterminées par spectrophotométrie et comptage-γ sont voisines de 2,5 g l^{-1} pour la solution n° 1 et de 1,3 g l^{-1} pour la solution n° 2.

Peroxyde d'hydrogène à 110 volumes "Electro", pour analyse, Prolabo.

L'appareillage comprend un installation de titrage décrite par ailleurs [3] et une spectrophotomètre Cary 14.

† Adresse actuelle: Institut de Recherche Nucléaire, 25068 Rez, Prague, Tchécoslovaquie.

Résultats

Titrage du plutonium en présence d'américium. A une prise d'essai d'environ 11 g de solution de plutonium, on ajoute des quantités croissantes d'américium. La solution est dosée suivant la méthode habituelle et les résultats, rapportés en mg de plutonium par gramme de prise d'essai, sont rassemblés dans le Tableau 1.

Les résultats obtenus en présence d'ajouts d'américium présentent une erreur systématique par excès. Cette erreur a tendance à augmenter avec la quantité d'américium ajoutée, mais ne lui est pas proportionnelle.

Influence de l'étape d'oxydation. Quelle qu'en soit la cause (présence de peroxyde d'hydrogène ou oxydation de l'américium), l'importance de l'interférence dépend probablement de l'étape d'oxydation nécessaire pour amener le plutonium au degré d'oxydation (VI). Aussi avons-nous essayé de remplacer ou de faire précéder l'ajout d'oxyde d'argent(II) par un traitement de la prise d'essai à l'acide perchlorique concentré porté à fumées blanches. Les résultats obtenus pour des prises d'essai contenant 5 mg d'américium

TABLEAU 1

Titrage du plutonium en présence d'américium

Am ajouté (ml de solution n° 1)	Am/Pu (%)	Pu trouvé (mg g^{-1})	
0	1	5,420	
0	1	5,425	$\bar{x}$ = 5,422
0	1	5,420	
			$\Delta (x - \bar{x})$
0,25	2,1	5,427	+0,005
0,5	3,1	5,435	+0,013
0,75	4,1	5,434	+0,012
1,0	5,1	5,455	+0,033
2,0	9,4	5,501	+0,079
5,0	21,3	5,488	+0,066

TABLEAU 2

Influence de l'agent oxydant

Am ajouté (ml de solution n° 1)	Agent oxydant utilisé	Δt (min)	Ce(IV)/Fe(II) (g/g)	Erreur observée (g solution Ce(IV) ~ 10^{-2} M)
—	—	—	2,6443 ± 0,0005	
2	AgO	45	2,43670	4,041
2	$HClO_4$	45	2,60195	0,735
2	$HClO_4$ + AgO	70	2,62348	0,148
2	$HClO_4$ + AgO	165	2,61951	0,248
2	$HClO_4$ + AgO	230	2,62116	0,233

en l'absence de plutonium sont rassemblés dans le Tableau 2: ils sont exprimés par la différence entre la quantité de solution de cérium(IV) qui serait nécessaire pour oxyder le fer(II) ajouté s'il était présent seul et la consommation réellement observée.

Le traitement par l'acide perchlorique semble diminuer sensiblement l'interférence, ce qui pourrait s'interpréter par une meilleure destruction du peroxyde d'hydrogène. Nous ne pouvons cependant pas exclure l'hypothèse qu'une partie au moins de l'interférence soit due à l'oxydation partielle de l'américium: on peut en effet prévoir que la facilité d'obtention et la stabilité des valences supérieures dépendent de l'acidité du milieu qui a varié au cours des essais ci-dessus.

Le temps Δt écoulé entre la fin de l'étape d'oxydation et l'ajout de fer(II) a peu d'influence, ce qui signifie que la formation de peroxyde d'hydrogène par radiolyse au cours du dosage demeure peu importante.

Il faut noter que l'erreur observée dans le premier essai (4 g de solution de cérium(IV)) est très supérieure à celle que nous obtenons dans les mêmes conditions en présence de plutonium (0,7 g dans l'essai comparable du Tableau 1). Dans tous les cas, l'erreur observée est supérieure à celle qui est due à l'oxydation parasite du fer(II) par les ions Ag^+ (environ 0,08 g de solution de cérium(IV)) que nous avons signalée dans une précédente communication [4].

Oxydation de l'américium. Pour vérifier l'hypothèse de cette oxydation, nous avons enregistré, par rapport à une solution de référence nitrique M—sulfurique 0,5 M, les spectres d'absorption des solutions suivantes:
2 ml de la solution d'américium n° 1 dilués à 10 ml par le mélange sulfonitrique: seul apparaît le pic de l'américium(III) (A = 0,853 à 503 nm).
2 ml de la solution d'américium n° 1 + 2 ml d'acide perchlorique concentré, amenés à fumées blanches puis dilués à 10 ml par le mélange sulfonitrique. Le spectre tracé 3,5 h après l'oxydation montre que 4% de l'américium(III) ont disparu (A = 0,817). Il n'y a pas d'américium(V) décelable. La déformation de la ligne de base entre 940 et 1100 nm, sans doute due au fait que cette solution est plus concentrée en acide que la solution de référence, ne permet pas de se prononcer sur l'existence d'américium(VI). En supposant toutefois que l'américium(III) disparu soit intégralement oxydé en (VI), l'erreur résultante correspondrait à environ 0,25 g de solution de cérium(IV).
2 ml de la solution d'américium n° 1 oxydés par l'oxyde argent(II) et dilués à 10 ml par le mélange sulfonitrique. Le spectre tracé 4 h après l'oxydation montre que 13% de l'américium(III) ont disparu (A = 0,743). L'américium(VI) est indécelable, mais le pic observé à 717 nm indique que 10% environ de l'américium sont oxydés en (V) (A = 0,014). L'erreur résultante correspondrait approximativement à 0,55 g de solution de cérium(IV).

Mise en évidence du peroxyde d'hydrogène dans la solution d'américium. L'addition de titane(IV) à la solution d'américium n° 1 préparée environ 40 jours plus tôt donne la coloration jaune orangée caractéristique du

complexe Ti(IV)—H_2O_2. D'autre part, le titrage appliqué à une prise d'essai de 2 ml de cette même solution dans les conditions habituelles, mais en omettant l'étape d'oxydation par AgO — ce qui exclut l'existence d'américium à un degré d'oxydation autre que (III) — fait apparaître une consommation anormalement faible de cérium(IV). Les résultats sont rassemblés dans le Tableau 3.

En supposant quantitative la réaction $2Fe(II) + H_2O_2 + 2H^+ \rightarrow 2Fe(III) + 2H_2O$, la consommation observée de fer(II) correspondrait à une concentration de peroxyde d'hydrogène dans la solution d'américium de 1,4 à $1{,}8 \cdot 10^{-2}$ M. Il est probable, étant donné l'instabilité de ce composé, que la teneur réelle dans l'échantillon avant dilution est plus élevée.

Importances relatives des deux causes d'interférence. Dans le Tableau 4, nous avons rassemblé les résultats obtenus parallèlement en spectrophotométrie et en titrage sur des prises d'essai, effectuées après l'étape d'oxydation, d'une solution d'américium à environ 0,5 g l^{-1}. Nous constatons que dans le cas où la solution n'a été oxydée que par l'oxyde d'argent(II), l'erreur observée dans le titrage est très importante (environ $5 \cdot 10^{-2}$ meq d'oxydoréduction). Elle ne peut être due qu'au peroxyde d'hydrogène (la solution n° 2 a été préparée une semaine environ avant ces essais) puisque la concentration en américium(III) n'est pas significativement différente de celle de la solution de référence non oxydée "R". Dans le cas où la solution a préalablement été traitée par l'acide perchlorique, la concentration mesurée en américium(III) est beaucoup plus petite et elle augmente au cours du temps. Si l'américium manquant était au degré d'oxydation (V) ou (VI), l'erreur observée devrait être plus importante (2,4 ou 3,6 g de solution de cérium(IV) respectivement) et nous devrions observer les pics d'absorption correspondants ($A \approx 0{,}07$ à 717 nm ou $A \approx 0{,}11$ à 996 nm respectivement), ce qui n'est pas le cas. En revanche, nous observons un précipité noir au fond de la fiole: soit que celui-ci adsorbe l'américium, soit plus vraisemblablement qu'il soit lui-même un composé peu soluble d'américium peut-être à un degré d'oxydation supérieur à (III) (peroxyde ou sel double avec Ag^+), l'américium repasse lentement en solution à l'état trivalent. En effet, le reste de la solution resté au contact du précipité durant 24 h est plus concentré en américium (III) que la solution de référence non oxydée "R".

TABLEAU 3

Mise en évidence du peroxyde d'hydrogène par titrage

Am ajouté (ml de solution n° 1)	Solution de Fe(II) (g)	Solution de Ce(IV) (g)	Ce(IV)/Fe(II) (g/g)	Erreur observée (g de solution Ce(IV) ~ 10^{-2} M)
0	20,049	52,966	2,6418	
0	19,976	52,777	2,6420	
2	20,026	47,213	2,3576	5,694
2	19,954	45,348	2,2726	7,368

TABLEAU 4

Comparaison du spectre d'absorption et du titrage de solutions d'américium oxydées

Δt[a] (h)	Absorbance 503 nm	Absorbance 812 nm	Prise d'essai[b] (ml)	Ce(IV)/Fe(II) (g/g)	Erreur observée[c] (g solution Ce(IV))
4 ml de solution d'américium n° 2—dilués à 10 ml par HNO_3 M—H_2SO_4 0,5 M (solution de référence non oxydée "R")					
	0,906	0,157			
20 ml de solution d'américium n°2—oxydation AgO (300 mg) — dilués à 50 ml par HNO_3 M—H_2SO_4 0,5 M					
			0	2,3295 ± 0,0006	
1,5	0,902	0,157			
1,5			10	2,0845	4,942
4			10	2,0767	5,083
5	0,902	0,157			
20 ml de solution d'américium n° 2 + 2 ml $HClO_4$ conc. — fumées blanches — ajout 10 ml HNO_3 M—H_2SO_4 0,5 M — oxydation AgO (300 mg) — dilués à 50 ml par HNO_3 M—H_2SO_4 0,5 M					
			0	2,3225 ± 0,0006	
1,5			10	2,3080	0,303
4			10	2,3084	0,283
4,3	0,504	0,091			
5,8	0,569	0,102			
6			10	2,3056	0,346
24	1,004	0,185			

[a]Temps écoulé entre la fin de l'étape d'oxydation et la mesure d'absorbance ou l'ajout de fer(II).
[b]Prise d'essai de la solution préparée comme indiqué dans le tableau.
[c]Calculée à partir de l'étalonnage de la solution de fer(II) effectué le jour même.

Dans le Tableau 5, figurent les résultats obtenus par titrage de prises d'essai ne contenant que du peroxyde d'hydrogène. Il en ressort que même la double oxydation perchlorique—oxyde d'argent(II) peut être insuffisante pour détruire complètement celui-ci: l'erreur correspond au dosage de 4% de la quantité introduite. En revanche, l'erreur n'est pas significative dans le cas du dernier essai, bien que l'on n'ait pas effectué le traitement perchlorique, indiquant que cette destruction est aléatoire.

Si la quantité de peroxyde d'hydrogène introduite est trop importante, l'erreur observée peut être en sens inverse: c'est ce que l'on constate avec une prise d'essai de 0,5 ml à 110 volumes (10 meq oxydant ou réducteur). L'oxyde argent(II) ne peut en oxyder qu'une faible partie ($\approx$ 2,4 meq) et le fer(II) ne peut en réduire qu'une petite quantité supplémentaire (~0,5 meq). Le peroxyde d'hydrogène restant réduit alors le cérium(IV).

TABLEAU 5

Influence du peroxyde d'hydrogène

Prise d'essai H_2O_2 110 vol (ml)	Dilution	Prise d'essai (ml)	Oxydation[a]		Ce(IV)/Fe(II) (g/g)	Erreur observée[b] (g solution Ce(IV))
			$HClO_4$	AgO		
0	—	—	non	non	2,3271 ± 0,0006	
0	—	—	non	292 mg	2,3228	0,086
0,5	—	—	non	300 mg	>3,7	
0	—	—	non	non	2,3225 ± 0,0005	
1	50	1	oui	300 mg	2,2415	1,621
1	50	1	non	300 mg	2,3180	0,091

[a]La prise d'essai a été diluée en milieu HNO_3 M—H_2SO_4 0,5 M avant chaque étape d'oxydation.
[b]Calculée à partir de l'étalonnage de la solution de fer(II) effectuée le jour même.

Conclusion

L'interférence de l'américium dans le dosage du plutonium par la méthode à l'oxyde d'argent(II) ne devient notable que pour des rapports Am/Pu ⩾ 2%. Lorsque ce rapport varie de 2 à 20%, l'erreur positive résultante évolue de 10^{-3} à quelques 10^{-2} en valeur relative, mais n'est pas reproductible.

La cause principale de cette erreur est la radioactivité de ^{241}Am: le peroxyde d'hydrogène formé par radiolyse n'est pas totalement détruit par l'oxyde argent(II) ni par un traitement préliminaire de la prise d'essai par l'acide perchlorique à fumées blanches, bien que cette destruction paraisse plus complète en présence de plutonium qu'en son absence (Pu catalyserait l'oxydation de H_2O_2). Il peut s'y ajouter, dans certains cas, une oxydation partielle de l'américium à un degré d'oxydation supérieur à (III). Ces deux causes ont le même effet, à savoir une oxydation de fer(II) en supplément de celle due à Pu(VI).

BIBLIOGRAPHIE

1 J. Corpel et F. Regnaud, Anal. Chim. Acta, 35 (1966) 508.
2 P. Cauchetier, C. Guichard et F. Regnaud, AIEA SM 201/55 (1975).
3 P. Cauchetier et C. Guichard, Rapport CEA-R-4233 (1971).
4 P. Cauchetier, C. Guichard et F. Regnaud, Anal. Chim. Acta, 80 (1975) 188.

Analytica Chimica Acta, 96 (1978) 195—198

Short Communication

THE DETERMINATION OF NITROGEN IN TANTALUM BY PROTON ACTIVATION ANALYSIS

K. STRIJCKMANS, C. VANDECASTEELE and J. HOSTE*

Institute of Nuclear Sciences, Rijksuniversiteit Ghent, Proeftuinstraat 86, B-9000 Ghent (Belgium)

(Received 25th July 1977)

The non-destructive determination of nitrogen in some refractory metals (Ta, Nb, Ti and W) has been described previously [1]. The method uses the $^{14}N(p, n)^{14}O$ reaction; the 2313-keV γ-rays of 70.5-s ^{14}O are measured with a Ge(Li) or NaI(Tl) detector, and sensitivities of 0.4—30 $\mu g\ g^{-1}$ can be obtained. The results for nitrogen in titanium (113 ± 8 $\mu g\ g^{-1}$) were compared with those obtained by other analytical methods as part of a program sponsored by BCR of the European Communities. The mean values by different methods ranged, however, from 89 to 142 $\mu g\ g^{-1}$. The present communication reports results for nitrogen in tantalum by another nuclear method, namely, through the $^{14}N(p, \alpha)^{11}C$ reaction.

As shown in Table 1, the interfering $^{11}B(p, n)^{11}C$ reaction cannot be avoided by an appropriate choice of the incident particle energy as the respective thresholds are at 3.1 and 3.0 MeV. Obviously, the $^{10}B(d, n)^{11}C$ reaction allows an interference-free determination of boron, if the deuteron energy is below 5.9 MeV, so that the interference can be corrected for. By irradiating tantalum with protons or deuterons, only a low activity of ^{181}W is induced, so that a non-destructive determination is possible if γ,γ-coincidence measurements are applied to measure ^{11}C. However as shown in Table 1, other impurities such as oxygen and carbon give rise to β^+-emitters such as ^{13}N and ^{18}F, so that decay curve analysis is required.

Standardization

The standardization was carried out by means of the "average cross-section" method. As a nitrogen standard, "Nylon 6" cylinders or a stack of "Kapton" polyimide foils were used. The boron standard was H_3BO_3 pressed into pellets at a pressure of 12 000 psi. This standard can be used with a beam of up to 100 nA. At higher intensities dehydration can occur.

Experimental

The irradiation and measurement conditions are summarized in Table 2. The samples were irradiated under vacuum (10^{-4} torr) in the extracted

TABLE 1

Nuclear reactions induced by 15-MeV protons and 5-MeV deuterons

Reaction	Threshold (MeV)	Radiation emitted	Half-life
1. $^{14}N(p, n)^{14}O$	6.3	β^+, γ	70.5 s
2. $^{13}C(p, n)^{13}N$	3.2	β^+	10.0 min
3. $^{16}O(p, \alpha)^{13}N$	5.5	β^+	10.0 min
4. $^{14}N(p, \alpha)^{11}C$	3.1	β^+	20.4 min
5. $^{11}B(p, n)^{11}C$	3.0	β^+	20.4 min
6. $^{18}O(p, n)^{18}F$	2.5	β^+	109.7 min
1. $^{12}C(d, n)^{13}N$	0.3	β^+	10.0 min
2. $^{10}B(d, n)^{11}C$	$Q > 0$	β^+	20.4 min
3. $^{14}N(d, \alpha n)^{11}C$	5.9	β^+	20.4 min
4. $^{17}O(d, n)^{18}F$	$Q > 0$	β^+	109.7 min

TABLE 2

Irradiation and measurement conditions

Particle		protons	deuterons
Energy		15 MeV	6 MeV
Energy (incident)		14 MeV	4.3 MeV
Flux monitor		Cu foil, 25 μm	Ni foil, 12.5 μm
Beam intensity normalization		$^{65}Cu(p, n)^{65}Zn$	$^{60}Ni(d, n)^{61}Cu$
Half-life		244 d	3.41 h
Gamma-ray energy		1115.5 keV	283 keV
Removed surface layer		20 μm	12 μm
Etching solution		HF (50%) + HNO_3 14 N, room temp.	
Irradiation time for:	standard	1 min	1 min
	sample	5 min	20 min
Beam intensity for	: standard	0.1 μA	0.1 μA
	: sample	3—4 μA	10 μA
Cooling time for	: standard	3 h	60 min
	: sample	2 h	20 min
Counting time		1 min	1 min
Period of counting		2 h	1 h

cyclotron beam. The measurements were carried out with a γ,γ-coincidence measuring system. Two 7.6 × 7.6-cm NaI(Tl) detectors at 180° were coupled to a fast coincidence unit, which triggered the slow coincidence input of a multichannel analyser.

Results and discussion

Deuteron activation gives a two-component decay curve: ^{13}N(10.0 min) and a long-lived background activity. No component corresponding to 20.4-min ^{11}C is detected. The detection limit for boron is difficult to determine quantitatively. However, when the entire short-lived activity is taken as an upper limit for ^{11}C, a detection limit for boron of 0.1 $\mu g\ g^{-1}$ is obtained.

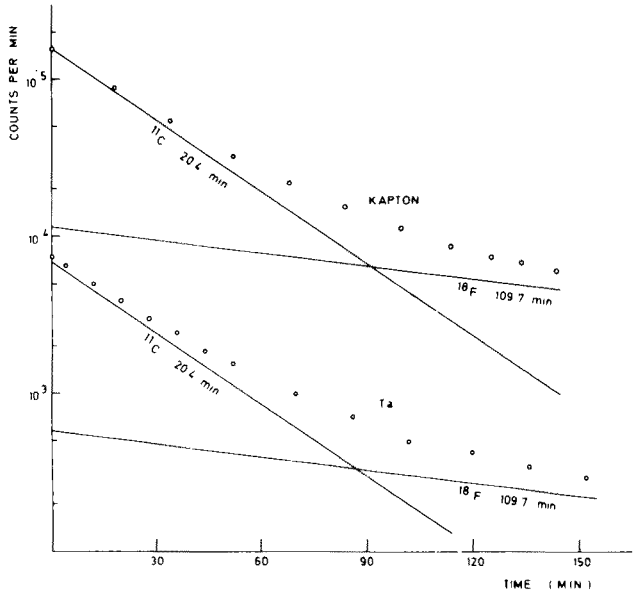

Fig. 1. Decay curve of a Ta sample and a Kapton standard irradiated with 15-MeV protons.

Proton activation yields a three-component decay curve: ^{13}N (10.0 min), ^{11}C (20.4 min) and ^{18}F (109.7 min). As shown in Fig. 1, if a cooling time of 2—3 h is used, no ^{13}N is detected. Replicate (14) determinations yielded a mean value of 10.72 $\mu g\ g^{-1}$ and a standard deviation of 0.74 $\mu g\ g^{-1}$. Both standards used — nylon and kapton — gave the same results, within experimental error. The boron interference is less than 1.7%, since at 15 MeV, 1 $\mu g\ g^{-1}$ of boron corresponds [2] to an apparent nitrogen concentration of 1.7 $\mu g\ g^{-1}$. The results obtained are in reasonable agreement with those obtained by the $^{14}N(p, n)^{14}O$ reaction [1] (9.18 ± 0.99 $\mu g\ g^{-1}$), if one considers the spread usually obtained when different analytical methods for nitrogen in metals at the $\mu g\ g^{-1}$ level are compared.

Conclusion

Results for nitrogen in tantalum obtained by non-destructive proton activation analysis via $^{14}N(p, \alpha)^{11}C$ are comparable to those obtained by the $^{14}N(p, n)^{14}O$ reaction. Both methods also give similar precision (7—10%). The first method can only be applied non-destructively for some favourable matrices, such as tantalum; for most other refractory metals, chemical separation of ^{11}C is necessary. The latter method is applicable for Ta, Ti, W and Nb. A further advantage of the $^{14}N(p, n)^{14}O$ reaction is that it is interference-free, at least below 22 MeV, whereas the $^{11}B(p, n)^{11}C$ reaction can interfere with the $^{14}N(p, \alpha)^{11}C$ reaction so that the boron content must be determined separately.

Grateful acknowledgement is made to R. Kieffer for skilful technical assistance, to the "Centre de recherche du Cyclotron" of the University of Liège for the use of the cyclotron and to the I.I.K.W. for financial support. Thanks are also due to J. Pauwels (CBNM, Geel) for providing the samples.

REFERENCES

1 K. Strijckmans, V. Vandecasteele and J. Hoste, Anal. Chim. Acta, 89 (1977) 255.
2 C. Engelmann, J. Radioanal. Chem., 7 (1971) 281.

Analytica Chimica Acta, 96 (1978) 199—201

Short Communication

SPECTROPHOTOMETRIC DETERMINATION OF URANIUM IN SEA WATER AFTER EXTRACTION WITH ALIQUAT-336

P. G. BARBANO* and L. RIGALI

Centro Applicazioni Militari dell'Energia Nucleare, S. Piero a Grado, Pisa (Italy)

(Received 16th May 1977)

For the analytical separation of uranium from sea water several methods have been proposed, based on techniques such as coprecipitation, ion exchange, flotation and solvent extraction [1, 2]. Of these techniques, extraction appears to be the most convenient from the points of view of simplicity and rapidity. Most solvent extraction methods, however, lack the necessary reproducibility or selectivity, so that complicated evaluations of the extraction yield or further purification steps are needed [3, 4].

Uranium(VI) is extracted from chloride solutions by quaternary ammonium salts [5]; an extraction coefficient higher than 10^3 has been obtained with 0.1 M Aliquat-336 in diethylbenzene, from aqueous 3.5 M LiCl—0.2 M HCl solutions. Under the same extraction conditions, many elements that cause serious interferences in the determination of uranium e.g. thorium, hafnium, zirconium, and rare earths, are poorly or negligibly extracted.

In this communication, an extraction method, based on Aliquat-336 solutions, is described for the quantitative separation of uranium in sea water. The uranium can then be determined spectrophotometrically by a modification of the well-known arsenazo-III procedure proposed by Korkisch and Gödl [6] for natural waters.

Experimental

Reagents and apparatus. Commercial grade monomethyltricaprylammonium chloride (Aliquat-336, General Mills Inc., U.S.A.) dissolved in xylene (5%, w/v) was used as extractant. Arsenazo III (B.D.H) was used in aqueous solution (0.05%, w/v). All other chemicals were reagent grade.

Sea-water samples were collected near the coast of Tirrenia (Pisa) in polythene bottles and immediately acidified with 2 ml of 11 M HCl per litre. No further acid was added before the analysis. A Beckman DU spectrophotometer was used with 4-cm cells.

Recommended procedure. Transfer 300 ml of acidified sea water to a 500-ml separatory funnel, make the solution 3.5 M in lithium chloride and extract (manually) twice for 10 min with 15 ml of the extractant. Combine the organic extracts and strip them twice for 5 min with 15 ml of 0.15 M HNO_3.

Centrifuge, to obtain good phase separation. Combine the aqueous phases, evaporate almost to dryness, dissolve the residue in 5 ml of 10 M HCl and again evaporate to eliminate nitric acid completely.

Transfer the residue to a 50-ml Erlenmeyer flask by adding 5 ml of 10 M HCl in portions. To this solution, add 10 mg of ascorbic acid and then 550 mg of zinc. Cover the flask, and shake it carefully until all the zinc has dissolved. Then add 0.5 ml of arsenazo-III solution. Measure the absorbance at 665 nm against a blank obtained by carrying 300 ml of distilled water through the complete procedure. Refer the absorbance readings to a calibration curve constructed by following the complete reduction procedure.

Results and discussion

Table 1 gives the results obtained for sea-water samples by the recommended procedure. To check the recovery of the uranium, some samples were spiked with different amounts of uranium. The uranium concentration found is practically independent of the volume taken for analysis; the mean concentration of uranium is 3.3 $\mu g\ l^{-1}$, in good accordance with data recently reported for the Tyrrhenian sea [7].

In strongly acidic media, thorium, zirconium, and hafnium interfere seriously with the determination of uranium by arsenazo III [8, 9]. Molybdenum (10 μg) also interferes [6]. Thorium, hafnium and molybdenum are not co-extracted significantly with uranium by Aliquat-336 so that 200-fold amounts of these elements do not interfere. Zirconium is extracted more effectively but a 50-fold excess can be tolerated.

As far as other foreign ions are concerned, rare earths are not extracted to any significant extent by Aliquat-336 and interference from iron(III) is eliminated by reduction with ascorbic acid. The elements more usually encountered as pollutants in waters give a colour reaction with arsenazo-III only in weakly acidic media and do not interfere with the determination of

TABLE 1

Uranium determinations in sea-water samples

Sample	Volume taken for analysis (ml)	U added (μg)	U found (μg)	Recovery (μg)
1	150	—	0.51	—
2	300	—	0.99[a]	—
3	500	—	1.66	—
4	300	1.0	2.0	1.0
5	300	2.0	3.1	2.1
6	300	4.0	5.2	4.2
7	300	10.0	10.8	9.8

[a]Mean of five determinations (standard deviation = 0.03). All other data are the means of at least two determinations.

TABLE 2

Effect on the determination of uranium of variable amounts of foreign ions added to 300 ml of sea water

Foreign ion	Amount added (μg)	U found (μg)	Foreign ion	Amount added (μg)	U found (μg)
Mo(VI)	100	1.0	Th	100	1.0
	200	1.0		200	0.9
Zr	50	1.0	Hf	100	0.9
	100	1.2		200	1.0

uranium(IV) in 9 M HCl. In a series of tests, 100 μg of copper(II), cadmium(II), cobalt(II), vanadium(V) and mercury(II) were added directly to the measuring solution before the reduction with zinc; no interference was found in the determination of 1 μg of uranium.

REFERENCES

1 J. P. Riley and G. Skirrow, Chem. Oceanogr., Vol. 2., Academic Press, 1965.
2 G. Leung, Y. S. Kim and H. Zeitlin, Anal. Chim. Acta, 60 (1972) 229.
3 J. D. Wilson, R. K. Webster, G. W. Milner, G. A. Barnett and A. A. Smales, Anal. Chim. Acta, 23 (1960) 505.
4 J. Korkisch and W. Koch, Mikrochimica Acta (Wien), (1973) 157.
5 K. B. Brown, USAEC Report ORNL-3785 (April 1965).
6 J. Korkisch and L. Gödl, Anal. Chim. Acta, 71 (1974) 113.
7 C. Franchini, Arch. Oceanogr. Limnol. (Venice), 18 (1973) 39.
8 S. B. Savvin, Talanta, 8 (1961) 673.
9 S. B. Savvin, Talanta, 11 (1964) 7.

Analytica Chimica Acta, 96 (1978) 203—205

Short Communication

DENSITOMETRIC MICRODETERMINATION OF ANTHRACENE AND SOME ANTHRAQUINONE DERIVATIVES AFTER SEPARATION BY T.L.C.

TH. A. KOUIMTZIS* and I. N. PAPADOYANNIS

Laboratory of Analytical Chemistry, University of Thessaloniki, Thessaloniki (Greece)

(Received 28th June 1977)

In connection with the photo-oxidation of anthracene adsorbed on aluminum oxide, the separation [1] and determination [2] of some anthraquinone derivatives was achieved by t.l.c. with benzene—carbon tetrachloride—acetic acid (50 : 75 : 0.8) as solvent system. Each zone was scraped off the plate and quantitative evaluation of the individual components (anthraquinone, quinizarin, chrysazin and alizarin) was carried out by an extraction—spectrophotometric technique.

The above technique is time-consuming and relatively large amounts of the compounds are needed for quantitative evaluation. Densitometric methods are being used increasingly for the quantitative evaluation of compounds separated by t.l.c. and the present work reports the results of in situ measurements by light absorption, reflection, or emission by quinizarin, chrysazin, alizarin, 1-hydroxyanthraquinone, anthraquinone and anthracene after their chromatographic separation.

Experimental

Reagents. The purity of anthracene, anthraquinone, quinizarin and chrysarin (Fluka), alizarin (E. Merck), and 1-hydroxyanthraquinone (Aldrich-Europe) was checked by melting point and chromatographic tests. Standard solutions were prepared by dissolving the appropriate amounts in a mixture of benzene—chloroform—methanol (90 : 5 : 5).

A standard solution of 2,4,7-trinitro-9-fluorenone (TNF; Aldrich-Europe) was prepared by dissolving 0.5 g in 100 ml of acetone.

Silica gel G was from E. Merck. All solvents were analytical-grade reagents.

Apparatus. The measurements of light absorption, reflection or emission were performed with a Universal Densitometer, Vitatron type TLD 100 automatic "flying-spot" scanner. Peak areas, automatically integrated by the recorder, were expressed in integrator units.

Thin layer chromatography. T.l.c. plates (0.25 mm thick) were prepared as follows: 30 g of silica gel G were mixed by constant stirring with 80 ml of 0.1 M phosphate solution buffered at pH 5.0. The slurry obtained was spread over glass plates, 20 × 20 cm, in the usual way, allowed to dry for 30 min, and activated at 110°C for 1 h; plates were stored over silica gel.

Sample solutions (1—10 μl) were spotted gradually on the plates by means

of a microsyringe. The plates were developed in an equilibrated chamber, filled with a solvent system of benzene—carbon tetrachloride—acetic acid (50:75:0.6), until the solvent front ascended 13 cm from the spotting line.

Quantitative evaluation. The plates were scanned and light absorption, reflection, or emission was measured for the coloured compounds (quinizarin, chrysazin, alizarin and 1-hydroxyanthraquinone). The spots of anthracene were scanned only for light emission. The solution of TNF was spread over the anthracene spot to form the coloured anthracene—TNF complex, and the plate was scanned again for the light absorption and reflection of this spot. The integrator units for each compound were referred to the corresponding calibration curves, constructed for each compound in the same way.

Results and discussion

T.l.c. separation of the six derivatives suitable for densitometry was achieved by means of the known chromatographic system [1], modified slightly because of the presence of an extra compound (1-hydroxyanthraquinone) in the analyzed mixture. Thus the pH of the buffered layer was increased to 5.0 and the amount of acetic acid in the solvent system was decreased; this chromatographic system gives good separation of the six compounds. The chromatographic spots are compact and suitable for densitometric registration.

The coloured spots of quinizarin, chrysazin, alizarin and 1-hydroxyanthraquinone were scanned for light absorption and reflection. These compounds are intensely fluorescent; their spots were also scanned for light emission.

Anthracene spots are fluorescent and were scanned for light emission. These spots were visualized by spraying with a solution of 0.5% TNF in acetone [3]; the intense red-brownish spots of the molecular complex were scanned for light absorption and reflection.

The amount of each compound in the mixture was calculated from calibration curves constructed in the following way to increase the precision. Various amounts of the compounds studied were spotted on a coated plate. The plate was then developed in the same way as the unknown sample, the spots were scanned, and the integrator units were plotted against known amounts of the compound. The calibration curves are given in Fig. 1; the sensitivity of the fluorescence measurements is higher than that of reflectance or transmittance. The detection limits of these compounds corresponding to a signal-to-noise ratio of 2:1, are in the range 10—40 ng for fluorescence measurements.

Various attempts to obtain densitometric registration of the colourless, non-fluorescent, anthraquinone spots were unsuccessful; no molecular complex is formed with TNF. A faint yellow colour, obtained by spraying these spots with a solution of $SbCl_3$ in CS_2, was not suitable for quantitative evaluation because it faded rapidly. The amount of anthraquinone in the spots was determined by extraction-spectrophotometry.

The results from five independent determinations performed on separate thin-layer plates with an artificial mixture of the six compounds are shown

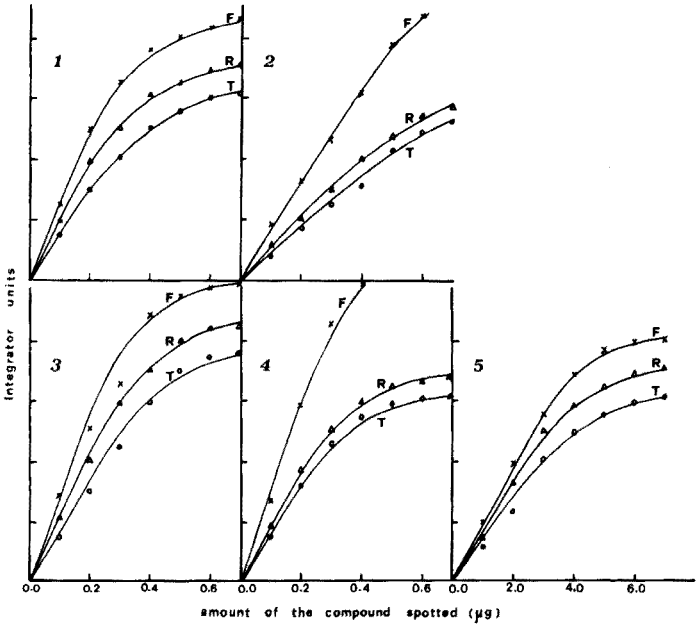

Fig. 1. Calibration curves of (1) 1-hydroxyanthraquinone, (2) alizarin, (3) chrysazin, (4) quinizarin, and (5) anthracene. F = fluorescence, R = reflectance, T = transmittance.

TABLE 1

Results of the densitometric determination of anthracene and anthraquinone derivatives in mixtures after separation by t.l.c.

Compound	R_F x100	Added (μg)	Found[a] (μg)		
			R	*T*	*F*
Anthracene	85	2.00	1.95 ± 0.06	1.92 ± 0.07	2.02 ± 0.06
Quinizarin	49	0.16	0.15 ± 0.04	0.16 ± 0.04	0.17 ± 0.02
Chrysazin	38	0.25	0.24 ± 0.05	0.23 ± 0.04	0.25 ± 0.04
1-Hydroxyanthraquinone	35	0.20	0.19 ± 0.05	0.17 ± 0.04	0.19 ± 0.03
Anthraquinone	31	—	—	—	—
Alizarin	7	0.25	0.23 ± 0.06	0.24 ± 0.05	0.26 ± 0.05

[a]Average value of 5 determinations. R = reflectance, T = transmittance, F = fluorescence.

in Table 1. The precision of the densitometric methods is satisfactory, and the sensitivity is ca. 100 times greater than that of the extraction—spectrophotometric method.

The authors are indebted to Professor G. Vasilikiotis for helpful discussions.

REFERENCES

1 E. Voyatzakis, G. Vasilikiotis and H. Alexaki-Tzivanidou, Anal. Lett., 5 (1972) 445.
2 G. Vasilikiotis and H. Alexaki-Tzivanidou, Microchem. J., 17 (1972) 655.
3 H. T. Gordon and M. J. Huraux, Anal. Chem., 31 (1959) 302.

Analytica Chimica Acta, 96 (1978) 207—210

Short Communication

RAPID EXTRACTION—ATOMIC ABSORPTION DETERMINATION OF BORON IN SEA WATER

ANA MARIA T. C. HORTA and ADILSON J. CURTIUS*

Departamento de Química da Pontifícia Universidade Católica do Rio de Janeiro (Brasil)

(Received 12th May 1977)

The determination of boron in sea water is important in biochemical, geochemical, and environmental studies. Several methods of analysis have been suggested [1—5], most of which are laborious and time-consuming or lacking in accuracy. Atomic absorption spectrometry was used by Spielholtz et al. [6] after a lengthy preconcentration by evaporation to 25% of the original volume. Those authors [6] overcame the poor inherent sensitivity of the method by extraction with 20% (v/v) 2-ethyl-1,3-hexanediol [7] in methyl isobutyl ketone in an acid medium. This chelation—extraction has been studied thoroughly and a simple, accurate, rapid, procedure for boron determination, suitable for automation, is proposed. The method was checked against a potentiometric procedure [1] for the analysis of some samples of surface water from the Brazilian coast.

Experimental

Reagents and apparatus. All reagents were reagent grade unless otherwise specified. The 2-ethyl-1,3-hexanediol (Merck-Schuchardt) was synthesis grade. Deionized water was used.

Artificial sea water was prepared as suggested by Lyman and Fleming [8]. Three standard solutions were made by dissolving known amounts of boric acid (a) directly in the extraction solution, (b) in artificial sea water and proceeding to chelation and extraction, and (c) in deionized water before chelation and extraction. The concentrations of boric acid were 0, 25, 50, 75, 100, 125, and 150 μg ml^{-1}. The extraction solution was 10% (v/v) 2-ethyl-1,3-hexanediol in methyl isobutyl ketone.

A Varian-Techtron Atomic Absorption Spectrophotometer, Model AA5, was used. The boron hollow-cathode lamp was used at 12 mA. Absorption measurements were made at 249.8 nm, with a 100 μm slit and $\times$10 scale expansion. A reducing flame (8.5 l min^{-1} of nitrous oxide and 4.0 l min^{-1} of acetylene) was employed to reduce the BO_2 present in the flame.

Recommended procedure. In a separatory funnel, mix 100 ml of the water sample or standard solution with 20 ml of 18 M H_2SO_4 and cool to room temperature. Add 10 ml of the extraction solution and shake for

1 min. Measure the upper layer in the instrument. Make a blank solution with 100 ml of deionized water, following the above-mentioned procedure.

This procedure was modified to study the optimized conditions for the extraction. Four different extraction solutions were made, containing 5, 10, 15 and 20% of 2-ethyl-1,3-hexanediol in methyl isobutyl ketone. The acid concentration was studied by adding 0, 5, 10, 20, 25, 30 and 35 ml of 18 M sulphuric acid to 85 ml of an aqueous solution containing 15 μg B ml^{-1}, completing the volume to 120 ml with deionized water.

Results and discussion

Extraction of boron. The effect of the reagent concentration in the organic solvent was studied for boron concentrations of 15 μg ml^{-1} and 10 μg ml^{-1}. For more than 10% (v/v) of reagent there was no improvement in the absorbance signal. This concentration was chosen because it is more economical and gives better sensitivity; the high viscosity of the reagent reduces the aspiration rate of the sample.

Absorbances of extracts from solutions containing 10.6 μg B ml^{-1} and different sulphuric acid concentrations were studied; the absorbance increased steadily in the range 0—3 M H_2SO_4, and then tended to level off in the range 4—5 M H_2SO_4. An acidity of 3 M was selected, because at higher concentrations the increase in absorbance was less pronounced, and insoluble sulphates may precipitate.

No variation in the signal was observed for extraction times ranging from $\frac{1}{4}$ to 20 min. A 12:1 ratio of aqueous-to-organic solution was necessary to avoid preconcentration stages such as evaporation to 25% of the original volume [6]. Also, at this ratio, the other components of sea water do not interfere, as can be seen by the coincidence of the calibration curves B and C (Fig. 1) obtained with standard solutions prepared in artificial sea water and in deionized water, respectively. Curve A, for standard solutions prepared directly in the organic chelation—extraction solution, shows that 66% of boron was extracted from the aqueous samples.

The ratios of the total variance to the instrumental variance and to the extraction variance [9] are of the same order of magnitude and less than those tabulated for the F distribution at the 95% confidence level. Thus the extraction stage does not contribute significantly to the error of the method when standard solutions and unknown samples are treated identically.

The limit of detection (defined here as the concentration that corresponds to twice the standard deviation near the blank level) was 1.0 μg ml^{-1} in the organic phase and the sensitivity of the method was 5.8 μg ml^{-1} 1%, in the organic phase.

From the curves in Fig. 1, the distribution ratio (total boron in the organic phase divided by total boron in the aqueous phase) could be determined. The value found (23.2) makes it possible to calculate the fractions extracted at different aqueous-to-organic ratios.

Boron in sea water samples. Samples filtered through a Millipore BSWP membrane (pore diameter 0.22 μm) and unfiltered samples did not show

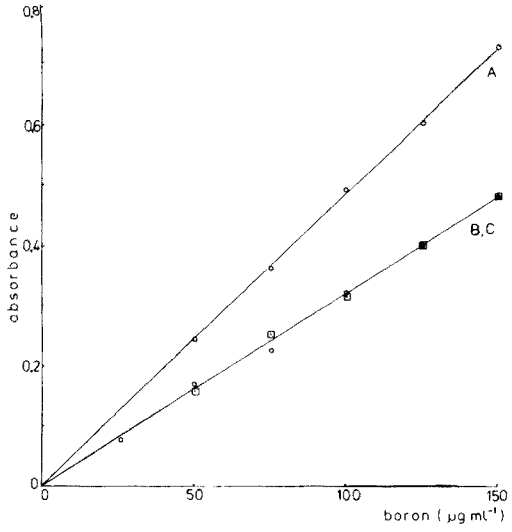

Fig. 1. Calibration curves for standard solutions prepared (A) directly in the organic solution; (B) in artificial sea water; (C) in deionized water.

significant differences in boron concentration. Samples extracted in borosilicate glass and in polyethylene containers also showed no difference. The samples were collected in polyethylene bottles and kept in a refrigerator until analysis.

Table 1 shows the boron content of some samples of Brazilian coastal surface waters. The agreement with a potentiometric method described by Gast and Thompson [1] is excellent. The Araruama Lagoon and the Rodrigo de Freitas Lagoon have high and low salinities, respectively. The average of the sea water samples, corrected for a salinity of 35 °/₀₀, was 4.6 ± 0.1 μg ml^{-1}, in agreement with the average of 4.5 ± 0.23 μg ml^{-1} for waters from several localities reported in the literature [10].

TABLE 1

Boron in Brazilian coastal surface waters

Locality	Boron concentration (μg ml^{-1})	
	Atomic absorption	Potentiometry
Cabo Frio	4.8 ± 0.1	4.8
Ipanema	4.2 ± 0.1	4.1
Leme	4.8 ± 0.1	4.8
Aracaju	4.7 ± 0.1	4.8
Araruama Lagoon	9.0 ± 0.1	9.1
R.de Freitas Lagoon	1.6 ± 0.1	1.9

The authors thank CAPES, FINEP, and CNPq for financial support.

REFERENCES

1 J. A. Gast and T. G. Thompson, Anal. Chem., 30 (1958) 9, 1549.
2 R. Greenhalgh and J. P. Riley, Analyst, 87 (1962) 970.
3 L. R. Uppstrom, Anal. Chim. Acta, 43 (1968) 475.
4 J. Lotrian and A. Johannin-Gilles, Spectrochim. Acta Part B, 24 (1969) 479.
5 M. Marcantonatos, G. Gamba and D. Monnier, Anal. Chim. Acta, 67 (1973) 220.
6 G. I. Spielholtz, G. C. Toralballa and J. J. Willsen, Mikrochim. Acta, (1974) 4, 649.
7 E. J. Agazzi, Anal. Chem., 39 (1967) 233.
8 J. Lyman and R. H. Fleming, J. Mar. Res., 3 (1940) 134.
9 K. Eckschlager, Errors, Measurements and Results in Chemical Analysis, Van Nostrand Reinhold, London, 1972, p. 120.
10 J. P. Riley and G. Skirrow (Eds.), Chemical Oceanography, Vol. 1, Academic Press, London, 1975, p. 405.

Analytica Chimica Acta, 96 (1978) 211—214

Short Communication

LIQUID—LIQUID EXTRACTION OF THE EDTA COMPLEXES OF LANTHANIDES WITH A QUATERNARY AMMONIUM SALT

CHUSHIRO YONEZAWA*

Division of Chemistry, Japan Atomic Energy Research Institute, Tokai-mura, Ibaraki-ken 319-11 (Japan)

HIROSHI ONISHI

Department of Chemistry, University of Tsukuba, Sakura-mura, Ibaraki-ken 300-31 (Japan)

(Received 14th July 1977)

Moore [1] described the extraction of americium and europium from an aqueous solution of ethylenediaminetetraacetate (EDTA) into a xylene solution of the quaternary ammonium salt, Aliquat-336; Moore [2] also used hydroxyethylethylenediaminetriacetic acid and diethylenetriaminepentaacetic acid for the same purpose. Irving and Al-Jarrah [3] extended the EDTA—Aliquat-336 system to the extraction of various metals. The present communication describes a detailed study of the extraction behavior of the EDTA complexes of lanthanides by solutions of Capriquat (trioctylmethylammonium chloride).

Experimental

Reagents and apparatus. Standard lanthanide solutions (10.0 μmol ml^{-1} of lanthanide) were prepared in 0.1 M hydrochloric acid. For the lanthanide tracer solutions (1.00 μmol ml^{-1} of lanthanide and 2.00 μmol ml^{-1} of EDTA), the following nuclides were used as tracers: ^{140}La, ^{144}Ce, ^{147}Nd, ^{153}Sm, ^{152}Eu, ^{160}Tb, ^{166}Ho, ^{170}Tm, ^{169}Yb and ^{177}Lu, together with ^{46}Sc and ^{88}Y. A hydrochloric acid solution of each nuclide and 10 ml of corresponding standard lanthanide solution were mixed and evaporated to dryness. The residue was dissolved in 2 ml of 0.10 M EDTA (disodium salt) and the solution was diluted to exactly 100 ml with water.

Capriquat (Dojin Laboratories, Kumamoto-shi, Japan) was dissolved in carbon tetrachloride or another organic solvent to give 0.1 M solutions.

An Aloka JDC-701, 44-mm diam. × 51-mm, well-type NaI(Tl) detector was used for radioactivity measurements. An ORTEC 6240 multichannel analyzer with ORTEC WIN-15 Ge(Li) detector, was used for examination of radiochemical purity of tracers. A Hitachi-Horiba Model M-5 pH meter was used.

Liquid—liquid extraction procedure. Lanthanide tracer solution (1 ml) and 1 ml of 0.010 M EDTA (disodium salt) were transferred to a stoppered

50-ml centrifuge tube. Dilute sodium hydroxide solution (8 ml) was added, and the solution was allowed to stand for 30 min. Then 10 ml of Capriquat solution was added, and the mixture was shaken for 5 min. After phase separation by centrifugation, the radioactivities of the organic and aqueous phases and the pH of the aqueous phase were measured.

Results and discussion

The distribution ratios of europium as a function of pH and organic solvent (diluent) are shown in Fig. 1. Carbon tetrachloride, benzene, toluene, and xylene gave the highest distribution ratio.

The effect of the initial EDTA concentration on the extraction of europium was studied with 1.00 μmol of europium and 1.0 mmol of Capriquat in 10 ml of carbon tetrachloride. The distribution ratio increased as the amount of EDTA was increased from 2 μmol to 12 μmol, and then became almost constant up to 102 μmol of EDTA.

The effect of the initial Capriquat concentration (solvent: carbon tetrachloride) on the extraction of cerium(III), europium and thulium was studied with 1.0 μmol of lanthanide and 12 μmol of EDTA. Nearly constant distribution ratios of cerium and europium were obtained at Capriquat concentrations higher than about 100 μmol/10 ml. The distribution ratio of

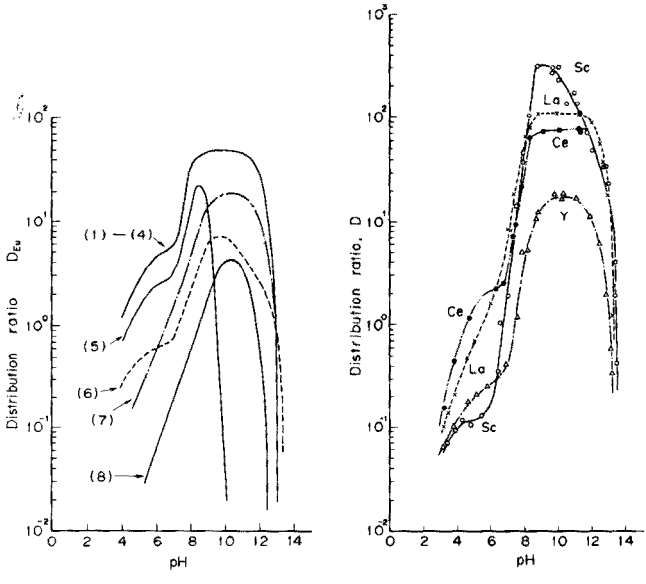

Fig. 1. Extraction of europium as a function of pH and organic solvent. [Eu] = 1.0 μmol/10 ml, [EDTA] = 12 μmol/10 ml, [Capriquat] = 100 μmol/10 ml. (1) Carbon tetrachloride; (2) benzene; (3) toluene; (4) xylene; (5) butyl acetate; (6) methyl isobutyl ketone; (7) 1,2-dichloroethane; (8) chloroform.

Fig. 2. Extraction of Sc(III), Y(III), La(III) and Ce(III). [M^{3+}] = 1.0 μmol/10 ml, [EDTA] = 12 μmol/10 ml, [Capriquat] = 1.0 mmol/10 ml.

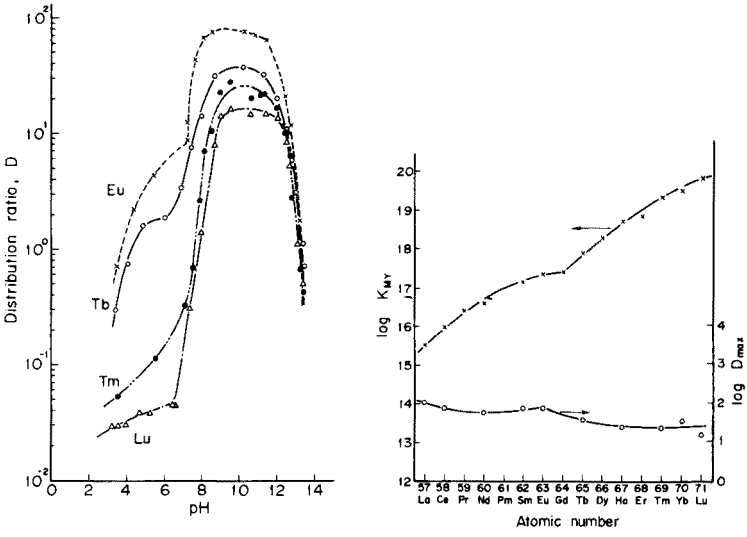

Fig. 3. Extraction of Eu(III), Tb(III), Tm(III) and Lu(III). [M^{3+}] = 1.0 μmol/10 ml, [EDTA] = 12 μmol/10 ml, [Capriquat] = 1.0 mmol/10 ml.

Fig. 4. Relation between log K_{MY} and log D_{max}. Extraction solvent: carbon tetrachloride.

thulium became almost constant at Capriquat concentrations higher than about 300 μmol/10 ml. Below these values, a plot of log D_{max} (D_{max}: maximum distribution ratio) against log Capriquat concentration gave a slope of about 1.4.

The distribution ratio of europium decreased with an increase in anion concentration; the effect was in the following order: $ClO_4^- > NO_3^- > Cl^- > SO_4^{2-}$. 1,2-Dichloroethane as solvent showed a greater effect than carbon tetrachloride. When the distribution ratio of europium at zero sulfate concentration was taken as unity (solvent: carbon tetrachloride), the distribution ratios were 0.91, 0.25, 0.091, 0.024 and 0.010 at sulfate concentrations of 10, 100, 300, 700 and 1000 μmol/10 ml, respectively.

The extraction behavior of scandium, yttrium, and lanthanides with 0.1 M Capriquat in carbon tetrachloride is shown in Figs. 2 and 3. Under the conditions used, 94—99% of lanthanides as well as scandium and yttrium can be extracted at ca. pH 10. Although Moore [1] has indicated the separation of light lanthanides from heavy ones, the present work shows that their separation is very difficult.

In Fig. 4, the maximum distribution ratios of lanthanides and the formation constants of lanthanide—EDTA complexes (K_{MY}) [4] are plotted against atomic number. No correlation is observed between log D_{max} and log K_{MY}.

REFERENCES

1 F. L. Moore, Anal. Chem., 37 (1965) 1235.
2 F. L. Moore, Anal. Chem., 38 (1966) 905.
3 H. M. N. H. Irving and R. H. Al-Jarrah, Anal. Chim. Acta, 74 (1975) 321.
4 L. G. Sillén and A. E. Martell, Stability Constants of Metal-Ion Complexes, Chemical Society, London, 1964; A. Ringbom, Complexation in Analytical Chemistry, Interscience, New York, 1963.

Analytica Chimica Acta, 96 (1978) 215—219

Short Communication

END-POINT ERRORS IN PHOTOMETRIC TITRATIONS IN THE CASE OF FORMATION OF BOTH 1:1 AND 2:1 METAL-INDICATOR CHELATES

HISAKUNI SATO

Laboratory for Industrial Analytical Chemistry, Faculty of Engineering, Yokohama National University, Ooka 2-31-1, Minami-ku, Yokohama-shi (Japan)

(Received 1st June 1977)

Metal indicators which form only a 1:1 chelate with the metal ion are obviously useful in complexiметric titrations [1, 2]. However, some indicators form 1:2 and/or 2:1 chelates in addition to the 1:1 chelate, and so complicate the titration. Kragten [3] has reported on the systematic error arising in the extrapolation method and on the conditions needed to reduce the error to less than 0.5% when one particular indicator chelate predominates during the titration.

When some triphenylmethane derivatives, such as xylenol orange (XO), are used as the indicator, MI and M_2I chelates are often formed. The latter is quite stable so that neither of the indicator chelates predominates during the titration. Such cases have not been dealt with theoretically, but seem to be rather important in practice. The standardization of EDTA with bismuth(III) and catechol violet [4] is an example.

The present communication deals with the systematic error of the extrapolated end-point of the absorbance curve for the case in which the conditional formation constant of M_2I is similar to the square of that of MI. The Pb—XO—EDTA system is taken as a practical example.

Equation for the systematic error

The chelate-formation reactions in a titration can be represented as

$$M + I^* \rightleftharpoons MI; \quad \beta_{11}^* = [MI]/[M][I^*] \tag{1}$$

$$2M + I^* \rightleftharpoons M_2I; \quad \beta_{21}^* = [M_2I]/[M]^2[I^*] \tag{2}$$

$$M + Y^* \rightleftharpoons MY; \quad K_{MY}^* = [MY]/[M][Y^*] \tag{3}$$

where M, I^*, Y^* represent the metal ion, indicator, titrant, respectively; charges are omitted for simplicity. β_{11}^*, β_{21}^*, and K_{MY}^* represent the conditional formation constants [5]. The mass-balance equations are

$$C_M = [M] + [MI] + 2[M_2I] + [MY] \tag{4}$$

$$C_I = [I^*] + [MI] + [M_2I] \tag{5}$$

$$C_Y = [Y^*] + [MY] \tag{6}$$

Absorbances at a certain wavelength may be written as

$$A_s = \epsilon_{11}[MI] + \epsilon_{21}[M_2I] + \epsilon_I[I^*] \tag{7}$$

$$A_I \equiv \epsilon_I C_I \tag{8}$$

$$A_s - A_I = (\epsilon_{11} - \epsilon_I)[MI] + (\epsilon_{21} - \epsilon_I)[M_2I] \tag{9}$$

If there is a wavelength for which the relationship

$$\epsilon_{21} - \epsilon_I = 2(\epsilon_{11} - \epsilon_I) \tag{10}$$

is valid, then eqn. (9) can be simplified to

$$A_s - A_I = (\epsilon_{11} - \epsilon_I)(2[M_2I] + [MI]) \tag{11}$$

The condition defined by eqn. (10), is often realized. "Normalized" absorbance can be defined as

$$A = \frac{1}{C_M} \cdot \frac{A_s - A_I}{\epsilon_{11} - \epsilon_I} \tag{12}$$

From eqns. (1)—(6), (11), and (12),

$$\frac{C_Y}{C_M} = \left(1 - \frac{[M]}{C_M} - A\right)\left(1 + \frac{1}{K_{MY}^*} \cdot \frac{1}{[M]}\right) \tag{13}$$

$$A = \frac{C_I}{C_M} \cdot \frac{\beta_{11}^*[M] + 2\beta_{21}[M]^2}{1 + \beta_{11}^*[M] + \beta_{21}^*[M]^2} \tag{14}$$

The equation for the photometric titration curve can be obtained from eqns. (13) and (14) by the elimination of [M].

For the extrapolation method, the tangent at the inflection point is considered to be best. However, it is difficult to obtain the parameter relations at the inflection point because of the complexity. Therefore, the tangent at another point is chosen here.

If M_2I predominates at the beginning, and [MI] increases gradually during a titration, the relationship

$$A_0 \approx 2[M_2I]/C_M \approx 2C_I/C_M \tag{15}$$

is valid. At $A = C_I/C_M \equiv A_{1/2}$

$$[M]_{A_{1/2}} = (\beta_{21}^*)^{1/2} \tag{16}$$

The equation of the tangent for the titration curve at $A_{1/2}$ is

$$\frac{C_Y}{C_M} - \left(\frac{C_Y}{C_M}\right)_{A_{1/2}} = \left\{\frac{d(C_Y/C_M)}{dA}\right\}_{A_{1/2}} \cdot \left(A - \frac{C_I}{C_M}\right) \tag{17}$$

By the extrapolation of this tangent to $A = 0$, the end-point can be obtained:

$$\left(\frac{C_Y}{C_M}\right)_{end} = \left(\frac{C_Y}{C_M}\right)_{A_{1/2}} - \frac{C_I}{C_M}\left\{-1 - \frac{\beta_{21}^{*1/2}}{K_{MY}^*} - \left(\frac{C_M\beta_{21}^*}{C_I K_{MY}^*} - \frac{\beta_{21}^*}{K_{MY}^*} + \frac{1}{C_I}\right) \times \left(\frac{\beta_{11}^*}{2\beta_{21}^*} + \frac{1}{\beta_{21}^{*1/2}}\right)\right\} \tag{18}$$

The systematic error of the end-point can be represented as:

$$e = \left(\frac{C_Y}{C_M}\right)_{end} - 1$$

$$= -\frac{1}{C_M K_{MY}^*} + \frac{\beta_{11}^*}{2K_{MY}^*}\left(1 - \frac{C_I}{C_M}\right) + \frac{\beta_{21}^{*1/2}}{K_{MY}^*}\left(2 - \frac{C_I}{C_M}\right) + \frac{\beta_{11}^*}{2C_M\beta_{21}^*} \qquad (19)$$

Thus, the end-point error for this extrapolation method can be estimated from the conditional formation constants and the approximate values of C_M and C_I when conditions (10) and (15) are satisfied.

The first term in eqn. (19) can usually be neglected in comparison with other terms. The larger the value of K_{MY}^*, the smaller the value of e. When C_I/C_M is less than 0.1,

$$e \approx \frac{1}{K_{MY}^*}\left(\frac{\beta_{11}^*}{2} + 2\beta_{21}^{*1/2}\right) + \frac{\beta_{11}^*}{2C_M\beta_{21}^*} \qquad (20)$$

This approximate value of e is always positive. If the last term in eqn. (19) or (20) is less than 10^{-2}, then $A_0 > 1.97\ C_I/C_M$, and condition (15) is almost satisfied.

In the derivation of eqn. (19), approximations are not included except for the effect of dilution during the titration. If this effect is taken into account, the first and the last terms in eqn. (19) are multiplied by the dilution ratio, $g_{1/2}$, at $A_{1/2}$: $g_{1/2} = (V_0 + v_{1/2})/V_0$, where V_0 is the titrand volume at the beginning of the titration and $v_{1/2}$ is the volume of titrant added at $A_{1/2}$. C_M and C_I in eqn. (19) are now the concentrations at the beginning of the titration. The absorbance values must be corrected for dilution. Equation (12) then becomes

$$A = \frac{1}{C_M} \cdot \frac{g \cdot A_s - g_I \cdot A_I}{\epsilon_{11} - \epsilon_I} \qquad (21)$$

Pb—XO—EDTA system

Table 1 lists the conditional formation constants at some pH values. By using these constants, the systematic error and A_0 values for the Pb—XO—EDTA system can be evaluated (Table 2). Accurate titrations can be expected unless the total concentration of lead(II) is too low.

Some titration curves at different wavelengths for the same amount of lead(II) are shown in Fig. 1. The change in absorbance decreases almost linearly between 565 and 570 nm, because the molar absorptivity condition (eqn. 10) holds. At 580 nm or longer wavelengths, the absorbance decrease shows a concave curve, whereas the titration curves at 520 and 540 nm are of convex type. Practically, successful titrations are possible at pH 5—6 with a hexamine buffer; acetate buffer is not suitable, because of the formation of lead(II)—acetate complexes.

TABLE 1

Conditional formation constants for Pb—XO and Pb—EDTA

pH	$\log \beta_{11}^{*a}$	$\log \beta_{21}^{*a}$	$\log K_{MY}^{*b}$
4.5	5.48	10.96	
5.0	6.24	12.45	11.4
5.5	7.10	13.95	
6.0	8.01	15.38	13.2
6.5	8.86	16.73	

[a] Calculated from the data of H. Sato et al. [6].
[b] Cited from Ringbom's book [5].

TABLE 2

Systematic error and A_0 value for Pb—XO—EDTA system

pH	$C_M = 10^{-3}$ M		$C_M = 10^{-4}$ M	
	e	A_0	e	A_0
5	0.04%	$2.00\ C_I/C_M$	0.41%	$1.99\ C_I/C_M$
6	0.004	2.00	0.04	2.00

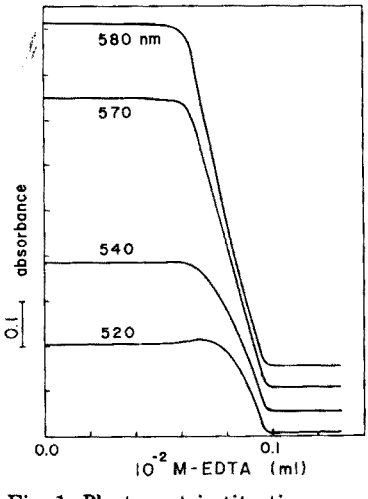

Fig. 1. Photometric titration curves for Pb(II)—XO—EDTA. $C_M = 1.99 \times 10^{-5}$ M; $C_I = 3.46 \times 10^{-6}$ M; pH 5.67.

Table 3 shows the titration results for different amounts of lead(II) at 565 nm. The concentration of the lead(II) stock solution was 0.9958×10^{-2} M (prepared from the pure metal). From the titration results, the concentration was evaluated as 0.9945×10^{-2} M, when the EDTA solution was standardized

TABLE 3

Titration results for the Pb—XO—EDTA system
($C_I = 3.46 \times 10^{-6}$ M, pH = 5.53 (hexamine—$HClO_4$), 565 nm, V_0 50.0 ml.)

10^{-2} M Pb(II) taken (ml) $f_{Pb} = 0.9958$	10^{-2} M EDTA consumed (ml) $f_Y = 1.0229$	Deviation from the regression line (ml)[a]
0.100	0.097_2	-0.002_4
1.000	0.975_4	$+0.000_8$
2.000	1.945_3	-0.001_5
3.000	2.919_8	$+0.000_8$

[a] $V_y = 0.9722\ V_{Pb} + 0.0024$

against standard zinc(II) solution [1]. The relative deviation was 0.13%. This error is attributed to measuring errors in several steps. Thus, even when MI and M_2I are formed, the systematic end-point error should be very small. Similar situations may be found in titration systems involving other metal ions and other sulfonephthalein derivatives as indicators.

REFERENCES

1 H. Sato and K. Momoki, Anal. Chem., 42 (1970) 1477.
2 E. Still, Suom. Kemistil. B., 41 (1968) 33.
3 J. Kragten, Mikrochim. Acta, (1971) 821.
4 Analytical Methods Committee, Analyst, 100 (1975) 675.
5 A. Ringbom, Complexation in Analytical Chemistry, Interscience, New York, 1963.
6 H. Sato, Y. Yokoyama, and K. Momoki, Anal. Chim. Acta, 94 (1977) 217.

Analytica Chimica Acta, 96 (1978) 221—223

Short Communication

NOUVELLE METHODE DE PREPARATION DE TUBES A PERMEATION

J. GODIN et Cl. BOUDENE*

Unité I.N.S.E.R.M. 122, Laboratoire de Toxicologie, Faculté de Pharmacie, Rue J. B. Clément, 92290 Chatenay-Malabry (France)

(Reçu le 4 juillet 1977)

La mesure des polluants dans l'atmosphère, l'étude physico-chimique des mélanges de gaz, la recherche des mécanismes d'action toxique des polluants sur l'homme, l'animal et les végétaux a conduit l'expérimentateur à mettre au point des techniques de mélange de composés gazeux à faibles concentrations. Parmi les techniques actuellement connues, deux méthodes sont largement utilisées; ce sont les tubes à perméation [1, 2] et les cellules de diffusion [3]. Le procédé que nous présentons est inspiré de ces deux techniques. Il consiste à préparer les mélanges polluants de titres connus par perméation du composé à travers une colonne de silicone de petit diamètre. La grande perméabilité des silicones aux gaz permet, en effet, comparativement au téflon, de réduire considérablement la surface de perméation (les coefficients de perméabilité des deux matériaux sont très différents: ainsi pour l'oxygène, ils sont de 60 pour le caoutchouc de diméthylsilicone et de 0,0004 pour le Téflon; les coefficients des autres polymères étudiés par Robb [4] se situent entre ces deux valeurs extrêmes). Déjà, les silicones ont reçu quelques applications pour la préparation de mélanges gazeux: oxyde de carbone [5], mercure [6], divers polluants [7] et également pour la confection de dosimètres portables pour oxydes d'azote [8].

Partie expérimentale

Un tube de verre (Fig. 1) non scellé dans sa partie supérieure est rempli dans sa partie inférieure en aspirant du diméthylsiloxane monomère (Prolabo RTV 141 A) contenant 10% (p/p) d'agent polymérisant (Prolabo RTV 141 B). L'extrémité est obturée provisoirement pendant 12 h pour permettre la polymérisation, l'ensemble étant placé verticalement dans une étuve à 50°C.

Le remplissage de ce tube s'effectue par sa partie supérieure en introduisant à l'intérieur du réservoir l'extrémité d'un tube de 3,2 mm de diamètre relié à la bouteille du gaz liquéfié. Pendant cette opération, le tube est refroidi à une température inférieure au point d'ébullition du composé. Après remplissage, le tube est maintenu à basse température dans de la carboglace pulvérulente pendant toute la durée du scellement de l'ampoule. Pour éviter aux vapeurs des composés organiques de charbonner, l'intérieur

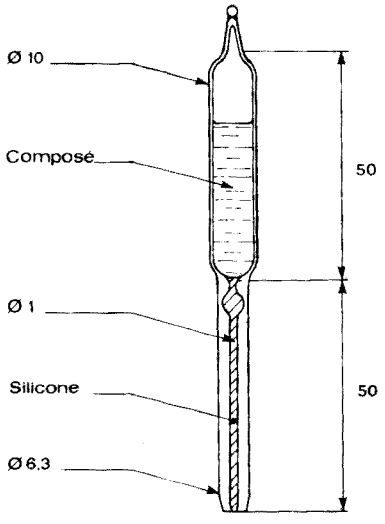

Fig. 1. Tube à perméation. Cotes en mm.

du tube est balayé par un léger courant d'azote pendant la fusion du verre. Les tubes ainsi préparés ont été utilisés après un mois de conditionnement dans l'enceinte thermostatée destinée à la production du gaz (Tracor 412).

Resultats

Pour les besoins du laboratoire, trois composés ont été utilisés pour le remplissage des tubes, le sulfure de carbone, le méthylmercaptan et le chlorure de vinyle. Les débits de gaz calculés sur quelques mois de fonctionnement sont respectivement de: 7,75 $\mu g\ h^{-1}$ (CV, 1,63%), 7,47 $\mu g\ h^{-1}$ (CV, 1,86%) et 45,32 $\mu g\ h^{-1}$ (CV, 3,58%). Les pesées sont effectuées sur une balance au 0,01 de mg (Mettler H20T). Les performances de ces tubes sur de longues périodes de temps font actuellement l'objet d'une étude approfondie. Il est cependant possible d'affirmer que ces tubes sont utilisables pour l'étalonnage d'appareils de mesure.

Ces résultats montrent également qu'il est possible d'obtenir des débits de gaz comparables à ceux obtenus avec les tubes à perméation en Téflon.

Discussion

L'intérêt le plus important de ces tubes est que leur confection ne présente pas de difficulté; de plus, la résine silicone et son agent de polymérisation sont disponsibles commercialement. L'étanchéité des tubes est assurée par la plasticité du polymère et par son gonflement sous l'influence du composé contenu dans le tube. De plus, la forme du tube est étudiée pour favoriser l'adhérence du polymère sur sa paroi. Comparativement, la réalisation des tubes à perméation en Téflon par un laboratoire non spécialisé est plus délicate notamment pour obtenir une étanchéité parfaite.

Un autre intérêt de ces tubes est qu'étant donné la grande perméabilité des silicones à beaucoup de composés organiques, il est possible d'envisager, comme pour le sulfure de carbone, de les utiliser pour la génération de vapeurs de substances organiques liquides à température ordinaire. Rappelons à titre de comparaison que les coefficients de perméabilité sont respectivement de 9000 pour le sulfure de carbone, 1080 pour le benzène, 60 pour l'oxygène et 28 pour l'azote [4].

Le débit de gaz fourni par les tubes peut être modifié en jouant sur la longueur et le diamètre de la partie du tube contenant le polymère. De même, les dimensions du réservoir peuvent être modifiées en fonction de la durée de vie désirée du tube.

Comme pour les tubes en Téflon, leur confection est limitée par la résistance des tubes à la pression des gaz présents à l'intérieur de l'enceinte qui ne peut dépasser quelques kg cm^{-2}.

BIBLIOGRAPHIE

1 A. E. O'Keefe et G. C. Ortman, Anal. Chem., 38 (1966) 760.
2 B. E. Saltzmann, W. R. Burg et G. Ramaswany, Environ. Sci. Technol., 5 (1971) 1121.
3 A. P. Altshuller et I. R. Cohen, Anal. Chem., 32 (1960) 802.
4 W. L. Robb, Ann. N.Y. Acad. Sci., 146 (1968) 119.
5 D. Brocco et M. Possanzini, Anal. Lett., 7 (1974) 153.
6 G. L. Corte, G. Dowd et L. Dubois, Am. Ind. Hyg. Ass. J., 36 (1975) 873.
7 J. Godin et Cl. Boudène, C.R. Acad. Sci. Sér. D., 283 (1976) 563.
8 B. I. Ferber, F. A. Sharp et R. W. Freedman, Am. Ind. Hyg. Ass. J., 37 (1976) 32.

Analytica Chimica Acta, 96 (1978) 225—227

Book Reviews

Gary D. Christian, *Analytical Chemistry*, 2nd edn., J. Wiley, New York, 1977, xvi + 648 pp., price £11.35, US $19.50.

This is a text-book for non-chemistry majors. The emphasis is on the application of analytical chemistry within the life sciences; a strongly classical approach is adopted. The text is self-contained in the sense that it includes theory, and the practical details for suitable laboratory experiments. Each chapter concludes with review-type questions and recommended references for further reading; the student who gains access to all those listed, and has time to read them, will certainly have done well.

That Christian has had a useful measure of success within his chosen scope is revealed by the fact that this second edition is offered only 6 years after the appearance of the book in its original form. Many changes have been made in this new edition, although the general organization of the text is essentially the same. Some topics have been dropped (e.g. chapters on laboratory safety, sampling, classical gas analysis, use of computers, optical rotatory dispersion etc.), several chapters have been revised and expanded, and some new chapters have been added (e.g. on non-aqueous titrations and drug analysis). Eight of the experiments in the first edition have been dropped, but 14 new ones give a total of 51 for which full laboratory instructions are supplied.

The standard throughout is that of an introductory text; the lay-out is attractive, and the price reasonable. Those who teach the categories of student for whom this book was written should put it on the list of possibles for class adoption.

Larry Kevan and Lowell D. Kispert, *Electron Spin Double Resonance Spectroscopy*, J. Wiley, New York, 1976, vii + 427 pp., price £18.00, US $30.70.

This text, written by authors with wide experience of the techniques involved in electron nuclear double resonance (ENDOR) and electron-electron double resonance (ELDOR), gives an excellent introduction to the subject; the treatment greatly augments that given by Atherton in his "Electron Spin Resonance" in 1973.

The basic concepts are given with the minimum amount of mathematics. The operation of commercial spectrometers and the experimental techniques are described clearly; there are numerous examples of liquid and solid phase ENDOR and ELDOR and a discussion of their biochemical applications, with emphasis on protons. Reviews of the appropriate literature through

1974 are given, and most of the chapters also include references to work published in 1975.

This is an excellent production, free from misprints, with excellent diagrams, and good indexes. The application of double resonance techniques has increased steadily over the past 10 years; although ENDOR and ELDOR are very specialised techniques, they are powerful methods of obtaining important analytical and structural information for complex molecules and free radicals, and their application will increase. This is a good text for those who wish to start to get into this field.

V. G. Berezkin, V. R. Alishoyen and I. B. Nemirovskaya, *Gas Chromatography of Polymers*, Elsevier, Amsterdam, 1977, xiii + 223 pp., price Dfl. 103.00, US $41.95.

This, Volume 10 of the Journal of Chromatography Library, is a translation of the second edition of the book first published in Russia in 1972; the additional references to work published in 1972—1975 are mainly from Russian sources. The translation is excellent; the general standard of production of this volume maintains the established high standard of this Series.

The basic approach of this book is sound, and the underlying themes, i.e. that many of the applications of chromatography to polymeric systems have yet to be optimized, and that there are many possible applications yet to be exploited, are justified. The main approaches have been to the analysis of monomers and solvents, to the study of polymer formation reactions, to the determination of volatile compounds in polymer systems, to the kinetics and mechanism of transformations of polymers at elevated temperatures, and to the use of reaction g.c., pyrolysis g.c., and inverse g.c., in which the polymer system under study is used as the stationary phase.

This book gives a good systematic summary of the earlier applications of g.c. to polymers, and also makes several suggestions as to how these studies can be extended in the future. The treatment is restricted to synthetic polymers. The omission of any form of index is unfortunate and makes it difficult to find out quickly what is and what is not in this book.

D. M. W. Anderson

J. Inczedy, *Analytical Applications of Complex Equilibria*, Ellis Horwood, Chichester, pp. 415, price £17.50, US $35.90.

This book is a translation, updated and extended, of the author's original (1970) Hungarian text. It contains four principal chapters. The first deals with the chemistry and properties of coordination complexes, and the fundamental theory underlying the formation of and equilibria affecting

complexes in solution. The second chapter describes most of the accepted methods for the determination of equilibrium constants of complexes. Chapter three, the largest one, considers how complex equilibria can be applied to improve the understanding of the major processes of analytical chemical determinations. The final chapter contains tables of equilibrium constants.

Although other texts cover some of the material contained in this book, none quite deals with the subject in the way Professor Inczedy has chosen. His treatment of a generally underestimated feature of training in analytical chemistry should do much to encourage the research worker to undertake equilibrium calculations with some confidence. This is a thoroughly workmanlike and eminently readable text which introduces the non-specialist to the intricacies of complex equilibrium calculations in a direct, simple way. Emphasis is given to the Ringbom concept of conditional constants, and wherever appropriate, worked examples are given to illustrate the practicality of calculations for establishing the optimal conditions for a particular analytical determination.

Price-wise, this is unfortunately too expensive a book to recommend for general student use, although there is much in it of value for graduate students studying conventional instrumental methods of chemical analysis. It should certainly be readily available for consultation by anyone seeking to use equilibrium calculations to assess the feasibility or otherwise of analytical procedures involving complexes in aqueous solution.

W. I. Stephen

ERRATUM

E. Merciny, J. M. Gatez et G. Duyckaerts, Étude par Spectroscopie d'Absorption de la Complexation des Lanthanides Trivalents par les Acides Aminocarboxyliques, *Anal. Chim. Acta*, 93 (1977) 227—237.

Page 227, ligne 13 du résumé, lire "ou huit pour les terres yttriques" au lieu de "on huit pour les terres yttriques".
Page 228, ligne 33: lire "Choppin et al. [6] arrivent à la conclusion" au lieu de "Choppin et al. [6] arrive à la conclusion".
Page 230, légende de la figure 1, ligne 5: lire "Les lignes verticales" au lieu de "Les lignes verticaux".
Page 230, ligne 13 du texte: lire "en fonction du pH" au lieu de "en fonction de pH".
Page 231, ligne 9: lire "la localisation" au lieu de "le localisation".
Page 231, ligne 14: lire "les mêmes raisons" au lieu de "les même raisons".
Page 231, ligne 22: lire "683.50" au lieu de "683.60".
Page 231, ligne 28: lire "les figures 2, 3 et 4" au lieu de "les figures 2, 3".
Page 232, ligne 11 du texte: lire "des chélatants monoazotés" au lieu de "des chélatants monoazotées".
Page 232, ligne 15 du texte: lire "particulière" et non "particulaire".
Page 233, tableau 2, avant dernière ligne: $\Delta\lambda$ = "2.60" et non "2.50".

(continued from page 4 of cover)

Short Communications

VOL. 96 No. 1 ANALYTICA CHIMICA ACTA JANUARY 1, 1978

CONTENTS

(continued on inside page of the cover)